Baculovirus Synergism: Investigating Mixed Alphabaculovirus and Betabaculovirus Infections in the False Codling Moth, *Thaumatotibia leucotreta*, for Improved Pest Control

A thesis submitted in fulfilment of the
requirements for the degree of

DOCTOR OF PHILOSOPHY

of

RHODES UNIVERSITY

By

Michael David Jukes

December 2017

Declaration

I, Michael David Jukes (g08j1719) hereby declare that the thesis submitted is my own work. It is being submitted for the degree of Doctor of Philosophy at Rhodes University. It has not been previously submitted for assessment of any degree at any other university or other body, organisation outside of the university.

M. D. Jukes

Author's signature

08 March 2018

Date

Abstract

Baculovirus based biopesticides are an effective and environmentally friendly approach for the control of agriculturally important insect pests. The false codling moth (FCM), *Thaumatotibia leucotreta* (Meyrick) (Lepidoptera: Tortricidae), is indigenous to southern Africa and is a major pest of citrus crops. This moth poses a serious risk to export of fruit to foreign markets and the control of this pest is therefore imperative. The Cryptophlebia leucotreta granulovirus (CrleGV) has been commercially formulated into the products Cryptogran™ and Cryptex®. These products have been used successfully for over a decade as part of a rigorous integrated pest management (IPM) programme to control *T. leucotreta* in South Africa. There is however, a continuous need to improve this programme while also addressing new challenges as they arise. An example of a rising concern is the possibility of resistance developing towards CrleGV. This was seen in Europe with field populations of the codling moth, *Cydia pomonella* (Linnaeus) (Lepidoptera: Tortricidae), which developed resistance to the Mexican isolate of the Cydia pomonella granulovirus (CpGV-M). To prevent such a scenario occurring in South Africa, there is a need to improve existing methods of control. For example, additional baculovirus variants can be isolated and characterised for determining virulence, which can then be developed as new biopesticides. Additionally, the potential for synergistic effects between different baculoviruses infecting the same host can be explored for improved virulence. A novel nucleopolyhedrovirus was recently identified in *T. leucotreta* larval homogenates which were also infected with CrleGV. This provided unique opportunities for continued research and development.

In this study, a method using *C. pomonella* larvae, which can be infected by the NPV but not by CrleGV, was developed to separate the NPV from GV-NPV mixtures in an *in vivo* system. Examination of NPV OBs by transmission electron microscopy showed purified occlusion bodies with a single nucleopolyhedrovirus morphology (SNPV). Genetic characterisation identified the novel NPV as Cryptophlebia peltastica nucleopolyhedrovirus (CrpeNPV), which was recently isolated from the litchi moth, *Cryptophlebia peltastica* (Meyrick) (Lepidoptera: Tortricidae).

To begin examining the potential for synergism between the two viruses, a multiplex PCR assay was developed to accurately detect CrleGV and/or CrpeNPV in mixed infections. This assay was applied to various samples to screen for the presence of CrpeNPV and CrleGV. Additionally, a validation experiment was performed using different combinations of

CrpeNPV and/or CrleGV to evaluate the effectiveness of the mPCR assay. The results obtained indicated a high degree of specificity with the correct amplicons generated for each test sample. The biological activity of CrpeNPV and CrleGV were evaluated using surface dose bioassays, both individually and in various combinations, against *T. leucotreta* neonate larvae in a laboratory setting. A synergistic effect was recorded in the combination treatments, showing improved virulence when compared against each virus in isolation. The LC_{90} for CrpeNPV and CrleGV when applied alone against *T. leucotreta* was calculated to be 2.75×10^{6} and 3.00×10^{6} OBs.ml^{-1} respectively. These values decreased to 1.07×10^{6} and 7.18×10^{5} OBs.ml^{-1} when combinations of CrleGV and CrpeNPV were applied at ratios of 3:1 and 1:3 respectively. These results indicate a potential for developing improved biopesticides for the control of *T. leucotreta* in the field.

To better understand the interactions between CrleGV and CrpeNPV, experiments involving the serial passage of these viruses through *T. leucotreta* larvae were performed. This was done using each virus in isolation as well as both viruses in different combinations. Genomic DNA was extracted from recovered occlusion bodies after each passage and examined by multiplex and quantitative PCR. This analysis enabled the detection of each virus present throughout this assay, as well as recording shifts in the ratio of CrleGV and CrpeNPV at each passage. CrleGV rapidly became the dominant virus in all treatments, indicating a potentially antagonistic interaction during serial passage. Additionally, CrpeNPV and CrleGV were detected in treatments which were not originally inoculated with one or either virus, indicating potential covert infections in *T. leucotreta.* Occlusion bodies recovered from the final passage were used to inoculate *C. pomonella* larvae to isolate CrpeNPV from CrleGV. Genomic DNA was extracted from these CrpeNPV OBs and examined by restriction endonuclease assays and next generation sequencing. This enabled the identification of potential recombination events which may have occurred during the dual GV and NPV infections throughout the passage assay. No recombination events were identified in the CrpeNPV genome sequences assembled from virus collected at the end of the passage assay.

Lastly, the efficacy of CrpeNPV and CrleGV, both alone and in various combinations, was evaluated in the field. In two separate trials conducted on citrus, unfavorable field conditions resulted in no significant reduction in fruit infestation for both the virus and chemical treatments. While not statistically significant, virus treatments were recorded to have the lowest levels of fruit infestation with a measured reduction of up to 64 %.

This study is the first to report a synergistic effect between CrleGV and CrpeNPV in *T. leucotreta*. The discovery of beneficial interactions creates an opportunity for the development of novel biopesticides for improved control of this pest in South Africa.

Table of Contents

List of Figures

Chapter 1:

Chapter 2:

Chapter 3:

Chapter 4:

Chapter 5:

Chapter 6:

List of Tables

Chapter 1:

Chapter 3:

Chapter 4:

Chapter 5:

Chapter 6:

Chapter 7:

Chapter 10:

List of Equations

Chapter 5:

Chapter 6:

List of Abbreviations

Abbreviations:

%	-	Percentage
×g	-	Time gravity
°C	-	Degrees Celsius
µl	-	Microliter
AGE	-	Agarose gel electrophoresis
ANOVA	-	Analysis of variance
BASF	-	Baden aniline and soda factory
BLAST	-	Basic Local Alignment Search Tool
bp	-	Base pair
BRERC	-	Bristol Regional Environmental Records Centre
BV	-	Baculovirus
CGA	-	Citrus Growers Association
CM	-	Codling moth
CTAB	-	Cetrimonium bromide
D1	-	Dose 1
D2	-	Dose 2
D3	-	Dose 3
D4	-	Dose 4
D5	-	Dose 5
D6	-	Dose 6
DAFF	-	Department of agriculture, forestry and fisheries
ddH_2O	-	Double distilled water DNA
DNA	-	Deoxyribonucleic acid
EDTA	-	Ethylenediaminetetraacetic acid
egt	-	*ecdysteroid uridine 5′-diphosphate - glucosyltransferase*
EPF	-	Entomopathogenic fungi
EPN	-	Entomopathogenic nematodes
EPPO	-	European and Mediterranean Plant Protection Organization
EU	-	European Union
FCM	-	False codling moth

gDNA	-	Genomic deoxyribonucleic acid
GLIMMER	-	Gene Locator and Interpolated Markov Modeler
gran	-	Granulin
GV	-	Granulovirus
H	-	High concentration
Ha	-	Hectares
IBM	-	International Business Machines Corporation
IGR	-	Insect growth regulator
IPM	-	Integrated pest management
JD	-	J domain
L	-	Low concentration
LC	-	Lethal concentration
LC_{50}	-	Lethal concentration (50 %)
LC_{90}	-	Lethal concentration (90 %)
LD	-	Lethal dose
lef	-	Late expression factor
LSD	-	Least significant difference
LT	-	Lethal time
M	-	Molar
MEGA	-	Molecular Evolutionary Genetics Analysis
mg	-	Milligram
ml	-	Millilitre
mM	-	Millimolar
MNPV	-	Multiple nucleopolyhedrovirus
mPCR	-	Multiplex polymerase chain reaction
MR	-	Missing region
MSSCP	-	Multitemperature single-stranded conformational polymorphism
MTR	-	Map to reference
NCBI	-	National Center for Biotechnology Information
NGS	-	Next Generation Sequencing
nm	-	Nanometre
NPV	-	Nucleopolyhedrovirus
NTC	-	No template control

OB	-	Occlusion Body
ODV	-	Occlusion derived virion
ORF	-	Open reading frame
P0	-	Passage 0
P1	-	Passage 1
P2	-	Passage 2
P3	-	Passage 3
P4	-	Passage 4
P5	-	Passage 5
PCR	-	Polymerase chain reaction
pif	-	*per os* infectivity factor
PM	-	Peritrophic membrane
polh	-	Polyhedrin
PPECB	-	The Perishables Products Export Control Board
PTM	-	Potato tuber moth
qPCR	-	Quantitative polymerase chain reaction
R	-	Rand
REN	-	Restriction endonuclease
RH	-	Relative humidity
RNA	-	Ribonucleic acid
SA	-	South Africa
SD	-	Standard deviation
SDS	-	Sodium dodecyl sulphate
SIT	-	Sterile insect technique
SNPV	-	Single nucleopolyhedrovirus
SPSS	-	Statistical Package for the Social Sciences
TAE	-	Tris base, acetic acid and EDTA
TEM	-	Transmission electron microscope
UGMUG	-	University of Gdansk and Medical University of Gdansk
UK	-	United Kingdom
US	-	United States
USA	-	United States of America
UV	-	Ultraviolet radiation

v/v	-	volume per volume
w/v	-	weight per volume

Viruses:

AcMNPV	-	Autographica californica MNPV
AdhoNPV	-	Adoxophyes honmai NPV
AdorNPV	-	Adoxophyes orana NPV
AfMNPV	-	Anagrapha falcifera NPV
AgMNPV	-	Anticarsia gemmatalis MNPV
AgseGV	-	Agrotis segetum GV
AgseNPV	-	Agrotis segetum NPV
AngeMNPV	-	Anticarsia gemmatalis MNPV
BmNPV	-	Bombyx mori NPV
CapoNPV	-	Catopsilia pomona NPV
ChfuNPV	-	Choristoneura fumiferana NPV
CnmeGV	-	Cnaphalocrocis medinalis GV
CpGV	-	Cydia pomonella granulovirus
CrleGV	-	Cryptophlebia leucotreta GV
CrpeNPV	-	Cryptophlebia peltastica NPV
CuniNPV	-	Culex nigripalpus NPV
DapuNPV	-	Dasychira pudibunda NPV
EpapGV	-	Epinotia aporema GV
HearNPV	-	Helicoverpa armigera NPV
HearSNPV	-	Helicoverpa armigera SNPV
LafiNPV	-	Lambdina fiscellaria NPV
LdMNPV	-	Lymantria dispar MNPV
LdNPV	-	Lymantria dispar NPV
LoobMNPV	-	Lonomia obliqua MNPV
MabrNPV	-	Mamestra brassicae NPV
NeleNPV	-	Neodiprion lecontei NPV
NeseNPV	-	Neodiprion sertifer NPV
OpMNPV	-	Orgyia pseudotsugata multicapsid NPV
PeluSNPV	-	Perigonia lusca SNPV

PhopGV	-	Phthorimaea operculella granulovirus
PlxyMNPV	-	Plutella xylostella MNPV
PsunNPV	-	Pseudaletia unipuncta NPV
RoMNPV	-	Rachiplusia ou MNPV
SfMNPV	-	Spodoptera frugiperda MNPV
SpalNPV	-	Spodoptera albula NPV
SpexNPV	-	Spodoptera exempta NPV
ThleNPV	-	Thaumatotibia leucotreta NPV
TnGV	-	Trichoplusia ni GV
TnSNPV	-	Trichoplusia ni SNPV
XecnGV	-	Xestia c-nigrum GV

Research Outputs

Conferences:

International:

Jukes, M.D., Knox, C.M., Hill, M.P. and Moore, S.D., 2014. The isolation, genetic and biological characterisation of a novel South African Phthorimaea operculella granulovirus. Oral presentation at the International Congress on Invertebrate Pathology and Microbial Control and 47th Annual Meeting of the Society for Invertebrate Pathology conference held at Johannes Gutenberg-Universität, Mainz, Germany. 3-7 August.

Jukes, M.D., Knox, C.M., Hill, M.P., Moore, S.D., Rabalski, L. and Szewczyk, B., 2016. Baculovirus synergism: investigating mixed alphabaculovirus and betabaculovirus infections in the false codling moth, *Thaumatotibia leucotreta*, for improved pest control. Oral presentation at the International Congress on Invertebrate Pathology and Microbial Control and 49th Annual Meeting of the Society for Invertebrate Pathology conference held at Da Vinci Centre, Tours, France. 24-28 July.

Jukes, M.D., Rabalski, L., Knox, C.M., Hill, M.P., Moore, S.D. and Szewczyk, B., 2017. Baculovirus synergy: mixed Alphabaculovirus and Betabaculovirus infections for the control of *Thaumatotibia leucotreta* in South Africa. Oral presentation at the IOBC-WPRS Working Group "Microbial and Nematode Control of Invertebrate Pests" to be held at the Agricultural University of Georgia, Tbilisi, Georgia. 11-15 July 2017.

Local:

Jukes M.D., Knox C.M., Hill M.P., Moore S.D., 2013. The isolation and genetic characterisation of a novel South African Phthorimaea operculella granulovirus. Oral presentation South African Society of Microbiology conference held at Forever Resorts Warm Baths, Bela-Bela, South Africa. 24-27 November.

Jukes M.D., Knox C.M., Hill M.P., Moore S.D., 2015. Isolation, genetic characterisation and evaluation of biological activity of a novel South African Phthorimaea operculella granulovirus (PhopGV). Oral presentation Congress of the ESSA and ZSSA conference held at Rhodes University, Grahamstown, South Africa. 12-17 July.

Jukes, M.D., Knox, C.M., Hill, M.P., Moore, S.D., Rabalski, L. and Szewczyk, B., 2016. Baculovirus synergism: investigating mixed alphabaculovirus and betabaculovirus infections in the false codling moth, *Thaumatotibia leucotreta*, for improved pest control. Oral presentation at the 9th Citrus Research Symposium conference held at Champagne Sports Resort, Drakensberg, South Africa. 21-25 August.

Articles:

Peer reviewed publications

Jukes, M.D., Knox, C.M., Hill, M.P., Moore, S.D., 2014. The isolation and genetic characterisation of a South African strain of Phthorimaea operculella granulovirus, PhopGV-SA. Virus Res. 183, 85–88. doi:10.1016/j.virusres.2014.01.013. IF 2.526

Jukes, M.D. et al., 2016. The comparative analysis of complete genome sequences from two South African betabaculoviruses: Phthorimaea operculella granulovirus and Plutella xylostella granulovirus. *Archives of Virology*, 161(10), pp.2917–2920. Available at: http://link.springer.com/10.1007/s00705-016-2978-5. IF 2.255

van der Merwe, M., Jukes, M., Rabalski, L., Knox, C., Opoku-Debrah, J., Moore, S., Krejmer-Rabalska, M., Szewczyk, B., Hill, M., 2017. Genome Analysis and Genetic Stability of the Cryptophlebia leucotreta Granulovirus (CrleGV-SA) after 15 Years of Commercial Use as a Biopesticide. Int. J. Mol. Sci. 18, 2327. doi:10.3390/ijms18112327. IF 3.226

Conference Bulletin:

Jukes, M.D., Rabalski, L., Knox, C.M., Hill, M.P., Moore, S.D. and Szewczyk, B., 2017. Baculovirus synergy: mixed Alphabaculovirus and Betabaculovirus infections for the control of *Thaumatotibia leucotreta* in South Africa. IOBC-WPRS Working Group "Microbial and Nematode Control of Invertebrate Pests" bulletin. 129, pp.170-174.

Patents:

Moore, S.D., Hill, M.P., Knox, C.M., Marsberg, T., Jukes, M.D., Szewczyk, B., Rabalski, L. and Chambers, C., 2016. Biological control agent - Genetic Study of sNPV. South African Provisional Patent Application No. 2016/05197

Acknowledgements

I would like to acknowledge the following people for their support and assistance in the completion of this work:

- My supervisor, Prof Caroline Knox, for her advice, support, assistance, and many hours of input over the past few years in helping me complete this study.
- My co-supervisors, Prof Sean Moore and Martin Hill, for the advice, assistance with experiments, and continual encouragement.
- A special thanks to Kate Bryan, for her support, motivation, and continued love.
- The research group at the University of Gdansk and Medical University of Gdansk, Dr Lukasz Rabalski, Martyna Krejmer-Rabalska, Maciej Kosińskiand, and Prof Boguslaw Szewczyk for their assistance, advice, and generosity.
- Dr Candice Coombes and Dr Tamryn Marsberg for their assistance with insect rearing and Wayne Kirkman and Mellissa Peyper for their help with the field trials.
- Marvin Randal and Shirley Pinchuck for their assistance with electron microscopy.
- My lab group for their assistance, advice, and positivity.
- My friends for their support and encouragement.
- My mother, Jill Shirley, and my siblings, Nicola-Ann Knowler and Christopher Jukes, for their support and encouragement, live long and prosper.
- Citrus research international, Rhodes University, the National Research Foundation and River Bioscience for financial and resource support.

Chapter 1

Literature review

1.1. Introduction

The South African agricultural sector is of great importance; it employs tens of thousands of people and generates billions of Rand towards the local economy. According to the South African Department of Agriculture, Forestry and Fisheries (DAFF), the citrus industry contributes significantly towards this sector. The export and local citrus fruit markets generated a gross income of approximately 15 billion Rand (1 billion US Dollar) in the 2016/17 season (DAFF, 2017). However, this industry faces many challenges, including plant diseases and the loss of citrus fruit due to damage caused by insect pests. According to Bedford et al. (1998), the industry is challenged by around 100 different insect pests including locusts, aphids, scale insects, thrips, flies, ants, beetles and moths. Of primary interest to this project is the lepidopteran pest *Thaumatotibia leucotreta* (Meyrick) (Lepidoptera: Tortricidae), more commonly known as the false codling moth (FCM). This pest feeds directly on the citrus fruit causing extensive damage. It also poses a major risk to South African citrus exports due to its classification as a phytosanitary pest in regions to which citrus is exported such as the European Union (EU) and the United States of America (USA) (PPECB, 2017). The challenge to control this pest is further exacerbated by increases in regulation placed on chemical pesticides in the EU and USA and thus limiting available control options (Ansell, 2008; Bielza et al., 2008). This creates a need to develop novel and effective control measures against *T. leucotreta* to ensure the sustainability of this industry. To date, the most effective approach has been through the utilisation of an integrated pest management (IPM) programme, which aims to combine chemical pesticides, cultural practices, biological pesticides, and other control options into a single strategic approach to combat *T. leucotreta* and other pests in this industry (Moore and Hattingh, 2017; Moore, 2017). A major component of this IPM programme is the baculovirus-based biological pesticide (biopesticide) Cryptogran™, which has been successfully used for over 10 years (Moore et al., 2015). However, the recent emergence of resistant *Cydia pomonella* (Linnaeus) (Lepidoptera: Tortricidae) populations in Europe towards another commercial biopesticide, which consists of the baculovirus Cydia pomonella granulovirus (CpGV), intensifies the need to develop and evaluate novel techniques. These could then be

incorporated into IPM programmes in the future to ensure the continuous control of *T. leucotreta* in this important industry in South Africa.

This chapter therefore aims to review the literature related to the host insect: *T. leucotreta.* The control options which are available or under development for use against this pest are presented. Current biological control options, particularly baculovirus-based biopesticides, which are used in the citrus industry will be discussed in greater detail. As a baculovirus biopesticide is currently utilised in the citrus industry, the potential for synergistic effects in mixed baculovirus infections is also reviewed. The chapter concludes with the justification for this study followed by the aims, objectives and a brief outline of the following chapters.

1.2. *Thaumatotibia leucotreta*, a major pest in South African agriculture

1.2.1. Taxonomy and distribution of *T. leucotreta*

The insect pest of interest in this study is the lepidopteran moth *Thaumatotibia leucotreta*, commonly known as the false codling moth. It was first taxonomically described as *Argyroploce leucotreta* (Meyrick) and later revised to *Cryptophlebia leucotreta* by Clarke, (1955). Since then, this species has been reclassified to its current genus *Thaumatotibia* in the family Tortricidae as shown in Table 1.1 (Komai, 1999).

Table 1.1. Taxonomic classification of *Thaumatotibia leucotreta* (Meyrick) (Lepidoptera: Tortricidae).

Taxa	Scientific classification
Kingdom	Animalia
Phylum	Arthropoda
Class	Insecta
Order	Lepidoptera
Family	Tortricidae
Genus	*Thaumatotibia*
Species	*T. leucotreta*
Binomial name	*Thaumatotibia leucotreta* (Meyrick, 1912)

The distribution of *T. leucotreta* is primarily within sub-Saharan Africa in the countries Angola, Burkina Faso, Burundi, Cameroon, Cape Verde Islands, Congo, Eritrea, Ethiopia, Gambia, Ghana, Ivory Coast, Kenya, Madagascar, Malawi, Mali, Mozambique, Niger, Nigeria, Rwanda, Senegal, Sierra Leone, Somalia, South Africa, Sudan, Swaziland, Tanzania, Togo, Uganda, Zambia and Zimbabwe (Figure 1.1). Other countries where *T. leucotreta* is found

which are not shown in this map include Israel, Mauritius, Réunion and Saint Helena (Stibick, 2007).

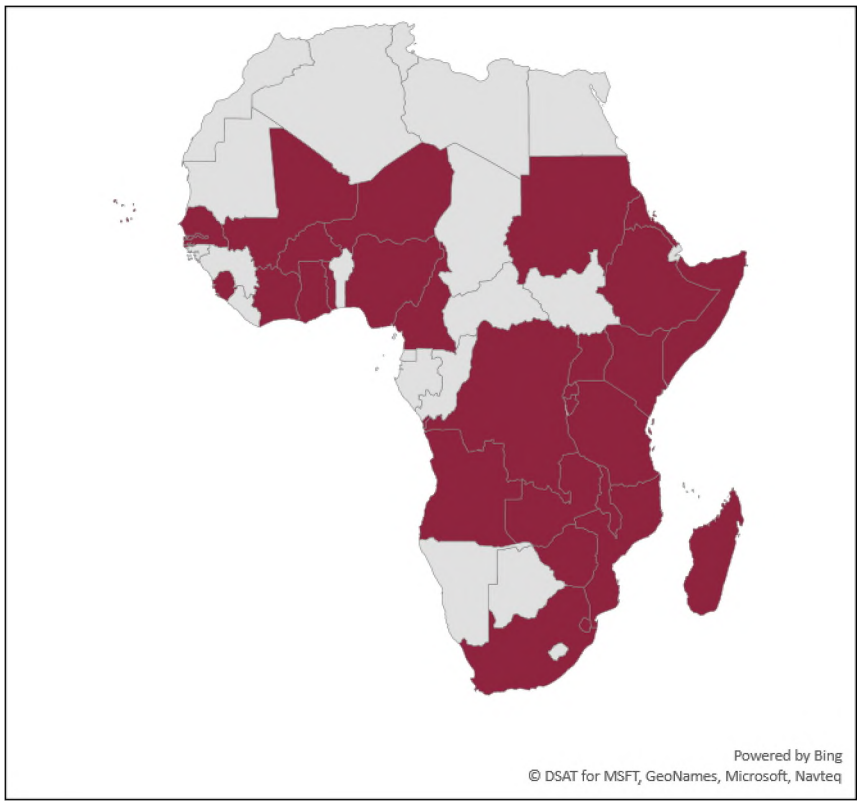

Figure 1.1. Geographic distribution of *Thaumatotibia leucotreta* across the African continent shown in maroon (Stibick, 2007).

Importantly, the distribution of *T. leucotreta* does not include Europe, North America or Asia. However, data collected by the Global Biodiversity Information Facility indicates three separate occurrences of *T. leucotreta* in Europe: twice in the United Kingdom, and once in Belgium (BRERC, 2017; Butterfly Conservation, 2017; Vanreuse et al., 2017). While the identification of individual moths does not necessarily confirm the establishment of *T. leucotreta* in Europe, it is of concern that this pest could further invade and become a significant risk to agricultural industries in this region (EPPO, 2013). Similarly, the introduction of *T. leucotreta* into North America has been evaluated with research showing that this region offers large areas in which the environment is suitable for the pest to become established (Stibick, 2007; Venette et al., 2003). A single occurrence of *T. leucotreta* was reported in California, whereby a single male moth was caught and identified during large scale surveillance programmes using pheromone traps. However, follow-up surveys were unsuccessful in identifying additional individuals (Gilligan et al., 2011). These incidences of *T. leucotreta* and

the potential of future expansion of this pest into these regions has resulted in this insect being classified as a significant phytosanitary risk (European Commission, 2017; Stibick, 2007).

1.2.2. **Host range and economic importance**

Given the large distribution of *T. leucotreta* and its classification as a phytosanitary risk, it is important to consider the host range on which this pest feeds. This pest has been identified to have a broad host range including many wild plants and economically import crops (EPPO, 2013; Stibick, 2007; Venette et al., 2003). A summarised list of cultivated plants that are agriculturally and economically important and which form part of the host range for *T. leucotreta* are shown in Table 1.2.

Table 1.2. Cultivated host plants of *T. leucotreta* (EPPO, 2013).

Scientific Name	Common Name
Capsicum spp.	Pepper
Citrus spp.	Orange
Gossypium spp.	Cotton
Litchi chinensis	Litchi
Macadamia spp.	Macadamia
Mangifera indica	Mango
Persea americana	Avocado
Prunus spp.	Apricot/Peach
Psidium guajava	Guava
Punica granatum	Pomegranate
Solanum melongena	Eggplant
Vitis spp.	Grape
Zea mays	Corn

Thaumatotibia leucotreta affects a wide range of cultivated plants and can have considerable economic impact due to the damage it causes (Table 1.2). Of these cultivated plants, several are listed as important fresh produce industries in South Africa, including peaches, apricots, grapes, pomegranates, oranges, mandarins, guavas, and litchis, together contributing approximately R1 billion to local markets (DAFF, 2017).

Citrus is produced in the Limpopo, Eastern Cape, Western Cape, Mpumalanga, Kwazulu-Natal, Northern Cape, and North West provinces of South Africa, with the former having the largest farming areas as shown in Figure 1.2 (CGA, 2017). Approximately 1.7 megaton of citrus was exported in the 2015/16 season to Europe, the Middle East, Asia, the Russian Federation and North America (DAFF, 2016; PPECB, 2017). A major risk to the South African

citrus export industry to these regions is the interception of exported fruit which is contaminated with restricted organisms that pose a phytosanitary risk (PPECB, 2017). With the inclusion of *T. leucotreta* as a phytosanitary risk in the EU (European Commision, 2017), the interception of infested fruit is more likely to have a significant economic impact on the citrus export industry.

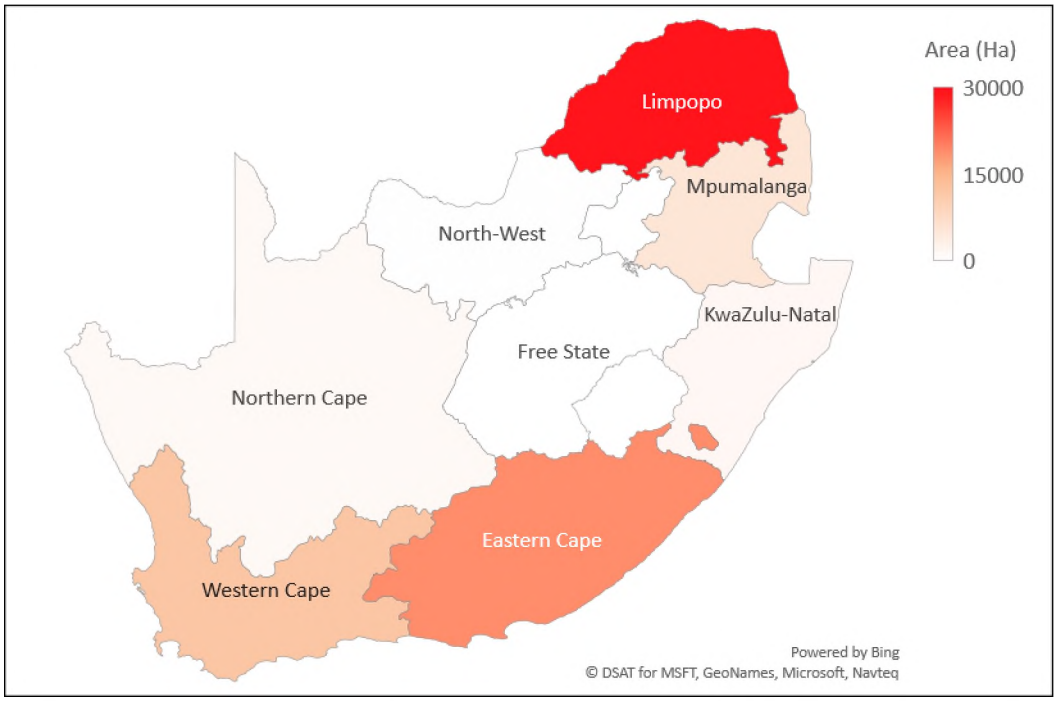

Figure 1.2. Citrus producing area (Ha) for each province in South Africa (CGA, 2017).

1.2.3. **The life cycle of *T. leucotreta***

The life cycle of *T. leucotreta* begins with the laying of eggs by a fertile moth, usually on the surface of a host plant primarily on the citrus fruit. These eggs continue to develop and after a few days neonate larvae emerge and begin to feed upon the fruit of the host plant. Once fully developed, larvae drop and burrow into the upper layers of the surrounding soil to pupate. Adult moths eclose from these pupae. The subsequent mating of male and female moths enables the cycle to begin again with the laying of eggs. Each stage of the *T. leucotreta* life cycle is described in greater detail below and is shown in Figure 1.3.

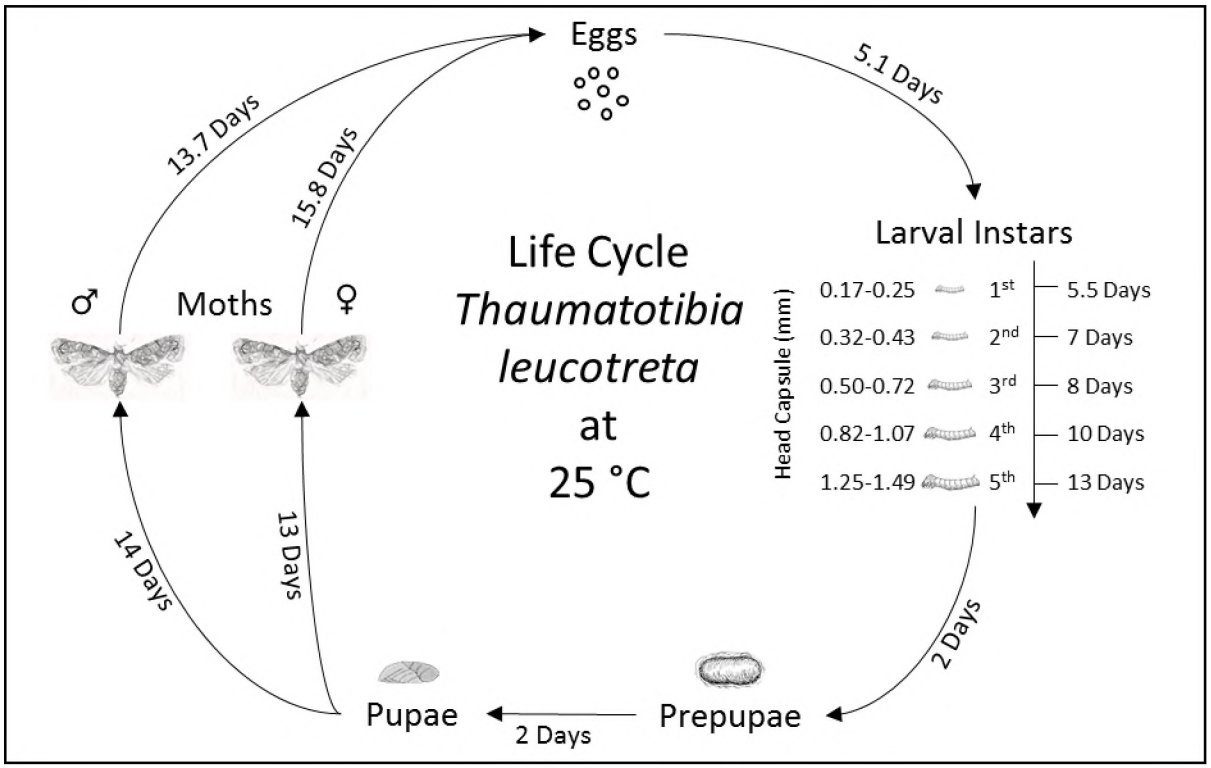

Figure 1.3. The life cycle of *Thaumatotibia leucotreta* at 25 °C showing the duration of each stage of development (Daiber, 1980, 1979a, 1979b, 1979c).

The biology of the *T. leucotreta* egg was first described by Daiber, (1979a). The eggs are cream-coloured with an oval-shape and have a length of 0.77 ± <0.001 mm and a width of 0.6 ± <0.001 mm. Female moths lay between 100 and 250 eggs with developmental times varying depending on environmental temperature and humidity. Higher humidity was found to increase the percentage of eggs which hatch. Temperatures between 20 and 30 °C resulted in egg-hatching rates of between 10 and 3 days respectively. Additionally, a lower threshold temperature between 11.7 to 11.9 °C was identified to be a range at which most of the examined eggs did not develop. Once eggs fully develop, neonate *T. leucotreta* larvae hatch and begin to feed. Depending on temperature and nutrition, larvae can take between 56 and 13 days to develop in temperature ranges of between 15 and 25 °C respectively (Daiber, 1979c). *Thaumatotibia leucotreta* undergoes five instars as shown in Figure 1.3, each of which can be determined by measurement of the head capsule width (Hofmeyr et al., 2016). Once fully developed, *T. leucotreta* larvae exit the infested host and drop to the ground, burrowing a few centimetres into the soil to spin cocoons and pupate.

The final stage of development for *T. leucotreta* is the adult moth. The life span of the adult has also been shown to be temperature dependent. The duration of development decreases from 24.5 and 34.5 days at 10 °C to 13.7 and 15.8 days at 25 °C for male and female moths

respectively (Daiber, 1980). It was also reported that the duration until oviposition of female moths increased with decreasing temperature from 6 days at 25 °C to 23 days at 10 °C. Conversely, the average number of eggs per female moth decreased with decreasing temperature from 456 eggs at 25 °C to less than 1 at 10 °C. It is important to note that the duration of development in variable environments, with similar average temperatures to the constant environments, were observed to differ. For example, the lower threshold for egg development was calculated at 11.7-11.9 °C. However, in variable environments with similar average temperatures, development was observed to increase beyond what was expected for this threshold (Daiber, 1979b). Similarly, female moths were observed to lay more eggs in variable environments than was observed in the corresponding constant environments with the same average temperature (Daiber, 1980). This data shows that observations made at constant temperatures can differ from the corresponding average temperature of variable environments as would be observed under natural conditions.

The final aspect of the *T. leucotreta* life cycle is the number of generations which occur annually. As reported above, the duration of each life stage can vary considerably which results in between six and eight generations per year in South Africa (Daiber, 1980; Stofberg, 1954). The number of eggs laid per individual female moth, the duration of larval development, and the number of generations per year enable *T. leucotreta* to be a major pest on many economically important crops in South Africa.

1.2.4. **Control options for *T. leucotreta***

The control of *T. leucotreta* in South Africa utilises an IPM programme, which was defined by Bajwa and Kogan, (2002) as a system which assists in selection of pest control tactics either individually or in a coordinated approach. This results in an ideal cost/benefit situation when considering the producers, society, and the environment. As such, an IPM programme for the control of *T. leucotreta* strategically combines chemical and biological options along with cultural practices, mating disruption, and sterile insect technique among others to achieve high levels of pest control (Moore and Hattingh, 2017) (Figure 1.4). The combination of these control options into a single programme has been calculated to have a combined efficacy of around 97 % (Moore et al., 2015).

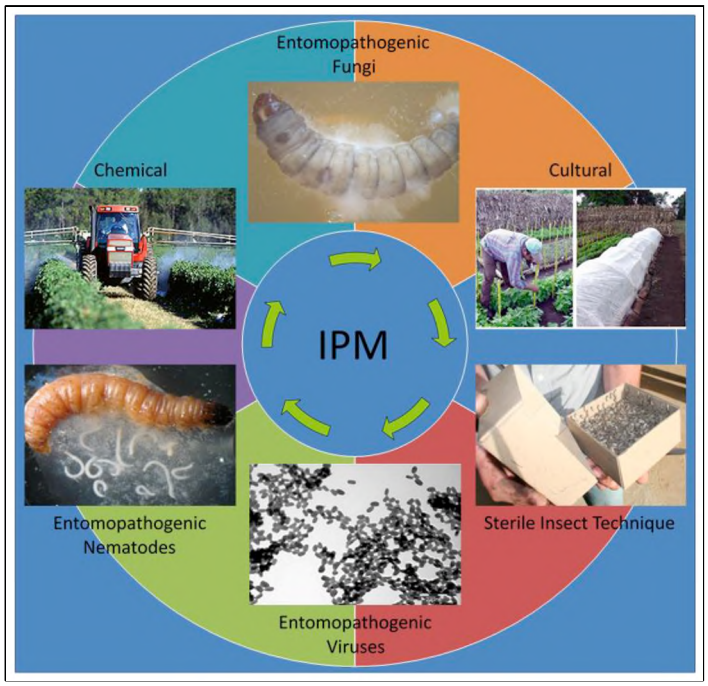

Figure 1.4. Integrated pest management (IPM) programmes against *T. leucotreta* utilise chemical pesticides, cultural practices, sterile insect technique, entomopathogenic nematodes, fungi and viruses in a strategic manner.

Several chemical products have been registered and are used to control *T. leucotreta* in citrus. These include, but are not limited to, two chitin synthesis inhibitors, Alsystin® (Bayer CropScience Pty Ltd, Germany) and Nomolt® (BASF, Germany), two pyrethroids Cypermethrin (Efekto, South Africa) and Meothrin (Philagro, South Africa), a spinosyn registered as Delegate (Dow AgroSciences, USA), another with anthranilic diamide named Coragen (DuPont, USA), and an insect growth regulator containing methoxyfenozide formulated as the product Runner (Dow AgroSciences, USA) (Moore and Hattingh, 2012; Moore, 2017).

While chemical pesticides have been shown to achieve high levels of *T. leucotreta* control, increased regulation has seen a dramatic decrease in the number of chemistries which can currently be used (Ansell, 2008; Bielza et al., 2008). As such, several alternative methods have been developed to maintain high levels of control. The first example of this is the sterile insect technique (SIT), which has been used in South Africa for several years to reduce levels of *T. leucotreta* infestation in the field. This method utilises mass-reared adult moths which are gamma irradiated resulting in sterile insects. These moths are then transported and aerially released over target crops where they unsuccessfully mate (Carpenter et al., 2007). Cultural practices are also an important part of IPM programmes. An example of this is orchard sanitation which is a primary form of *T. leucotreta* control. This involves the clearing of fallen

fruit which could be infested as well as the removal of infested and injured fruit still hanging on trees which would attract moth oviposition (Newton, 1989). Simple practices such as this can have significant effects in the reduction of *T. leucotreta* levels in the field. A third example of an alternative control method is that of mating disruption programmes. These utilise synthetic pheromones to disorientate the adult moths during their mating period. Four pheromone based mating disruption products are registered for use against *T. leucotreta* in South Africa namely Checkmate FCM-F (Chempak, South Africa), Isomate FCM (Nulandis, South Africa), Splat-FCM (River Bioscience, South Africa), and Last Call™ FCM (Insect Science, South Africa) (Moore and Hattingh, 2012; Moore, 2017).

There are also several biological control options which have been or are being developed to control *T. leucotreta* in South Africa (Coombes et al., 2016; Knox et al., 2015; Malan et al., 2011; S. Moore et al., 2004; Zimba et al., 2016). These include entomopathogenic nematodes (EPN), entomopathogenic fungi (EPF), viruses, and parasitoids. EPNs and EPFs have been studied due to their ability to target the soil-associated life stages of *T. leucotreta*, these being the fifth instar larvae and pupae. They also have a major advantage over chemical methods as EPN and EPF control agents can target the cryptic life stages of *T. leucotreta*, either within infested fruit or larvae which have burrowed into the upper layer of soil to pupate. Both EPNs and EPFs have been tested and shown to be effective in the field. Studies have also been conducted to bio-prospect and evaluate South African species of nematode against *T. leucotreta* (Malan et al., 2011; Steyn et al., 2017). These studies have identified several EPNs which are highly virulent against fifth instar larvae and pupae. Additionally, emerging moths were shown to be infected with these EPNs which not only improved control but also enhanced the distribution of the control agent post application. An EPN based product, CryptoNem (River Bioscience, South Africa), has been developed and registered for use in the control of the soil-associated life stages of *T. leucotreta* in South Africa. Several EPF isolates have also been evaluated against *T. leucotreta,* both in laboratory and field settings (Coombes et al., 2017, 2016, 2013). These isolates have shown enormous potential in the field and warrant further investigation and possible development into commercial products. The EPF, *Beauveria bassiana,* has been formulated and registered as the products Broadband™ (BASF, Germany) and Eco-Bb (Plant Health Products, South Africa) for use in South Africa. These products consist of concentrated spores which are diluted and sprayed onto crops for the control of pests such as *Plutella xylostella* (Linnaeus) (Lepidoptera: Plutellidae), *Phthorimaea operculella* (Zeller) (Lepidoptera: Gelechiidae), and *T. leucotreta* among others.

A major component of IPM programmes, and of significant importance to this project, is the use of viruses in the control of *T. leucotreta* in South Africa. The betabaculovirus Cryptophlebia leucotreta GV (CrleGV) has been successfully developed into commercial products including Cryptex® (Andermatt, Switzerland) and Cryptogran™ (River BioScience, South Africa). These are registered for use in South Africa against *T. leucotreta* (S. Moore et al., 2004; Moore, 2017). The product Cryptogran™ is formulated with a naturally occurring endemic isolate of this virus which can infect the larval stages of *T. leucotreta*, enabling control of the life stage responsible for damaging fruit (S. Moore et al., 2004). This also reduces the environmental impact due to decreased use of chemical pesticides which may have a broader spectrum, potentially killing natural pest enemies and beneficial insects or having unwanted toxic residues. A review of field trials conducted with CrleGV products over more than 10 years of continuous commercial use in South Africa concluded that these biopesticides were at least as effective as their chemical counterparts and could be utilised within pre-existing IPM programmes offering increased control over *T. leucotreta* (Moore et al., 2015). There is also recent evidence that Cryptogran™ may supress *Cryptophlebia peltastica* (Meyrick) in the field, however, these results are preliminary and have not yet been published (C. Hendriks pers. comm). Samples collected in 2000 and 2015 of the CrleGV isolate used in the production of Cryptogran™ were used to evaluate the virulence (severity of disease caused by the virus) and genome stability of this virus over a 15-year period (Thomas and Elkinton, 2004; van der Merwe et al., 2017). It was found that the virus genome was highly stable over this period with only a few single nucleotide polymorphisms identified within open reading frames (ORFs). Additionally, the biological activity was found to have remained relatively consistent over this period indicating that the virus continues to be highly effective for use against *T. leucotreta* in the field (van der Merwe et al., 2017).

While there are many existing options in use for the control of *T. leucotreta*, continued development of novel biopesticides is essential in ensuring this pest can be adequately managed in the future. Only one baculovirus is currently known to infect *T. leucotreta* and, although several novel isolates of this virus have been identified and characterised (Opoku-Debrah et al., 2014), it is important to continue bioprospecting for novel isolates and species which can be used against this pest. Such isolates or species could be further developed which would potentially result in additional biopesticides that can be incorporated into IPM programmes.

1.3. Baculoviruses and their role as biological control agents

Baculoviruses are a large family of double-stranded DNA viruses which infect several arthropod species. Many of these are pests in the agricultural industry while others are themselves economically important (reviewed by Harrison and Hoover, 2011). The first identification of a baculovirus induced infection was in *Bombyx mori* (Linnaeus) (Lepidoptera: Bombycidae), due to its use in the production of silk and hence, its economic importance. The pathology of the infection, which results in the liquefaction of the host, was studied in greater detail and named jaundice (Nysten, 1808). Subsequently, the causative agent of jaundice was identified and allowed for the continued study of baculoviruses. More recently, baculoviruses have been extensively exploited with success as biological pesticides in the control of pests in the agricultural industry. Their use in this economically important industry and the application of baculoviruses in the biotechnology field has led to significant research and advancement into understanding their biology, genetics and life cycle (Haase et al., 2015; Moscardi et al., 2011; Rohrmann, 2013).

1.3.1. Taxonomy and nomenclature

Historically the family *Baculoviridae* consisted of two genera, the nucleopolyhedroviruses (NPVs) and granuloviruses (GVs), with these classifications based on morphological structure. More recently, genetic classification using estimates of evolutionary distances and phylogenetic analysis based on alignments of concatenated *lef*-8, *lef*-9 and *polh* nucleotide sequences of members in the family resulted in the formation of four genera shown in Table 1.3 (Jehle et al., 2006; Lauzon et al., 2004). The first of the revised genera, is the Alphabaculoviruses, all of which are NPVs that infect lepidopteran species. This genus is further divided into two groups, 1 and 2, with the first group consisting of two clades A and B. The *Betabaculovirus* genus comprises all GVs which specifically infect lepidopteran species. The last two genera in the family *Baculoviridae*, the Gammabaculoviruses and Deltabaculoviruses, comprise the remaining NPVs each of which infect hymenopteran and dipteran hosts respectively. To date, 71 baculovirus genomes have been sequenced from these four genera and are present on GenBank (NCBI, USA). Many of them have found their way into commercial applications, some of which are discussed in Section 1.3.5.

Table 1.3. Taxonomic classification of baculoviruses (Jehle et al., 2006)

Genera	Type species	Host
Alphabaculovirus	Autographica californica multiple NPV	Lepidopteran
Betabaculovirus	Cydia pomonella GV	Lepidopteran
Gammabaculovirus	Neodiprion lecontei NPV	Hymenopteran
Deltabaculovirus	Culex nigripalpus NPV	Dipteran

The nomenclature used for baculoviruses is typically based upon the first host from which it was isolated. This created several complications whereby the same baculovirus could be isolated independently from two separate hosts and subsequently received two different names (Lange et al., 2004). The system for abbreviating the names of baculoviruses is based on the binominal name of the host species and uses the first letter of the host genus name followed by the first letter of the species epithet combined with either GV or NPV depending on the virus. For example, the NPV isolated from *Autographica californica* was named Autographica californica MNPV and abbreviated as AcMNPV. However, this also presented problems with the potential for identical virus abbreviations being created (Rohrmann, 2013). To overcome these challenges, a system for the classification of a baculovirus as a new or existing species was developed based primarily on phylogenetic analysis combined with genomic composition, morphological, and pathological traits (Jehle et al., 2006; Lange et al., 2004; Lauzon et al., 2004). Furthermore, the abbreviations used for new baculoviruses would comprise both the first two letters of the host genus and species combined with either NPV or GV depending on the virus. For example, Cryptophlebia leucotreta GV would be referred to as CrleGV (Rohrmann, 2013). However, due to the extensive use of older abbreviations, such as AcMNPV, Lymantria dispar MNPV (LdMNPV), and CpGV, the use of two letters was maintained for these viruses alone while the new approach was only adopted for novel isolates.

1.3.2. **Baculovirus morphology**

The morphology of baculovirus particles is closely tied to the life cycle of the virus with occluded and budded virions observed. Baculoviruses consist of an occluded virion which is encapsulated in a protein matrix which form the common occlusion body (OB) morphology. OBs are often grouped into two major divisions: these are either granular (GV) and polyhedral (NPV) shaped (Rohrmann, 2013). These comprise of occlusion-derived virions (ODVs) which are enveloped particles consisting of either one or multiple rod shaped nucleocapsid/s which

each contain the viral genomic DNA (gDNA) (Figure 1.5A). For both GV and NPV OBs, ODVs are occluded within the major structural protein matrix and comprise either the granulin or polyhedrin protein respectively (Rohrmann, 2013). NPV OBs contain multiple ODVs with these having either a single nucleocapsid or multiple nucleocapsids, which are referred to as single-NPV (SNPV) or multiple-NPV (MNPV) respectively (Figure 1.5C) (Rohrmann, 2014). Granulovirus OBs each comprise of a single ODV containing one nucleocapsid (Figure 1.5D). OBs are essential in the horizontal transfer of baculoviruses in the environment and this morphology is exploited for use in the field of biological control.

The second morphology observed in baculoviruses is the budded virion. Budded virions differ from OBs in that the nucleocapsids acquire their envelope during egress from infected cell which contain several trans-membrane proteins such as gp64 or the F-protein (Figure 1.5B) (Wang et al. 2016). Budded virions are not occluded and instead enable the systemic spread of the virus within an infected host.

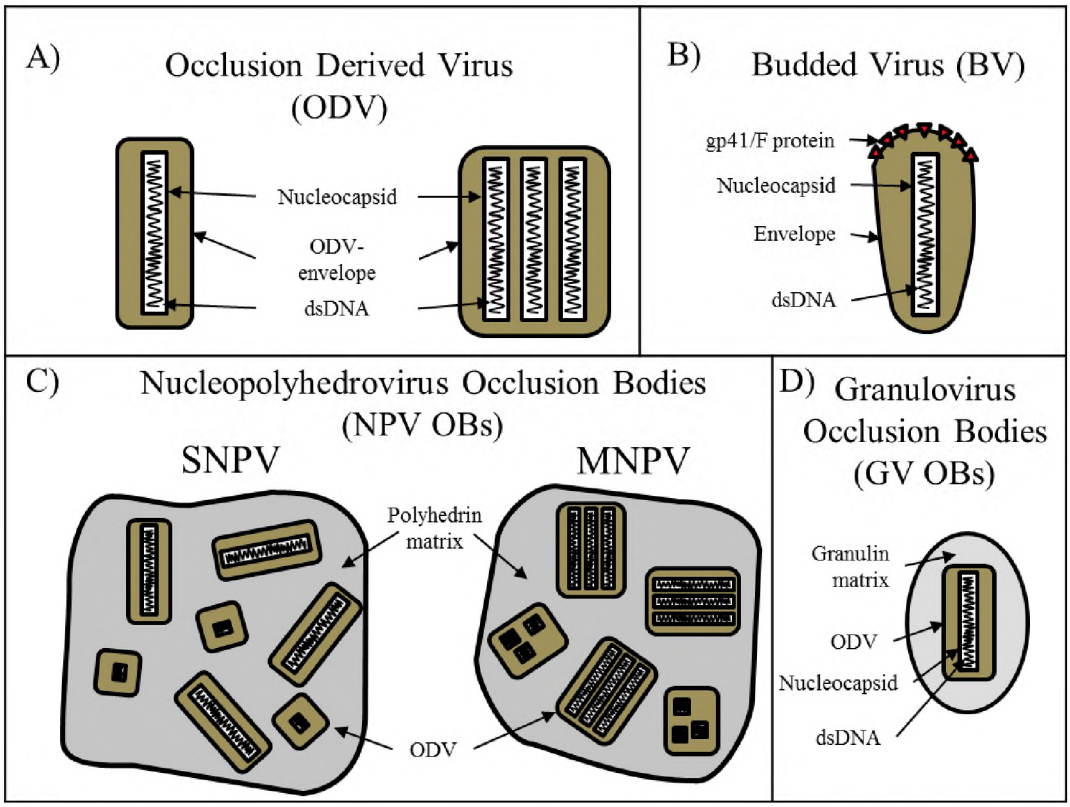

Figure 1.5. Diagram of the baculovirus morphology showing the A) occlusion derived virion, B) budded virus, C) nucleopolyhedrovirus occlusion bodies and D) granulovirus occlusion bodies

The size and shape of baculovirus OBs varies significantly, not only between NPV and GV particles, but also between species. GV OBs are ovoid in shape, ranging in size from 0.2-0.4

μM, while NPV OBs are larger ranging in size from 0.6-2 μM in diameter and having an irregular shape (Rohrmann, 2013). NPVs with unusual OB shapes have also been described. For example, tetrahedral particles with an average size of 1.5 μM were described by Senthil Kumar et al. (2015). The budded virion enables baculoviruses to effectively replicate within a host while OBs allow the spreading of the virus to new hosts in an environment. The role of each in the viral life cycle is described in the following section.

1.3.3. **Life cycle and transmission of baculoviruses**

The life cycle of baculoviruses comprises two stages: primary and secondary infection (Figure 1.6), which are extensively reviewed by Rohrmann, (2013), Friesen, (2007), Possee et al. (2010) and Harrison and Hoover, (2012). The primary infection process begins with the ingestion of OBs by a larva feeding on contaminated food sources (Figure 1.6A). Once OBs enter the midgut, the crystalline lattice surrounding the ODV/s begins to break away due to the high alkalinity present. The released ODVs penetrate the peritrophic membrane (PM) to reach and infect the midgut epithelial cells (Figure 1.6B). Some baculoviruses utilise additional protein factors such as enhancins to damage and degrade the PM. This assists the ODV entry into the midgut epithelial cells. Entry into the midgut epithelial cells is achieved by fusion of the ODV envelope to the host cell plasma membrane. The ODV envelope also contains *per os* infectivity factors (PIFs) which are required for binding and fusion to occur. Successful entry of ODVs results in the release of the viral nucleocapsids into the cytoplasm. These travel to the nucleus where virus replication is initiated (Figure 1.6C).

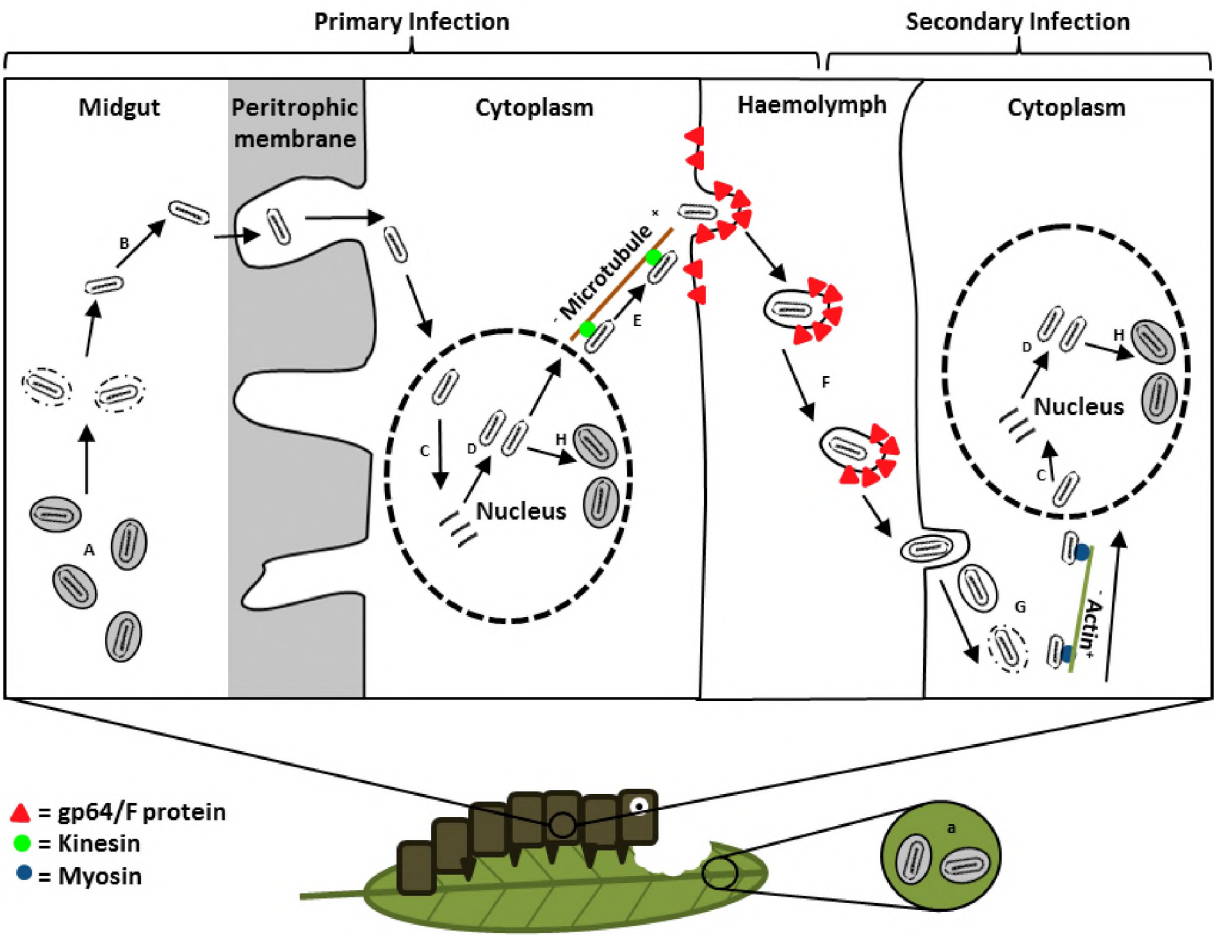

Figure 1.6. Diagram of the baculovirus primary and secondary infection cycles showing the transmission route through an infected host (adapted from Possee et al., 2010).

Following entry of the nucleocapsids into the nucleus, viral DNA is uncoated which enables the expression of genes. Gene expression is temporally regulated by specific promoters, with different stages such as early (immediate early and early) and late (late and very late) identified. Early genes are transcribed by host RNA polymerase II while late and very late genes are transcribed by a viral RNA polymerase. The expression of these genes initiates the production of replication proteins, structural proteins, transcription proteins, and proteins involved in virion assembly (Figure 1.6D). With the replication of viral DNA and production of structural proteins occurring, nucleocapsids begin to assemble before exiting the nucleus via pores in the nuclear membrane to travel to the plasma membrane. Here the nucleocapsids bud through the plasma membrane which now contains viral proteins resulting in the budded virions (Figure 1.6E). The budded virions proceed to spread infection to other cells and tissues in the host causing a systemic infection. Entry into these cells in achieved through endocytosis of the budded virions, after which the membrane fuses with the endosomal membrane allowing release of the nucleocapsid into the cytoplasm (Figure 1.6F and G). These nucleocapsids move

to the nucleus, release the viral genomic DNA and begin replication in the same manner as described for those in the midgut epithelial cells.

Systemically infected cells begin to produce nucleocapsids which receive an envelope, and associated envelope proteins, while in the infected nuclei forming ODVs. These ODVs are then occluded in the major structural protein, either granulin or polyhedrin for granuloviruses and nucleopolyhedroviruses respectively producing viable OBs (Figure 1.6H). Once virus replication is complete, host lysis occurs which results in liquification of the infected larvae. This releases OBs into the environment. The OBs can then be ingested by another host enabling the infection process to begin again. The life cycle of baculoviruses makes them ideal candidates for biological pesticides as the process not only kills the target pest, but also results in the production of additional virus particles which can lead to secondary infections in the field.

1.3.4. **Baculovirus genetics**

Baculoviruses are double-stranded DNA viruses with genomes ranging between 80,000 bp and 180,000 bp. Gammabaculoviruses have been identified to have the smallest genomes which encode for approximately 120 genes while larger alpha and betabaculovirus genomes have been identified to encode more than 180 genes (Rohrmann, 2013). Baculovirus genes are characterised into several functional groups including replication, transcription, and structural. While there is considerable variation in the gene content of baculoviruses, all sequenced genomes have been determined to contain a set of 37 conserved genes referred to as core genes (Table 1.4) (Garavaglia et al., 2012; Rohrmann, 2013). An additional set of 25 lepidopteran-conserved genes have also been identified to be present in all alpha and betabaculoviruses as well as in some gammabaculoviruses (Rohrmann, 2013).

Table 1.4. Core genes present in all baculovirus genomes by functional group (Rohrmann, 2013)

Transcription	Late expression factor 4	**Replication**	Alkaline nuclease	**Structural**	Ac66
	Late expression factor 5		DNA helicase		Ac109
	Late expression factor 8		DNA polymerase		Ac142
	Late expression factor 9		Late expression factor 1		Ac144
	P47		Late expression factor 2		Gp41
	Very late factor 1	**Auxiliary**	38k phosphatase		ODV– envelope 18
ODV structure	*Per os* infectivity factor 0		Sulfhydryl oxidase		ODV– envelope 25
	Per os infectivity factor 1		Ubiquitin		P6.9
	Per os infectivity factor 2	**Unknown Function**	Ac78		Vp39 capsid
	Per os infectivity factor 3		Ac81		Vp91
	Per os infectivity factor 4		Ac93		Vp1054
	Per os infectivity factor 5		Ac101		
	Per os infectivity factor 6		Ac103		

In addition to the core and lepidopteran-conserved genes, many others have also been of great interest, particularly those which have an impact on virulence or speed of kill. A study by Serrano et al. (2015) investigated the effect that several Spodoptera exigua NPV genes had on pathogenicity and speed of kill in *Spodoptera exigua* larvae. Six genes, *se4*, *se5*, *se28*, *se76*, *se87*, and *se129*, were studied by generating knockout mutants. Deletion of *se28* was observed to increase pathogenicity while the deletion of *se4*, *se5*, and *se76* resulted in a decrease. Another gene which has been a subject of interest is *ecdysteroid uridine 5′-diphosphate - glucosyltransferase* (*egt*) which encodes for a protein that has been shown to prolong feeding as well as the duration between larval instars in infected insects. Experiments involving the deletion of this gene have shown an increase in the speed of kill and may have implications for improved biological control (Bianchi et al., 2000; Chen et al., 2000; Cory et al., 2004; Hoover et al., 2011; Katsuma and Shimada, 2015; Pinedo et al., 2003). The continued discovery of genes involved in virulence and speed of kill will assist in the identification of which baculovirus isolates may be ideal candidates for use in biological control.

1.3.5. **Development of baculovirus biological control**

1.3.5.1. **Baculovirus based biopesticides**

Baculovirus-based biopesticides have been developed and used in the agricultural industry since the 1960s in many countries to control a wide variety of important lepidopteran pests (Haase et al., 2015; Moscardi, 1999; Moscardi et al., 2011). More recently, South Africa has begun to have an increasing role in the continued use and development of novel baculovirus-based biopesticides (Knox et al., 2015). The success of baculoviruses as biopesticides has led to the development of several commercial products, listed in Table 1.5, which have been successfully utilised across the globe.

Table 1.5. Examples of baculoviruses developed into commercial biological pesticides for the control of lepidopteran pests (adapted from Moscardi et al., 2011; Sahayaraj, 2014).

Baculovirus	Product	Host Insect	Reference
AdorNPV	Capex® 2	*Adoxophyes orana*	Cunningham, 1995; Erlandson, 2008
AngeMNPV	Baculovirus Nitral, Coopervirus, Baculovirus AEE	*Anticarsia gemmatalis*	Moscardi, 2007, 1999
CpGV	Madex®, VirosoftCP4®, Carpovirusine®, Cyd-X®	*Cydia pomonella*	Provost et al., 2015; Vincent et al., 2007
CrleGV	Cryptogran™, Cryptex®	*Thaumatotibia leucotreta*	Moore et al., 2004, 2015
HearNPV	Helicovir™, Bolldex®	*Helicoverpa armigera*	Moore and Kirkman, 2010
LdNPV	Gypcheck®	*Lymantria dispar*	Erlandson, 2008
NeleNPV	Lecontvirus®	*Neodiprion lecontei*	Erlandson, 2008
NeseNPV	Neocheck-S®, Virox®	*Neodiprion sertifer*	Erlandson, 2008
PhopGV	PTM Baculovirus, Matapol®	*Phthorimaea operculella*	Moscardi, 1999; Sosa Gómez et al., 2008
SpexNPV	Spod-X, Ness-A, Ness-E	*Spodoptera exigua*	Erlandson, 2008

AdorNPV - Adoxophyes orana NPV, AngeMNPV - Anticarsia gemmatalis MNPV, CpGV - Cydia pomonella GV, HearNPV - Helicoverpa armigera NPV, CrleGV - Cryptophlebia leucotreta GV, LdNPV - Lymantria dispar NPV; NeleNPV - Neodiprion lecontei NPV, NeseNPV - Neodiprion sertifer NPV, PhopGV Phthorimaea operculella GV, SpexNPV - Spodoptera exigua NPV.

While there are many more commercially formulated biopesticides than are shown in Table 1.5, some of those listed have been extensively used. This includes CpGV and CrleGV, each of which have demonstrated the efficacy of baculovirus-based biopesticides. For example, *C. pomonella* is a major pest in European apple orchards and as such has had several baculovirus-based biopesticides developed against it. The use of CpGV was reviewed by Lacey et al., (2008) with regards to the specificity, production, application, and use in IPM programmes among other aspects of the virus. It was shown to infect many agriculturally important pests such as *C. pomonella*, *Grapholita molesta* (Busck) (Lepidoptera: Tortricidae), *Cydia nigricana* (Fabricius) (Lepidoptera: Tortricidae), and *T. leucotreta* among others while importantly not affecting beneficial insects such as honeybees. This degree of specificity makes baculoviruses an ideal control method compared to some chemical pesticides. The chemical pesticides may have detrimental effects on naturally occurring species that may be natural enemies of other non-target insects and so potentially result in increased levels of secondary pests (Arthurs et al., 2007). Due to its ability to effectively control *C. pomonella*, CpGV has been applied in field trials and/or commercially in North America, Argentina, Australia, New Zealand, Europe, Israel, and South Africa (Lacey et al., 2008).

CpGV, Helicoverpa armigera NPV (HearNPV), and CrleGV have been developed into commercial products and/or utilised in South Africa to control *C. pomonella*, *Helicoverpa armigera* (Hübner) (Lepidoptera: Noctuidae), and *T. leucotreta* respectively (Knox et al., 2015). A strong example of a baculovirus proving to be highly effective is that of CrleGV against *T. leucotreta* in South Africa. This baculovirus was developed into two biological pesticides and has been utilised in South Africa for over 10 years (Moore et al., 2015; Moore and Kirkman, 2010). In a review by Moore et al., (2015) it was reported that across several field trials of CrleGV, *T. leucotreta* infestation levels were reduced by an average of 72 %. Like CpGV, it was also noted that the effects of the biopesticide on non-target insects was insignificant along with several naturally occurring enemies of citrus pests remaining unaffected.

While many baculoviruses have been successfully developed into commercial biopesticides, there remain several challenges and limitations which require further research and development.

1.3.5.2. **Challenges encountered in the development of baculovirus biopesticides**

There are many challenges and limitations encountered in the development and application of baculoviruses. These include ultraviolet (UV) susceptibility, development of resistance in targeted hosts, the speed of kill, and virulence.

UV susceptibility of baculovirus particles has been the focus of some studies due to the rapid inactivation of virions when exposed to UV radiation (Arthurs et al., 2008; Shapiro, 1995). This is a major challenge for commercial baculovirus products, which will decrease in efficacy the longer they are exposed to environmental UV radiation in the field. To overcome this challenge, studies have investigated the use of nano-zinc oxide-binding peptides on the surface of OBs which improved UV resistance (Li et al., 2015). Another study investigated the protein Bm65 from the baculovirus Bombyx mori NPV (BmNPV) (Tang et al., 2015). Overexpression of the Bm65 protein decreased the rate of particle inactivation following UV radiation. Here, the authors suggest that the protein may be involved with the repair of DNA damaged by UV exposure.

Another potential challenge in the baculovirus biopesticide industry is the potential for resistance in target insects towards commercial products to develop. Currently, only one example of resistance development has been observed. European populations of *C. pomonella* showed decreased susceptibility towards a commercially formulated baculovirus CpGV that was isolated in Mexico (CpGV-M) (Asser-Kaiser et al., 2007). The discovery of resistance in *C. pomonella* populations to CpGV-M led to the isolation and characterisation of novel CpGV isolates. These have since been used to manage the resistant populations (Eberle et al., 2008). Furthermore, these studies have also identified the locus involved with the resistance development in *C. pomonella* and the associated genetic differences in the isolates which could overcome this resistance (Asser-Kaiser et al., 2011, 2010; Eberle, 2010; Eberle and Jehle, 2006; Gebhardt et al., 2014).

Studies have also investigated whether resistance towards baculoviruses could be generated in a laboratory setting by repeatedly exposing insect hosts to the same virus. In doing so, researchers could better understand the rate at which resistance might occur in natural populations. Nakai et al. (2017) performed a series of experiments exposing more than 150 generations of the smaller tea tortrix, *Adoxophyes honmai* (Yasuda) (Lepidoptera: Tortricidae), neonate larvae to Adoxophyes honmai NPV (AdhoNPV) OBs. A significant decrease in virulence was observed by the 3rd generation and continued to a point where a resistance ratio

of 550 was observed by generation 26. By generation 153, a survival rate of 94-100 % was recorded at the highest achievable dose of OBs. Comparing this against two susceptible host strains indicated a 400,000 and 816,260-fold increase in the required dose in order to achieve the same levels of virulence (Nakai et al., 2017).

Nakai et al. (2017) further investigated whether the observed resistance was occurring in the midgut, affecting primary infection, or haemocoelically, preventing secondary infection. The results obtained indicated that the resistance was occurring in both the primary and secondary infection routes. This study also concluded that the resistance trait was stable and persisted in the host after exposure to the virus was temporarily ceased. With resistance observed in both field and laboratory settings, an interesting observation was made that resistance traits were measured to occur faster in populations obtained from the field than those originating from a laboratory colony (Briese and Mende, 1983). This is likely due to the field population having a larger potential for resistance genes whereas laboratory populations have a more homogenous gene pool (Briese and Mende, 1983). While these observations have serious implications for the effectiveness of baculovirus-based biopesticides, it is important to note that no such resistance has been recorded for CrleGV, which has been used for extended periods of time in the field. Despite this, the continued development of novel control options remains essential to ensure resistance could be effectively mitigated should it occur in other insects such as *T. leucotreta*. This would provide a safeguard for the continued productivity and sustainability of the citrus industry in South Africa.

Another challenge facing baculovirus-based biopesticides is the virulence and speed of kill against a specific host. This has been an area of considerable focus as these aspects have the greatest influence on the efficacy of commercial products. A study by Opoku-Debrah et al. (2016) investigated the virulence of seven CrleGV isolates against geographically distinct populations of *T. leucotreta*. The results obtained showed that certain isolates had improved virulence towards some of these populations. This could have important implications for both improved biological control as well as mitigating potential resistance-development to any one CrleGV isolate.

These studies describe only some of the challenges involved in the development of baculovirus biopesticides. This necessitates ongoing research into the continued development of innovative solutions to overcome both these and novel obstacles which may be encountered.

1.3.6. **Synergistic interactions for improved biological control**

To overcome the many challenges involved in the use of baculovirus-based biopesticides, continual research is required to develop improved control options. The use of mixed baculovirus infections has been investigated as an option to mitigate several of these challenges including overcoming resistance and improved virulence (Arrizubieta et al., 2015a, 2015b; Biedma et al., 2015; Graillot et al., 2016; Lara-Reyna et al., 2003). Several types of interactions have been described which can occur in mixed virus infections (Table 1.6). For example, a mutualistic interaction between two viruses would result in both having improved replication which would not be observed with either in isolation. Alternatively, antagonism results in improved replication for one virus at the expense of the other (Cheng and Lynn, 2009).

Table 1.6. Types of interactions which can occur in mixed infections (Cheng and Lynn, 2009)

Type of interaction	Effect on virus 1	Effect on virus 2
Mutualism	Beneficial	Beneficial
Commensalism	Beneficial	No effect
Neutralism	No effect	No effect
Antagonism	Beneficial	Detrimental
Amensalism	Detrimental	No effect
Competition	Detrimental	Detrimental

Numerous studies have been conducted to investigate the interactions and effects in baculovirus coinfections. Interest has been placed on the possibility of improving the insecticidal activity for viruses used as biocontrol agents while also providing additional biological understanding into how these viruses interact with one another and their hosts. Several studies have investigated the interactions between mixtures of different baculovirus genotypes. The first of these involved various mixtures of eight Helicoverpa armigera SNPV (HearSNPV) genotypes (Arrizubieta et al., 2015a). Bioassays were performed using six variants obtained from Lebrija, referred to as HearLB1-6, and a Spanish wildtype isolate HearSP1 which was identified to have two genotypes, HearSP1A and HearSP1B, which co-occluded. Each of the variants were tested singly and in a variety of combinations on second instar *H. armigera* larvae using a droplet dose bioassay. While the relative potency of the viruses differed only slightly when used individually, combinations of the variants showed up to a 3.6-fold increase in relative potency. Another study investigated mixtures of CpGV genotypes against a colony of *C. pomonella*. This colony had been demonstrated to be resistant

to some of these genotypes, such as CpGV-M, while others, such as CpGV-R5, were able to overcome this resistance and establish an infection (Graillot et al., 2016). Interestingly, when a mixture of these genotypes was applied to the resistant colony, both were shown to replicate. This indicated that the R5 genotype assists CpGV-M and enables it to overcome the resistance.

Studies have also been conducted utilising different baculovirus species to investigate interactions during coinfection. An example of this was demonstrated in *Trichoplusia ni* (Hübner) (Lepidoptera: Noctuidae) larvae whereby AcMNPV was mixed with either Trichoplusia ni SNPV (TnSNPV) or Trichoplusia ni GV (TnGV) to evaluate potential synergistic interactions (Lara-Reyna et al., 2003). The authors reported synergistic interactions with AcMNPV in both mixtures with increases of 8 and 10 times the lethal concentration when combined with TnSNPV and TnGV respectively. Another study by Wennmann et al. (2015) investigated the effect of Agrotis segetum granulovirus (AgseGV) and Agrotis segetum nucleopolyhedrovirus B (AgseNPV) coinfections in neonate larvae of the common cutworm, *Agrotis segetum* (Denis & Schiffer-müller) (Lepidoptera: Noctuidae). Larvae were treated with each virus singly as well as in mixtures comprising a set dose of the GV (9×10^5 OBs/ml) mixed with either a low (8×10^2 OBs/ml) or high (3.7×10^4 OBs/ml) dose of the NPV. No significant increase or decrease was observed in larval mortality when infected with a mixture of the viruses compared to each virus in isolation. Another study involved mixtures of Anticarsia gemmatalis MNPV (AgMNPV) and Epinotia aporema GV (EpapGV) which were coinfected in the larvae of *Anticarsia gemmatalis* (Hübner) (Lepidoptera: Noctuidae) (Biedma et al., 2015). Although EpapGV was shown to not cause infection in *A. gemmatalis* larvae, mixtures of this virus with AgMNPV increased larval mortality rates and decreased the median survival time more than would be observed with the NPV in isolation. The authors speculated that these improvements might be due to components present in the EpapGV OBs which damaged the peritrophic membrane and increased NPV access to the midgut epithelial cells.

Similarly, experiments have also been performed whereby capsules from one virus were mixed with another virus to determine whether improvements in virulence could be achieved. One example involved the infection of *Mythimna unipuncta* (Haworth) (Lepidoptera: Noctuidae), the true armyworm moth, with mixtures of Pseudaletia unipuncta NPV (PsunNPV) and viral capsules extracted from Pseudaletia unipuncta GV. These mixed infections showed improvement in infectivity of the NPV (Tanada et al., 1975; Tanada and Hukuhara, 1971).

These studies demonstrate how mixed baculovirus infections can be significant in both improving the virulence and speed of kill of baculoviruses which are intended to be further developed into biological pesticides. There remains a knowledge gap in this research area regarding mixed GV and NPV infections, particularly interactions between each virus and the host and whether these may affect one another during coinfection. Furthermore, additional research into whether mixed formulations could further assist in both preventing and/or controlling resistant insect populations, as was demonstrated with resistant *C. pomonella* larvae and mixtures of CpGV-M and CpGV-R5, is needed.

1.4. Justification for this study

The South African citrus industry is of major importance to the local economy and faces significant threats to its continued productivity. An example of such a threat is *T. leucotreta*, which causes considerable damage to citrus fruit with harmful implication for export to foreign markets. Control of this pest has received much attention resulting in the development of an IPM programme incorporating chemical, cultural, and biological methods into a strategic framework. The baculovirus, CrleGV, is a major component of this IPM programme and has been continuously applied in the field for over a decade. Although this product has been shown to be effective in reducing *T. leucotreta* infestations, novel and improved methods of control are required to combat potential obstacles such as the development of resistance in host populations. Recent experiments conducted at the University of Gdansk and Medical University of Gdansk (UGMUG) in Poland, in collaboration with Citrus Research International (CRI, South Africa), indicated the presence of a previously unknown NPV in homogenates of virus infected *T. leucotreta* cadavers. This is the first ever record of an NPV infecting a *Thaumatotibia* species. The discovery of this virus offers the potential to produce a second independent NPV-based biopesticide for the control of *T. leucotreta* in the field. Furthermore, the observation of two baculoviruses infecting the same insect host provides a unique opportunity to investigate potential synergistic effects that could lead to increased virulence and improved biopesticides.

1.5. Aims and objectives

The overall aim of this project was to evaluate the potential for synergistic interactions between a novel NPV and CrleGV in *T. leucotreta* larvae for improved pest control.

The specific objectives were to: 1) isolate and confirm the presence of the NPV in *T. leucotreta* homogenate samples using transmission electron microscopy, 2) analyse the complete genome

sequence of this novel NPV, 3) develop a conventional PCR-based method for the detection and differentiation of CrleGV and the NPV in *T. leucotreta* homogenate samples, 4) develop a quantitative PCR (qPCR) assay for the quantification of NPV and GV OBs isolated from virus infected *T. leucotreta* larvae, 5) evaluate the biological activity of the NPV and CrleGV on *T. leucotreta* both individually and in combinations in the laboratory, 6) determine the ratio of NPV and GV OBs in larval cadavers after multiple passage in *T. leucotreta* using a qPCR assay, 7) generate the complete genome sequence of the NPV recovered from the final passage to evaluate potential recombination events between the NPV and CrleGV, and 8) evaluate the biological activity of the NPV and CrleGV on *T. leucotreta* both individually and in combinations in the field.

1.6. Overview of chapters

Chapter 2 describes the development of a method for isolation of mixed NPV-GV OBs from *T. leucotreta* homogenate samples which were subsequently imaged using transmission electron microscopy. NPV OBs were purified from resultant mixtures by passing the viruses through *C. pomonella* larvae. Purified NPV and CrleGV OBs were then embedded in resin, sectioned, and further imaged by transmission electron microscopy.

Chapter 3 reports the complete genome of the NPV with primary focus on comparisons with closely related baculoviruses through gene parity plots and mauve alignments. These analyses compare gene content and genome organisation with respect to other alphabaculoviruses. The phylogeny of this novel NPV is also determined in this chapter.

The development of PCR-based techniques for the detection and quantification of each virus is discussed in **Chapter 4**. Using conventional PCR, a multiplex assay was developed to screen samples for the presence or absence of CrleGV or the NPV. The development of a qPCR assay is further discussed in this chapter. This assay enabled the quantification of OBs isolated from larval samples obtained from the biological assays for each virus.

The biological activity of each virus, both individually and in various combinations, is described in **Chapter 5**. These biological assays were carried out against *T. leucotreta* neonate larvae using a surface dose inoculation method. The results from the mixed virus treatments are further analysed to determine whether synergistic effects were occurring.

Chapter 6 describes the passage of NPV and GV OBs, alone and in combination, through *T. leucotreta* larvae. The OBs recovered from the passage assay were further examined by qPCR to determine how the composition of the viruses change. The final passage was further applied

to *C. pomonella* larvae to isolate the NPV OBs enabling the detection of potential recombination events. Analysis of these NPV samples was carried out by generating restriction endonuclease profiles and through the assembly of complete genome sequences using next generation sequencing.

The application of CrleGV and the NPV, alone and in combinations, in the field is reported in **Chapter 7**. Two separate trials were performed in the Sundays River Valley in the Eastern Cape province.

Lastly, **Chapter 8** is a general discussion of the results obtained from the previous chapters. Emphasis is placed on differences in the biological activity observed between viruses used independently or in combinations. These results are discussed with a view to further develop the viruses into improved biopesticides for use in South Africa. A discussion is given for future perspectives and recommendations for improving the results obtained in this study.

Chapter 2

Detection and isolation of an NPV from coinfected *Thaumatotibia leucotreta* larval homogenates

2.1. Introduction

As part of a collaborative project with UGMUG and CRI, CrleGV infected *T. leucotreta* larvae, referred to as *T. leucotreta* homogenate samples, were prepared and sent to UGMUG to sequence the viral genome. These samples spanned a 15-year period and were analysed with next generation sequencing (NGS) and multitemperature single strand conformation polymorphism (MSSCP) technologies to examine whether changes in the CrleGV genomes had occurred (unpublished data; van der Merwe et al., 2017). During the *de novo* assembly of the CrleGV genome, a novel alphabaculovirus, initially referred to as Thaumatotibia leucotreta Nucleopolyhedrovirus (ThleNPV), was detected. The discovery of this novel NPV, capable of infecting *T. leucotreta*, created a series of objectives which form the basis of this project. The first of these objectives was to develop a technique to purify ThleNPV OBs from a mixed sample which also contained CrleGV. The process by which NPV or GV OBs are purified is well documented. However, few studies have investigated the purification of OBs from mixed samples and fewer still on the separation of OBs from two baculoviruses in a single sample.

In general, the purification of baculovirus OBs utilises centrifugation and ultra-centrifugation techniques enabling the separation of viral particles from debris found within the sample (Abdulkadir et al., 2013; Ardisson-Araújo et al., 2014; Ishii et al., 2002; Jukes et al., 2014; Senthil Kumar et al., 2015). Highly purified baculovirus OBs are regularly obtained with the use of density gradient and differential centrifugation. However, these protocols are mainly used for the isolation of viral particles from samples which contain only one species of baculovirus. Significant difficulties can be expected when attempting to isolate an NPV from a sample which also contains a GV. This is due to the overlap in particle size as GV particles range in size from 0.13 to 0.5 µm (Dhladhla, 2012; Haase et al., 2015; Jehle et al., 2006; Laarif et al., 2006; Sciocco-Cap et al., 2001), while NPV particles are known to range from 0.15 µm to far greater sizes of 15 µm (Eberle, 2010; Haase et al., 2015; Jehle et al., 2006; Wennmann, 2014).

An alternative method which could potentially separate the NPV and GV OBs is the use of an *in vivo* system whereby a specific "heterologous" host is infected as a means of isolating one virus from the other. Baculoviruses, especially NPVs have been shown to be able to infect multiple hosts with varying levels of susceptibility. Some NPVs have been reported to have broad host ranges of 10 or more moth species (Graillot et al., 2017; Harrison, 2009; Matindoost et al., 2015). In contrast, GVs are considered to have narrow host ranges, only capable of infecting one or two different hosts (Jackson and Sutter, 1985; Jung and Kim, 2006; Knox et al., 2015; Mascarin and Delalibera, 2012; Moscardi, 1999). For example, both CrleGV and ThleNPV are capable of infecting *Thaumatotibia leucotreta*, but there may exist differences in their host ranges. This may enable the NPV to establish an infection in a heterologous host which is known to not be susceptible to CrleGV. A potential heterologous host is *C. pomonella,* which is more commonly known as codling moth. *C. pomonella* has previously been reported to be susceptible to only one GV, CpGV, and the NPVs AcMNPV and Anagrapha falcifera MNPV (AfMNPV) (Lacey et al., 2002). Additionally, *C. pomonella* has been shown to not be susceptible to CrleGV infection making it an ideal choice for a heterologous host (Jehle et al., 1995). Given the relatively close phylogenetic relationship of *C. pomonella* to *T. leucotreta* (both in the family Tortricidae) and the broader host range typically demonstrated by NPVs, it may allow for ThleNPV to establish an infection (Harrison, 2009; Hostetter and Puttler, 1991). Larval cadavers from such an experiment could then be examined for the presence or absence of OBs, potentially producing only those from the NPV.

The aim of this chapter was to develop a method for the purification of NPV OBs from mixed NPV-GV samples. The first objective was to identify NPV OBs in homogenate samples using a centrifugation-based purification method and a transmission electron microscope (TEM). The second objective was to examine whether mixed CrleGV-ThleNPV samples could trigger a baculovirus infection in *C. pomonella* to recover pure NPV particles for later use. Successfully infected *C. pomonella* larvae would then be examined for NPV OBs, again using a TEM.

2.2. Materials and methods

2.2.1. Sucrose cushion purification

The purification of ThleNPV from mixed NPV-GV homogenate samples provided by River Bioscience (Hermitage, South Africa) was attempted using a modified sucrose cushion centrifugation method (Wennmann and Jehle, 2014). Samples, typically 4 ml each, of mixed NPV-GV homogenate were added to an equal volume of 0.1 % SDS (w/v) and sonicated four times at 60 Hz for 15 seconds each. These were then aliquoted into 2 ml tubes with larger debris

removed by two or three low speed centrifugation steps at 400-700 ×g for 20 seconds. After each centrifugation step, supernatants were collected and pooled together with the pellets re-suspended in 1 ml 0.1 % SDS (w/v) before the next low speed centrifugation. The pooled supernatants were centrifuged at 12,100 ×g for 10-15 minutes to pellet OBs with the resulting supernatants discarded and each pellet suspended in 100-200 µl TE buffer (10 mM Tris, 1mM EDTA, pH 7.2). Sucrose cushions were prepared in new 2 ml tubes, containing 1 ml of 50 % sucrose (w/v) in TE buffer, and cooled to 4 °C. The suspended samples were carefully loaded atop each sucrose cushion and centrifuged at 12,100 ×g for 30 minutes. The supernatant from each cushion was discarded and each pellet was washed twice by suspension in 2 ml 0.1 % SDS (w/v) followed by centrifugation at 12,100 ×g for 10 minutes. The supernatant was again discarded, and the final pellet was suspended in 100 µl ddH_2O and stored at -20 °C.

2.2.2. **Transmission electron microscopy**

Transmission electron microscope grids were prepared using a modified method previously described by Abdulkadir et al. (2013) and Opoku-Debrah et al. (2013). In brief, 5 µl of purified OBs were placed onto a carbon formvar grid for 60 seconds. Filter paper was then used to remove excess liquid from the grid. The grid was then stained using 5 µl 1% uranyl acetate (w/v) for 30 to 60 seconds, with NPV OBs typically stained for shorter durations than GV OBs. Excess uranyl acetate was removed from the grid using filter paper, with grids left overnight to dry. Grids were viewed using a Libra 120 (Zeiss, Germany) TEM. Images were captured and analysed using the Mega view (G2) Olympus analysis software (Olympus, Japan). Prepared grids were stored in a grid case at room temperature.

2.2.3. ***Cydia pomonella* infection assay**

OBs purified from 6 ml of *T. leucotreta* cadaver homogenate, using the 50 % sucrose purification method, were enumerated using a haemocytometer and dark field microscopy as previously described (Hunter-Fujita et al., 1998; Opoku-Debrah et al., 2013). The virus concentration was estimated at 1.02×10^{11} OBs.ml^{-1} from which a 1:10 dilution was prepared using ddH_2O. This dilution, referred to as V1, was used in the neonate and late instar infection assays described below.

2.2.3.1. **Neonate infection assay**

A single dose infection assay was carried out using neonate *C. pomonella* larvae and replicated three times. Eggs were provided by Entomon Technologies (Stellenbosch, South Africa) on strips of wax paper which were cut into small sections, placed in petri dishes, and sealed with

Parafilm (Bemis NA, USA). Eggs were then incubated in a controlled environment at ± 26 °C and a relative humidity (RH) of 30 – 60 % which was maintained with a humidifier until neonate larvae hatched.

Artificial diet was prepared by first autoclaving 13 g of bacteriological agar in 400 ml ddH_2O along with 400 ml ddH_2O at 120 °C for 15 minutes. Pre-mixed *Helicoverpa armigera* diet (235.27 g) supplied by River BioScience (South Africa) was baked at 200 °C for 10 mins to sterilise. To this, 1,527 µl propionic acid and 154 µl phosphoric acid were added. The autoclaved agar was then mixed in, followed by the sterilised ddH_2O, which was added until a viscous solution was achieved (Marsberg, 2016). The diet was distributed into two 24 well plates and allowed to dry. To the first plate, 50 µl ddH_2O was inoculated onto the surface of each diet plug while 50 µl of V1 was inoculated onto the surface of each diet plug on the second plate, forming the control and virus plates respectively. Newly hatched neonate *C. pomonella* larvae were then transferred to the artificial diet, ensuring each well received one larva. Plates were closed, wrapped in paper towel and stored in a controlled environment at ±26 °C and a RH of 30 – 60 % for 14 days

After 7 days infection assays were evaluated by examining diet plugs for the presence or absence of larval frass. After 14 days, plugs were again examined for frass with each plug individually checked for larvae. Healthy larvae were collected from the control plates and used in Section 2.2.3.2. Data was recorded and processed in Excel 2016 (Microsoft, USA).

2.2.3.2. **Late instar infection assay**

A 24 well plate containing artificial diet was treated with 50 µl ddH_2O and V1 with each individually applied to a set of 12 wells. Larvae reared on artificial diet for 14 days (4^{th} & 5^{th} instar) were collected and transferred to the treated plate ensuring each well received a larva. The plate was closed, wrapped in paper towel and stored in a controlled environment at ± 26 °C at a RH of 30 – 60 % for 7 days. Following this, plates were examined with larvae recorded as alive (healthy or infected) or dead. Where possible, cadavers were individually collected and stored at -20 °C for future use.

2.2.4. **Crude purification of GV and NPV OBs**

Purification of NPV OBs from larval cadavers were performed using a modified centrifugation method (Wennmann and Jehle, 2014). Insect cadavers were placed into sterile 2ml tubes into which 1 ml of 0.1 % SDS (w/v) was added. The cadavers were homogenised using sterile pipette tips and vortexed for 1-2 min. Homogeneous cadavers were centrifuged at 100 ×g for

10-30 seconds with the supernatants collected in new 2 ml tubes. The pellets were re-suspended in 1 ml of 0.1 % SDS and centrifuged a second time at 100 ×g for 10-30 seconds. The resulting supernatants were pooled together with the respective supernatants previously collected. The pooled supernatants were then centrifuged at 2,500 ×g for 5 minutes. From this, the supernatants were then discarded, with each pellet re-suspended in 1 ml ddH_2O prior to a final centrifugation at 2,500 ×g for 5 minutes. The final pellet was collected and re-suspended in 150-200 µl ddH_2O.

2.2.5. Cross sectioning and analysis of OBs by transmission electron microscopy

2.2.5.1. Virus preparation

ThleNPV OBs were first bulked up using the samples collected from the late instar infection assay described in Section 2.2.3.2. To do this, OBs were purified from one of the cadavers collected (referred to as C_6) using the method described above (Section 2.2.4.) and enumerated as per Section 5.2.1. The late instar infection assay was repeated, substituting V1 with a 1:10 dilution of the C_6 OBs. After 14 days, plates were examined with insects recorded as alive (larva, pupa or moth) or dead. Cadavers were collected, pooled together and used to purify OBs.

CrleGV OBs were purified from 1 g of infected *T. leucotreta* larvae. This was achieved using a modified glycerol gradient purification method described by Hunter-Fujita et al. (1998) and Opoku-Debrah et al. (2013).

2.2.5.2. OB sectioning and imaging

ThleNPV and CrleGV OBs purified from larval cadavers were embedded in resin using a modified method (Cross et al., 2001). After embedding, OBs were sectioned with a microtome and imaged with a TEM. For each virus, 50 µl of purified OBs were pelleted at 12,100 ×g for 10 minutes and left to dry overnight. To each pellet, 1 ml 2.5 % glutaraldehyde in sodium phosphate ($NaPO_4$, 0.1 M pH7.3) was added and left for two days at 4 °C. Pellets were then washed twice in $NaPO_4$ each for 10 minutes. Pellets were then fixed in 1 % OsO_4 in PO_4 (w/v) for 90 minutes. The pellet was again washed twice in $NaPO_4$ each for 10 minutes. The pellet was then dried in five solutions of ethanol starting at 30 %, followed by 50, 70, 80, and 90 %, each for 5 minutes. Absolute ethanol was applied to each pellet twice for 10 minutes. Propylene oxide was added to each pellet for 20 minutes, followed by 60-minute treatments of 75:25, 50:50 and 25:75 propylene to resin solutions. After each of these treatments, pure resin was added to the pellet and left overnight at 4 °C.

The pure resin was replaced with 1.5 ml fresh pure resin and incubated at 60 °C for 36 hours. The pellet, now embedded in hardened resin was removed from the incubator and sectioned at 70 nm using a PowerTome XL (RMC Boeckeler, USA) with sections placed on 200 mesh copper grids. Grids were stained with two stains, first with 5 % uranyl acetate (w/v) for 20 minutes and then with Reynolds lead citrate (0.44 g lead citrate, 0.59 g sodium citrate, 2.6 ml 1M sodium hydroxide and 4 ml ddH_2O) for 3 minutes with ddH_2O used to wash the grid after applying each stain (Reynolds, 1963).

Grids were visualised using a Libra 120 (Zeiss, Germany) TEM. Images were captured and analysed using the Mega view (G2) Olympus analysis software (Olympus, Japan).

2.3. Results

2.3.1. Sucrose cushion purification

To isolate OBs from the mixed *T. leucotreta* homogenate samples, a modified sucrose cushion purification method was used. Following sucrose cushion purification, samples were examined by TEM with the resulting images shown in Figure 2.1.

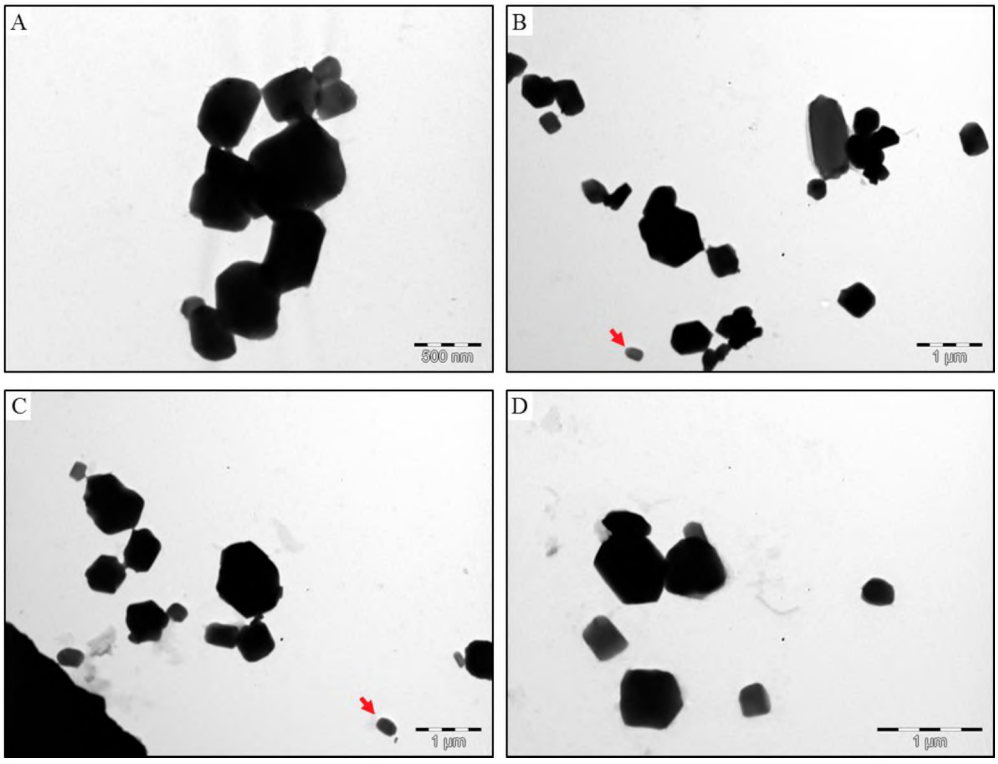

Figure 2.1. TEM images of NPV-like OBs extracted from mixed NPV-GV homogenate samples by 50 % sucrose cushion centrifugation. The red arrows indicate OBs with a GV morphology.

The use of a sucrose cushion purification provided the first observation of NPV-like OBs in the homogenate samples. Figure 2.1 shows several large OB like particles with an average length of 582 ± 230 nm (n = 30). These particles showed a high degree of variation in shape, with the smaller particles appearing more ovoid while the larger particles were amorphous. The smaller particles were around 313 nm and the larger particles around 1313 nm in length. Furthermore, several GV-like OBs were observed in the purified sample (red arrows in Figure 2.1B and C).

2.3.2. *Cydia pomonella* infection assay

Mixed CrleGV and NPV OBs were semi-purified from *T. leucotreta* homogenate samples through a sucrose cushion and tested against neonate *C. pomonella* larvae using a surface dose inoculation method in triplicate. Approximately 5.1×10^8 OBs were applied to the surface of each plug of diet in a 24 well plate, with a second plate treated with ddH_2O used as a control. Wells were examined at 7 and 14 days for the presence or absence of frass with an example of the plate set-up and results for replicate 3 shown in Figure 2.2. From this assay the percentage mortality was calculated and is shown in Figure 2.3.

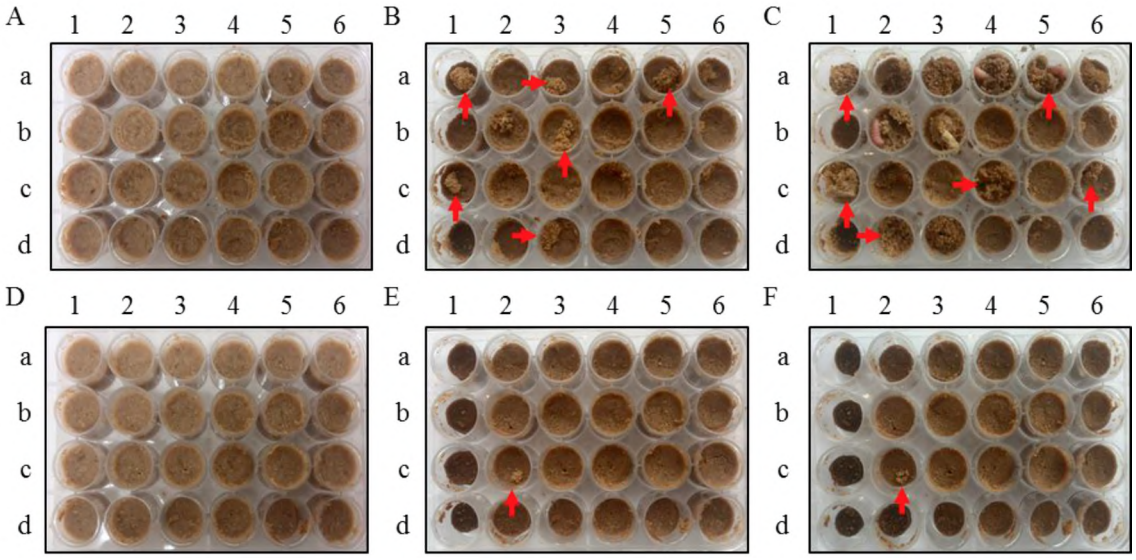

Figure 2.2. *Cydia pomonella* infection assay (Replicate 3) showing control plates at A) 0 days, B) 7 days and C) 14 days post infection and plates inoculated with a mixture of ThleNPV and CrleGV at D) 0 days, E) 7 days and F) 14 days post infection. Red arrows indicate wells with actively feeding larvae and the presence of frass.

A comparison of control and virus treated plates is shown in Figure 2.2. Plates A, B and C show the control treatments for replicate 3 at 0, 7 and 14 days after the addition of *C. pomonella* larvae respectively. Plates D, E and F show the virus treated plate for the same replicate at 0, 7 and 14 days post inoculation and addition of *C. pomonella* larvae respectively. The

accumulation of frass on the surface of the diet plugs is visible in plates B, C, E and F (examples shown with red arrows) with healthy larvae identified in wells a4, a5 and b2 of panel C. Control plates for replicates 1 and 2 showed comparable results, whereas minimal frass accumulation was observed on the virus inoculated plates across the three replicates.

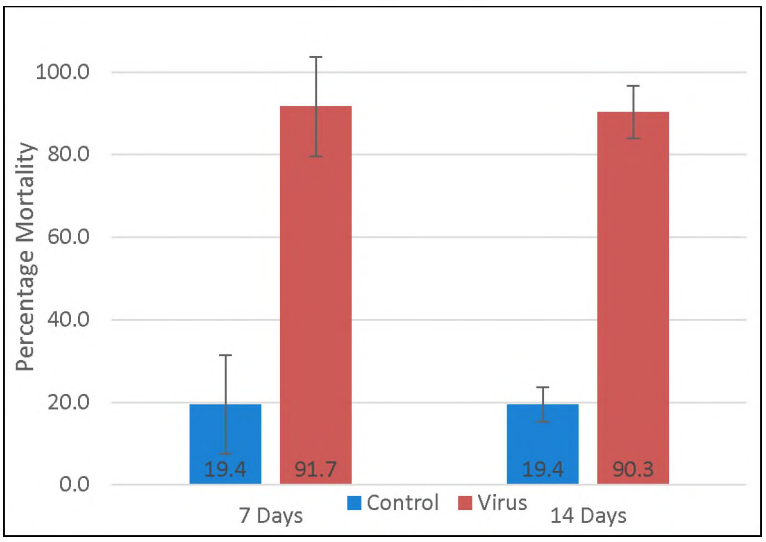

Figure 2.3. Percentage mortality (std. deviation) of *C. pomonella* neonate larvae at 7 and 14 days after exposure to CrleGV and NPV OBs.

An average control mortality of 19.4 % (± 12 SD) and a virus induced mortality of 91.7 % (± 4.2 SD) was observed at 7 days post inoculation (Figure 2.3). The average control mortality did not change after 14 days, whereas a slight decrease was observed in the virus treatment with an average mortality of 90.3 % (± 6.4 SD) recorded.

2.3.3. **Preparation of ThleNPV OBs**

C. pomonella larvae (4th and 5th instar) were treated with the same virus mixture and concentration as used in the neonate infection assay (Section 2.3.2.). This enabled the collection of cadavers for downstream analysis (Figure 2.4).

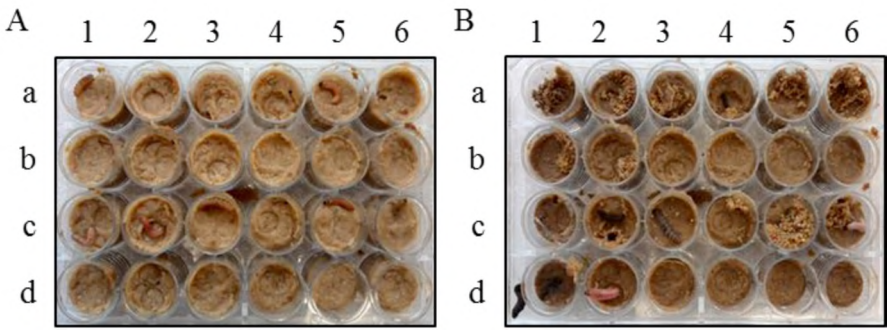

Figure 2.4. Infection of 4nd and 5rd instar *C. pomonella* with CrpeNPV and CrleGV OBs. Control wells in row a, b1 & b2 and virus inoculated wells in row c, d1 & d2. A) 0 days post infection and B) 7 days post infection.

A total of 16 4th and 5th instar larvae were transferred to the plate shown in Figure 2.4A. The wells in row a and wells b1 and b2 (eight wells) were surface inoculated with water and served as a control. The wells in row c and wells d1 and d2 (eight wells), were surface inoculated with the virus treatment. For the purposes of this experiment, to collect infected larvae, the combination of the treated and control larvae on a single plate was considered to not be a problem. After an additional 7 days, three larvae had died in control wells a3, a4, and a5 shown in Figure 2.4B. The virus treated plate was recorded to have 6 dead larvae with those in wells c5 and d2 still alive. Cadavers were collected individually, with the cadavers in wells c1 and c6 observed to exhibit typical baculovirus symptomology with a pale white colour and mostly liquified.

OBs were purified from the larva collected from well c6 above using the purification method described in Section 2.2.4 and are referred to as C_6. TEM grids of the OBs purified from the C_6 sample were prepared and are shown in Figure 2.5.

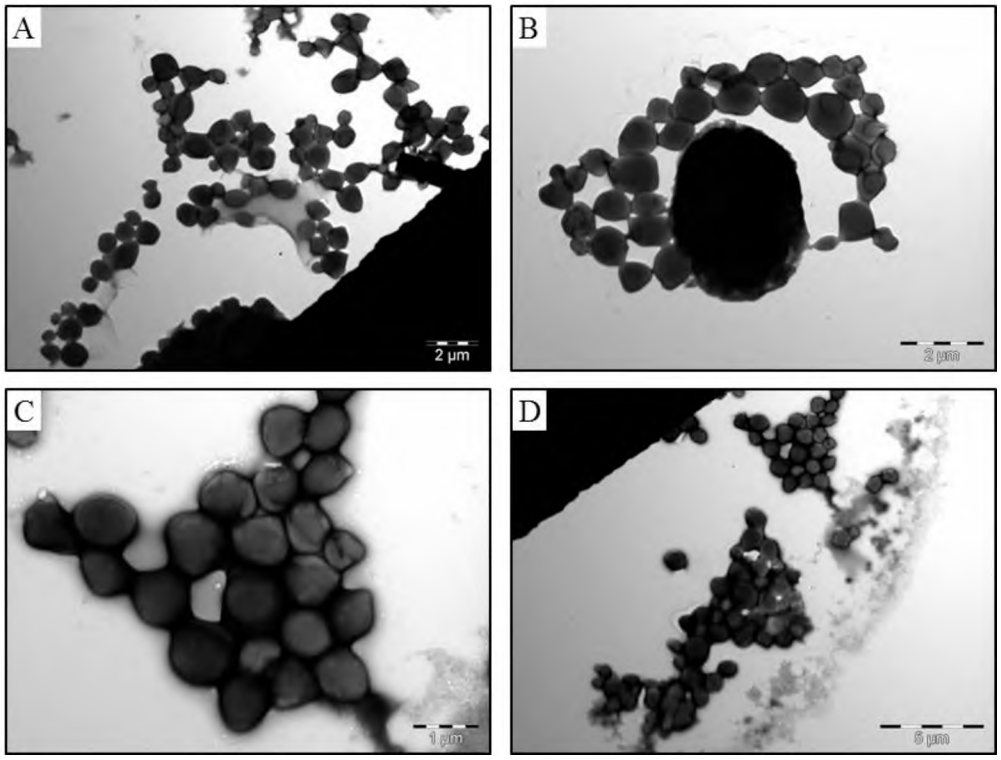

Figure 2.5. NPV-like OBs isolated from C_6 *Cydia pomonella* larval cadaver after infection with a mixture of CrleGV and ThleNPV OBs. Panels A-D show different sections of a single carbon formvar grid containing NPV-like OBs isolated from this single larval cadaver.

Several NPV-like OBs were observed following purification from the C_6 cadaver as shown in Figure 2.5. These particles had a circular to irregular shape with an average size of 1335.6 ± 442.3 nm by 1306.7 ± 500.8 nm (n = 30). Minor amounts of debris were also visible as is shown in Figure 2.5D.

The C_6 OBs were further applied to healthy 4th and 5th instar *C. pomonella* larvae to obtain additional virus for downstream applications. Images of the plate at 0, 7, and 14 days post infection are shown below in Figure 2.6.

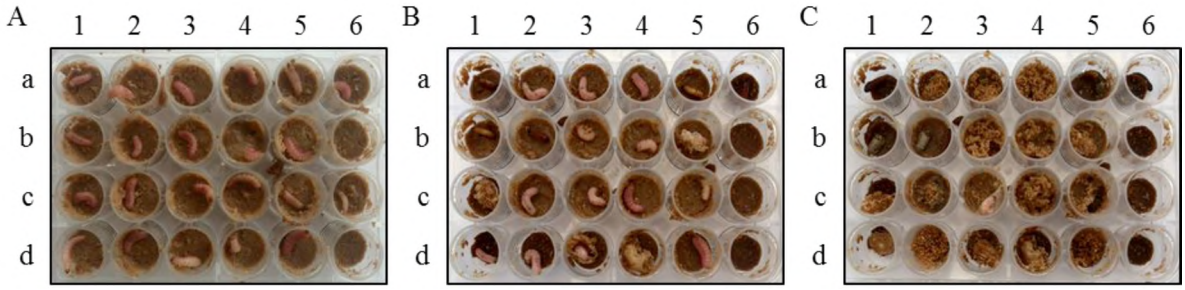

Figure 2.6. Infection of 4th and 5th instar *C. pomonella* with ThleNPV OBs. Control wells in rows a and b and virus inoculated wells in rows c and d. A) 0 days post infection, B) 7 days post infection and C) 14 days post infection.

A total of 12 larvae were exposed to wells treated with water, serving as a control (rows a and b in plates A, B and C). Only one larva died from the control group (well b6) while three moths, (wells a5, b1 and b2) and two pupae (wells a1 and a6), were observed after 14 days. The virus inoculated wells showed elevated levels of larval mortality with 10 larvae dying, from which eight cadavers were collected. The remaining larvae in wells c3 and c4 were observed to be healthy.

ThleNPV OBs were again purified from the eight larval cadavers collected, using the purification method described in Section 2.2.4. Furthermore, CrleGV OBs were purified by glycerol gradient ultracentrifugation (shown in Figure 2.7) from multiple larval cadavers supplied by River Bioscience (South Africa) as described in Section 2.2.5.1.

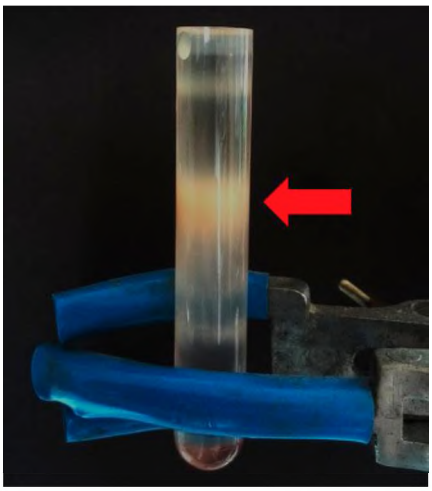

Figure 2.7. Photograph of the CrleGV OB band (Red arrow) observed after density (30 - 80 % glycerol) gradient ultracentrifugation.

TEM grids of the purified ThleNPV and CrleGV OBs were prepared with images of each shown below in Figure 2.8. Panels A, B and C show CrleGV OBs and panels D, E and F show ThleNPV OBs.

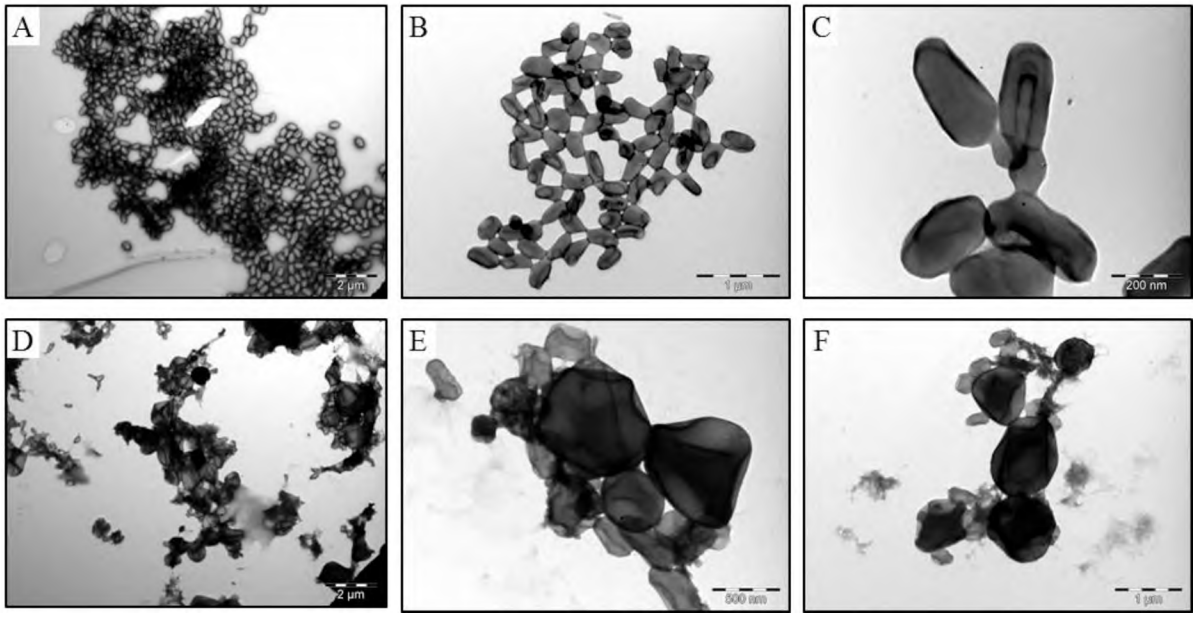

Figure 2.8. TEM images of ThleNPV and CrleGV OBs purified from infected *C. pomonella* and *T. leucotreta* larvae respectively. The abundance and purity of CrleGV OBs in panels A, B and C and ThleNPV OBs in panels D, E and F are shown.

Images of the CrleGV OBs (Figure 2.8A, B and C) showed a uniform ovoid shape with a high concentration and purity of particles observed. The average size of these particles was 341 ± 31 nm (n = 30) in length and 175 ± 31 nm (n = 30) in width. The ThleNPV OBs (Figure 2.8D, E and F) were more irregular in shape with an average size of 686 ± 284 nm (n = 30). A large deviation in NPV particle size was calculated with the smallest particles around 238 nm and

the largest around 1429 nm. Lastly, while a high concentration of NPV OBs was obtained, the purity of these was much lower than for the CrleGV OBs, with debris still present (visible in Figure 2.8D and F).

2.3.4. **OB sectioning and transmission electron microscopy**

Purified CrleGV and ThleNPV OBs shown in Figure 2.8, were embedded in resin and sectioned with a microtome. These sections were then imaged by TEM with the results shown in Figure 2.9 and Figure 2.10.

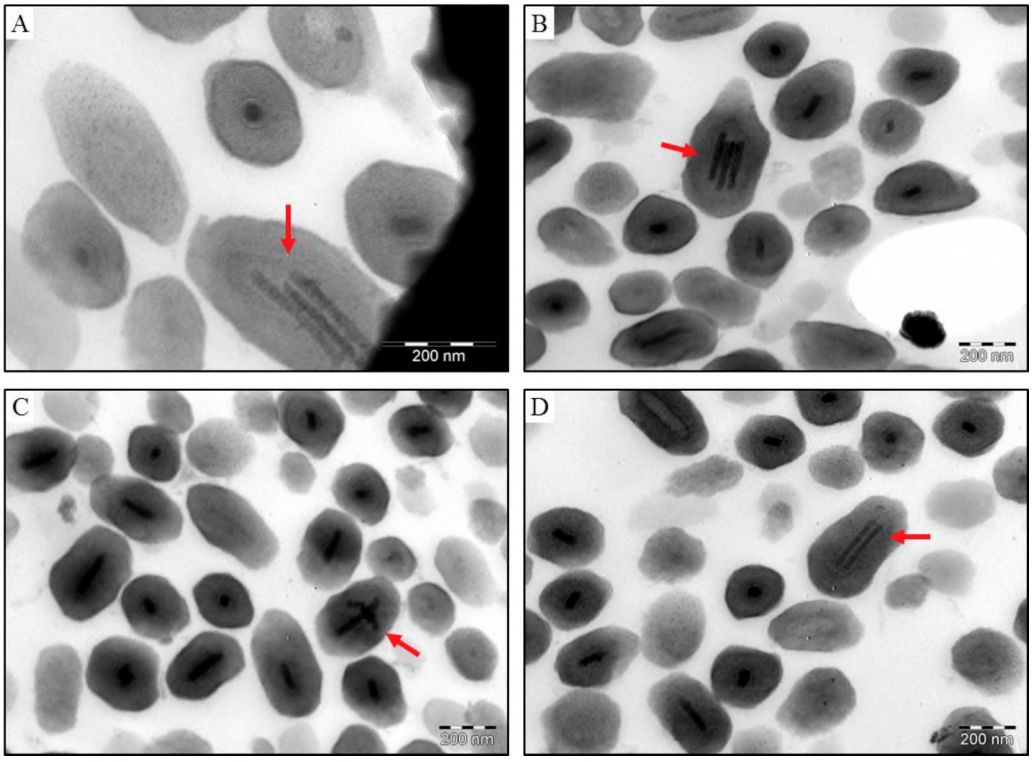

Figure 2.9. TEM images of CrleGV OBs embedded in resin and sectioned with a microtome. Red arrows indicate OBs with multiple nucleocapsids per ODV. Panels A-D show different sections of a single carbon formvar grid with the red arrows highlighting OBs with multiple ODVs.

The characteristic GV OB morphology was observed for most virus particles with a single ODV surrounded by the major occlusion protein granulin. The average length was 363 ± 50 nm (n = 10) and width was 20 ± 18 nm (n = 10). OBs which were sectioned along the length of the particle also enabled the ODVs to be measured, with an average length of 155 ± 36 nm (n = 10) and width of 37 ± 11 nm (n = 10).

Additionally, CrleGV OBs with multiple nucleocapsids per ODV were also observed. Figure 2.9A, B and D, each include a single OB with two or more nucleocapsids in the ODV, shown with red arrows. In Figure 2.9A, the ODV envelope is visible within the OB which appears to

surround all three nucleocapsids (red arrow). Figure 2.9C also includes an OB with an unusual ODV arrangement, shown with a red arrow.

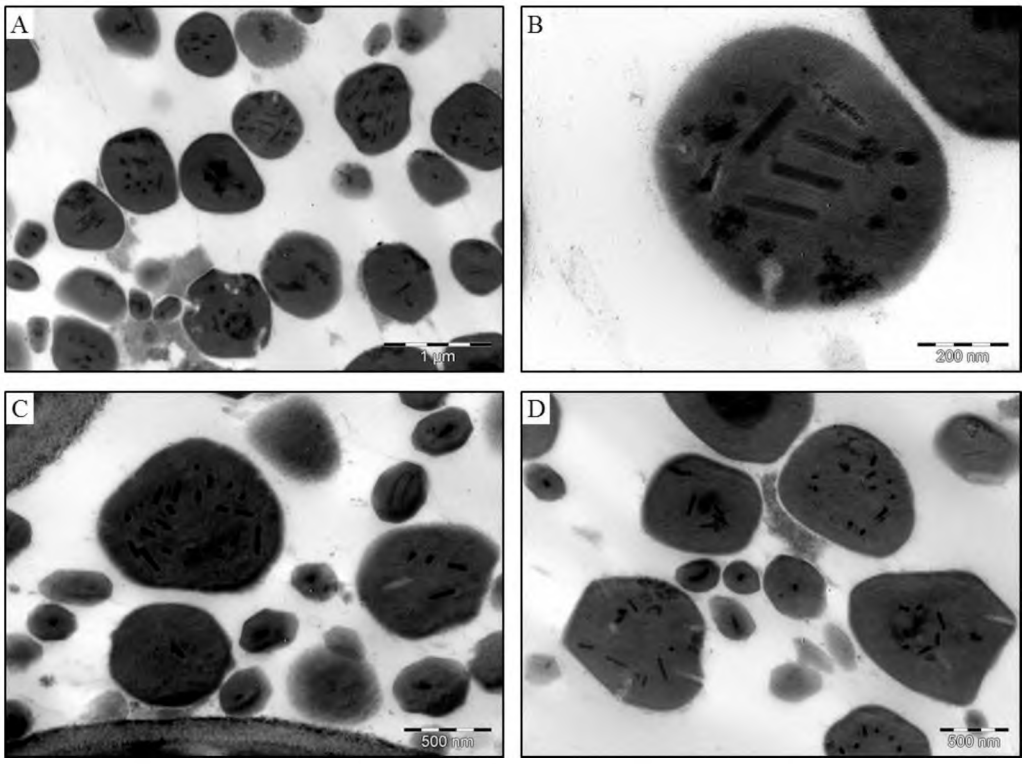

Figure 2.10. TEM images of ThleNPV OBs embedded in resin and sectioned with a microtome. Panels A-D show different sections of a single carbon formvar grid.

TEM images of the ThleNPV OBs confirmed that the particles isolated and observed were baculovirus particles (Figure 2.10). The morphology of these particles was again irregular with the size of the sectioned particles at 655 ± 263 nm (n = 10) and 595 ± 221 nm (n = 10), when measured across two axes (x and y). The average length of selected ODVs was 138 ± 29 nm (n = 10) with a width of 26 ± 8 nm (n =10) measured. Furthermore, the number of ODVs present in several particles was determined, with an average of 7 ± 7 (n = 10) recorded per OB, across the sectioned plane of the particle.

2.4. Discussion

A novel NPV was identified in CrleGV infected *T. leucotreta* homogenate samples by next generation sequencing. To study this virus, it was essential to develop a method for purifying and separating the NPV from a NPV-GV mixture. The use of a modified sucrose cushion protocol enabled the first observation of the NPV OBs. These OBs had a morphology and size typical of other NPVs (Serrano et al., 2015). However, while this protocol laid down a process for obtaining NPV OBs, the purity was questionable with GV-like OBs still observed in these

samples when examined by TEM. Consideration was given to the differences between GV and NPV OB morphology, particularly their size difference, which may have provided a possible solution for purification and separation. While some positive results were obtained, centrifugation methods could not be reproduced successfully and would require additional optimisation before consistent results might be obtained.

It was thus hypothesised that the purification of the NPV could be achieved *in vivo* whereby a heterologous host, which was susceptible to the NPV but not the GV, would enable the separation of the viruses. The first aspect of this hypothesis which required demonstration was whether the NPV could establish an infection in this heterologous host while confirming that CrleGV could not (Jehle et al., 1995). *Cydia pomonella* larvae were exposed to semi-purified NPV-GV mixtures and examined at 7 and 14 days post inoculation. The results obtained from this experiment showed a clear increase in mortality for larvae exposed to the virus mixture compared to control larvae. A minor decrease in larval mortality was observed in the virus-treated larvae after 14 days due to the evaluation method used. A possible explanation for this might be a low level of feeding activity by a single neonate larva in the virus treatment. This prevented detection of a live larva at the 7-day check-up. However, after 14 days surface frass from this larva was apparent, thus categorising this larva as alive. This resulted in the slight decrease in mortality recorded for the 14-day versus the 7-day check-ups. However, it could not be proven whether the increased mortality observed in this assay was caused by the NPV as no follow-up analysis could be immediately carried out. This was due to the small size of the neonate larvae which prevented larval cadavers from being collected and further examined.

To resolve this, an experiment was carried out with 4th and 5th instar *C. pomonella* larvae which were again exposed to the same virus mixture and concentration. From this, a single cadaver (C_6) was successfully collected, from which OBs were purified and examined by TEM. Images showed the presence of NPV OBs, referred to as ThleNPV OBs, like those first observed from the sucrose cushion purification of the mixed NPV-GV samples. Importantly, no GV-like OBs were observed among the OBs purified from the sample, supporting previous evidence that exposure of *C. pomonella* to CrleGV does not result in infection (Jehle et al., 1995). These results show that the infection of *C. pomonella* with a mixture of NPV-GV OBs can be used as an *in vivo* system to separate the NPV from the GV. These results further confirm that the increased mortality observed in the *C. pomonella* neonate infection was due to the presence of ThleNPV OBs in the mixture. However, a potential drawback in the methodology used was the application of virus using surface dose inoculation which could contaminate the surface of the

larvae. A possible solution to this could be the use of an alternative method such as droplet feeding.

The OBs purified from C_6 were then used to infect additional 4th and 5th instar *C. pomonella* larvae to generate additional OBs. CrleGV OBs were also purified from infected *T. leucotreta* larvae by glycerol gradient purification. These OBs were embedded into resin followed by sectioning and examination by TEM. Across all ThleNPV OBs measured, an approximate size of 500-600 nm was recorded. However, due to the irregular morphology of these viruses, no clear length or width could be defined. To overcome this, OBs were measured along a predefined axis (x and y) for each image to determine the diameter, but this resulted in large deviations for each measurement due to the wide range of OB sizes recorded for ThleNPV. In contrast, the ovoid shape CrleGV OBs enabled the length and width to be easily measured for particles which were sectioned along the longitudinal axis.

ODVs were clearly visible in the ThleNPV OBs which had been sectioned, with a maximum of ~ 22 ODVs visible along one of the cross-sectional planes. These OBs were observed to have a SNPV morphology due to the lack of nucleocapsid clusters in the ODVs. The variation observed in ODV number may indicate that the inclusion of capsids into the NPV OB may be a random event. In contrast, CrleGV OBs each typically contained only one nucleocapsid per ODV indicating an ordered assembly process. An unexpected result was also observed whereby several CrleGV OBs were shown to differ from this typical morphology with multiple nucleocapsids per ODV contained within a single particle. The arrangement of these nucleocapsids in the ODV is reminiscent of multiple nucleopolyhedrovirus morphology, albeit with far fewer ODVs and nucleocapsids, whereby the nucleocapsids are clustered into groups (Rohrmann, 2014). The accumulation of multiple nucleocapsids per ODV in CrleGV OBs has been reported previously by Dhladhla (2012) with the proportion of these considerably less than the single nucleocapsid per ODV morphology.

For both CrleGV and ThleNPV, accurate measurement of ODV sizes was difficult to determine, due to their orientation within the OB. It was unclear whether the ODVs measured had been fully sectioned along their longitudinal axis or whether a partial section was visible. This problem has been previously reported by Dhladhla, (2012) for CrleGV. Several particles were measured to provide an estimate of the ODV size, with CrleGV ODVs having an average length and width of 155 nm and 37 nm respectively. ThleNPV ODVs had similar sizes with an average length of 138 nm and width of 26 nm.

In conclusion, this chapter describes the successful observation of an NPV from mixed GV-NPV samples. An *in vivo* system was tested and was observed to effectively purify the NPV from the GV. Virus particles obtained from this system were successfully viewed by TEM which showed an sNPV, ThleNPV, which infects both *T. leucotreta* and *C. pomonella*. The next chapter (Chapter 3) involves the analysis of the complete genome sequence for this novel NPV. Further molecular analysis of the purified GV and NPV OBs is described in Chapter 4.

Chapter 3

ThleNPV genome sequence analysis

3.1. Introduction

As discussed in the previous chapter, ThleNPV was first identified during the sequencing of CrleGV samples using next generation sequencing (NGS). This enabled the assembly of a consensus sequence of the complete ThleNPV genome. Following assembly, the genome sequence could then be compared against other published NPV genomes. The sequencing of baculovirus genomes has become an important aspect of baculovirology, enabling identification and phylogenetic analysis. It further allows genomic organisation and gene composition to be studied (Roelvink et al., 1995; Rohrmann, 2013). Several NGS technologies are commonly used to determine the genome sequence of baculoviruses including the Roche 454 platforms (Roche, Switzerland), the Illumina MiSeq and HiSeq platforms (Illumina, USA), the Ion Torrent platforms (Applied Biosystems, USA), and the Nanopore platforms (Oxford Nanopore Technologies, UK) (Shokralla et al., 2012).

To date, 78 baculovirus genomes have been fully sequenced of which 54 are in the genus *Alphabaculovirus* (lepidopteran NPVs), 20 in the genus *Betabaculovirus* (lepidopteran GVs), three in the genus *Gammabaculovirus* (hymenopteran NPVs), and one in the genus *Deltabaculovirus* (dipteran NPVs) (Wang et al., 2016). Novel baculoviruses are frequently identified, sequenced and added to this growing database. Examples of this include Perigonia lusca SNPV (PeluSNPV), Cnaphalocrocis medinalis GV (CnmeGV), Dasychira pudibunda NPV (DapuNPV), Catopsilia pomona NPV (CapoNPV), Lonomia obliqua MNPV (LoobMNPV), Cryptophlebia peltastica NPV (CrpeNPV), and Lambdina fiscellaria NPV (LafiNPV) with each of these sequenced and published within the last three years (between 2015 and 2017) (Aragão-Silva et al., 2016; Ardisson-araújo et al., 2016; Han et al., 2016; Krejmer et al., 2015; Marsberg, 2016; Rohrmann et al., 2015; Wang et al., 2016). CrpeNPV, a novel NPV, was recently isolated at Rhodes University (South Africa) from *C. peltastica* which is more commonly known as litchi moth is of particular relevance to this study (Marsberg, 2016). Investigations regarding the host range, morphology, and evaluation of the biological activity for CrpeNPV have been reported. Interestingly, CrpeNPV shares many characteristics with ThleNPV. This includes similar host ranges with both viruses capable of infecting *C.*

pomonella and *T. leucotreta*, similar geographic distributions within southern Africa, and sharing similar OB morphology. Comparison of the genome sequences of ThleNPV and other baculovirus, such as CrpeNPV, assist in understanding the novelty of an isolate while also providing a foundation for future analysis.

The wealth of information generated by sequencing of baculovirus genomes has greatly increased over time, advancing the field of baculovirology. This has enabled the identification of conserved genes, variation in genomes, and provided the data necessary for the comparison of novel isolates. For example, the largest baculovirus genome is that of Xestia c-nigrum GV (XecnGV) with a length of 178,733 base pairs (bp) and 181 open reading frames (ORFs) (Hayakawa et al., 1999). On the other hand, Neodiprion lecontei NPV (NeleNPV) comprises the smallest genome with a length of 81,755 bp and a total of 89 ORFs (Lauzon et al., 2004). While there is a large amount of genomic and gene diversity observed among species in the *Baculoviridae* family, several genes have been shown to be present among all known baculoviruses. These genes, of which there are currently 37, are named the core genes and are typically involved in the viruses' infection and transmission cycle (Garavaglia et al., 2012). A second set of 23 genes has been identified to be conserved among all lepidopteran (alpha- and betabaculoviruses) with 11 additional genes further limited to group 1 alphabaculoviruses (Chen et al., 2008; Garavaglia et al., 2012; Herniou et al., 2003; Jiang et al., 2009).

Using the information outlined above, the analysis of NPV genomes typically begins with the identification of ORFs and subsequently searching for homologous genes. Once ORFs within the genome are identified, an annotated map can be produced showing the genome structure of a given baculovirus (Ardisson-Araújo et al., 2014; Crook et al., 1997; Cuartas et al., 2015; Wang et al., 2016). This information can then be utilised allowing further comparison against other baculoviruses whereby changes in genome structure and organisation can be investigated through the generation of gene parity plots (Cuartas et al., 2015; Wang et al., 2016). These plots essentially compare the positions of homologous genes in two baculovirus genomes, showing the movement of genes along with inverted and conserved co-linear regions. Additional information, such as percentage identity, is also generated through the comparison of homologous genes and this enables the identification of conserved genes. Lastly, the evolutionary history of baculoviruses can be inferred by pairwise distance calculation and phylogenetic comparison of shared genes, such as the core genes or other conserved genes (Cuartas et al., 2015; Herniou et al., 2001; Jehle et al., 2006; Lange et al., 2004; Wang et al., 2016).

This chapter describes the analysis of the ThleNPV genome sequence. First, a comparison with CrpeNPV was performed by multiple alignment to evaluate the degree of similarity between these sequences. Next, translated ORF sequences were checked for homology with those from other baculoviruses. This information was used to generate a genome map for ThleNPV. Thirdly, gene parity plots were generated against three other NPVs: a group 1A, a group 1B, and a group 2 alphabaculovirus. Lastly, the phylogeny of ThleNPV was determined in relation to 57 other baculoviruses.

3.2. Materials and methods

3.2.1. Complete genome sequence of ThleNPV

Genomic DNA (gDNA) was extracted from *T. leucotreta* larval homogenate samples by Citrus Research International and sent to UGMUG to generate the complete genome sequence of CrleGV using next generation sequencing. During this process, the complete genome sequence for ThleNPV was also determined using the MiSeq (Illumina, USA) platform. The Nextera library preparation kit (Illumina, USA) was used for the sequencing as per the manufacturer's instructions generating paired reads of approximately 300 bp. Reads were *de novo* assembled using Geneious R8 into a single consensus sequence and checked for ambiguous nucleotides. ORFs were identified using Glimmer in Geneious R8 with these annotations added to the ThleNPV genome sequence. The complete genome sequence and ORF annotations of ThleNPV were used in downstream analyses.

3.2.2. Multiple alignments and PCR amplification of gaps

A pairwise nucleotide alignment between ThleNPV and CrpeNPV was performed in Geneious R7 using the ClustalW method and the ClustalW cost matrix. For each genome, the first nucleotide of the polyhedron gene was set as bp 1. Oligonucleotides were designed using the Geneious R7 primer design tool, targeting regions in the alignment where gaps were identified. gDNA was extracted from CrpeNPV OBs using a modified cetyltrimethyl-ammonium bromide (CTAB) method (Opoku-Debrah et al., 2013). In 1.5 ml tubes, 200 µl of purified OB samples were treated with 90 µl Na_2CO_3 (1 M) before incubation at 37 °C for 30 minutes. Next 120 µl Tris-HCl (1 M, pH 6.8), 50 µl SDS (10% w/v) and 20 µl Proteinase K (25 $mg.ml^{-1}$) were added and further incubated at 37 °C for 30 minutes. Prior to a final 30-minute incubation at 37 °C, 10 µl RNase A (10 $mg.ml^{-1}$) was added.

The samples were then centrifuged at 12,100 ×g in an MiniSpin® (Eppendorf, Germany) desktop centrifuge for 2 minutes. The supernatants were transferred to 2 ml tubes to which each

400 µl of CTAB buffer (54mM CTAB, 0.1 M Tris-HCl pH 8.0, 20 mM Na_2EDTA, 1.4 M NaCl, preheated to 70 °C) was added. Samples were incubated at 70 °C for 45 minutes. Following this, 400 µl chloroform (pre-cooled to 4 °C) was added to each sample, with each being inverted several times before centrifugation at 6,700 ×g for 10 minutes. The upper aqueous phase of each sample was collected in a new 2 ml tube followed by the addition of 400 µl ice-cold isopropanol (-20 °C) to allow DNA to precipitate overnight in a freezer at -20 °C.

Samples were centrifuged at 12,100 ×g for 20 minutes with each supernatant carefully discarded. A volume of 1 ml of ice-cold (-20 °C) 70 % ethanol (v/v) was added to each pellet followed by a final centrifugation at 12,100 ×g for 5 minutes. The supernatants were again discarded with each pellet left to dry, ensuring all ethanol had evaporated. DNA pellets were re-suspended in 20 µl ddH_2O

PCR reactions containing 1µl of the forward and 1 µl reverse oligonucleotides (10µM), 12.5 µl Taq ReadyMix PCR kit (KAPA Biosystems, USA) and 1 µl template genomic DNA (gDNA) were prepared. Reactions were made up to a total volume of 25 µl with ddH_2O and prepared alongside a no template control (NTC). PCR amplifications were performed in a SimpliAmp Thermal Cycler (Applied Biosystems, USA) with an initial denaturation cycle of 95 °C for 3 minutes followed by 30 cycles of 95 °C for 30 seconds, 55 °C for 30 seconds, and 72 °C for 1 minute 20 seconds. A final elongation cycle of 72 °C for 3 min was used.

Amplicons were visualised by 1 % agarose gel electrophoresis stained with ethidium bromide and separated at 90 v for 30-45 minutes in 1 × TAE buffer (40 mM Tris-acetate, 20 mM acetic acid, 1 mM EDTA). Agarose gels were visualised using the ChemiDoc™ XRS+ (Bio-Rad, USA) and images were captured with the Image Lab™ (Bio-Rad, USA) software.

Amplicons were sent to Inqaba Biotech (South Africa) for sequencing. The resulting sequences were edited and aligned using the ClustalW pairwise alignment method in Geneious R7 against the respective regions in the ThleNPV and CrpeNPV genomes.

3.2.3. **Genome annotations**

ORFs in the ThleNPV genome sequence were translated into amino acids using a standard codon table in Geneious R7. Data was exported into the FASTA file format and submitted to the online search tool HMMER (http://www.ebi.ac.uk/Tools/hmmer/). The output generated was used to identify homologous proteins with these details used to amend the ORF annotations.

3.2.4. **Gene parity plots**

The amino acid sequences for ThleNPV ORFs were generated in Geneious R7 and submitted to pBLAST (NCBI). The percentage identity, where possible, was recorded for each ORF against three other NPVs: AdhoNPV (GenBank: NC_004690), Orgyia pseudotsugata multiple NPV (OpMNPV) (GenBank: NC_001875), and AcMNPV (GenBank: NC_001623). Data was exported into Excel 365 (Microsoft) and used to generate parity plots against each of these viruses. Mauve alignments were also generated between ThleNPV and AdhoNPV, OpMNPV and AcMNPV in Geneious R7 using the default settings.

3.2.5. **Phylogenetic analysis**

Estimations of evolutionary divergence between six NPVs, namely ThleNPV, CrpeNPV, AdhoNPV, AdorNPV, AgseNPV and LdMNPV, were determined using the Kimura-2-paramter (K2P) model in MEGA 7 (Kimura, 1980; Kumar et al., 2008). Concatenated *lef*-8, *lef*-9 and *polh* nucleotide sequences extracted from the complete genome sequences of each virus were first aligned using ClustalW in Geneious R11 before analysis in MEGA 7 (Supplementary Table 10.1). A gamma distribution was applied to the analysis with 1000 bootstrap replicates with gaps and missing data removed.

A data set of the 37 core genes from 58 baculoviruses including ThleNPV was used to generate the phylogeny of this virus in MEGA 7 (Supplementary Table 10.1) (Kumar et al., 2016). The evolutionary history was inferred by using the Maximum Likelihood method based on the JTT matrix-based model (Jones et al., 1992). 1000 bootstrap replicate trees were inferred with the initial tree(s) for the heuristic search obtained automatically by applying Neighbor-Join and BioNJ algorithms to a matrix of pairwise distances estimated using a JTT model. The topology was then selected using the superior log likelihood value. The final tree was drawn to scale, with branch lengths measured in the number of substitutions per site. All positions containing gaps and missing data were removed. The betabaculovirus CpGV, the deltabaculovirus Culex nigripalpus NPV (CuniNPV), and the gammabaculovirus Neodiprion sertifer NPV (NeseNPV) were used as an outgroup.

3.3. Results

3.3.1. **Comparison of the ThleNPV and CrpeNPV genomes**

The complete genome of ThleNPV was assembled from reads generated during the sequencing of CrleGV in *T. leucotreta* homogenate samples. Following *de novo* assembly of reads into larger contigs, the sequence of ThleNPV was identified and determined to be 115,728 bp in

length with a GC content of 37.2 %. A total of 126 ORFs were identified with GLIMMER in Geneious R9. Similarities in morphology and host range between ThleNPV and CrpeNPV lead to the comparison of the genome sequences of these viruses.

Pairwise alignment of ThleNPV with CrpeNPV showed a 99.2% pairwise identity. Two gaps of 17 bp in ORF 12 (ac-26) and 934 bp in ORF 35 (djbp or J domain) were identified in the alignment. Oligonucleotides were designed to bind the regions flanking these gaps referred to as the MR and JD amplicons respectively (Table 3.1).

Table 3.1. Oligonucleotides targeting the J-Domain and Ac-26 region of the ThleNPV genome sequence

Name	Length	Position	Sequence (5' to 3')	Amplicon Size (bp)	Tm (°C)
JD-F	20	34882-34901	TGTACCGTGTTTCAGACTAC	1389/455	54.8
JD-R	20	36270-36251	TTCCAGTTTCGATCTAACCG		55.2
MR-F	20	10975-10994	TAACCACCGTGATGTTCTTG	536/518	55.7
MR-R	20	11510-11491	ATACACACTTTTGTTTCGGC		54.8

To examine these regions, gDNA was successfully extracted from CrpeNPV OBs and used as template for amplification of the MR and JD regions. Amplicons were resolved by 1% AGE with an image of these products captured (Figure 3.1).

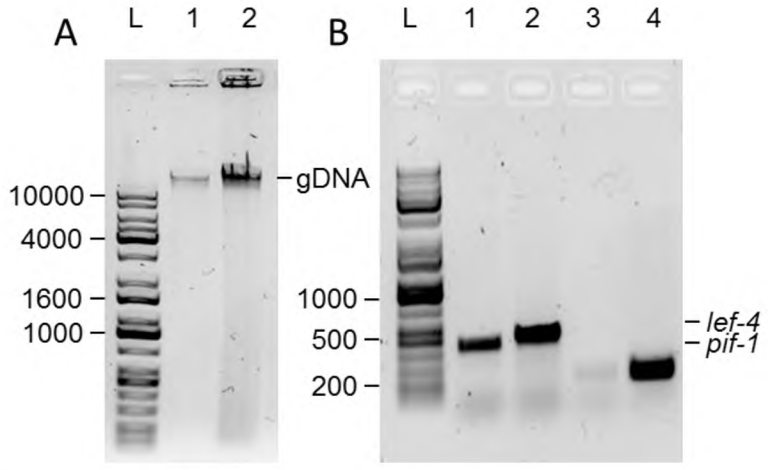

Figure 3.1. A) Inverted AGE image of genomic DNA extraction. Lane 1 – CrleGV gDNA; Lane 2 – CrpeNPV gDNA. B) PCR amplicons for the JD and MR regions using CrpeNPV as template. Lane 1 - JD; Lane 2 – MR; Lane 3 – NTC (-ve) and Lane 4 – Control (+ve). L – KAPA Universal Ladder.

Single amplicons were produced for each of the target regions. The JD amplicon was determined to be around 500 bp in size as shown by the band in lane 1 of Figure 3.1B. Lane 2

shows the MR amplicon which was approximately 550 bp in size. No band was observed in the negative control shown in lane 3. These amplicons were sent for sequencing with the results aligned against the respective regions in the CrpeNPV and ThleNPV genomes.

The MR sequence was 484 bp after trimming ambiguous nucleotides from the 5' and 3' ends with 63% of the bases in the sequence reported as high quality. This sequence was aligned against the region spanning from 10960 (shown as position 1) to 11525 (shown as position 566) in the ThleNPV-CrpeNPV alignment shown in Figure 3.2.

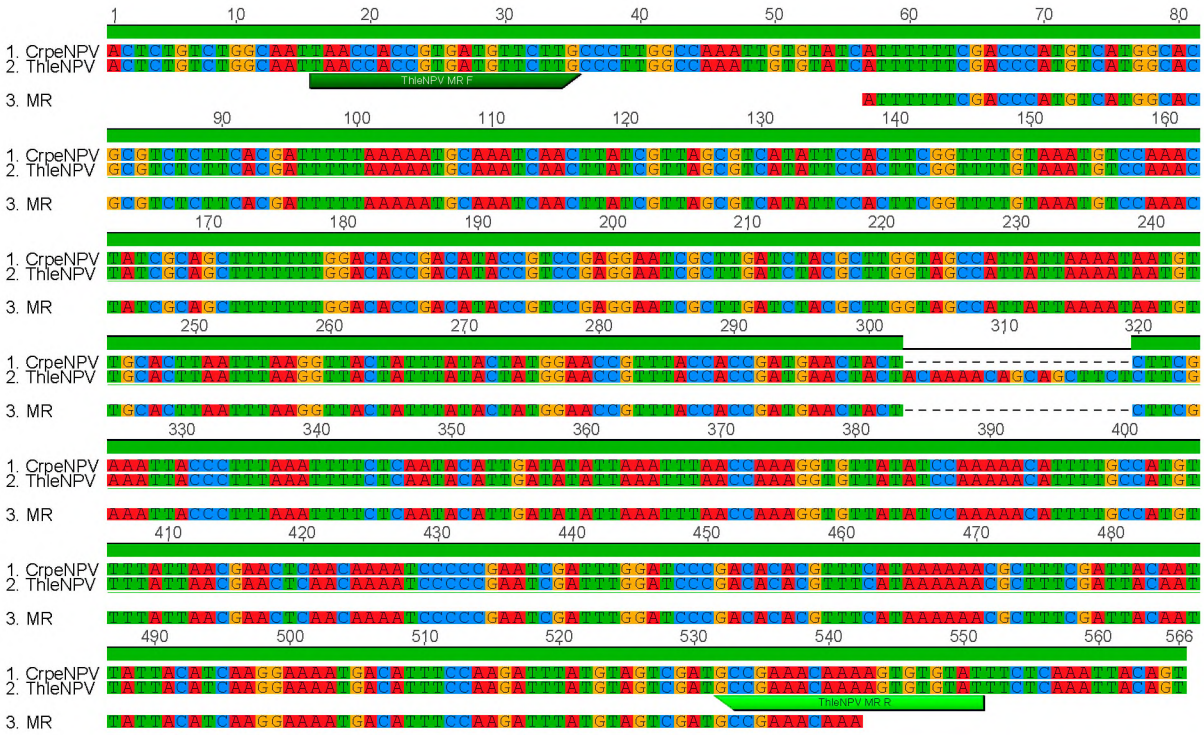

Figure 3.2. Pairwise alignment of the MR amplicon to the respective regions in ThleNPV and CrpeNPV. The green bar shows alignment identity with the forward and reverse oligonucleotide binding regions annotated on the sequence.

Alignment of the MR amplicon sequence to the ThleNPV and CrleGV genome showed a gap spanning from base pair 303 to 319 in the alignment. These base pairs were also absent in the CrpeNPV genome sequence, while the ThleNPV genome showed a 17 bp insertion. The lack of this insertion in the CrpeNPV genome results in a significant truncation of the ac-26 gene (ORF 12) from 114 aa as observed in ThleNPV to 16 aa.

Sequencing of the JD amplicon produced a sequence of 420 bp after trimming of ambiguous nucleotides from the 5' and 3' ends with 84.3% of the sequence reported as high quality. This sequence was aligned against the region spanning from 34871 (shown as position 1) to 36306 (shown as position 1436) in the ThleNPV-CrpeNPV alignment shown in Figure 3.3.

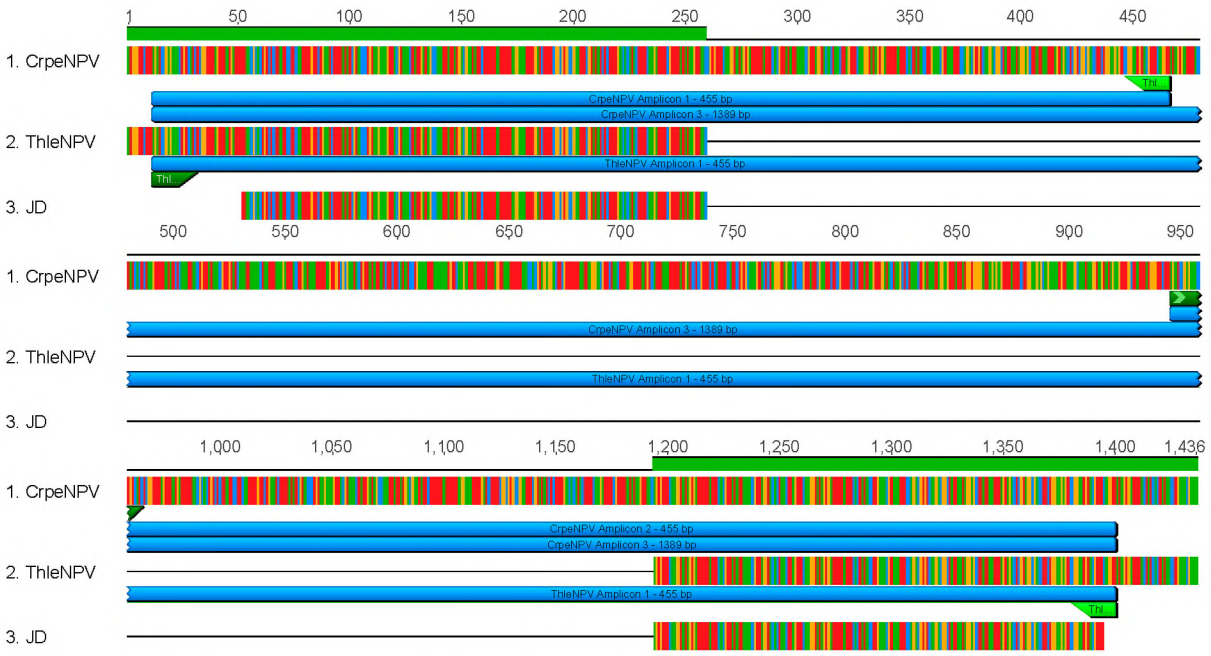

Figure 3.3. Pairwise alignment of the JD amplicon to the respective regions in ThleNPV and CrpeNPV. The green bar shows alignment identity with the forward and reverse oligonucleotide binding regions annotated on the sequence.

Alignment of the JD amplicon sequence against the target region in ThleNPV and CrpeNPV showed a gap of 934 bp ranging from position 260 to 1193. This gap was also observed in the ThleNPV sequence. The binding regions for the forward and reverse primers are also shown in Figure 3.3, with the forward and reverse primers determined to each bind twice in the CrpeNPV genome and once in the ThleNPV, with the various amplicons each would generate shown as blue annotations.

Alignment of the ThleNPV and CrpeNPV, with these regions corrected according to the PCR results, showed a 99.998 % identity with only two nucleotide differences still present in the alignment. The first of these differences was an insertion of an additional adenine nucleotide at position 5916 in the CrpeNPV genome. The second difference was a single nucleotide polymorphism at position 77182 whereby a C was observed in ThleNPV and a T was observed in CrpeNPV.

3.3.2. **Genome mapping and annotation**

Analysis of the ORFs in the ThleNPV genome was completed using HMMER with the results used to annotate the sequence and generate a linear map (Figure 3.4).

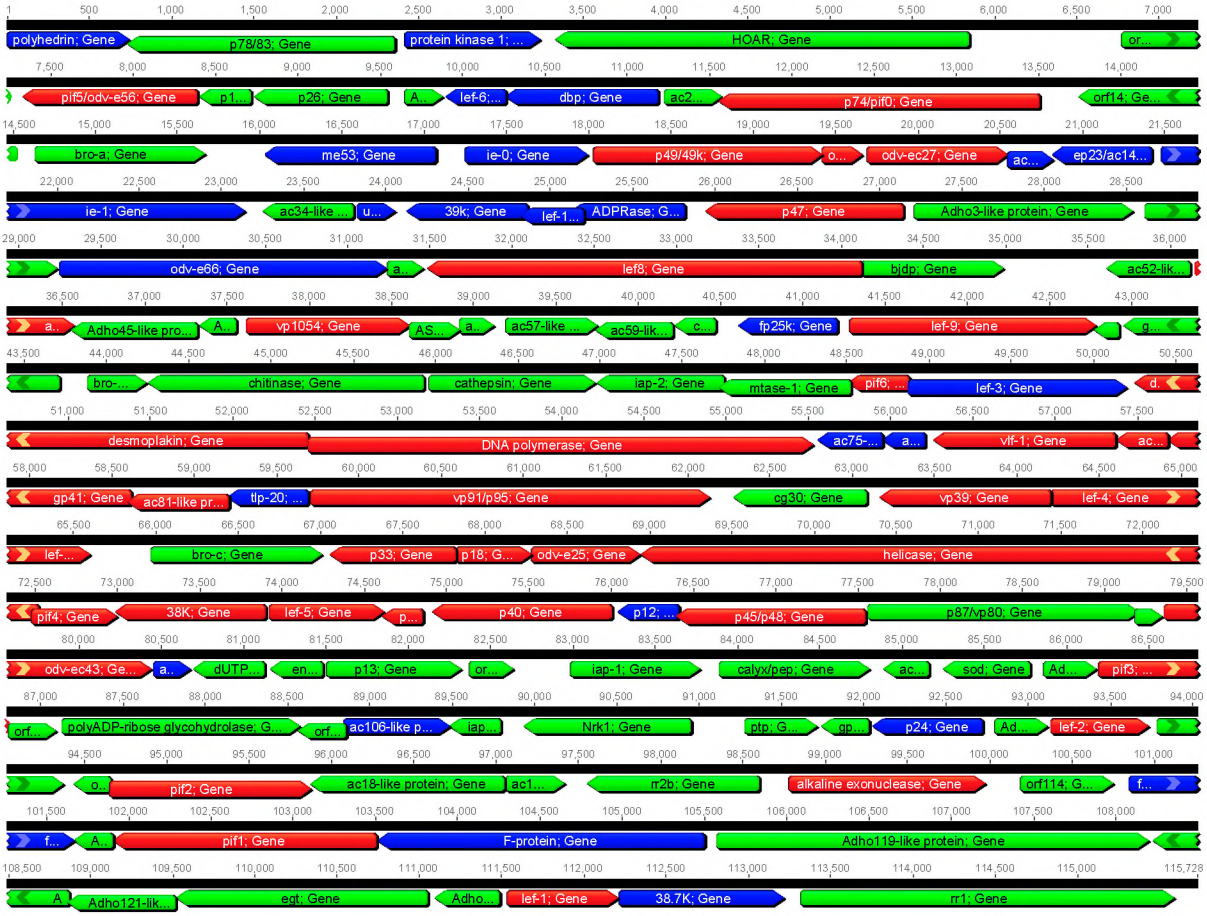

Figure 3.4. Linearised genome map of ThleNPV showing the core genes (red) lepidopteran conserved (blue) and other baculoviral gene (green) annotations. Nucleotide position is shown with nucleotide 1 set at the start of the polyhedrin gene.

All 37 core genes were identified in the ThleNPV genome shown in red in Figure 3.4. A total of 26 lepidopteran conserved and 63 other baculoviral genes were also identified, shown above in blue and green respectively. These genes are further characterised by their function in Table 3.2. The functional groups identified were replication, transcription, structural, oral infection, auxiliary, and unknown with 14, 10, 34, 7, 24 and 37 genes in each respectively.

Table 3.2. Core, lepidopteran specific, other baculoviral and missing genes in the ThleNPV genome arranged by function

Gene types	Core genes	Lepidopteran conserved genes	Other baculoviral genes
Replication	DNA polymerase (Thle58), helicase (Thle74), lef2 (Thle106), alk-exo (Thle113), lef1 (Thle124)	dbp (Thle11), me53 (Thle16), ie-1 (Thle23), lef11 (Thle27), lef3 (Thle56)	lef12 (Thle31), dUTPase (Thle86), endonuclease/ac79 (Thle87), rr1 (Thle126)
Transcription	p47 (Thle29), lef8 (Thle34), lef9 (Thle47), vlf-1 (Thle61), lef4 (Thle69), lef5 (Thle77)	pk-1 (Thle3), lef6 (Thle10), ie-0 (Thle17), 39k (Thle26)	
Structure	p49/49k (Thle18), odv-e18 (Thle19), odv-ec27 (Thle20), ac53 (Thle37), vp1054 (Thle40), desmoplakin (Thle57), ac78 (Thle62), gp41 (Thle63), ac81 (Thle64), vp91/p95 (Thle66), vp39 (Thle68), p33 (Thle71), p18 (Thle72), odv-e25 (Thle73), 38k (Thle76), p6.9 (Thle78), p40 (Thle79), p45/p48 (Thle81), odv-ec43 (Thle84)	polyhedrin (Thle1), odv-e66 (Thle32), fp25k (Thle46), tlp-20 (Thle65), p12 (Thle80), p24 (Thle104), F-protein (Thle118)	p78/83-orf1629 (Thle2), p10 (Thle7), cg30 (Thle67), vp80 (Thle82), calyx/pep (Thle91), PARG (Thle97), gp16 (Thle103), pkip (Thle107)
Oral infection	pif5/odv-e56 (Thle6), p74/pif0 (Thle13), pif6 (Thle55), pif4 (Thle75), pif3 (Thle95), pif2 (Thle109), pif1 (Thle117)		
Auxiliary		ubiquitin (Thle25), ADPRase (Thle28), fgf (Thle115), 38.7k (Thle125)	HOAR (Thle4), p26 (Thle8), bro-a (Thle15), djbp (Thle35), chaB-like (Thle45), ctl (Thle48), gp37 (Thle49), bro-b (Thle50), chitinase (Thle51), cath (Thle52), iap-2 (Thle53), mtase (Thle54), bro-c (Thle70), p13 (Thle88), iap-1 (Thle90), sod (Thle93), iap-3 (Thle100), Nrk1 (Thle101), ptp (Thle102), egt (Thle122)
Unknown		ac145 (Thle21), ep23/ac146 (Thle22), ac75 (Thle59), ac76 (Thle60), ac108 (Thle85), ac106 (Thle99)	Thle5, Adho30 (Thle9), ac26 (Thle12), Thle14, ac34 (Thle24), Adho3 (Thle30), ac43 (Thle33), ac52 (Thle36), Adho45 (Thle38), Adho44 (Thle39), ASB110/ac55 (Thle41), ac56 (Thle42), ac57 (Thle43), ac59 (Thle44), ac110 (Thle83), Thle89, ac117 (Thle92), Adho107 (Thle94), Thle96, Thle98, Adho101 (Thle105), Thle108, ac18 (Thle110), ac19 (Thle111), Thle112, Thle114, Adho113 (Thle116), Adho119 (Thle119) Adho120 (Thle120), Adho121 (Thle121), Adho123 (Thle123)

3.3.3. Genome organisation: mauve alignments and parity plots

Genome organisation was investigated by generating mauve alignments and gene parity plots for ThleNPV against three other NPVs. These analyses show changes in genome organisation because of recombination, duplication, rearrangement or horizontal transfer events with mauve alignments showing the organisation of homologous regions (coding and non-coding) while gene parity plots show the organisation of homologous genes between two or more closely-related organisms. As such, a high degree of corroboration should be observed between these analyses. Each comparison was performed in relation to the polyhedrin gene, which was set as ORF 1.

3.3.3.1. Comparison of ThleNPV to AcMNPV

The first comparison was performed between AcMNPV and ThleNPV with the mauve alignment shown in Figure 3.5A and the parity plot shown in Figure 3.5B.

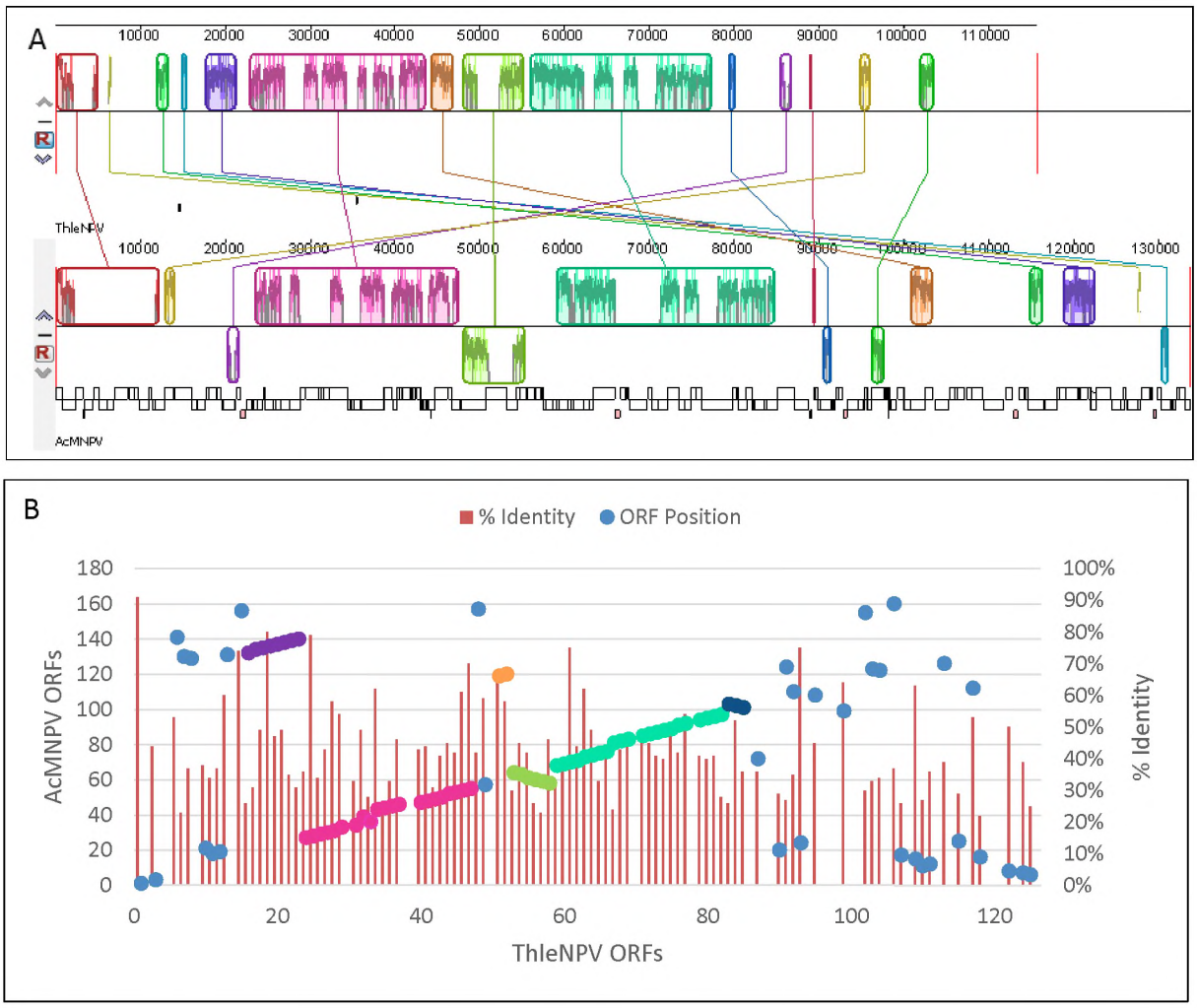

Figure 3.5. A) Mauve alignment showing the organisation of similar regions between the ThleNPV (top bars) and AcMNPV (bottom bars) genome sequences. Inverted regions in

relation to the *polyhedrin* genes are show as bars below each line. B) gene parity plot indicating changes in ORF position and the percentage identity between ThleNPV and AcMNPV.

Comparison of the AcMNPV and ThleNPV genomes by mauve alignment and gene parity showed several changes in genome organisation (Figure 3.5). Three large co-linear regions were identified between these genomes shown in purple, pink and light green (Figure 3.5A) with these encompassing ORFs 16-23, 24-47 and 59-82 in ThleNPV respectively (Figure 3.5B). Two inverted regions were also distinguished across ORFs 53-58 (green) and 83-85 (dark blue) in ThleNPV. Various other ORFs were also identified to have changed position in these genomes shown as individual blue dots across the graph.

Also shown in Figure 3.5B is the percentage identity between homologous ORFs in AcMNPV and ThleNPV. A total of five ORFs showed a percentage identity greater than 75% namely; ORF 1 (polyhedrin), ORF 19 (odv-e18) ORF 25 (ubi), ORF 61 (vlf-1), and ORF 93 (sod). The grouping of these genes is shown in Table 3.2 with two of these (ORFs 1 and 25) considered lepidopteran conserved while two others (ORFs 19 and 61) are core genes.

3.3.3.2. **Comparison of ThleNPV to OpMNPV**

The ThleNPV genome was next compared against OpMNPV (NC_001875) which is a group 1B alphabaculovirus. The mauve alignment and parity plots for this comparison are shown in Figure 3.6A and B.

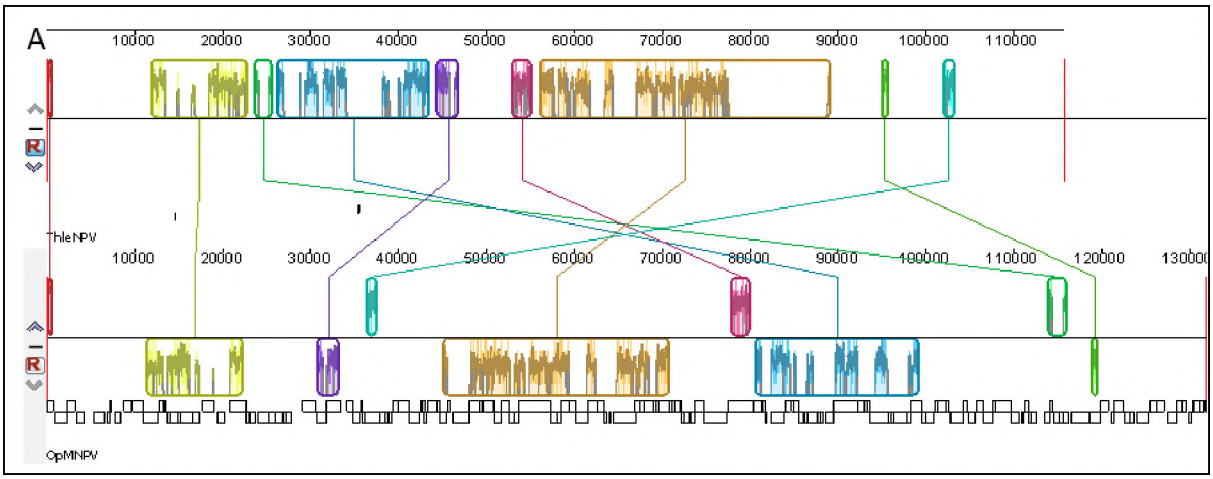

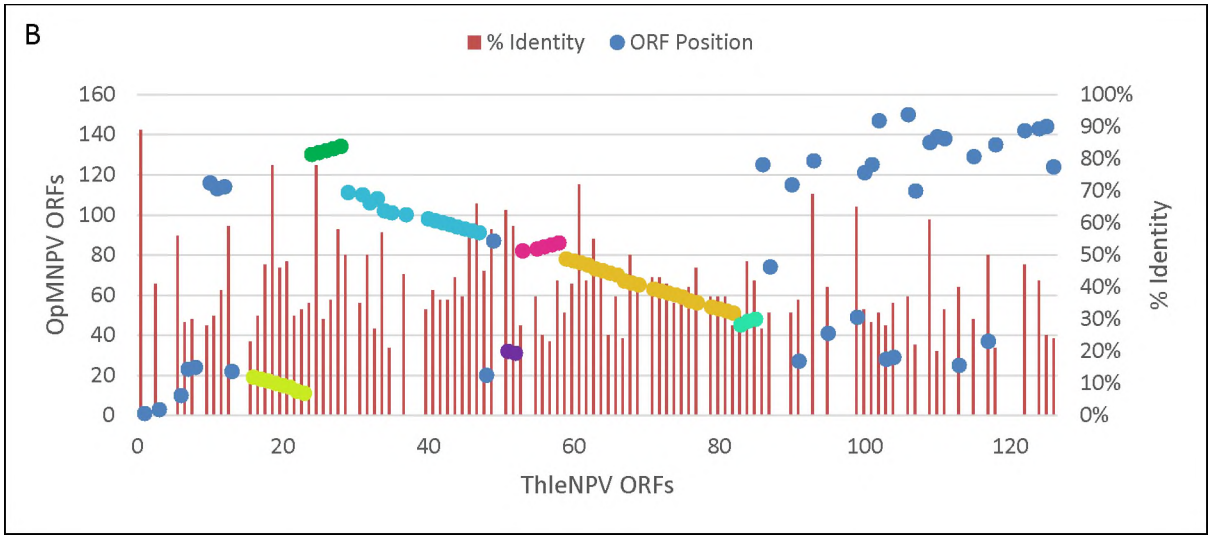

Figure 3.6. A) Mauve alignment showing the organisation of similar regions between the ThleNPV (top bars) and OpMNPV (bottom bars) genome sequences. Inverted regions in relation to the *polyhedrin* genes are show as bars below each line. B) gene parity plot indicating changes in ORF position and the percentage identity between ThleNPV and OpMNPV.

A major distinction was observed between the arrangement of ORFs in ThleNPV to OpMNPV, with large regions, highlighted in yellow, blue and orange, shown to be inverted in relation to the *polyhedrin* gene (Figure 3.6A). These inversions are shown in Figure 3.6B across ORFs 16-23 (yellow), 29-47 (light blue), 52-53 (purple), and 59-85 (orange) in ThleNPV and ORFs 19-11, 111-91, 32-31, and 78-48 in OpMNPV respectively. Three co-linear regions were also identified across ORFs 24-28 (green), 53-58 (pink), and 83-85 (light green) in ThleNPV to ORFs 130-134, 82-86, and 45-48 in OpMNPV respectively. Several of the ThleNPV ORFs which occur towards the 3' region of the genome were identified to have remained in the same region of the OpMNPV genome such as ORFs 90, 93, 105, and 118. There are however exceptions such as 91, 103, and 113 which were identified as ORFs 27, 28, and 25 in the OpMNPV genome.

The percentage identity between homologous ORFs in OpMNPV and ThleNPV are also shown in Figure 3.6B. Only three ORFs showed a percentage identity greater than 75% namely, ORF 1 (polyhedrin), ORF 19 (odv-e18) and ORF 25 (ubi). Two of these (ORFs 1 and 25) are lepidopteran conserved while ORF 19 is a core gene (see Table 3.2).

3.3.3.3. Comparison of ThleNPV to AdhoNPV

The ThleNPV genome was compared against AdhoNPV (NC_004690) which is a group 2 alphabaculovirus. The results for the mauve alignment and parity plot are shown in Figure 3.7 A and B respectively.

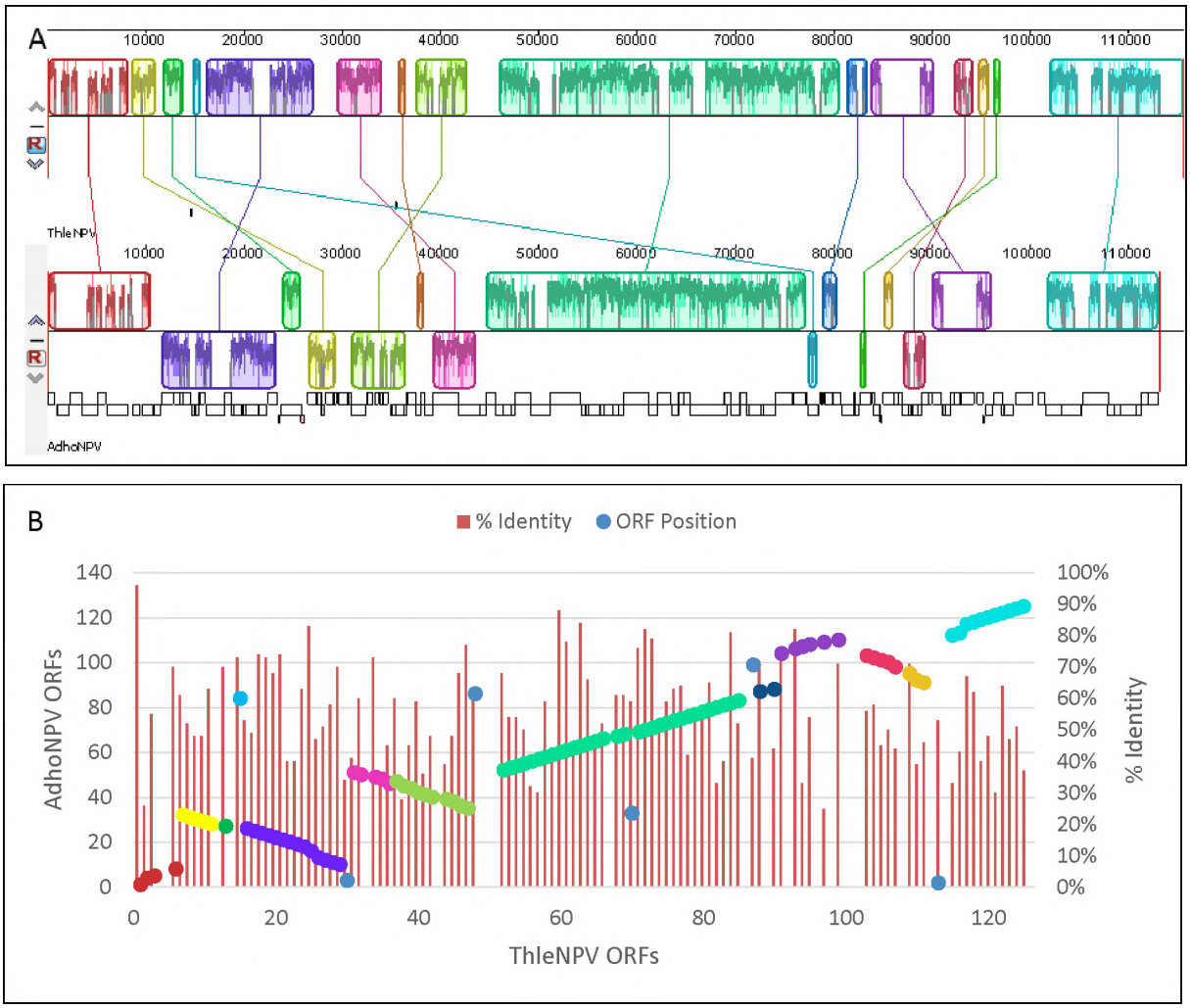

Figure 3.7. A) Mauve alignment showing the organisation of similar regions between the ThleNPV (top bars) and AdhoNPV (bottom bars) genome sequences. Inverted regions in relation to the *polyhedrin* genes are show as bars below each line. B) gene parity plot indicating changes in ORF position and the percentage identity between ThleNPV and AdhoNPV

Analysis of the ThleNPV and AdhoNPV genomes showed 11 co-linear regions, six of which were inverted. The largest co-linear region, shown in light green in Figure 3.7A, included ORFs 52-85 in ThleNPV and ORFs 52-83 in AdhoNPV with one additional ORF included in this region, namely AdhoNPV ORF 33 identified as ORF 70 in ThleNPV (Figure 3.7B). Preceding this co-linear region are four smaller inverted regions shown in yellow, purple, pink and green which include ThleNPV ORFs 7-13, 16-29, 31-37, and 38-47 which correspond to ORFs 32-27, 26-10, 51-47, and 45-35 in AdhoNPV respectively. Like ThleNPV ORF 70, AdhoNPV ORF 84 was identified earlier in the ThleNPV genome as ORF 15. These ORFs (ThleNPV ORF 70 and 15) were both identified a baculovirus repeat ORFs (*bro* genes). Two smaller inverted co-linear regions were identified towards the 3' region of these genomes shown in

light red and orange which included ThleNPV ORFs 103-107 and 109-111 respectively. The last four co-linear regions included ThleNPV ORFs 1-3, 88/90, 91-99, and 115-125.

The percentage identity between homologous ORFs in AdhoNPV and ThleNPV are shown in Figure 3.7B. Ten ORFs showed a percentage identity greater than 75% namely, ORF 1 (polyhedrin), ORF 25 (ubi), ORF 60 (ac-76), ORF 61 (vlf-1), ORF 63 (gp41), ORF 71 (p33), ORF 72 (p18), ORF 73 (odv-e25), ORF 84 (odv-ec43), and ORF 93 (sod). Of these three (ORFs 1, 25, and 60) are lepidopteran conserved and six (ORFs 61, 63, 71, 72, 73, and 84) are core genes (see Table 3.2).

3.3.4. **ThleNPV phylogeny**

To evaluate the evolutionary divergence of ThleNPV, an analysis of concatenated lef-8, lef-9 and polh nucleotide sequences was conducted using the Kimura-2-parameter (K2P) in MEGA 7. The distances and standard errors between ThleNPV and three other Tortricid NPVs namely CrpeNPV, AdhoNPV and AdorNPV were determined (Table 3.3). Additionally, the NPVs LdMNPV and AgseNPV were included as an outgroup.

Table 3.3. Kimura-2-parameter estimates of the evolutionary divergence between concatenated *lef*-8, *lef*-9 and *polh* sequences from six baculovirus species. The lower diagonal shows the number of base substitutions per site between sequences while the upper diagonal shows the standard error. The distance values and standard error between ThleNPV and CrpeNPV are shown in bold.

		Standard error					
	Virus	**AdhoNPV**	**AdorNPV**	**AgseNPV**	**CrpeNPV**	**LdMNPV**	**ThleNPV**
Distances	**AdhoNPV**		0.004	0.023	0.016	0.026	0.016
	AdorNPV	0.053		0.023	0.016	0.026	0.016
	AgseNPV	0.600	0.607		0.019	0.015	0.019
	CrpeNPV	0.455	0.458	0.537		0.025	**0.000**
	LdMNPV	0.719	0.742	0.493	0.663		0.025
	ThleNPV	0.455	0.458	0.537	**0.000**	0.663	

The K2P distances between ThleNPV and CrpeNPV were estimated at 0.000 ± 0.000 (Table 3.3). The estimated distances between ThleNPV and the Tortricid NPVs AdhoNPV and AdorNPV were 0.455 ± 0.016 and 0.458 ± 0.016 respectively. The estimated distances between ThleNPV and the Noctuid NPV AgseNPV and the Lymantrid NPV LdMNPV were higher at 0.537 ± 0.019 and 0.663 ± 0.025 respectively.

The phylogeny of ThleNPV was inferred by maximum likelihood in MEGA 7. This was generated using a concatenation of 37 core gene amino acid sequences from 58 baculoviruses with CpGV, CuniNPV and NeseNPV set as the outgroup shown in Figure 3.8.

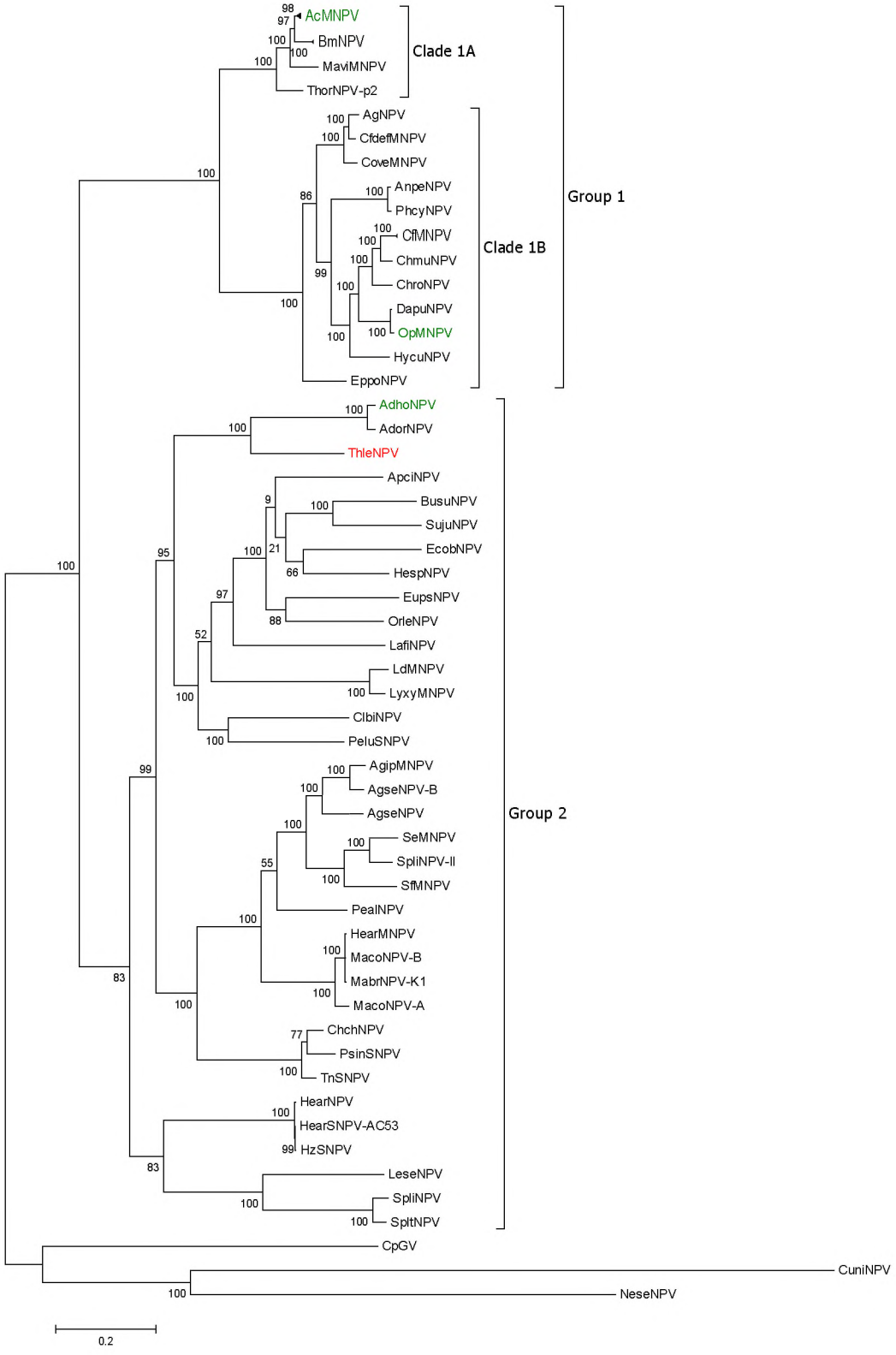

Figure 3.8. Molecular phylogenetic analysis of ThleNPV (red text) by the Maximum Likelihood method based on 37 concatenated core gene amino acid sequences from 58 baculoviruses. AdhoNPV, OpMNPV and AcMNPV are shown with green text.

The tree with the highest log likelihood (-425850.6591) is shown in Figure 3.8. The percentage of trees in which the associated taxa clustered together is shown next to the branches. In total 9381 positions were utilised in the final dataset to generate the tree. ThleNPV was found within the group 2 alphabaculoviruses clustering most closely with AdhoNPV and Adoxophyes orana NPV (AdorNPV). This clustering was observed in 100% of trees generated, with ThleNPV shown to be distinct from the most closely related viruses included in this analysis.

3.4. Discussion

The aim of this chapter was to describe the complete genome sequence of ThleNPV by comparison against other selected baculoviruses. This would first involve the alignment of genome sequences from ThleNPV against the recently identified CrpeNPV to evaluate the degree of similarity between these isolates. Following this, the ThleNPV genome would be further characterised by identification of all ORFs followed by comparison of genome organisation by mauve alignments and parity plots against three baculoviruses: namely, AcMNPV, OpMNPV, and AdhoNPV. The last objective was to examine the phylogeny of ThleNPV in relation to other alphabaculoviruses.

The first objective for this chapter was to compare the genome sequences of CrpeNPV and ThleNPV by pairwise alignment. This analysis revealed the genomes to be almost identical (99.2%) with disagreements observed in only two regions. The first region, referred to as MR, was identified within ORF 12 (ac-26) and showed a gap of 17 bp in the CrpeNPV genome. PCR amplification of this region from CrpeNPV gDNA and subsequent sequencing confirmed the presence of this gap. These results further indicate a frame shift within ORF 12 which would result in a severe truncation of the encoded protein. It is however important to note that this ORF is neither a core gene nor a conserved gene. This modification is not likely to have a significant deleterious effect on the virus. PCR amplification and sequencing of the second gap observed in the alignment, referred to as JD (J-Domain), from CrpeNPV gDNA showed a repeat region had been incorporated into the CrpeNPV genome during assembly. The JD PCR sequence matched that of the ThleNPV, indicating an error within the CrpeNPV assembly. Following incorporation of these results into the ThleNPV and CrpeNPV genomes, a pairwise identity of 99.998 % and a size discrepancy of 1 bp was observed thus confirming that these viruses are essentially identical sequences. These results further support the accuracy of the

genome sequences since two separate assemblies resulted in near identical outcomes once major discrepancies had been resolved by PCR and sanger sequencing. Regarding ORFs, only 105 ORFs were originally reported in the CrpeNPV genome (Marsberg, 2016), while 126 were identified in the ThleNPV genome. Comparison with the ThleNPV genome confirmed the presence of all 37 core genes, including the lef-3, lef-6, ptp, vp80, iap-2, and iap-3 genes which were previously unidentified. Additional lepidopteran conserved along with other baculoviral genes were also identified in the CrpeNPV and, due to the identical nature of the CrpeNPV and the ThleNPV genomes, both have at least 126 ORFs. Furthermore, several genes identified in other baculoviruses genome were absent in the ThleNPV genome. These include lef7 and p94, which have been identified in some group II NPVs as well as arif-1, ac105, ac29, and lef10, which are present in most group II genomes. Interestingly, several lepidopteran NPV conserved genes were identified to be absent in the ThleNPV genome: namely exon-0 and sf58 (Rohrmann, 2013). This finding supports the novelty of ThleNPV as a unique group II species.

The next objective was the comparison of the ThleNPV genome against three other NPVs to identify changes in genome structure and organisation. Several large co-linear regions were observed in the comparisons against AcMNPV and OpMNPV. However, AdhoNPV was observed to maintain the greatest amount of structural similarity with multiple co-linear regions identified. Interestingly, of the 11 co-linear regions observed between ThleNPV and AdhoNPV, six indicate that large inversions occurred during the divergence of these species, resulting in significantly different genome organisations. Comparison with the AdhoNPV genome further revealed the highest number of conserved genes, most of which were identified as core genes. Additionally, two ORFs, polyhedrin (polh) and ubiquitin (ubi), were found to be conserved between all three genome comparisons. The ORF odv-e18 was also found to be conserved in both the AcMNPV and OpMNPV comparisons, with the percentage in AdhoNPV falling just short of the set threshold at 73%. Two other ORFs, very late factor-1 (vlf-1) and super oxide dismutase (sod), were observed to be conserved in two of the comparisons while all other conserved ORFs were only identified within one other genome comparison. Although most of the conserved ORFs were identified to encode core genes, three encoded lepidopteran conserved genes and one encoded a baculoviral gene. The lepidopteran conserved gene, polyhedrin, is known to be the major structural component of NPV OBs and thus is likely conserved to ensure viable OBs are formed (Rohrmann, 2013). Ubiquitin and sod are auxiliary genes involved in cell cycle response/stress response and virus entry/superoxide inactivation respectively (Li et al., 2003; Rohrmann, 2013; Van Strien et al., 1996). Based on the level of

conservation it would appear these functions are significantly important in the virus infection cycle. The remaining gene, ac-76, while having been identified as a lepidopteran conserved gene, does not have a known function (Rohrmann, 2013). This gene may warrant further investigation given the level of conservation observed to help elucidate its function.

The comparisons discussed above show that the ThleNPV genome is unique in structure from other baculoviruses and therefore likely represents a novel group II alphabaculovirus. Research conducted by Jehle et al. (2006) determined a set of criteria by which lepidopteran-specific baculoviruses could be defined as a unique species. These criteria specify that K2P distances determined using concatenated *polh*, *lef*-8 and *lef*-9 nucleotide sequences less than 0.015 indicate two or more isolates belonging to the same species while values larger than 0.050 indicate two or more isolates belonging to distinct species. Isolates with distance values ranging between 0.015 and 0.050 require additional analysis before classification. Following these criteria, the results show that CrpeNPV and ThleNPV are the same species having an estimated distance of 0. Additionally, distance estimates between ThleNPV and other Tortricid NPVs (AdhoNPV and AdorNPV) show that this virus is a unique baculovirus species having values greater than 0.050.

The final objective for this chapter was to determine the molecular evolution of ThleNPV. The group 1 and 2 alphabaculovirus clusters were clearly identified in the phylogenetic tree with the 1A and 1B clades easily distinguished. ThleNPV was identified as a group 2 alphabaculovirus which clustered most closely with AdhoNPV and AdorNPV. The bootstrap support for this clustering was observed to be 100, showing further support for ThleNPV as a separate species to AdhoNPV and AdorNPV.

Similar to the work described in this chapter, a study by Wang et al. (2016) utilised similar techniques in the analysis of a novel group 1 alphabaculovirus CapoNPV. It is interesting to note that gene parity plots generated between CapoNPV and AcMNPV, which were reported to be closely related by phylogenetic analysis, revealed these genomes to be essentially identical in gene organisation; a single large co-linear region and only one minor inversion was observed. Conversely, although the ThleNPV and AdhoNPV genomes were shown to similarly cluster together by phylogenetic analysis, a far greater amount of genome reorganisation was observed. It is possible to speculate that there are several branches missing around the AdhoNPV-ThleNPV cluster which would be populated by NPVs. Each of these might show a more gradual progression to the level of genome reorganisation observed between these viruses

to a point where a similar observation is made to that of the CapoNPV and AcMNPV cluster. These results may therefore imply that there are many undiscovered group 2 NPVs that are closely related to AdhoNPV and ThleNPV, which would populate this region of the baculovirus evolutionary tree.

This chapter described the complete genome sequence of ThleNPV. A total of 126 ORFs were identified, each of which were grouped by function. Comparison of ThleNPV and CrpeNPV showed these viruses to have essentially identical genome sequences, indicating that these viruses are indeed the same species of baculovirus. For this reason, and an observation that the virus replicates at higher levels in *C. peltastica* (S. Moore pers. comm), the name CrpeNPV was adopted for ThleNPV and is used in all subsequent chapters. This identification directed us to a source of purified CrpeNPV OBs, which is readily available and can therefore be used in downstream applications foregoing the need to separate and purify the virus through *C. pomonella* larvae. Analysis of the CrpeNPV (ThleNPV) genome further revealed AdhoNPV to share the greatest amount of genome organisation, while phylogenetic analysis showed this virus and AdorNPV to be the most closely-related organisms. In conclusion, these results support CrpeNPV as a novel baculovirus species that falls within the group 2 *Alphabaculovirus* genera.

Chapter 4

Development of PCR based techniques to detect and quantify CrleGV and CrpeNPV in mixed infections

4.1. Introduction

The previous chapters discussed techniques which were evaluated to isolate the NPV from mixed NPV-GV *T. leucotreta* homogenate samples. First, a 50 % sucrose cushion was applied to these mixed samples, providing the first observation of NPV-like OBs. Next, a technique to separate the NPV OBs was developed by infecting larvae of a heterologous host, *C. pomonella*, with mixed NPV-GV treatments. The resulting infection was shown to only produce NPV OBs which, along with CrleGV OBs were examined by TEM. Chapter 3 showed that ThleNPV, which was isolated from *T. leucotreta* homogenate samples, was identical to CrpeNPV. With this identification, an accessible source of CrpeNPV OBs became available from infected *C. peltastica* larvae, which could be used in downstream applications where necessary.

The objective for this chapter was the development of highly sensitive molecular techniques which could be used to quantitatively and qualitatively evaluate mixed infections of CrpeNPV and CrleGV. Typically, the presence of a baculovirus in a sample can be identified by amplification of a target region of the genome followed by sequencing and analysis with BLAST (NCBI, USA). The granulin (*gran*) or polyhedrin (*polh*) genes have been identified as highly conserved regions which, along with the *lef*-8 and *lef*-9 genes, have been previously utilised to identify lepidopteran specific baculoviruses (Herniou et al., 2003; Jehle et al., 2006). This process becomes more complicated when considering samples containing mixtures of two or more baculoviruses, whereby the use of degenerate oligonucleotides targeting these conserved regions could result in multiple amplicons of similar sizes which cannot be easily differentiated. To overcome this, the multiplex PCR (mPCR) technique is used. This technique uses a mixture of highly specific oligonucleotides which bind only the target gDNA, producing multiple amplicons each with a unique size. Multiplex PCR has been used in several studies to screen samples for the presence of various baculoviruses including EpapGV, AgseNPV A and B, AgseGV, and Choristoneura fumiferana NPV (ChfuNPV) (Kemp et al., 2011; Manzán et al., 2008; Wennmann and Jehle, 2014). In each study, the resulting amplicons were specifically

generated to be easily distinguishable and thus serve a qualitative function for screening of samples.

This technique can be applied in this project to screen samples for the presence of CrpeNPV and CrleGV in mixed infections to evaluate whether potential synergistic interactions are occurring between these viruses. The mPCR analysis could also be applied to *T. leucotreta* homogenate samples which were collected over a 15-year period from 2000 to 2015 by CRI to determine when CrpeNPV first entered the *T. leucotreta* colony (van der Merwe et al., 2017).

A second molecular technique, which can be applied to samples generated from mixed CrpeNPV and CrleGV infections in downstream experiments, is quantitative PCR (qPCR). The qPCR technique allows for the accurate quantification of a sample, based on the rate at which a target region amplifies in relation to a known set of standards. qPCR utilises a fluorescent dye which intercalates with double-stranded DNA or oligonucleotides with fluorescent tags. After each cycle of amplification, the level of fluorescence increases and can be quantified by comparison to the standard. Previous research has utilised qPCR extensively to examine the frequencies of genotypes for baculoviruses such as AcMNPV and HearSNPV (Arrizubieta et al., 2015b; Zwart et al., 2008). Similarly, qPCR has also been used to quantify Spodoptera exempta NPV (SpexNPV) in agricultural pests to further understand covert infections (Graham et al., 2015) and to study the interaction of AgseGV and AgseNPV in mixed infections (Wennmann et al., 2015; Wennmann and Jehle, 2014). The development of a qPCR technique was necessary in this study to quantify the amount of virus present in larvae following mixed NPV-GV infections, which will be performed to evaluate potential interactions.

The aim of this chapter was to first develop oligonucleotides, based on the complete genome sequences of CrpeNPV and CrleGV, which can be used in mPCR and qPCR assays. Homogenate samples purified by sucrose cushion in Chapter 2 were examined by the mPCR analysis to demonstrate the production of the correct amplicons. CrpeNPV OBs, which were separated from mixed NPV-GV samples through the *in vivo* infection of *C. pomonella*, were also screened with the mPCR technique to determine which of the viruses were present. Once purified CrleGV and CrpeNPV gDNA was obtained, the mPCR assay was validated to ensure it accurately identified these viruses in samples. The mPCR analysis was then applied to a set of *T. leucotreta* homogenate samples which had been collected by CRI over a 15-year period to determine when CrpeNPV first entered the *T. leucotreta* colony. Finally, a qPCR technique

was developed for both CrleGV and CrpeNPV which can be used to quantify these viruses in samples generated from mixed infections.

4.2. Materials and methods

4.2.1. Oligonucleotide design for mPCR and qPCR assays

Oligonucleotides were designed and tested using the Primer3 (v4.0.0) online tool and Geneious R7 software based on the complete CrleGV and CrpeNPV genome sequences (Kearse et al., 2012; Untergasser et al., 2012). Regions which did not form hairpin/secondary structures and primer dimers while also having an optimal melting temperature of 59 °C were automatically selected in the Primer3 software. Two oligonucleotide sets were designed to bind the *late expression factor 4* (*lef4*) and *glycoprotein 41* (*gp41*) genes in CrleGV, producing partial amplicons of 378bp and 197 bp respectively (Table 4.1). A second set of oligonucleotides was designed to bind the *per os factor* (*pif1*) gene in CrpeNPV, producing a partial amplicon of 187 bp. Oligonucleotide specificity was checked *in silico* against both the CrpeNPV and CrleGV genome sequences. The ClGV-lef4 and CpNPV-pif1 oligonucleotides were utilised in the mPCR analysis while the ClGV-gp41 and CpNPV-pif1 sets were used in the qPCR analysis.

Table 4.1. Oligonucleotide design against CrpeNPV *pif1* gene and CrleGV *lef4* and *gp41* genes.

Name	Length	Sequence (5'-3')	Amplicon Size (bp)	Tm (°C)
CpNPV-pif1F	20	ATCGGGATGGTTGGTCAAGT	187	59.0
CpNPV-pif1R	20	CAACGCATGTATTCGTCCGT		59.0
ClGV-L4F	21	TTCGCTTTCTAAACCGCTGTC	378	59.2
ClGV-L4R	22	AGGATGACGTTCCTAATGACGG		59.9
ClGV-gp41F	20	TAGGGCCAACAATACAGCCA	197	59.0
ClGV-gp41R	20	CATGGGCCGATTCGTTGATT		58.9

4.2.2. CrleGV and CrpeNPV gDNA extraction

Genomic DNA was extracted from CrleGV and CrpeNPV OBs using a modified CTAB extraction method. CrpeNPV OBs were purified from infected *C. peltastica* larvae and the CrleGV OBs were purified from infected *T. leucotreta* larvae as described in section 2.2.5.1 (Marsberg, 2016). gDNA was visualised by 1 % AGE as described previously in Section

3.2.2. DNA concentrations and purity (A260/280 and A260/230) were measured using a Nanodrop 2000 (Thermo Scientific, USA) (Supplementary Table 10.2).

gDNA was visualised by 0.6 % agarose gel electrophoresis stained with ethidium bromide and separated at 90 v for 30-45 minutes in 1 × TAE buffer (40 mM Tris-acetate, 20 mM acetic acid, 1 mM EDTA). Agarose gels were visualised using the ChemiDoc™ XRS+ (Bio-Rad, USA) and images were captured with the Image Lab™ (Bio-Rad, USA) software.

4.2.3. **Multiplex PCR assay**

An end-point multiplex PCR assay was developed to screen samples for the presence of either CrleGV or CrpeNPV genomic DNA. PCR reactions were set-up with each containing 12.5 µl Taq ReadyMix HotStart PCR kit (KAPA Biosystems, USA). To this 1µl of the CpNPV-pif1F and ClGV-lef4F oligonucleotides (10µM) and 1 µl of the CpNPV-pif1R and ClGV-lef4R oligonucleotides (10µM) were added. Between 1 and 2 µl of gDNA was added as template. Reactions were made up to a total volume of 25 µl with ddH_2O. No template controls (NTC) were included in each PCR run whereby template gDNA was replaced with ddH_2O. Initially, Phthorimaea operculella GV (PhopGV) gDNA and granulin specific oligonucleotides were used as a control to ensure reagents and equipment were functioning correctly (Jukes, 2015). Thereafter, a mixture of the CrpeNPV-pif1 and CrleGV-lef4 amplicons were used as template for positive control reactions. Where possible, master mixes of the oligonucleotides, Taq ReadyMix and ddH_2O were prepared before being aliquoted into the corresponding PCR tubes to which the template gDNA was added. PCR amplifications were performed in a SimpliAmp Thermal Cycler (Applied Biosystems, USA) with an initial denaturation cycle of 95 °C for 3 minutes followed by 30 cycles of 95 °C for 30 seconds, 55 °C for 30 seconds, and 72 °C 30-45 seconds. A final elongation cycle at 72 °C for 1 minute followed these cycles. Amplicons were visualised by 1% AGE as described previously in Section 3.2.2.

4.2.4. **Quantitative PCR development**

A qPCR assay was developed to quantify the amount of CrpeNPV or CrleGV OBs in a sample. qPCR test reactions, consisting of six standards, an unknown sample, and an NTC reaction were performed for each virus to evaluate the technique. The concentration of OBs in CrpeNPV and CrleGV samples were first evaluated using a haemocytometer and dark field microscopy as previously described (Hunter-Fujita et al., 1998; Opoku-Debrah et al., 2013). For each virus, standards were generated using 10 µl gDNA extracted from these OBs using the CTAB DNA extraction protocol described in Section 3.2.2. A 10-fold serial dilution of gDNA from each

virus was carried out using nuclease free qPCR grade H_2O. These dilutions were labelled D1 to D6 with D1 representing the standard with the highest gDNA concentration and D6 the lowest (Table 4.2). These concentrations were selected to cover a broad range from 10^2 to 10^7 OBs.μl^{-1} to ensure unknown samples could be accurately quantified.

Table 4.2. Concentrations for the CrpeNPV and CrleGV qPCR standards.

Standard	Concentration (OBs.μl^{-1})	
	CrpeNPV	**CrleGV**
D1	4.88×10^7	3.73×10^8
D2	4.88×10^6	3.73×10^7
D3	4.88×10^5	3.73×10^6
D4	4.88×10^4	3.73×10^5
D5	4.88×10^3	3.73×10^4
D6	4.88×10^2	3.73×10^3

For CrleGV, 4 µl of the CrleGV D3 dilution was used as the test sample with an estimated concentration of 1.49×10^7 CrleGV OBs added to the reactions. For CrpeNPV, 4 µl of a five-fold dilution of the CrpeNPV D3 standard was used as the test sample with an estimated concentration of 3.90×10^5 CrpeNPV OBs in the test reaction. CrpeNPV reactions were also performed in duplicate to further evaluate the accuracy of the method.

Each reaction comprised 10 µl KAPA SYBR green ReadyMix (KAPA Biosystems, USA) which was added to nuclease free optically clear PCR tubes. For CrleGV, 1 µl of the ClGV-gp41F and 1µl ClGV-gp41R oligonucleotides (10 µM) were added to this. Alternatively, for the CrpeNPV reactions 1 µl of the CpNPV-pif1F and 1 µl CpNPV-pif1R oligonucleotides (10 µM) were added to the Taq ReadyMix. Nuclease free qPCR grade H_2O (4 µl) was added to each reaction to make it up to 16 µl. Each reaction then received 4 µl of gDNA from the corresponding standard or unknown samples, making a total of 20 µl with each thoroughly mixed by vortexing for a few seconds. No template control reactions did not contain gDNA, instead 4 µl of nuclease free qPCR grade H_2O was used.

CrpeNPV reactions were performed in duplicate, with the contents of each reaction doubled to 40 µl during reaction preparation. Each reaction was then split into two PCR tubes with each receiving 20 µl of the mixture. Where possible, mixtures were prepared as master mixes in nuclease free 1.5 ml tubes, which were then aliquoted out when necessary. Reactions were run

using the MiniOpticon Real-Time PCR system (Bio-Rad, USA) with the cycle parameters as follows: an initial denaturation cycle of 95 °C for 3 minutes followed by 40 cycles of 95 °C for 30 seconds, 55 °C for 30 seconds, and 72 °C for 20 seconds with fluorescence measured after each cycle. A final denaturation cycle at 95 °C for 30 seconds was performed followed by generating the melt curve starting at 53 °C increasing to 95 °C at 0.5 °C intervals each of 30 seconds. Fluorescence levels were captured after each interval of 0.5 °C. Data was analysed using the CFX Manager™ Software (Bio-Rad, USA) to generate the amplification curves for each reaction, the melt peak for all amplicons generated and the standard curve for quantification of the test samples.

4.3. Results

4.3.1. Multiplex PCR of samples purified by 50% sucrose cushion

As discussed in Chapter 2, *T. leucotreta* homogenate samples were purified using a 50 % sucrose method. Subsequent imaging of these samples showed the presence of NPV and GV OBs. Genomic DNA was extracted from these OBs using the CTAB method and examined by mPCR using the ClGV-lef4 and CpNPV-pif1 oligonucleotides with the results shown in Figure 4.1.

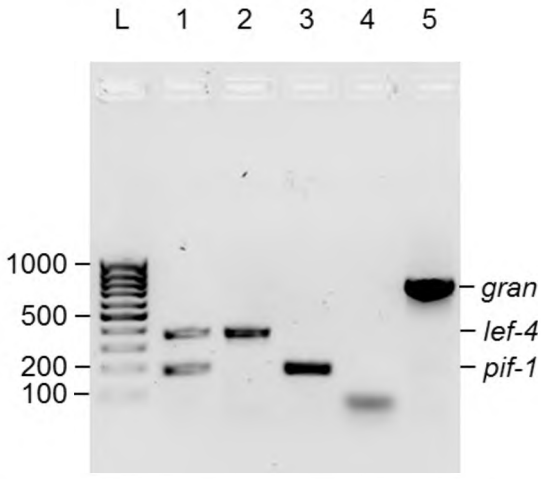

Figure 4.1. Inverted AGE image of mPCR analysis using CrleGV and CrpeNPV gDNA extracted by 50% sucrose cushion. Lane 1 - mPCR, Lane 2 – ClGV-lef4 oligonucleotides, Lane 3 – CpNPV-pif1 oligonucleotides, Lane 4 – NTC and Lane 5 - control. L – GeneRuler 100 bp DNA ladder.

Multiplex PCR analysis of DNA extracted from the 50% sucrose cushion showed the production of two amplicons of approximately 200 bp and 400 bp in Lane 1. These match the expected sizes of the CrpeNPV-pif1 and CrleGV-lef4 amplicons respectively (Table 4.1). Lanes 2 and 3 show the production of the lef4 and pif1 amplicons individually from the same

template gDNA used in Lane 1 with each observed to be approximately 400 bp and 200 bp in size respectively. No amplicon was observed in the no template control while an amplicon of approximately 800 bp was observed in the positive control containing PhopGV gDNA and granulin oligonucleotides (Jukes et al., 2014). The control was included to show that the reagents and equipment were functioning correctly.

4.3.2. **Multiplex PCR of CrpeNPV OBs purified by infection of *Cydia pomonella***

With the mPCR shown to generate amplicons of the correct sizes, samples obtained from the infection of *C. pomonella* larvae with mixed CrleGV and CrpeNPV OBs discussed in Chapter 2 could be evaluated. Two cadavers referred to as C_1 and C_6 were collected from which OBs were purified. Genomic DNA was extracted from both the C_1 and C_6 OBs, a sample of the mixed *T. leucotreta* homogenate tested above and CrleGV OBs which were purified by glycerol gradient centrifugation in Chapter 2. Two of these samples, C_6 and CrleGV, were examined by TEM in Chapter 2 and were each shown to only contain CrpeNPV and CrleGV OBs respectively. Genomic DNA from these samples were analysed using the mPCR technique with the results shown in Figure 4.2A and B.

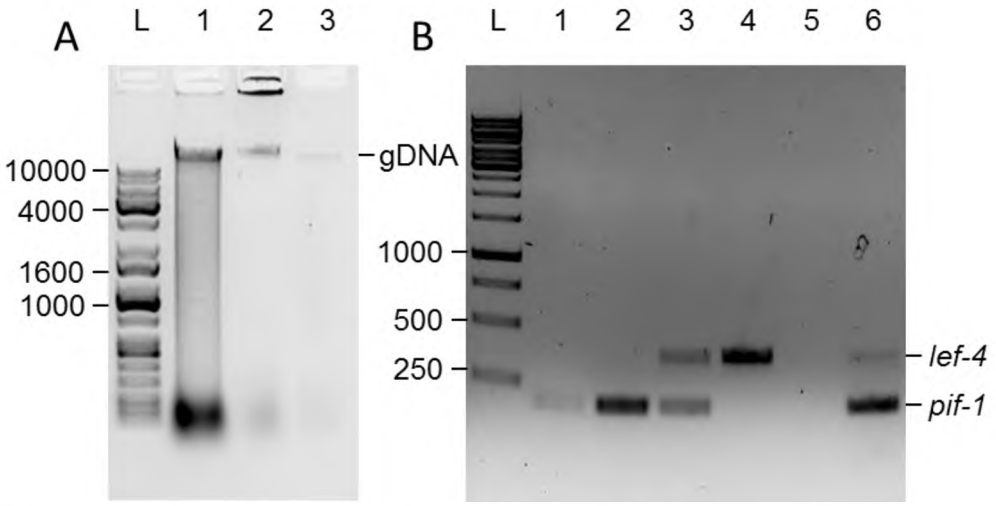

Figure 4.2. Inverted AGE image of A) gDNA extracts from *C. pomonella* larval cadavers and *T. leucotreta* homogenate. Lane 1 – C_1 cadaver, Lane 2 – C_6 cadaver, Lane 3 – *T. leucotreta* homogenate, L – KAPA Universal Ladder. B) mPCR analysis of extracted gDNA. Lane 1 – C_1 gDNA, Lane 2 – C_6 gDNA, Lane 3 – *T. leucotreta* homogenate gDNA, Lane 4 – CrleGV gDNA, Lane 5 - NTC, Lane 6 - +ve control, L – 1Kb GeneRuler DNA Ladder.

Two bands were observed above the 10,000 bp marker in lanes 1 and 2 from the C_1 and C_6 samples indicating successful isolation of gDNA (Figure 4.2A). A fainter DNA band was observed at the same position in lane 3 which was extracted from the *T. leucotreta* homogenate sample.

Results of the mPCR on the C_1 and C_6 gDNA are shown in Lanes 1 and 2 of Figure 4.2B. Each had a single amplicon of approximately 200 bp indicating amplification of the CrpeNPV-pif1 region. Two bands, one of approximately 400 bp and another of 200 bp were amplified from the *T. leucotreta* homogenate sample shown in Lane 3 indicating both the CrleGV and CrpeNPV amplicons. Multiplex PCR amplification of gDNA extracted from CrleGV OBs showed the production of a single amplicon of approximately 400 bp in Lane 4 as expected for the oligonucleotides targeting the CrleGV-lef4 region. No amplicons were observed in the NTC while two bands were observed in the positive control, one of 400 bp and another of 200 bp. This was expected as the mPCR amplicons shown in Lane 1 of Figure 4.1 were used as template for this positive control to ensure reagents and equipment were functioning correctly.

4.3.3. **Validation of multiplex PCR on artificially mixed samples**

The identification of ThleNPV and CrpeNPV as the same virus in Chapter 3 provided an easily accessible source of NPV OBs from infected *C. peltastica* larvae, which could be used in downstream experiments (Marsberg, 2016). Using gDNA extracted from CrpeNPV and CrleGV OBs, artificial mixtures of the viruses were prepared to test and validate the accuracy of the multiplex PCR technique. Extracted gDNA is shown below in Figure 4.3A with the mPCR results in Figure 4.3B. Oligonucleotide pairs were tested against gDNA from each virus and a combination of template gDNA. Furthermore, mixtures of the oligonucleotide sets were tested against gDNA from each virus and a combination of template gDNA.

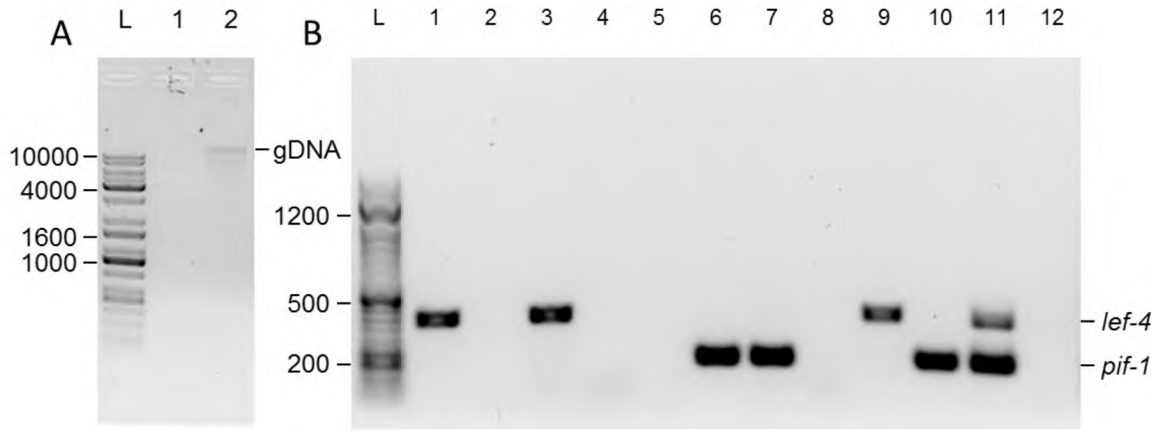

Figure 4.3. Inverted AGE image of A) gDNA extracts from Lane 1 - CrleGV and Lane 2 - CrpeNPV OBs. L – KAPA Universal DNA ladder B) mPCR oligonucleotide testing with CrleGV gDNA against Lane 1 – ClGV-lef4, Lane 2 – CpNPV-pif1, Lane 3 – ClGV-lef4 & CpNPV-pif1 oligonucleotides and Lane 4 – NTC. CrpeNPV gDNA against Lane 5 – ClGV-lef4, Lane 6 – CpNPV-pif1, Lane 7 – ClGV-lef4 & CpNPV-pif1 oligonucleotides and Lane 8 – NTC. ClGV and CpNPV gDNA against Lane 9 - ClGV-lef4, Lane 10 – CpNPV-pif1, Lane 11 – ClGV-lef4 & CpNPV-pif1 oligonucleotides and Lane 12 – NTC. L – PCR Bio III DNA ladder.

The ability of the mPCR to accurately produce the desired amplicons was tested in a series of PCR reactions with these resolved by AGE and shown in Figure 4.3B. Lanes 1 to 4 show the testing of the mPCR oligonucleotides with only CrleGV gDNA as template, lanes 5 to 8 show testing with only CrpeNPV gDNA as template, and lanes 9 to 12 show testing of the oligonucleotide sets with both CrleGV and CrpeNPV gDNA present. For the first set (lanes 1 to 4), amplicons of 400 bp were produced shown in lanes 1 and 3 while lanes 2 and 4 contained no amplicons. Lane 4 shows the negative control with no bands observed.

The second set (lanes 5 to 8) show amplicons of 200 bp in lanes 6 and 7 while lanes 5 and 8 were clear. Once again, no bands were observed in the no template control for this set shown in lane 8. In the last set (lanes 9 to 12) amplicons of 400 bp were observed in lanes 9 and 11 while amplicons of 200 bp were observed in lanes 10 and 11 with lane 12 producing no amplicons. No bands were observed in the negative control lane 12.

The amplicons produced in lanes 1, 6, 9 and 10 were sent to Inqaba Biotech (South Africa) for sequencing. Each sequence was aligned against the target regions in the CrpeNPV and CrleGV genomes and found to be 100 % identical.

4.3.4. Evaluation of CrleGV infected *T. leucotreta* homogenate samples spanning 15 years

Homogenate samples of CrleGV infected *T. leucotreta* larvae spanning 15 years from 2000 to 2015 were supplied by CRI. Analysis of these samples by mPCR could show when CrpeNPV first entered the *T. leucotreta* colony from which these homogenate samples were prepared. Genomic DNA was extracted from the 2000, 2003, 2006, 2009, 2012, and 2015 samples and is shown in Figure 4.4A. Additionally, gDNA was extracted from the 2013, 2014, and 2015 homogenate samples which are shown in Figure 4.4B.

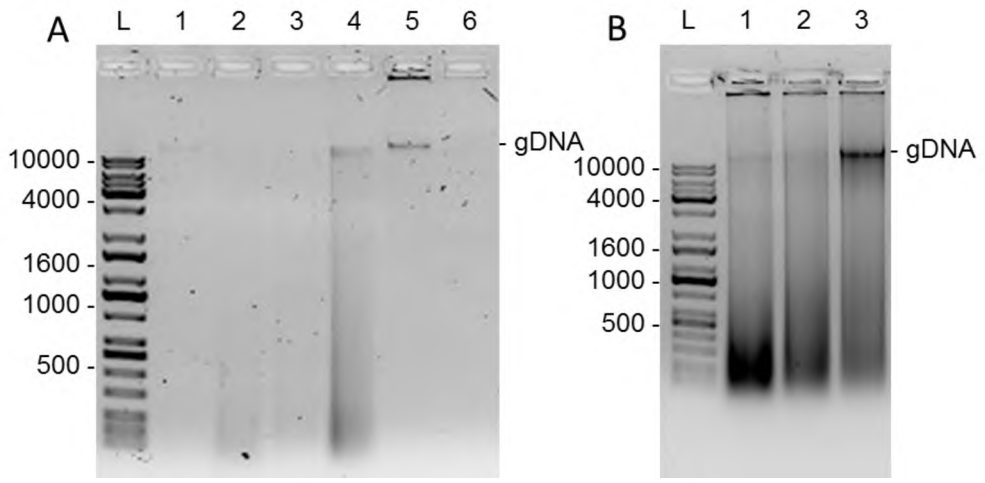

Figure 4.4. gDNA extractions from homogenate samples A) Lane 1 – 2015, Lane 2 – 2012, Lane 3 – 2009, Lane 4 – 2006, Lane 5 – 2003 and Lane 6 – 2000. B) Lane 1 – 2013, Lane 2 – 2014, Lane 3 – 2015. L – KAPA Universal DNA ladder.

gDNA was successfully obtained from the six homogenate samples with concentrations ranging from 3.2 to 100.2 ng/µl as shown in Figure 4.4A. Genomic DNA was also extracted from homogenate samples collected in 2013, 2014, and 2015 as shown in Lanes 1 to 3 of Figure 4.4B. These samples were subjected to the mPCR analysis to determine whether CrleGV and/or CrpeNPV were present in these samples (Figure 4.5A and B).

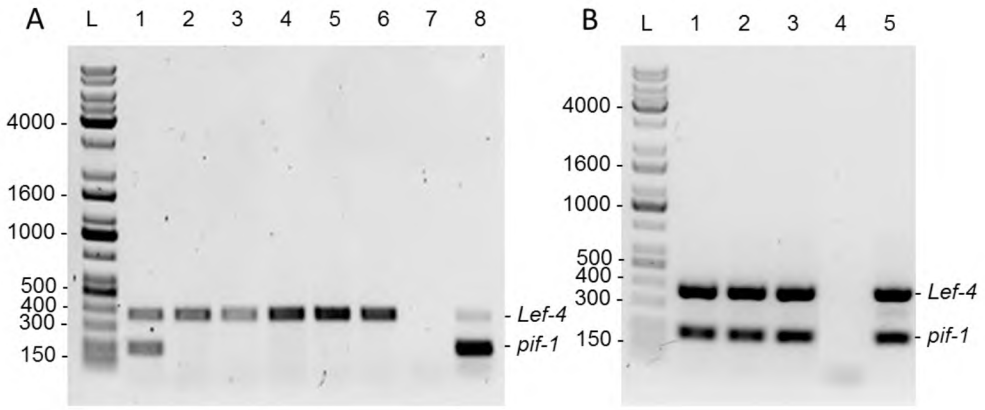

Figure 4.5. Inverted AGE image examining *T. leucotreta* homogenate samples spanning from 2000 to 2015 by mPCR. A) Lane 1 – 2015, Lane 2 – 2012, Lane 3 – 2009, Lane 4 – 2006, Lane 5 – 2003, Lane 6 – 2000, Lane 7 – NTC and Lane 8 – +ve control. B) Lane 1 – 2013, Lane 2 – 2014, Lane 3 – 2015, Lane 4 – NTC and Lane 5 – +ve control. L – KAPA Universal DNA ladder.

First, the multiplex PCR analysis was performed on samples from 2000, 2003, 2006, 2009, 2012, and 2015 alongside negative and positive controls (Figure 4.5A). Control reactions functioned as expected with no amplicons observed in the negative controls and two bands. A larger band of approximately 400bp indicating the CrleGV-lef4 amplicon and a smaller band

of approximately 200bp for the CrpeNPV-pif1 amplicon were observed in the positive controls. Alongside the control reactions, the larger band was observed in all sample reactions indicating the successful amplification of CrleGV-lef4 and the presence of CrleGV in these homogenates. A second band matching the CrpeNPV-pif1 amplicon from the positive control was only observed in the 2015 sample indicating that both CrleGV and CrpeNPV are present in this production homogenate.

To further examine when the virus entered the *T. leucotreta* colony from which the homogenates originated, additional samples from 2013 through to 2016 were examined using the mPCR analysis (Figure 4.5B). Again, no amplification occurred within the negative control while the CrpeNPV-pif1 and CrleGV-lef4 amplicons were observed in the positive control. For the homogenate samples collected from 2013, 2014, and 2015, both amplicons were observed as shown in Lanes 1 to 3. These results indicate that both CrleGV and CrpeNPV are present in the 2013, 2014, and 2015 samples with prior samples containing only CrleGV.

4.3.5. **Development of a quantitative PCR analysis**

The development of a quantitative PCR technique was evaluated using CrleGV and CrpeNPV gDNA. This technique would enable the quantification of CrleGV or CrpeNPV in downstream experiments involving mixed infections. It was first tested with CrleGV gDNA using the ClGV-gp41 oligonucleotides reported in Table 4.1. The technique was then tested with CrpeNPV gDNA in duplicate using the CpNPV-pif1 oligonucleotides. The qPCR amplification curves, melt peaks and standard curves are shown in Figure 4.6 for each virus.

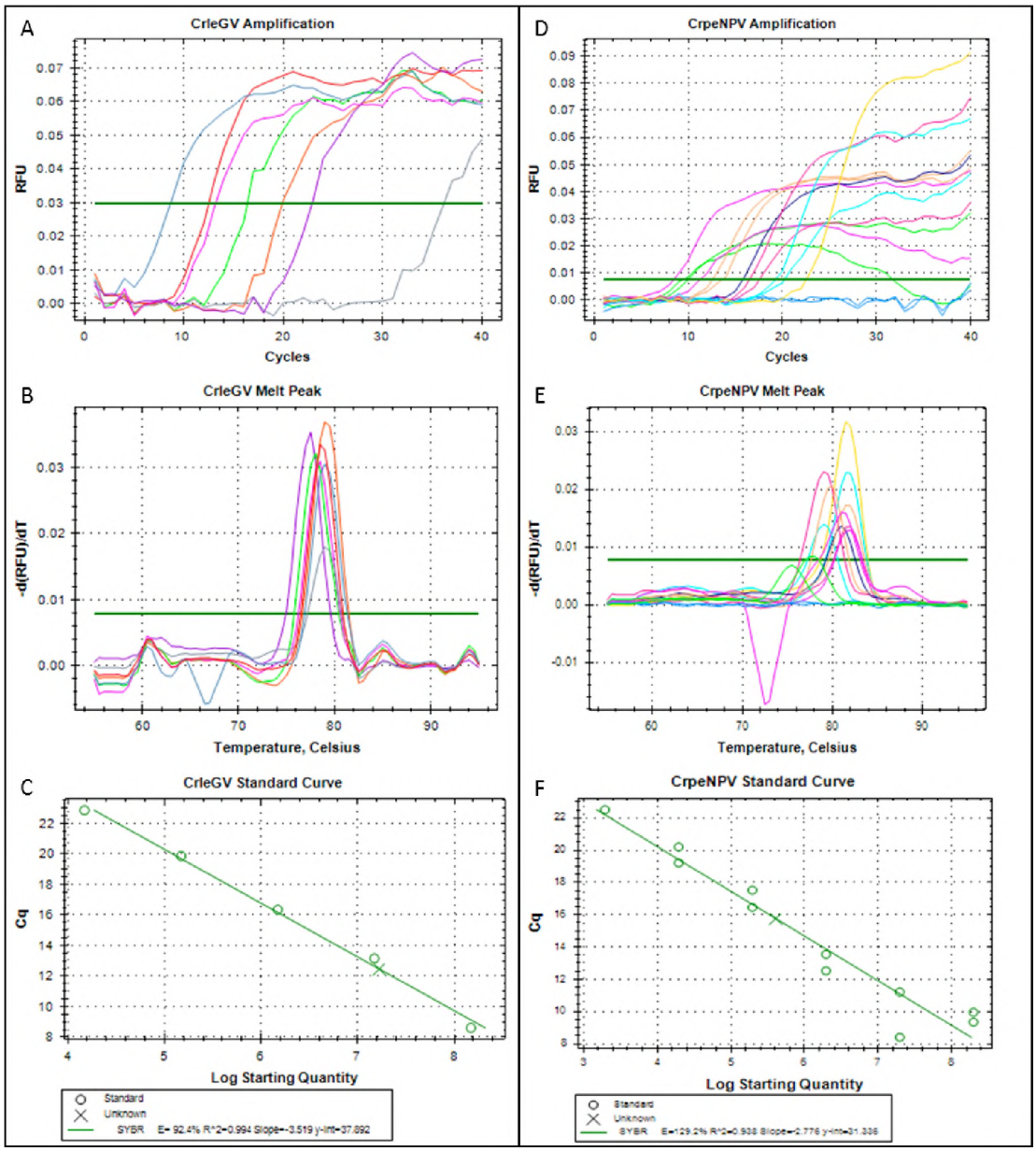

Figure 4.6. Evaluation of a qPCR analysis technique against CrleGV with the A) Amplification curve B) Melt peak and C) standard curves shown. For CrpeNPV the D) Amplification curve E) Melt peak and F) standard curves are also shown.

Development of a qPCR analysis to quantify CrleGV OBs in a test sample is shown in Figure 4.6A, B and C. Amplification curves for each reaction are shown in graph A, with the standards prepared from D2 to D6 each shown to peak after an increasing number of cycles. The unknown sample, shown in red, was observed to have a similar amplification curve as D3 which is shown in pink. The NTC began to produce an amplification curve after cycle 30 and is shown in grey. Standard one did not produce an amplification curve. A single melt peak was observed for CrleGV (Figure 4.6B) indicating a single amplicon was produced for each reaction. Figure 4.6C shows the standard curve produced from the CrleGV standards with the test sample

marked with an ×. This test sample was prepared to have an approximate concentration of 1.49 × 10^7 OBs with the analysis showing a measured concentration of 1.68 × 10^7 OBs and an R^2 value of 0.994.

A test sample of CrpeNPV OBs was also analysed using the qPCR analysis and the CrpeNPV-pif1 oligonucleotides with the results shown in Figure 4.6D, E and F. Amplification curves, shown in Figure 4.6D, were observed for almost all the standards and unknown samples with exception to standard D6 from replicate 1 and the unknown sample in replicate 2. No amplification curve was observed in the NTC. An uneven melt peak was observed for the CrpeNPV analysis as shown in Figure 4.6E, with melting temperatures observed to range from 74 to 84 °C. Analysis of the standard curve, Figure 4.6F, showed the concentration for the test sample to be 4.07 × 10^5 OBs which was close to the calculated value of 3.90 × 10^5 OBs with an R^2 value of 0.938 reported.

4.4. Discussion

This chapter describes the development of an mPCR analysis technique which can be used to screen samples for the presence of CrleGV and/or CrpeNPV in a single reaction. This technique was applied to several samples obtained previously in Chapter 2 as well as several homogenate samples spanning 15-years from 2000 to 2015. The technique was designed to produce amplicons from each virus, which could be easily distinguished from one another forming a qualitative assay. Two regions, pif1 and lef4, were targeted with amplicons of 187 bp and 378 bp, produced when complementary gDNA was present. Furthermore, the pif1 and gp41 oligonucleotides were designed to meet specific criteria, such as the length and melting temperature, enabling them to be further utilised in the qPCR analysis.

The mPCR analysis was first applied to *T. leucotreta* homogenate samples which had been purified by the sucrose cushion method described in Chapter 2. TEM results of this sample showed the presence of both CrleGV and CrpeNPV OBs and, therefore, it was expected that both amplicons would be produced using this sample. At this stage of the project, purified CrpeNPV OBs were unavailable, therefore, each set of oligonucleotides were tested individually against mixed gDNA samples with the expected amplicons produced. This result supports the earlier identification of both viruses in previous TEM images, while also indicating that each oligonucleotide set produced an amplicon of the expected size.

An analysis of the OBs extracted from the *C. pomonella* infection assay, described in Chapter 2, showed the production of only the CrpeNPV-pif1 amplicon after having been exposed to a

mixture of CrpeNPV-ThleNPV OBs. This supports the previous observation by TEM that only NPV OBs were present while also confirming that CrleGV cannot establish an infection in *C. pomonella* (Jehle et al., 1995). It further confirms that the OBs obtained from the *C. pomonella* cadavers were from CrpeNPV and that this host can be used as an *in vivo* system to separate the viruses from CrleGV-CrpeNPV mixtures. These OBs were also checked for the presence of CpGV using a PCR assay described by Motsoeneng, (2014) with oligonucleotides targeting the *egt* gene which produces an amplicon of 1455 bp. No amplicon was generated from the OBs isolated from *C. pomonella* while a positive control using CpGV-SA gDNA produced the expected result (data not shown). This indicated that CpGV was not present in the OBs purified through *C. pomonella* albeit within the limitations of this PCR assay. Additionally, the sample of CrleGV, which was purified by glycerol gradient and observed to contain only GV OBs by TEM, was also tested and found to contain no CrpeNPV OBs with only the larger CrleGV-lef4 amplicon produced.

Using CrleGV and CrpeNPV gDNA, an experiment was performed to fully demonstrate the ability of the mPCR analysis to detect these viruses. A series of validation PCR reactions were performed on gDNA from each virus alone and in combinations against the two mPCR oligonucleotide sets. Samples containing only CrleGV or CrpeNPV gDNA were exposed to each oligonucleotide set alone and in combination. Next, artificial mixtures of the gDNA from both viruses were exposed to each oligonucleotide set alone and in combination. In all instances, amplicons of the correct size were generated. These reactions showed that the ClGV-lef4 oligonucleotides specifically bind to the CrleGV template gDNA while the CpNPV-pif1 set could not. Reactions with the CpNPV-pif1 oligonucleotides showed specific binding to the CrpeNPV gDNA while the ClGV-lef4 set did not produce any non-specific amplicons. To further confirm these results, several amplicons were collected, sequenced, and aligned against the expected target region. In all alignments, sequences were found to be 100 % identical to the target region. This validation experiment confirmed that the correct amplicons are produced when applied to artificial mixtures of viral gDNA and that it can be reliably used to screen samples for CrleGV and CrpeNPV.

The mPCR technique has been applied in previous studies to detect baculoviruses in mixed infections (Kemp et al., 2011; Wennmann and Jehle, 2014). This technique has also been used to screen samples for the presence of baculoviruses in insect populations and in the production of biopesticides for quality control purposes (Manzán et al., 2008; Nealis et al., 2015). Following the validation experiment, the mPCR analysis developed in this study was used in

an applied manner. Homogenate samples which were collected over a 15-year period were screened to determine when CrpeNPV first entered the *T. leucotreta* colony. Samples were screened for the presence of CrleGV and CrpeNPV using this technique, with CrleGV expected in all homogenate samples as these larvae were intentionally infected with this virus around the time of collection. This was confirmed by the mPCR analysis results with the larger CrleGV-lef4 amplicon observed in all samples. The CrpeNPV-pif1 amplicon was observed in the 2013, 2014, and 2015 samples. This result was expected in the 2013 sample as this was the homogenate from which the virus was originally identified. It was, however, an unexpected finding that the virus had persisted in the *T. leucotreta* samples through to 2015, but before definitively stating that the earlier samples do not contain CrpeNPV, consideration should be given as to what the template threshold is for the mPCR analysis to produce positive results. This study did not evaluate the lower limits at which positive results can be obtained. For example, a sample with 99.9 % CrleGV and only 0.01 % CrpeNPV might not produce the pif1 amplicon resulting in a false negative result. This would then give the impression that CrpeNPV is present in the sample, potentially having undesirable consequences should this sample be used in downstream experiments or applications.

The last method to be developed was a qPCR technique which could be utilised to quantify the amount of CrpeNPV or CrleGV OBs in a sample. A study by Zwart et al. (2008) utilised a qPCR assay to quantify AcMNPV genotypes in mixed samples. The assay was shown to be accurate in quantifying the ratio of genotypes. Another study by Wennmann and Jehle, (2014) developed a qPCR assay to quantify AgseGV and AgseNPV in mixed infections. It was reported that the accurate quantification was dependent on the method utilised in purifying OBs. This was particularly relevant to this study, as the method applied to coinfected samples of *T. leucotreta* was guided by these findings to enable correct quantification of GV and NPV OBs. The preliminary results obtained showed that the technique could accurately quantify the test samples in relation to the predefined standards. Further improvement of this technique is possible as the amplification curves and melt peaks were not optimal, however, due to time and cost constraints this was not done here.

In conclusion, an mPCR analysis was developed which could successfully screen samples for CrpeNPV and CrleGV. Analysis of OBs recovered from *C. pomonella* confirmed that this host can be used in an *in vivo* system to separate CrpeNPV from CrleGV in downstream experiments or applied to a variety of homogenate and test samples. After a rigorous validation experiment, this technique was applied to homogenate samples spanning a 15-year period. These results

showed that CrpeNPV entered the *T. leucotreta* colony in 2013 and has persisted into the 2015 samples. This timing also coincides with when the *C. peltastica* colony was introduced into the facility. Finally, a qPCR technique was developed which can be used to quantify the amount of CrpeNPV and CrleGV in samples resulting from mixed infections. This technique could be applied to downstream experiments such as the biological assays.

Chapter 5

Biological assays of CrpeNPV and CrleGV on *Thaumatotibia leucotreta* neonates

5.1. Introduction

Chapters 2 and 4 showed the presence of a novel NPV in homogenate samples prepared from CrleGV infected *T. leucotreta* larvae. This novel virus, first identified as ThleNPV, was shown to be genetically identical to CrpeNPV, an alphabaculovirus isolated from *C. peltastic*a in Chapter 3. This identification created a direct source of NPV OBs for use in downstream experiments including the biological assays. With the development of molecular techniques, the next major objective was to evaluate the biological activity of CrpeNPV and CrleGV, both individually and in combinations. Analysis of these bioassays will assist in determining whether a synergistic interaction occurs in mixed infections, leading to increased virulence and ultimately improved biological control options.

Biological assays are used to establish the virulence of virus against a specific host. Various procedures have been developed to estimate the biological activity of baculoviruses, such as droplet feeding, diet incorporation, and surface dose assays with each having advantages and disadvantages (Grzywacz et al., 2004). For example, droplet feeding assays usually require larvae to be starved before treatment, introducing an additional stress factor. However, an advantage of this method is the ability to accurately quantify the amount of virus consumed by each larva, increasing the accuracy of the assay. Alternatively, surface dose assays reduce the amount of stress placed on the larvae but are less accurate in quantifying the amount of virus ingested. Depending on the methodology used, evaluation of biological activity is calculated as either the lethal concentration (LC), lethal dose (LD), or lethal time (LT) (Grzywacz et al., 2004). These values are represented by the proportion of the target population affected. For example, when estimating LC values, LC_{50} and LC_{90} are calculated each representing the concentration of virus required to achieve a 50 and 90 % mortality of individuals in a sample, respectively.

The biological activity of CrleGV has been previously reported in both laboratory and field applications. As discussed by Moore et al. (2011), the life stage evaluated in the laboratory for

which the LC or LD values are generated should be the same stage which would be targeted in the field. *T. leucotreta* is a cryptic pest of citrus in South Africa. For this reason, neonate larvae are the easiest to target in the field and are commonly used to evaluate the biological activity of CrleGV (Moore et al., 2011; Opoku-Debrah et al., 2016). Similarly, the method of application should assist in developing baculoviruses into biological control agents and, given that formulated viruses are typically applied using a spray system in the field, i.e. topically applied, the surface dose bioassay methodology has been shown to be an ideal choice for CrleGV and other baculoviruses (Abdulkadir et al., 2015; Grzywacz et al., 2004; Moore et al., 2015; Moore, 2002; Opoku-Debrah, 2008).

This study used the surface dose method to evaluate the biological activity of CrpeNPV and CrleGV on *T. leucotreta* neonate larvae. Furthermore, potential synergistic interactions in mixed infections with these viruses were evaluated. Synergistic interactions between baculoviruses has been an area of increased interest, given the possibility of positive effects which could improve the virulence of biological control agents. There are several interactions which can be observed including mutualistic, commensalistic, antagonistic, and neutral, depending on whether there is an improvement, a decline or no change in the biological activity (Cheng and Lynn, 2009). Interactions between baculoviruses have been previously studied with several reports showing improvements in virulence. The insecticidal activity of eight HearSNPV genotypes in different combinations was examined against *H. armigera* in a laboratory setting (Arrizubieta et al., 2015b). The results from this study showed that certain mixtures of these HearSNPV genotypes were more pathogenic than any one genotype in isolation and more than some of the other mixtures tested. Another study investigating interactions between baculoviruses demonstrated a synergistic effect between Anticarsia gemmatalis MNPV (AngeMNPV) and EpapGV (Biedma et al., 2015). *Anticarsia gemmatalis* larvae treated with a 1:120 mixture of AngeMNPV and EpapGV OBs, showed an increase in mortality and decrease in median survival time. Interestingly, no *A. gemmatalis* larvae died when exposed to EpapGV alone. Mixtures of AngeMNPV and EpapGV treated larvae were examined by PCR and shown to not result in co-infections of these viruses. This indicated that the synergistic effect was due to structural components in the EpapGV OB which assist AngeMNPV during infection. Conversely, a separate study investigating co-infections of AgseGV and AgseNPV in *Agrotis segetum* larvae, did not result in increased mortality when compared to single infections of these viruses (Wennmann et al., 2015). This study also noted a decrease in OB production in co-infected larvae suggesting a competitive interaction. In

either instance, be it synergistic or antagonistic, it is important to identify the type of interaction which can occur between baculoviruses which are intended for field use. Positive interactions could have valuable implications for the development of novel mixed biological control products. Alternatively, the identification of negative interactions could assist in improved planning of virus applications should both viruses be utilised within the field.

This chapter aims to determine the biological activity of CrpeNPV and CrleGV in two combinations and alone against *T. leucotreta* neonate larvae. First, biological assays were performed using a surface dose methodology with larvae fed on artificial diet. The results from these assays were used to determine the virulence of these viruses alone and in combination by determining the lethal concentration required to achieve 50 and 90 % mortality. Next, the results from the biological assays were further analysed to identify potential synergistic effects between CrpeNPV and CrleGV.

5.2. Materials and methods

5.2.1. CrleGV and CrpeNPV occlusion body enumeration

CrleGV OBs from infected *T. leucotreta* larvae and CrpeNPV OBs from infected *C. peltastica* larvae were purified by glycerol gradient purification as described in Chapter 2 and used in the biological assays. To confirm each sample of OBs contained only the desired virus, gDNA was extracted from a sample of each batch of OBs and screened using the mPCR method described in Chapter 4. For each virus, OBs were enumerated using a Helber counting chamber (Hawksley®, USA) with a depth 0.02 mm and dark field microscopy. For each virus, 10 µl of OB suspension was diluted 1:5 in ddH_2O and homogenised by vortexing for 15 sec. These dilutions were further diluted 1:5 in 0.07 % SDS producing 1:25 dilutions. The 1:25 dilutions were then sonicated at 60hz with four pulses of 15 seconds. Homogenised 1:25 dilutions were further diluted 1:60 for CrpeNPV and 1:80 for CrleGV, to produce final dilutions of 1:1250 and 1:200 respectively. Three samples, each of 5 µl, were loaded onto the counting chamber with OBs in the top left, bottom left, top right, bottom right and a random central large square, each consisting of 16 smaller squares, counted using a tally counter for each virus. The concentration of OBs was calculated using Equation 5.1.

Equation 5.1. Equation for the determination of OBs.ml^{-1} using a counting chamber.

$$OBs\ per\ ml = (D \times x) \div (N \times V)$$

Where D = dilution factor, x = Average No. of OBs counted, N = Number of small squares and V = Volume.

5.2.2. **Virus dose preparation**

Enumerated virus was used to prepare primary suspensions of 10 ml by diluting the CrpeNPV OBs extract 1:265 and the CrleGV OBs extract 1:66 resulting in concentrations of 5.01×10^{8} and 4.02×10^{9} OBs.ml^{-1} respectively. The primary suspensions were used to prepare 10 µl aliquots of each virus for downstream use and were stored at -20 °C when not in use. These aliquots were diluted 1:100 to produce working suspensions from which the bioassays were carried out. The primary suspensions were thawed intermittently when additional working suspensions were required. Working suspensions were used to prepare dose 1 (D1) for each virus by further diluting each 3.2 and 26.2-fold resulting in D1 concentrations of 1.57×10^{6} and 1.53×10^{6} OBs.ml^{-1} for CrpeNPV and CrleGV respectively. Subsequent doses 2 to 6 (D2-D6) were prepared by a 2.5-fold serial dilution from D1 as shown in Figure 5.1.

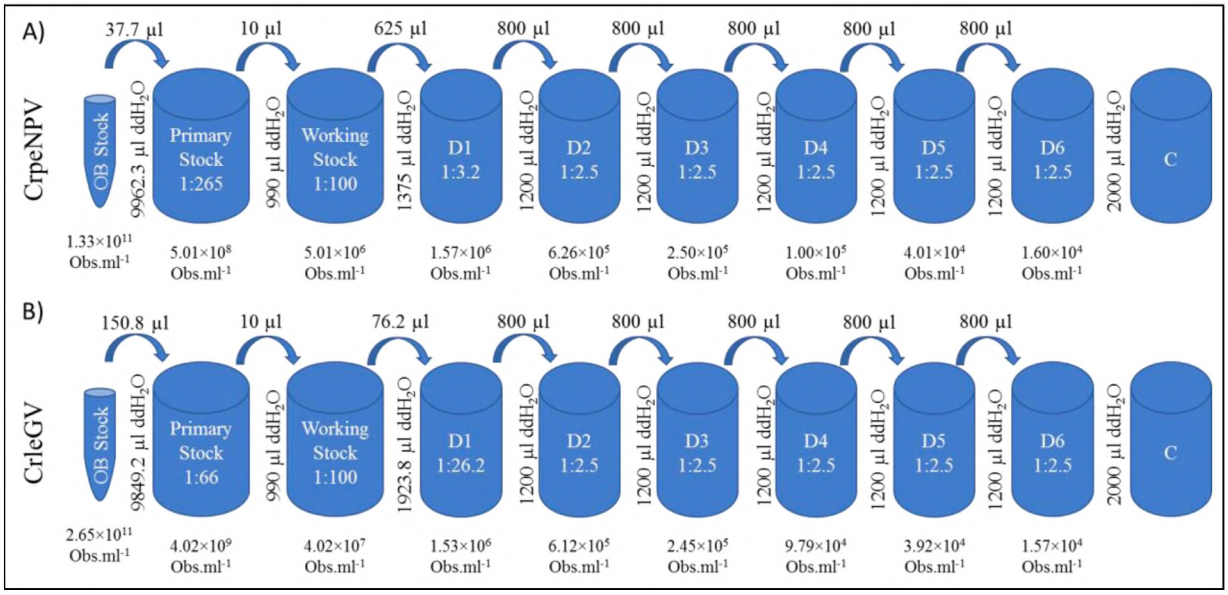

Figure 5.1. Virus dose preparation from primary and working stocks of A) CrpeNPV and B) CrleGV.

Virus treatments used in the mixed virus bioassays were prepared by first preparing D1 for each virus as mentioned above. For the GV:NPV mixture of 1:3, 1500 µl of CrpeNPV D1 was mixed with 500 µl CrleGV D1 and *vice versa* for the GV:NPV mixture of 3:1, with 1500 µl of CrleGV D1 mixed with 500 µl CrpeNPV D1. These mixed D1 samples were then vortexed and used to prepare the subsequent mixed doses 2 to 6 by following the same 2.5-fold serial dilution described above. The final concentrations for each dose are shown in Table 5.1.

Table 5.1. The calculated concentrations (OBs.ml^{-1}) for each of the six dosages used in the single and mixed CrleGV and CrpeNPV biological assays.

Virus (GV:NPV)	Dose 1	Dose 2	Dose 3	Dose 4	Dose 5	Dose 6	Control
NPV	1.57×10^{6}	6.26×10^{5}	2.50×10^{5}	1.00×10^{5}	4.01×10^{4}	1.60×10^{4}	0
1:3	1.56×10^{6}	6.23×10^{5}	2.49×10^{5}	9.96×10^{4}	3.98×10^{4}	1.59×10^{4}	0
3:1	1.54×10^{6}	6.15×10^{5}	2.46×10^{5}	9.85×10^{4}	3.94×10^{4}	1.58×10^{4}	0
GV	1.53×10^{6}	6.12×10^{5}	2.45×10^{5}	9.79×10^{4}	3.92×10^{4}	1.57×10^{4}	0

5.2.3. **Surface dose biological assays**

A total of 4 surface dose biological assay were carried out, each in triplicate for CrleGV and CrpeNPV, and 1:3 and 3:1 mixed CrleGV to CrpeNPV treatments. Each assay was carried out using neonate *T. leucotreta* larvae reared on artificial diet. Artificial diet was prepared by baking 250 g of diet (Moore et al., 2014) mixed with 200 ml of ddH_2O at 200 °C for 30 minutes in a flat baking dish. Plugs of diet were transferred into 24 well plates and compressed with a syringe plunger. *T. leucotreta* eggs laid on wax paper were incubated in petri dishes at 25 °C with a RH of ± 30-60 % until hatching. For each virus treatment, seven plates were prepared by inoculating each plate with either one of the six doses and ddH_2O as a control. Each well was surface inoculated with 50 µl of the respective dose or water for the control. Plates were left for the wells to dry with the lids on before transferring a single neonate larva to each inoculated well. Once all seven plates had been prepared, larvae were left to feed on the treated diet for 7 days in a controlled environment of 25 °C with a RH of ± 30-60 %. After 7 days, diet plugs in each well were inspected for surviving larvae or larval cadavers with the number of dead larvae tallied for each treatment.

5.2.4. **Biological assay data analysis and calculations**

Data obtained from each bioassay were analysed using the ToxRat V3.2.1 (ToxRat Solutions, Germany) software. Dose response effects were determined by linear regression using a probit model and linear maximum likelihood. Confidence limits were based on Fieller's theorem with a minimum acceptable p (Chi-Squared) significance level set to 0.1. Control mortality was compensated for in ToxRat using Abbott's correction. Lethal concentrations at 50 % (LC_{50}) and 90 % (LC_{90}) were calculated from the linear regression.

Synergistic interactions were evaluated using the Tammes-Bakuniak graphical method (Lara-Reyna et al., 2003). The LC_{50} or LC_{90} values of CrpeNPV and CrleGV in isolation were plotted along each axis defining the equitoxic line. The zone above this line indicates antagonistic effects while synergistic effects are identified below the line. The fiducial limits were further plotted for each virus, creating a zone around the equitoxic which indicates an additive effect. LC_{50} and LC_{90} values for the mixed treatments are plotted onto the respective graphs with the corresponding zone identified.

5.3. Results

5.3.1. CrleGV and CrpeNPV OB enumeration and dose preparation

Purified OBs were successfully obtained for each virus, with the purity of each examined by the mPCR technique developed in Chapter 4. Genomic DNA extracted from CrleGV and CrpeNPV OBs was amplified using a mixture of ClGV-lef4 and CpNPV-pif1 oligonucleotides (Figure 5.2).

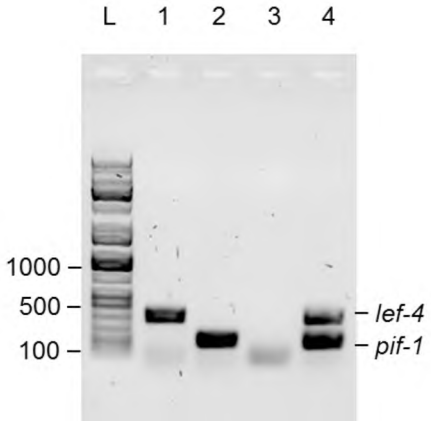

Figure 5.2. Inverted AGE image of the multiplex PCR analysis on the CrleGV and CrpeNPV OBs used in the biological assays. Lane 1 – CrleGV OBs, Lane 2 – CrpeNPV OBs, Lane 3 – NTC, Lane 4 – positive control. L – KAPA Universal DNA Ladder.

Single amplicons were observed in the mPCR analyses for each virus shown in lanes 1 and 2 of Figure 5.2. A band of approximately 400 bp was observed in the CrleGV sample shown in lane 1 matching the CrleGV-lef4 amplicon. A smaller band of approximately 200 bp was observed in the CrpeNPV sample in lane 2 matching the CrpeNPV-pif1 amplicon. Both the negative and positive controls produced the expected bands.

Before performing the biological assays, several pilot assays were performed (data not shown) to help identify the range of virus concentrations required to achieve between 20 and 90 % mortality, which is suitable for statistical analysis. Using the results from these pilot assays,

the dilution factors shown in Section 5.2.2 were calculated. Primary stocks of each virus were prepared to prevent excessive freeze-thawing of doses. This was done to prevent potential damage to the OBs due to changes in storage conditions and mitigate any resulting variation in virulence (Sireesha et al., 2010).

5.3.2. **Biological activity of CrleGV and CrpeNPV against *T. leucotreta* neonates**

Surface dose bioassays were performed using either CrleGV or CrpeNPV OBs against *T. leucotreta* neonate larvae. A total of three replicates were performed for each virus, with each consisting of six dosages used alongside a control containing ddH_20. The observed mortality, corrected mortalities and regression Probits are shown in Table 5.2 for each virus.

Table 5.2. Results from the CrleGV and CrpeNPV bioassays showing the mortality, corrected mortality and regression Probit values for each treatment.

CrleGV				CrpeNPV			
Treatment OBs.ml^{-1}	**Mortality (%)**	**Corrected Mortality (%)**	**Reg. Probit**	**Treatment**	**Mortality (%)**	**Corrected Mortality (%)**	**Reg. Probit**
Control	9.7	0.0		Control	9.7	0.0	
1.57×10^4	27.8	20.0	-0.795	1.60×10^4	27.8	20.0	-0.842
3.92×10^4	45.8	40.0	-0.433	4.01×10^4	41.7	35.4	-0.463
9.79×10^4	48.6	43.1	-0.072	1.00×10^5	50.0	44.6	-0.086
2.45×10^5	63.9	60.0	0.291	2.50×10^5	63.9	60.0	0.292
6.12×10^5	72.2	69.2	0.653	6.26×10^5	73.6	70.8	0.671
1.53×10^6	90.3	89.2	1.015	1.57×10^6	90.3	89.2	1.050

5.3.2.1. **CrleGV biological assay**

The first set of bioassays was performed using only CrleGV with virus dosages ranging from 1.57×10^4 to 1.53×10^6 OBs.ml^{-1}. The survival rate and concentration-effect curve for this bioassay are shown in Figure 5.3.

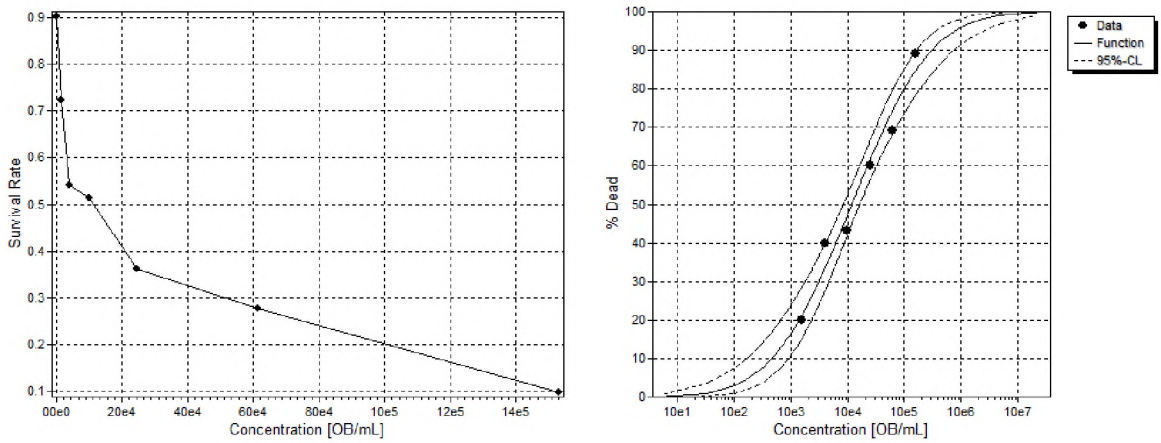

Figure 5.3. Analysis of surface dose bioassay 7 days' post infection using CrleGV against *T. leucotreta* neonate larvae A) Survival rate of larvae when treated with increasing concentrations of CrleGV OBs B) Concentration-effect curve indicating the percentage mortality with increasing concentrations of CrleGV OBs with the 95 % confidence level shown.

Regression analysis of the first bioassay using CrleGV against *T. leucotreta* neonate larvae indicated a Chi-squared value of 4.305 and p (Chi-squared) value greater than 0.1, indicating a good fit of the regression line. Furthermore, a statistically significant concentration response found with p (F) less than 0.001 with four degrees of freedom. Probit analysis of the data obtained indicated a LC_{50} of 1.17×10^5 and an LC_{90} of 3.00×10^6 OBs.ml^{-1} (Table 5.3) with the response corrected by 9.7 % for control mortality.

Table 5.3. The LC_{50} and LC_{90} for the CrleGV bioassay against *T. leucotreta* neonate larvae.

Lethal Concentration	Concentration (OBs.ml^{-1})	95 % confidence limits	
		Lower	Upper
LC_{50}	1.17×10^5	8.34×10^4	1.61×10^5
LC_{90}	3.00×10^6	1.62×10^6	7.47×10^6

5.3.2.2. CrpeNPV biological assay

The virulence of CrpeNPV alone was tested against neonate *T. leucotreta* larvae in a surface dose bioassay. Virus dosages ranged from 1.60×10^4 to 1.57×10^6 OBs.ml^{-1}. The survival rate and concentration-effect curve for this bioassay are shown in Figure 5.4.

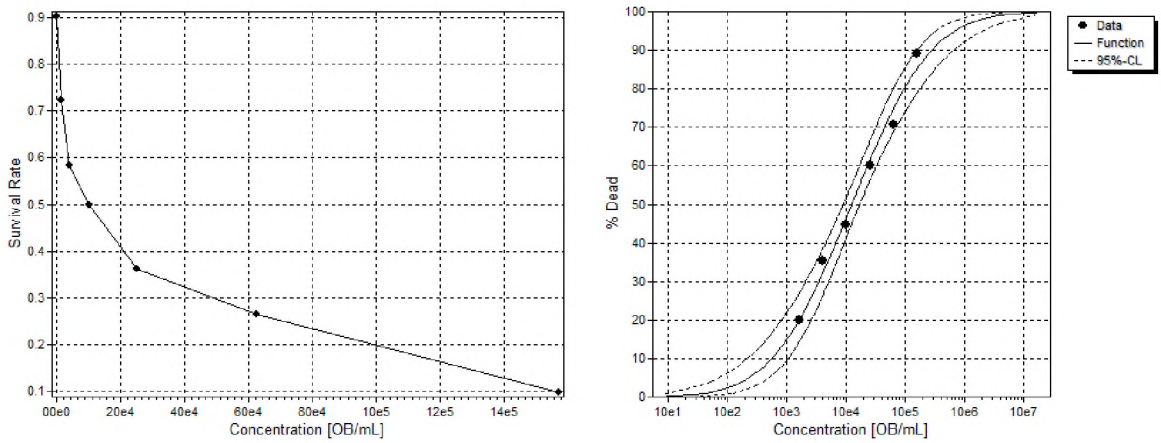

Figure 5.4. Analysis of surface dose bioassay 7 days' post infection using CrpeNPV against *T. leucotreta* neonate larvae A) Survival rate of larvae when treated with increasing concentrations of CrpeNPV OBs B) Concentration-effect curve indicating the percentage mortality with increasing concentrations of CrpeNPV OBs with the 95 % confidence level shown.

A Chi-squared value of 2.047 was calculated from the regression analysis of the CrpeNPV bioassay with the p (Chi-squared) value greater than 0.1 indicating a good fit of the regression line to the data. A statistically significant concentration response was found with p (F) less than 0.001 with four degrees of freedom. Probit analysis of the data obtained indicated an LC_{50} of 1.23×10^5 and an LC_{90} of 2.75×10^6 OBs/ml (**Table 5.4**) with a control response of 9.7 % corrected for.

Table 5.4. The LC_{50} and LC_{90} for the CrpeNPV bioassay against *T. leucotreta* neonate larvae.

Lethal Concentration	Concentration (OBs.ml^{-1})	95 % confidence limits	
		Lower	Upper
LC_{50}	1.23×10^5	8.88×10^4	1.67×10^5
LC_{90}	2.75×10^6	1.57×10^6	6.42×10^6

5.3.3. Biological activity of mixed CrleGV and CrpeNPV samples against *T. leucotreta* neonates

A second set of surface dose bioassays were performed using combinations of CrleGV and CrpeNPV OBs against *T. leucotreta* neonate larvae. These combinations were performed at a ratio of 3:1 or 1:3 of CrleGV and CrpeNPV respectively. For each of the mixed bioassays, a total of three replicates were performed for each combination, with each consisting of six mixed dosages used alongside a control. The observed mortality, corrected mortalities and regression Probits are shown in Table 5.5 for each virus.

Table 5.5. Results from the mixed CrleGV and CrpeNPV bioassays showing the mortality, corrected mortality and regression Probit values for each treatment.

CrleGV:CrpeNPV 3:1				CrleGV:CrpeNPV 1:3			
Treatment OBs.ml^{-1}	**Mortality (%)**	**Corrected Mortality (%)**	**Reg. Probit**	**Treatment**	**Mortality (%)**	**Corrected Mortality (%)**	**Reg. Probit**
Control	2.8	0.0		Control	5.6	0.0	
1.58×10^4	25.0	22.9	-0.856	1.59×10^4	20.8	16.2	-0.938
3.94×10^4	31.9	30.0	-0.393	3.98×10^4	37.5	33.8	-0.403
9.85×10^4	51.4	50.0	0.071	9.96×10^4	63.9	61.8	0.131
2.46×10^5	75.0	74.3	0.535	2.49×10^5	72.2	70.6	0.664
6.15×10^5	86.1	85.7	0.999	6.23×10^5	87.5	86.8	1.198
1.54×10^6	91.7	91.4	1.464	1.56×10^6	97.2	97.1	1.733

5.3.3.1. **CrleGV dominant biological assays**

The first of the virus combination bioassays was performed using a mixture of CrleGV and CrpeNPV at a ratio of 3:1 with virus dosages ranging from 1.58×10^4 to 1.54×10^6 OBs.ml^{-1}. Individual virus concentrations ranged from 1.17×10^4 to 1.15×10^6 OBs.ml^{-1} and 4.01×10^3 to 3.91×10^5 OBs.ml^{-1} for CrleGV and CrpeNPV respectively. The survival rate and concentration-effect curve for this bioassay are shown in Figure 5.5.

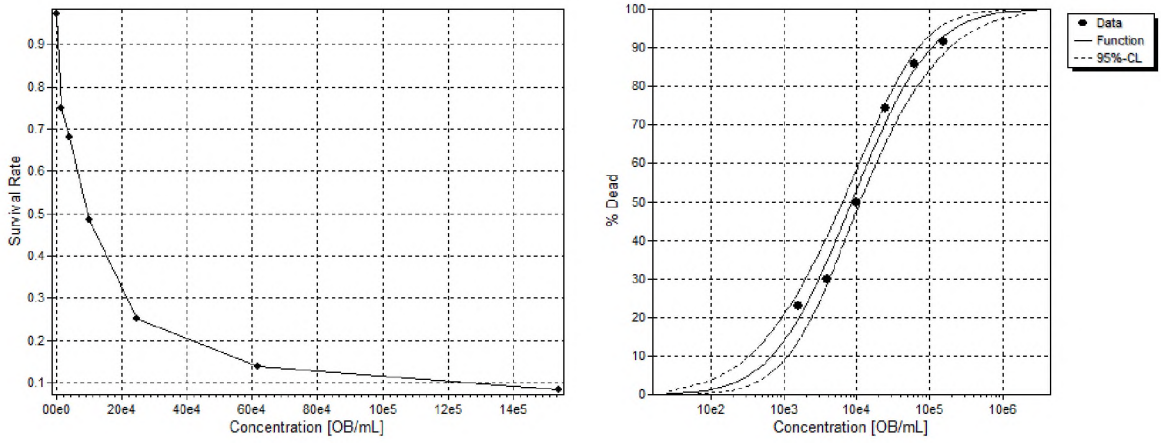

Figure 5.5. Analysis of surface dose bioassay 7 days' post infection using a 3:1 mixture of CrleGV and CrpeNPV-SA against *T. leucotreta* neonate larvae A) Survival rate of larvae when treated with increasing concentrations of OBs B) Concentration-effect curve indicating the percentage mortality with increasing concentrations of OBs with the 95 % confidence level shown.

The first bioassay using mixtures of CrleGV and CrpeNPV-SA at a ratio of 3:1 against *T. leucotreta* neonate larvae was calculated to have a Chi-squared value of 2.309 and p (Chi-squared) value greater than 0.1, indicating a good fit of the regression line to the recorded data. A p (F) value less than 0.001 was calculated indicating a statistically significant concentration response measured with four degrees of freedom. Probit analysis of the data obtained indicated an LC_{50} of 8.55×10^4 and an LC_{90} of 1.07×10^6 OBs.ml^{-1} (Table 5.6) with a control mortality of 2.8 % corrected for.

Table 5.6. The LC_{50} and LC_{90} for the 3:1 mixture of CrleGV and CrpeNPV-SA bioassay against *T. leucotreta* neonate larvae.

Lethal Concentration	Concentration (OBs.ml^{-1})	95 % confidence limits	
		Lower	Upper
LC_{50}	8.55×10^4	6.41×10^4	1.11×10^5
LC_{90}	1.07×10^6	7.07×10^5	1.90×10^6

5.3.3.2. CrpeNPV Dominant Biological Assays

The second set of virus combination bioassays was performed using a mixture of CrleGV and CrpeNPV at a ratio of 1:3 with virus dosages ranging from 1.59×10^4 to 1.56×10^6 OBs.ml^{-1}. Individual virus concentrations ranged from 3.92×10^3 to 3.82×10^5 OBs.ml^{-1} and 1.20×10^4 to 1.17×10^6 OBs.ml^{-1} for CrleGV and CrpeNPV respectively. The survival rate and concentration-effect curve for this bioassay are shown in Figure 5.6.

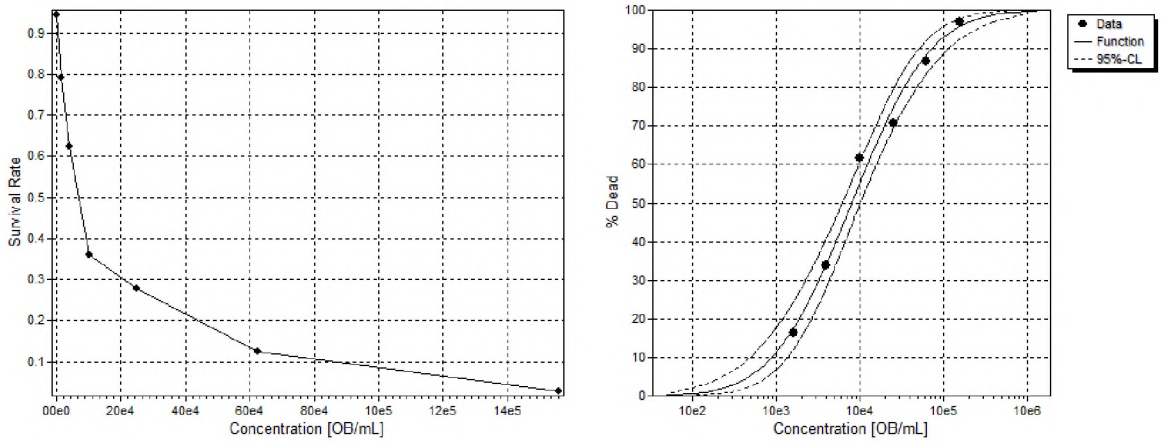

Figure 5.6. Analysis of surface dose bioassay 7 days' post infection using a 1:3 mixture CrleGV and CrpeNPV against *T. leucotreta* neonate larvae A) Survival rate of larvae when treated with increasing concentrations of OBs B) Concentration-effect curve indicating the

percentage mortality with increasing concentrations of OBs with the 95 % confidence level shown.

The second bioassay carried out using mixtures of CrleGV and CrpeNPV at a ratio of 3:1 against *T. leucotreta* neonate larvae was calculated to have a Chi-squared value of 2.446 with a p (Chi-squared) value greater than 0.1, indicating a good fit of the regression line to the recorded data. The p (F) value was again calculated to be less than 0.001 similarly indicating a statistically significant concentration response with four degrees of freedom. Probit analysis of the data obtained indicated a LC_{50} of 7.95×10^4 and an LC_{90} of 7.18×10^5 OBs.ml^{-1} (Table 5.7)

Table 5.7. The LC_{50} and LC_{90} for the 1:3 mixture of CrleGV and CrpeNPV bioassay against *T. leucotreta* neonate larvae.

Lethal Concentration	Concentration (OBs.ml^{-1})	95 % confidence limits	
		Lower	Upper
LC_{50}	7.95×10^4	6.14×10^4	1.00×10^5
LC_{90}	7.18×10^5	5.04×10^5	1.14×10^6

5.3.4. Evaluation of synergistic or antagonistic interactions between CrpeNPV and CrleGV

The interaction between CrleGV and CrpeNPV in the mixed bioassays was evaluated to determine whether a synergistic, additive or antagonistic interaction was occurring. The LC_{50} values and fiducial limits for the viruses in isolation were plotted along each axis defining these three zones as shown in Figure 5.7.

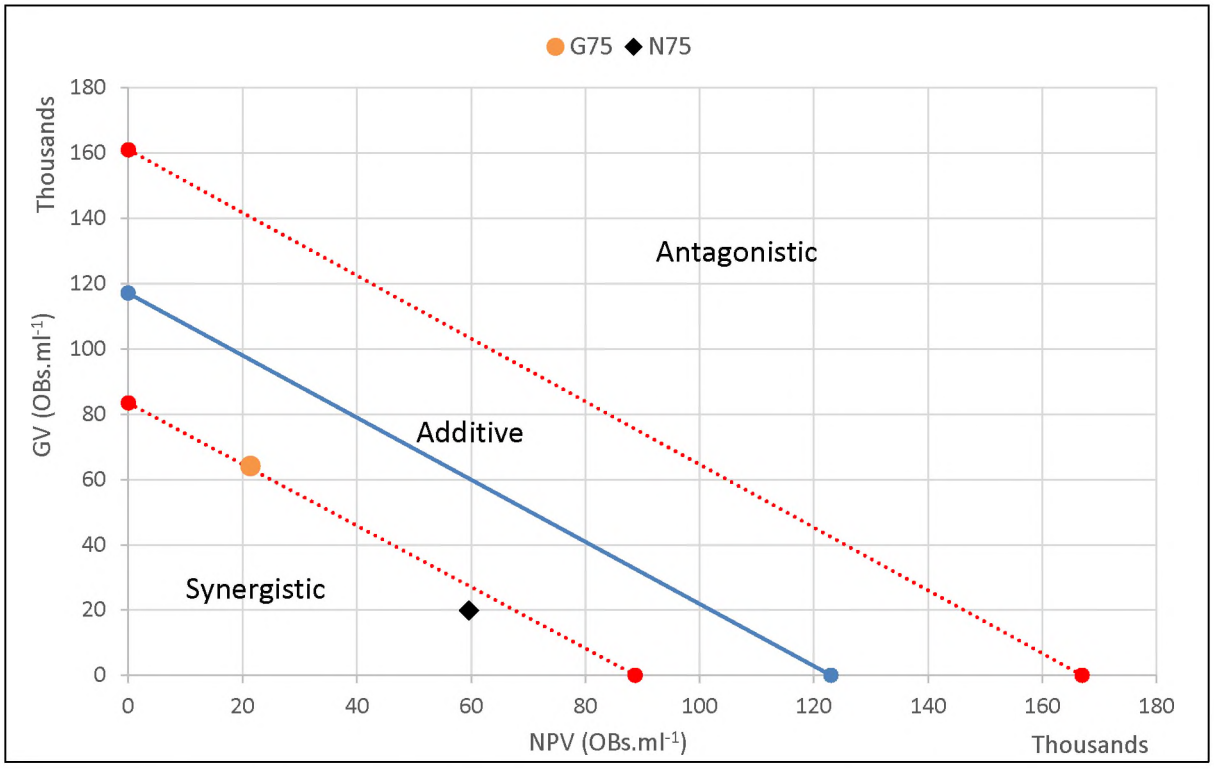

Figure 5.7. Thames-Bakuniak plot of the synergistic interaction between CrpeNPV and CrleGV at the LC_{50}. The solid line indicates the equitoxic line with the 95 % upper and lower fiducial limits shown by the dotted lines. The GV and NPV dominant mixtures are shown as a circle and diamond respectively (Lara-Reyna et al., 2003).

Analysis of the LC_{50} values for the viruses in the two combinations showed an additive effect in the CrleGV dominant mixture shown as the orange circle in Figure 5.7. This indicates no significant divergence from the LC_{50} values from each of the virus when applied in isolation effectively showing an additive effect. In contrast, the CrpeNPV dominant mixture was observed to have a synergistic effect, indicating a lower net concentration of each virus was required to achieve 50 % mortality. Overall, mixtures of CrpeNPV and CrleGV showed improved LC_{50} values with a 1.4-fold and 1.5-fold decrease observed for the GV dominant and NPV dominant treatments respectively.

The LC_{90} values for the mixtures were also examined using the same method with the results shown in Figure 5.8.

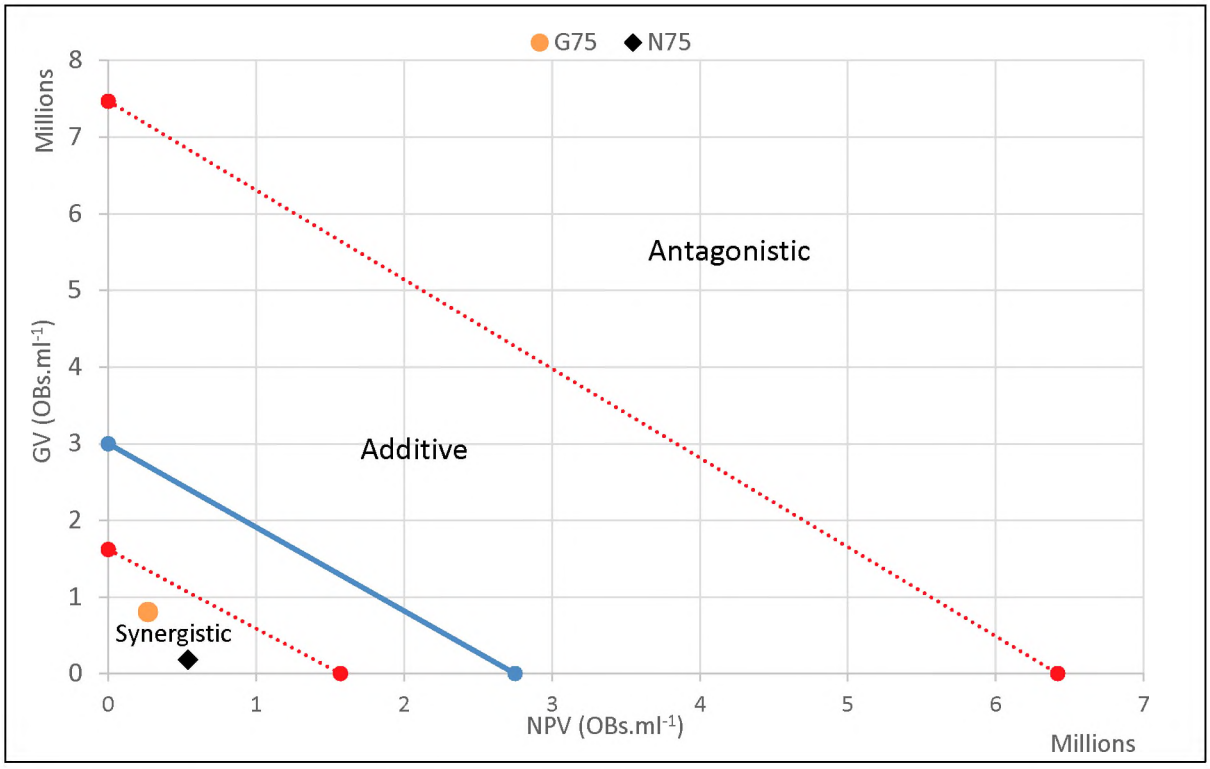

Figure 5.8. Thames-Bakuniak plot of the synergistic interaction between CrpeNPV and CrleGV at the LC_{90}. The solid line indicates the equitoxic line with the 95 % upper and lower fiducial limits shown by the dotted lines. The GV and NPV dominant mixtures are shown as a circle and diamond respectively (Lara-Reyna et al., 2003).

A synergistic effect was observed for both the CrleGV and CrpeNPV dominant mixtures at LC_{90}. Unlike the LC_{50} synergism plot, both mixtures were observed to fall well within the synergistic zone, indicating a more profound effect with increasing concentration (Figure 5.8). This improvement of LC_{90} was a 2.8-fold and 2.6-fold decrease for the GV dominant mixture when compared to the GV and NPV only treatments respectively. The NPV dominant mixture showed the highest level of improved LC_{90} values with a 4.2-fold and 3.8-fold decrease when compared to the GV and NPV only treatments respectively

5.4. Discussion

In this chapter, the biological activity of CrpeNPV and CrleGV was evaluated against *T. leucotreta* neonate larvae using a surface dose assay. Each virus was evaluated alone and in combinations with the data obtained used to determine the LC_{50} and LC_{90} values. This data was further analysed with the aim of identifying potential synergistic effects which result in increased mortality.

No major difference was observed in the LC_{50} or LC_{90} values obtained between each virus when applied to *T. leucotreta* neonate larvae individually. These results differ slightly to an

earlier study by Marsberg, (2016) whereby surface dose bioassays conducted with CrpeNPV and CrleGV against *T. leucotreta* neonate larvae showed a 1.8-fold decrease in LC_{50} in the NPV treatment when compared to the GV treatment (Table 5.8). This improvement was, however, not observed in the LC_{90} values. Additionally, the LC_{50} and LC_{90} values determined by Marsberg, (2016) were lower than observed in this study, with LC_{50} values 28 and 50-fold lower and LC_{90} values 25 and 27-fold lower for CrleGV and CrpeNPV respectively. It is unclear why this variation in the LC values was observed. However, there may have been differences in colony health, environmental conditions or the methods used for data analysis.

Table 5.8. Table of CrleGV and CrpeNPV LC_{50} and LC_{90} values against *T. leucotreta* previously reported by Marsberg, (2016).

Virus	LC_{50}	LC_{90}
CrpeSNPV	2.29×10^3	9.97×10^4
CrleGV	4.09×10^3	1.18×10^5

A comparison between the results obtained in the mixed treatments from this study to published data is not possible as this is the first evaluation of this kind on CrpeNPV. Two artificial mixtures of CrpeNPV and CrleGV were prepared and used in this chapter at ratios of 3:1 and 1:3 for each virus respectively. Studies involving mixtures of different baculovirus genotypes have employed 1:9, 1:3, and 1:1 ratios, with these chosen to help elucidate how different combinations of each virus would affect the virulence (Arrizubieta et al., 2015b; Simón et al., 2006; Virto et al., 2017). Comparison of the LC values for the mixtures against those recorded for each virus in isolation in this study showed increased levels of mortality, particularly at the LC_{90}. These results show that combinations of the viruses result in a synergistic effect, improving the biological activity especially when applying the viruses at higher concentrations. The improvement observed in mortality in these mixed infections supports studies which have shown similar results with mixtures of other baculoviruses (Arrizubieta et al., 2015a, 2015b; Biedma et al., 2015; Lara-Reyna et al., 2003). Combinations of AngeMNPV and EpapGV increased mortality rates from approximately 40 to 80 % and decreased the median survival time by 2 days in *A. gemmatalis* larvae. Similarly, combinations of AcMNPV with either TnSNPV or TnGV were found to have a synergistic effect improving the LC_{50} by 8 and 10.7 times respectively (Lara-Reyna et al., 2003).

It is also important to note that CrleGV has been successfully utilised as a commercial biological control agent of *T. leucotreta* in the field for over 10 years (Moore et al., 2015; S.

Moore et al., 2004). However, the risk of *T. leucotreta* developing resistance to this virus, as was seen with *C. pomonella* and CpGV in Europe (Asser-Kaiser et al., 2011, 2010, 2007; Jehle et al., 2014), shows the importance of identifying novel control agents and/or approaches which can help prevent such a scenario occurring in South Africa. The results obtained in this chapter suggest that CrpeNPV could be utilised as a separate control agent to CrleGV in the field, having achieved similar levels of reduction of *T. leucotreta* larvae in the biological assays. The addition of CrpeNPV as an individual control option to integrated pest management programmes would further decrease the risk of resistance developing to either CrleGV or CrpeNPV. The improved levels of control recorded in both mixed treatments could also lead to the development of several novel CrpeNPV and CrleGV formulations which could be tested and commercialised for field use. Another potential application of mixed CrpeNPV and CrleGV formulations may be to enable the continued use of both should resistance develop towards either virus individually. An example of this was observed in *C. pomonella* whereby resistance was recorded to the Mexican isolate CpGV-M which was shown to be unable to replicate. However, when mixed with the resistance overcoming isolate CpGV-R5, both CpGV-R5 and CpGV-M could replicate (Graillot et al., 2016). While further investigation is still required, the same might be observed with CrpeNPV and CrleGV with mixtures of these viruses potentially used to overcome resistance which could develop towards either virus or isolates of these viruses independently.

In conclusion, this chapter reports the biological activity of CrpeNPV and CrleGV applied alone and in combinations against *T. leucotreta* neonate larvae. A synergistic effect was observed in the mixed treatments with up to a 4.2-fold improvement observed. These results indicate that both CrleGV and CrpeNPV could be utilised as biological control agents in the field as separate formulations. Furthermore, improved control might be observed in the field when using mixtures of these viruses. The next chapter describes the infection of multiple generations of 3rd and 4th instar *T. leucotreta* larvae from which the resulting OBs are examined using the mPCR and qPCR techniques to evaluate CrpeNPV and CrleGV co-infections.

Chapter 6

The sequential passage of CrpeNPV and CrleGV in *Thaumatotibia leucotreta* larvae to evaluate mixed interactions

6.1. Introduction

In the previous chapter, the biological activity of CrpeNPV and CrleGV was evaluated against *T. leucotreta* neonate larvae both alone and in combination. A synergistic effect was observed between CrpeNPV and CrleGV, particularly in the NPV:GV mixture at a ratio of 3:1, indicating an interaction was occurring between these viruses during the infection process. However, the use of neonate larvae in the biological assays prevented sufficient larval tissue being recovered for additional downstream analysis using the multiplex and quantitative PCR assays for detection of each virus in deceased larvae. To further understand the interactions between CrpeNPV and CrleGV, a series of infections using four treatments, namely CrleGV and CrpeNPV and 3:1 (GV dominant or G3) and 1:3 (NPV dominant or N3) mixtures of these virus, were applied by serial passage against multiple *T. leucotreta* larvae. In this serial passage assay, virus was recovered at each stage to examine how mixed infections change across multiple consecutive infections.

The consecutive inoculation of baculovirus OBs from one population of larvae to another by serial passage has been shown to be an important technique with a variety of applications. The isolation of baculovirus genotypes has been successfully achieved by serial passage and plaque assay of infected insect cell lines (López-Ferber et al., 2003). Serial passage of baculoviruses has also been utilised in the adaptation of baculoviruses, such as CpGV or PhopGV, to heterologous hosts such as *Grapholita molesta* and *Tecia solanivora* (Gómez-Bonilla et al., 2011; Graillot et al., 2017; Moscardi, 1999). In each case, successive passage of CpGV or PhopGV in the respective heterologous host resulted in improved insecticidal activity while the CpGV isolate still conserved the same level of activity in its homologous host *C. pomonella*. Serial passage has also been shown to be useful in adapting non-permissive CpGV isolates to

C. pomonella larvae, which have been shown to exhibit selective resistance (Graillot et al., 2014).

The application of serial passage has also been used to examine the dynamics of baculoviruses in mixed infections, investigating the frequency at which different genotypes are present in diseased larvae. Studies by Clavijo et al., (2009) and Simón et al., (2006) examined the frequency of Spodoptera frugiperda MNPV (SfMNPV) complete and deletion genotypes in *Spodoptera frugiperda* larvae. Mixtures of these genotypes were used to infect larvae and the recovered OBs used to infect additional larvae by serial passage. Various mixtures including a 9:1 and 1:9 ratio of the deletion and complete genotypes respectively were used as the initial inoculum with infections continued up to a passage number of five. Interestingly, these studies found that the ratio of the deletion and complete genotypes in the artificial mixtures returned to the original frequency first observed in wildtype isolate from which these genotypes were recovered. Another study by Arrizubieta et al. (2015b) investigated the stability of co-occluded mixtures of HearSNPV genotypes following serial passage in *Helicoverpa armigera* larvae. The initial inoculum consisted of a binary mixture with a 1:1 ratio of these genotypes with the changes in frequency measured across five consecutive passages through fourth instar larvae. A significant change in genotype frequency was observed in OBs collected, shifting from a 1:1 to approximately 1:6 ratio by the final passage. Additionally, a decrease in the meantime to death and an increase in relative potency were observed by the final passage. While these studies demonstrate that baculovirus genotype mixtures are likely to shift in composition across multiple passages, little research, if any, has been performed to evaluate the changes in dual infections consisting of two different baculoviruses.

When studying the interactions between different baculoviruses, it is important to consider both potential covert infections and recombination events. For example, a review by Williams et al. (2017) discusses the various mechanisms and importance of covert baculovirus infections in lepidopteran insects. It was reported that laboratory insect populations are likely to contain covert baculovirus infections which under certain stress factors can become overt resulting in symptomatic baculovirus infections because of increased virus replication. An example of this was observed in *T. leucotreta* whereby the overcrowding of larvae in a laboratory setting triggered covert infections to become overt, resulting in the isolation of novel CrleGV isolates (Opoku-Debrah et al., 2013). Additional stress factors associated with triggering an overt infection in covertly infected larvae include changes in temperature, humidity, and starvation (David and Gardiner, 1966, 1965; Fuxa et al., 1999; Kouassi et al., 2009; Williams et al., 2017).

However, a superinfection, whereby a second virus challenges the host, has been shown to consistently trigger covert infections to become overt (Cooper et al., 2003; Fuxa et al., 2002; Kouassi et al., 2009; Williams et al., 2017). Consideration must therefore be given to a potential covert CrleGV and/or CrpeNPV infection becoming overt in *T. leucotreta* larvae during any laboratory experiment.

Serial passage of mixed baculovirus treatments has also been reported to result in recombination between the viral genomes during replication in infected larvae. For example, mixed infections of the closely related BmNPV and AcMNPV in both insect cell lines and the larvae of *Heliothis virescens* were examined post-coinfection for recombination events (Kamita et al., 2003). High frequency recombination was observed in certain coinfected insect cell lines while much lower frequencies of recombination were observed *in vivo*. The identification of recombinant viruses resulting from mixed baculovirus infections may have significant implications on the interactions occurring in superinfected hosts while also offering novel isolates for downstream analysis.

This chapter aimed to investigate interactions between CrpeNPV and CrleGV by serial passage through *T. leucotreta* larvae. The first objective for this chapter was to passage four virus treatments though *T. leucotreta* five times. Secondly, the resulting OBs were then analysed by mPCR and qPCR to identify which of these viruses were present and at what ratio. The final objective for this chapter was to examine potential recombination events which may have occurred between CrleGV and CrpeNPV through successive passage. This was accomplished by separating CrpeNPV OBs from mixed GV-NPV mixtures obtained from the fifth passage by inoculation of *C. pomonella* (see Chapter 2) followed by restriction endonuclease and NGS analysis of recovered virus.

6.2. Materials and methods

Five consecutive groups of 120 *T. leucotreta* larvae were reared on artificial *T. leucotreta* diet for 14 days. Each group was inoculated with four virus treatments and one control treatment after 7 days, with the preparation of each described below in Section 6.2.2. This was repeated on consecutive sets of larvae to achieve a passage number of 5 (Figure 6.1). The first passage (P1) was treated with virus stocks (P0) prepared to have equal concentrations to the highest dosages utilised for the bioassays in Chapter 5 at 1.57×10^6, 1.53×10^6, 1.56×10^6, and 1.54×10^6 OBs.ml^{-1} for the CrpeNPV alone, CrleGV alone, NPV dominant and GV dominant mixtures respectively. Subsequent passages (P2-P5) were treated with virus recovered from the

previous passage. Virus treatments for P2 to P5 were adjusted to match the P0 dose range which is described below in Section 6.2.2. Finally, OBs recovered from the final passage (P5), were used in a *C. pomonella* passage (CM) whereby P5 virus was inoculated onto artificial diet on which *C. pomonella* larvae fed. The resulting cadavers were collected and used to purify CrpeNPV OBs for downstream molecular analysis.

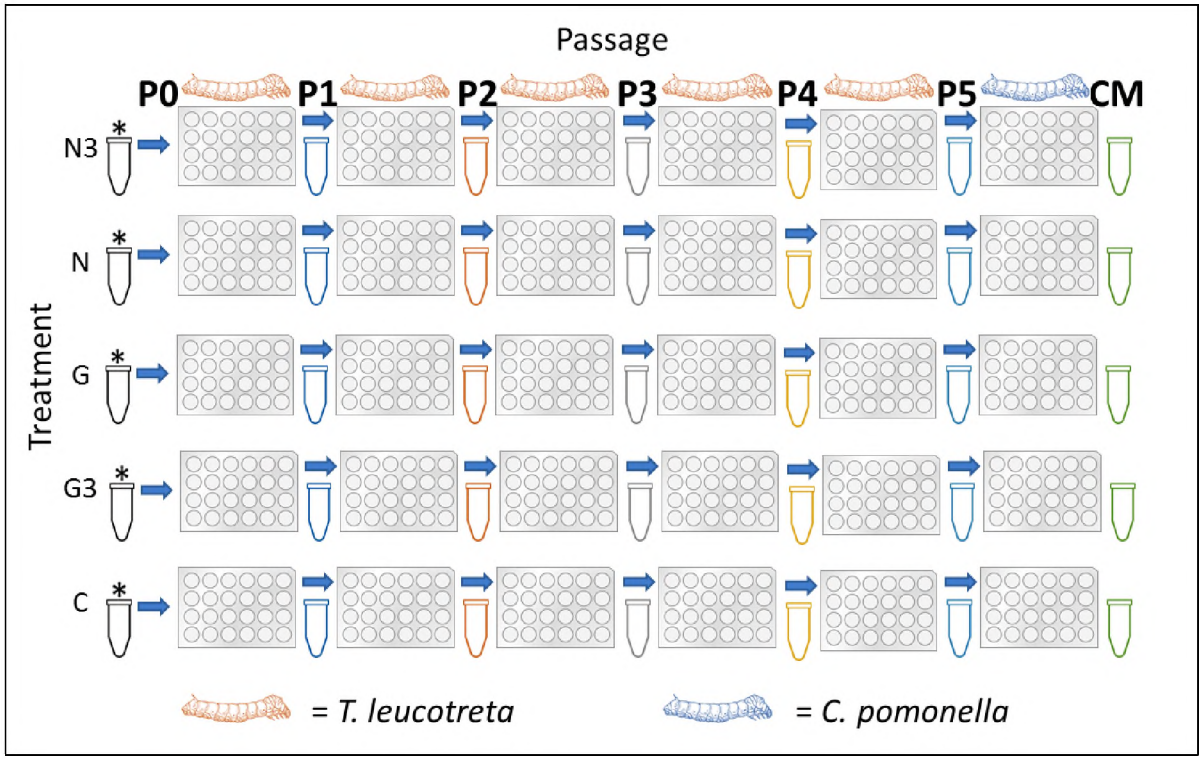

Figure 6.1. Schematic of the passage assay methodology showing the five treatments each consecutively applied to five sets (P1 to P5) of *T. leucotreta* larvae (orange) with the final treatments applied to *C. pomonella* larvae (blue). * - Prepared virus stocks P0. The treatments used were N3 - NPV dominant (NPV:GV at 3:1), N – CrpeNPV, G – CrleGV, G3 – GV dominant (NPV:GV at 1:3) and C – ddH_20 control.

6.2.1. **Rearing of 3rd and 4th instar *T. leucotreta* larvae**

Rearing began with the incubation of *T. leucotreta* egg sheets at 25 °C, with a RH of 30 to 60 % maintained until neonates began hatching. Prior to hatching, five 24 well plates, referred to as "Neonate plates", containing artificial *T. leucotreta* diet, were prepared as described in Chapter 5, Section 5.2.3. (Moore et al., 2014). Newly hatched neonate larvae were carefully transferred to the diet plugs, with one larva placed into each well. The plates were then further incubated in a controlled environment at 25 °C with a RH of 30 to 60 % for 7 days. After the sixth day, a second set of fresh artificial diet was prepared again in five 24 well plates, referred to as "Instar Plates". On the 7th day each Instar Plate was treated with one of the five virus/control inoculations described in Section 6.2.2. Twenty larvae were transferred onto each

of the 5 Instar Plates from the Neonate Plates and incubated at 25 °C with a RH of 30 to 60 % for 7 days.

Any additional larvae from the Neonate Plates were collected and stored at –20 °C. These larvae were later thawed, placed on a scale and viewed under a dissecting microscope. The width of the head capsule for 30 randomly selected larvae were measured using the scale to determine the larval instar (Hofmeyr et al., 2016).

Following incubation, Instar Plates were inspected for larval cadavers and/or healthy larvae, which were collected with those originating from the same plate pooled together. The number of cadavers and surviving larvae were recorded for each treatment. Importantly, all micro centrifuge tubes were weighed prior to and after the collection of cadavers to ascertain the mass of larval tissue acquired from each treatment. This process was repeated for each of the five serial passages, with the respective P0 to P5 virus inoculums for each treatment used to treat the Instar plates.

6.2.2. **Passage assay virus preparation**

The five virus treatments applied at P0, utilised in the first passage of this assay, were CrpeNPV (N), CrleGV (G), a NPV:GV mixture of 3:1 (N3), a NPV:GV mixture of 1:3 (G3), and a control containing ddH_2O (Figure 6.1). Virus treatments were applied at 1.57×10^6, 1.53×10^6, 1.56×10^6, and 1.54×10^6 OBs.ml^{-1} for the CrpeNPV, CrleGV, NPV dominant, and GV dominant mixtures respectively. The passage was carried out by preparing 2 ml of each virus treatment. Each of the five Instar plates for this passage were treated with one of the virus treatments by surface inoculating each diet plug with 50 µl of sample preparation.

Larval cadavers collected from the first passage as described in Section 6.2.1 were used to prepare the virus treatments P1 for the second passage, with the recovered virus P2 used to inoculate the third passage and so on up to a final passage of five. The preparation of the treatments for each passage involved the semi-purification of OBs, using the method described in Chapter 2, Section 2.2.4, with minor modifications made to the centrifugation steps with an increased speed of 10,000 × g used instead of 2,500 × g. All resulting pellets were resuspended in 200 µl ddH_2O. Following this, OB concentrations were enumerated as described in Chapter 5, Section 5.2.1. Samples of OBs recovered from P1 to P5 for each of the treatments were first diluted 1:1000 by transferring 2 µl of virus to 1,998 µl ddH_2O. These 1:1000 dilutions were then used to produce a final dilution whereby virus concentrations were adjusted to match the corresponding D1 dilution used to prepare the initial inoculum, P0. These dilutions were made

up to a final volume of 1.5 ml and used to inoculate the consecutive passages 2 to 5 and CM in the same manner as was done in the first passage.

To determine the concentration of OBs per mg tissue recovered, the number of OBs in each 200 µl sample was calculated using the data recorded following OB enumeration. Using the mass of tissue recovered and measured after each collection, the OBs per mg was calculated (Equation 6.1)

Equation 6.1. Calculation used to estimate the concentration of OBs per mg of tissue recovered from each treatment following each passage.

$$OBs.mg^{-1} = \frac{\left(\frac{OBs.ml^{-1}}{5}\right)}{mg\ tissue}$$

6.2.3. **Multiplex PCR analysis of OBs recovered from the passage assay**

For each treatment across all five passages (P1 to P5), 10 µl of semi-purified OBs were transferred into separate 1.5 ml microcentrifuge tubes and made up to 100 µl using ddH_2O. Baculovirus gDNA was individually extracted from each of these samples using the ZR Viral DNA (Zymo Research, USA) extraction kit as per manufacturer's instructions. DNA from each sample was eluted into 10 µl elution buffer. The concentration of gDNA was measured using a Nanodrop 2000 (Thermo Scientific, USA) (Supplementary Table 10.3). Further, 2 µl of each extraction was analysed by AGE using a 1 % gel stained with ethidium bromide and run at 90 V for 30-45 minutes to confirm gDNA integrity. Lastly, multiplex PCR reactions were set-up as described in Section 4.2.3 with 2 µl of extracted gDNA used as template for all reactions. Amplicons were separated by AGE on 1 % gels at 90 V for 45 minutes and visualised on a ChemiDoc™ XRS+ (Bio-Rad, USA) with images captured with the Image Lab™ (Bio-Rad, USA) software.

6.2.4. **DNA extraction from OBs recovered from the passage assay for qPCR analysis**

Using the data obtained for the mass of larvae recovered from each treatment in the passage assay, samples of OBs equal to 20 mg of tissues were transferred to 1.5 ml microcentrifuge tubes and made up to 100 µl with nuclease free H_2O. Genomic DNA was extracted from these samples using the ZR Viral DNA extraction kit as per the manufacturer's instructions. DNA from each sample was eluted with 20 µl of nuclease free water into RNase/DNase free 1.5 ml microcentrifuge tubes. All pipetting was performed using DNase/RNase free filter pipette tips.

DNA was also extracted using the same kit and method to prepare the qPCR standards. A GV and NPV standard was prepared from CrpeNPV and CrleGV OBs semi-purified from infected *T. leucotreta* larvae. OB concentration was determined with the use of a Neubauer Haemocytometer and dark field microscopy for each sample (see Chapter 5, Section 5.2.1). Extracted gDNA samples were screened by mPCR as described above in Section 4.2.3 to ensure each standard contained only the target virus. Reactions were performed twice for each virus each time with one of two different PCR ReadyMix solutions, these being the KAPA Taq EXtra HotStart ReadyMix (KAPA Biosystems, USA) and TEMPase Hot Start Master Mix Blue (Ampliqon, Denmark). Amplicons were separated by AGE on 1 % gels at 90 V for 45 minutes with images captured for each set of reactions.

6.2.5. Quantitative PCR analysis of CrpeNPV and CrleGV OBs recovered from the passage assay

Quantitative PCR was performed to evaluate the amount of CrleGV and CrpeNPV in larval samples collected from each treatment across all five passages. This was done using the method developed in Chapter 4 with some minor modifications made. Each reaction contained 10 µl KAPA SYBR Green ReadyMix (KAPA Biosystems, USA), 1 µl of the forward oligonucleotide, 1 µl of the reverse oligonucleotide, 7 µl ddH_2O, and 1 µl template gDNA (equivalent to 1 mg tissue). For the no template control ddH_2O was used instead of template gDNA extracted above. Using the gDNA extracted and screened by mPCR for the standards in the section above, six standard reactions were prepared for each virus with the concentrations of each shown in Table 6.1.

Table 6.1. Concentrations for the CrpeNPV and CrleGV qPCR standards used to analyse the OBs recovered from the passage assay.

Standard	Concentration (OBs.µl^{-1})	
	CrpeNPV	**CrleGV**
D1	1.60×10^7	8.30×10^7
D2	1.60×10^6	8.30×10^6
D3	1.60×10^5	8.30×10^5
D4	1.60×10^4	8.30×10^4
D5	1.60×10^3	8.30×10^3
D6	1.60×10^2	8.30×10^2

All reactions were performed in triplicate and prepared in a sterile PCR workstation hood. This was done by tripling the contents of each reaction to 60 µl during reaction preparation. These master mixes were then split into three PCR tubes each receiving 20 µl of the mixture. Where possible, reagents were prepared as master mixes in nuclease free 1.5 ml tubes which were then aliquoted out when necessary. All pipetting was performed using DNase/RNase free filter pipette tips in nuclease free 1.5 ml tubes and nuclease free optically clear PCR tube strips. Nuclease free qPCR grade H_2O was used in all reactions. Reactions were run using the CFX Connect Real-Time PCR system (Bio-Rad, USA) and data was analysed using the CFX Manager™ Software (Bio-Rad, USA). Additional data analysis was performed using Excel 365 (Microsoft, USA) with the ratio of GV and NPV calculated using the mean starting quality obtained from the qPCR analysis and Equations 6.2 and 6.3 respectively.

Equation 6.2. Calculation used to determine the ratio of CrleGV in each treatment from the passage assay based on the mean starting quantities (SQ) values determined by qPCR.

$$Ratio\ GV = \left(\frac{100}{GV\ SQ\ Mean + NPV\ SQ\ Mean}\right) \times GV\ SQ\ Mean$$

Equation 6.3. Calculation used to determine the ratio of CrpeNPV in each treatment from the passage assay based on the mean starting quantities (SQ) values determined by qPCR.

$$Ratio\ NPV = \left(\frac{100}{GV\ SQ\ Mean + NPV\ SQ\ Mean}\right) \times NPV\ SQ\ Mean$$

6.2.6. Evaluation of recombination in CrpeNPV

6.2.6.1. Purification of CrpeNPV and CrleGV mixes through *C. pomonella*

CrpeNPV and CrleGV OBs recovered from the final passage (P5) from each treatment were enumerated before adjusting the concentrations to match the respective D1 doses as described in Section 6.2.2. *C. pomonella* eggs provided by Entomon Technologies (South Africa) on strips of wax paper which were placed in petri dishes, sealed with parafilm, and incubated in a controlled environment at approximately 26 °C and a RH of 30 – 60 %. A total of 120 neonate larvae were reared on artificial diet as described in Section 2.2.3.1 in five 24 well plates.

After 7 days of incubation, fresh artificial diet was prepared and distributed across five new 24 well plates. Each plate was inoculated with the prepared doses from each of the treatments from the final passage, with each well receiving 50 µl inoculum. A control plate was prepared by inoculating each well with 50µl ddH_2O. *C. pomonella* larvae were transferred to the treated plates, with each receiving a total of 20 larvae. Additional larvae were collected and stored at -20 °C to enable measurement of head capsule sizes at a later stage to determine larval instar.

Treated plates with larvae were incubated for another 7 days in the controlled environment after which plates were examined for cadavers and surviving larvae with the results recorded for each treatment. Cadavers were individually collected from this assay in 1.5 ml tubes while all other larvae from each treatment were pooled together and stored at -20 °C.

6.2.6.2. Multiplex PCR and restriction endonuclease analysis of purified CrpeNPV-CM gDNA

OBs were purified from five *C. pomonella* cadavers (referred to as CrpeNPV-CM1 to CM5), which were all recovered from the CrpeNPV dominant treatment. Genomic DNA was extracted from these OBs using the ZR Viral DNA extraction kit (Zymo Research, USA) and screened using the mPCR analysis for the presence of CrpeNPV and/or CrleGV.

Additional gDNA was extracted from the CrpeNPV-CM OBs using the CTAB DNA extraction method described in Section 3.2.2, on which restriction endonuclease (REN) profiles were generated. Restriction enzymes were evaluated *in silico* against the complete CrpeNPV genome to identify two enzymes which would result in banding patterns which were well defined and did not result in fragments of similar sizes which would overlap. The enzymes *Pst*I and *Nde*I (Thermo Scientific, USA) were selected. Restriction digest reactions containing 3 µl (10 U/µl) of either *Pst*I or *Nde*I, 3 µl 10 × restriction enzyme buffer, 16 µl ddH_2O, and 9 µl template gDNA were prepared. Reactions were incubated at 37 °C in a water bath for 2 h. Samples were analysed by 0.6% AGE stained with ethidium bromide and resolved at 30 V for 16 h. Gels were visualised using the ChemiDoc™ XRS+ (Bio-Rad, USA) with image captured and band sizes estimated in the Image Lab™ (Bio-Rad, USA) software. I*n silico* profiles for both *Pst*I and *Nde*I were generated against the CrpeNPV complete genome sequence in Geneious R7 and used as a reference for comparison.

6.2.6.3. Complete genome sequencing of purified CrpeNPV-CM isolates

Genomic DNA was extracted from the CrpeNPV-CM OBs using the ZR Viral DNA extraction kit. DNA concentration was determined using a Quantus fluorimeter (Promega, USA) as per the manufacturer's instructions (Supplementary Table 10.4). Genomic DNA was sequenced using the MiSeq platform (Illumina, USA) with libraries prepared using the Nextera XT DNA sample preparation kit V3.0 (Illumina, USA) as per the manufacturers guidelines with dual indexes used. Following library clean-up, amplified libraries were checked using a 2200 TapeStation (Agilent, USA). Libraries were normalised and pooled together with other samples for sequencing.

Data was analysed in Geneious R7 with each CrpeNPV-CM genome assembled *de novo* forming larger contigs (Kearse et al., 2012). These contigs were then mapped to the CrpeNPV complete genome sequence. A second assembly method was also utilised whereby reads were mapped directly to the reference (MTR) CrpeNPV genome. All CrpeNPV-CM sequence assemblies were compared by multiple pairwise alignment against the reference CrpeNPV genome using the ClustalW alignment method to identify potential recombination events.

Oligonucleotides were designed and tested using the Geneious R7 software to flank a region which showed disagreement between the CrpeNPV-CM1 and CrpeNPV genome sequences (Table 6.2). PCR reactions were set-up as described in Section 4.2.3 with 2 µl of extracted CrpeNPV-CM3 gDNA used as template for the reaction. The resulting amplicon was sent to Inqaba Biotech (South Africa) for sequencing. The sequence was edited and aligned using the ClustalW method in Geneious R7 against the respective regions in the CrpeNPV-CM1 and CrpeNPV genomes by pairwise alignment.

Table 6.2. Oligonucleotide design against CrpeNPV-CM1

Name	Length	Sequence (5'-3')	Amplicon Size (bp)	Tm (°C)
CpNPV-CM1F	20	GGGCTGTAAGGTTCATTTTG	584	54.8
CpNPV-CM1R	20	AGTCGTGTCAGTAAACGTAG		54.9

6.3. Results

6.3.1. *T. leucotreta* tissue and occlusion body yield

The evaluation of CrpeNPV and CrleGV against *T. leucotreta* neonate larvae, both alone and in combination, using a surface dose biological assay identified a synergistic effect between these viruses when applied together. However, the use of neonate larvae resulted in minimal amounts of larval tissue being recovered from these assays preventing further analysis of these interactions using the molecular techniques developed in Chapter 4. To resolve this, several 4th instar *T. leucotreta* larvae with an average head capsule width of 0.941 ± 0.04 mm (n = 20) were treated with the D1 dosages from each of the treatments used in the biological assays. OBs recovered from these larvae were enumerated, followed by the preparation of a 1:1000 dilution which was then used to prepare inoculum for the following passage. The volume of the 1:1000 dilution used to prepare 1.5 ml of inoculum for the subsequent passages, with concentrations comparable to the original P0 dosages, are shown in Table 6.3 along with the concentrations of both the stock OB and dilution samples. OBs recovered following the fifth passage were prepared in a similar manner as above and used to inoculate 3rd and 4th instar *C.*

pomonella larvae with a mean head capsule width of 0.932 ± 0.06 (n = 20). This would enable the separation of CrpeNPV from the mixed GV:NPV treatments for downstream analysis. The mass of larval tissue recovered was also recorded with these results shown in Table 6.3.

Table 6.3. Dose preparation for each treatment across each of the five passages and final *C. pomonella* passage showing amount of tissue recovered and concentration of OBs.ml^{-1} of stock suspensions and 1:1000 dilution.

	Treatment	Tissue (mg)	Concentration (OBs.ml^{-1}) Stock	1:1000	Volume (µl)
Passage 0	**NPV:GV 3:1**	-	1.56×10^{6}	-	-
	NPV	-	1.57×10^{6}	-	-
	GV	-	1.53×10^{6}	-	-
	NPV:GV 1:3	-	1.54×10^{6}	-	-
	Control	-	0	-	-
Passage 1	**NPV:GV 3:1**	163.4	3.53×10^{11}	3.53×10^{8}	6.6
	NPV	160.2	5.41×10^{10}	5.41×10^{7}	43.5
	GV	181.2	6.25×10^{11}	6.25×10^{8}	3.6
	NPV:GV 1:3	113.2	2.71×10^{11}	2.71×10^{8}	8.5
	Control	905.3	0	0	-
Passage 2	**NPV:GV 3:1**	638.95	1.00×10^{12}	1.00×10^{9}	2.3
	NPV	308.68	1.94×10^{11}	1.94×10^{8}	11.9
	GV	487.98	1.05×10^{12}	1.05×10^{9}	2.2
	NPV:GV 1:3	286.88	9.35×10^{11}	9.35×10^{8}	2.5
	Control	636.6	0	0	-
Passage 3	**NPV:GV 3:1**	207.42	6.31×10^{11}	6.31×10^{8}	3.7
	NPV	246.01	7.12×10^{11}	7.12×10^{8}	3.2
	GV	564.76	1.13×10^{12}	1.13×10^{9}	2.0
	NPV:GV 1:3	501.38	1.31×10^{12}	1.31×10^{9}	1.8
	Control	566.4	0	0	-
Passage 4	**NPV:GV 3:1**	582.21	1.49×10^{12}	1.49×10^{9}	1.5
	NPV	545.60	1.41×10^{12}	1.41×10^{9}	1.6
	GV	724.60	1.63×10^{12}	1.63×10^{9}	1.4
	NPV:GV 1:3	585.38	1.44×10^{12}	1.44×10^{9}	1.6
	Control	574.0	0	0	-
Passage 5	**NPV:GV 3:1**	328.00	1.30×10^{12}	1.30×10^{9}	1.8
	NPV	296.59	1.15×10^{12}	1.15×10^{9}	2.0
	GV	285.55	1.33×10^{12}	1.33×10^{9}	1.7
	NPV:GV 1:3	250.69	9.58×10^{11}	9.58×10^{8}	2.4
	Control	549.1	0	0	-

The concentration of OBs recovered from infected *T. leucotreta* larvae ranged from 5.41×10^{10} OBs.ml^{-1} in the NPV treatment of passage 1 to a maximum of 1.63×10^{12} OBs.ml^{-1} observed in GV only treatment of passage 4. While the amount of tissue recovered from the control treatments was comparable to that of the virus treatments, a clear distinction was observed in the physical appearance of the larvae. Control larvae were alive at the time of final evaluation, had a pinkish colour and were actively feeding or moving around the wells. On the contrary, larvae from the virus treatments were almost all dead, with cadavers pale white in colour and some completely liquified. Any surviving larvae in the virus treatments were lethargic and reacted poorly to environmental stimuli, also having a pale white colour.

While the number of recovered larvae was recorded for each treatment across all five passages, the amount of tissue recovered per larva or the concentration of OBs per larva cannot be accurately calculated as tissue was difficult to collect, often having absorbed into the diet plugs because of extensive liquification following infection. To better estimate the concentration of OBs obtained per virus treatment, the concentration of OBs per mg of tissue recovered was determined and is shown in Figure 6.2.

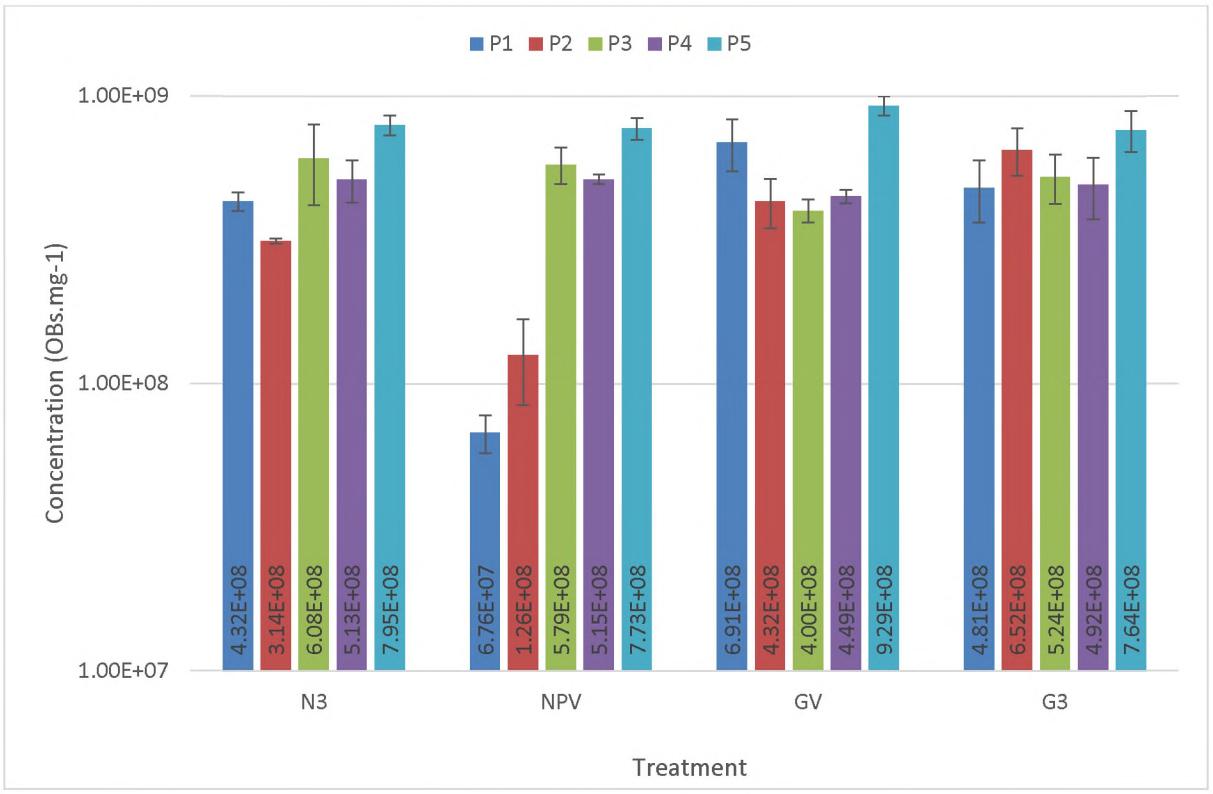

Figure 6.2. Concentration of OBs per mg tissue recovered from each treatment through five passages of *T. leucotreta* larvae. Passage assays P1 to P5 are shown with blue, red, green, purple and light blue bars for the N3 - NPV dominant, NPV - CrpeNPV, G - CrleGV and G3 - GV dominant treatments. The standard deviations are shown with the error bars.

The concentration of OBs per mg of tissue recovered from the passage assay treatments is shown in Figure 6.2. The average amount of OBs recovered per mg of tissue was $5.54 \times 10^8 \pm 2.13 \times 10^8$. The lowest concentration of OBs was observed in the CrpeNPV treatment after passage 1 with approximately 6.75×10^7 OBs.mg^{-1} recovered. The number of OBs in this treatment steadily increased approaching the average concentration by passage 3. It was also recorded that the CrleGV dominant mixture produced the highest average concentration of OBs per mg of tissue at $5.83 \times 10^8 \pm 1.22 \times 10^8$ although this was not greater than the other three treatments.

6.3.2. mPCR of *T. leucotreta* passages 1 to 5

Genomic DNA was extracted from OBs recovered during the passage assay. For each passage, five samples were screened: namely NPV:GV of 3:1, CrpeNPV, CrleGV, NPV:GV of 1:3, and a ddH_2O control treatment. A no template control and positive control were included in each mPCR analysis. The results for each passage are shown below in Figure 6.3A to E.

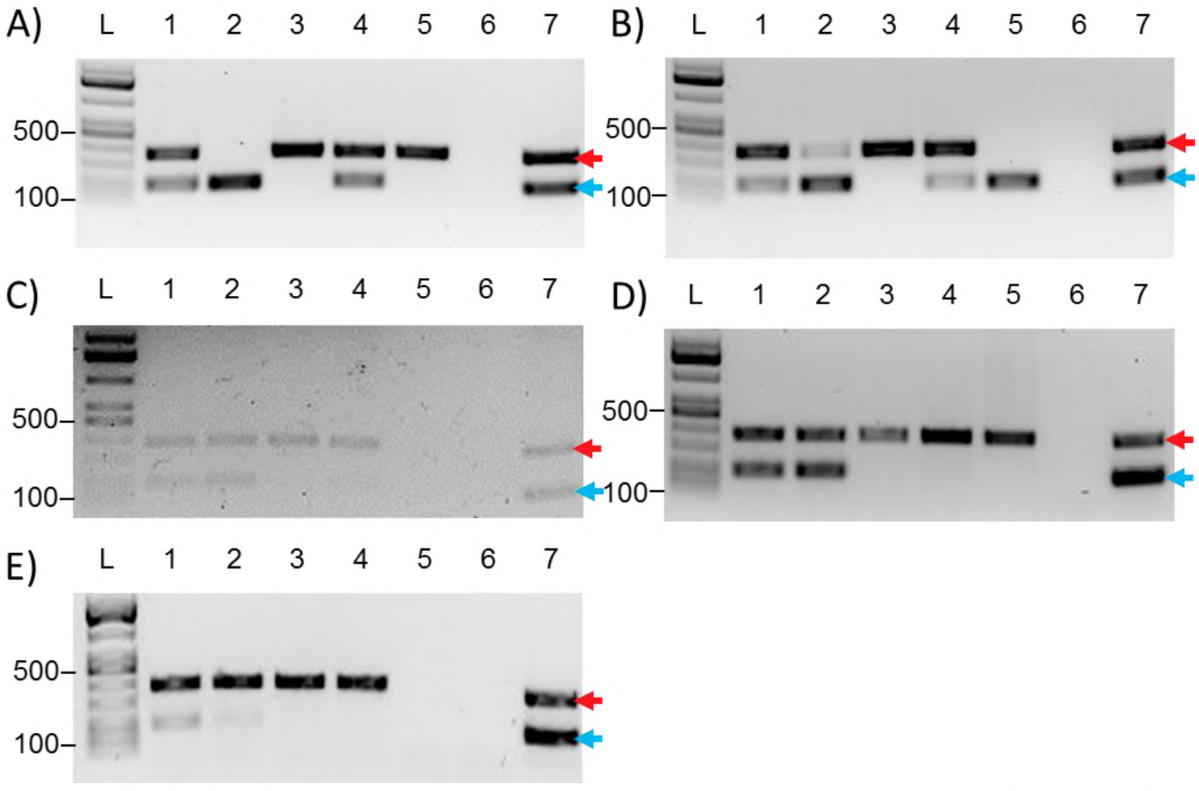

Figure 6.3. Multiplex PCR analysis of genomic DNA extracted from passages 1-5 in panels A-E respectively with treatments in Lane 1 - NPV:GV 3:1, Lane 2 - CrpeNPV, Lane 3 – CrleGV, Lane 4 – NPV:GV 1:3, Lane 5 – ddH_2O treatment, Lane 6 – NTC and Lane 7- positive control. L – KAPA Universal DNA Ladder (bp). Red marker – CrleGV-lef4 amplicon and Blue marker – CrpeNPV-pif1 amplicon.

The mixed treatment with NPV:GV at a ratio of 3:1 in Lane 1 of Figure 6.3 across all five passages showed the presence of two bands: a larger band of approximately 400 bp and a smaller band of approximately 200 bp. These bands match the expected sizes of the CrleGV-lef4 and CrpeNPV-pif1 amplicons respectively. The CrpeNPV treatments in Lane 2 of the analysis showed the presence of a 200 bp band in all passages while the larger CrleGV-lef4 band of approximately 400 bp was observed in passages 2 to 5. Lane 3 of each mPCR analysis shows the CrleGV treatment from each passage with only the larger band of approximately 400 bp observed in all samples. Lane 4 shows the mixed NPV:GV treatment at a ratio of 1:3, with the larger band of approximately 400 bp observed in all five passages while the smaller CrpeNPV-pif1 amplicon was only observed in passages 1 and 2. Multiplex PCR analysis of the control larvae treated with ddH_2O, shown in Lane 5, indicated the presence of CrleGV in passages 1 and 3 producing the larger ~400 bp amplicon while CrpeNPV was observed in passage 2 whereby the smaller CrpeNPV-pif1 amplicon of approximately 200 bp was observed. No amplicons were observed in the no template controls, while both the CrpeNPV-pif1 and CrleGV-lef4 amplicons were observed in the positive controls as expected. These controls confirm that the reagents and equipment were operating correctly.

6.3.3. qPCR analysis of CrleGV and CrpeNPV in the *T. leucotreta* passage assay

6.3.3.1. CrleGV and CrpeNPV amplification curves, melt peaks and standard curves

Quantitative PCR was performed on gDNA extracted from OBs recovered from each treatment across all five passages. The amplification curves, melt peaks, and standard curves for CrleGV and CrpeNPV are shown below in Figure 6.4. For both the CrpeNPV and CrleGV amplification curves and melt peaks, the standard and no template control lines are shown in green. All experimental reactions are coloured per treatment with replicates of each treatment sharing the same colour.

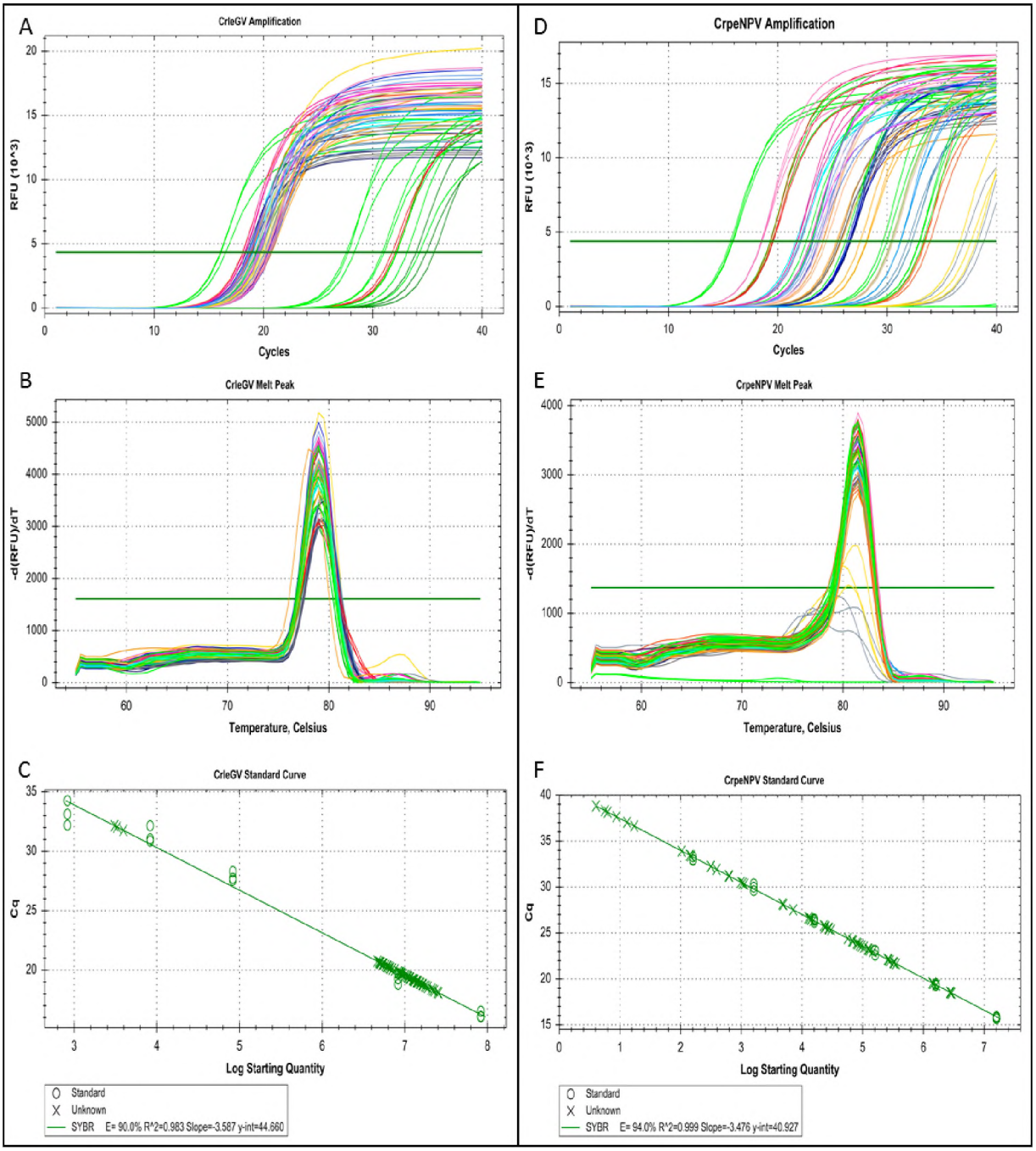

Figure 6.4. Quantitative PCR analysis results of the CrleGV and CrpeNPV passage assay. A) CrleGV amplification curve, B) CrleGV melt peak, C) CrleGV standard curve, D) CrpeNPV amplification curve, E) CrpeNPV melt peak and F) CrpeNPV standard curve.

Quantitative PCR for both CrpeNPV and CrleGV was performed on all 20 samples obtained from the passage with each tested in triplicate. Figure 6.4A, B, and C show the results from the CrleGV analysis. Consistent amplification of each standard (green lines) was observed in Figure 6.4A except for Standard 3 (D3) which was excluded from the analysis. All reactions were found to form an identical melt peak, as shown in Figure 6.4B, indicating the production of a single amplicon. The standard curve generated from the CrleGV qPCR analysis is shown

in Figure 6.4C with the unknown samples each marked with an ×. These are plotted along the regression line generated from the CrleGV standards each marked with an ○. The coefficient of determination (R^2) was 0.983 indicating a good fit of the data to the regression line. The amplification efficiency for the CrleGV qPCR reactions was 90 %, falling within the recommended range of 90-105 %.

Figure 6.4D, E and F show the results from the CrpeNPV qPCR analysis of the passage assay samples. All reactions produced ideal amplification curves as shown in Figure 6.4D, with the standards and NTCs coloured green and the unknown samples coloured separately by replicate. Importantly, no amplification curve was observed in the no template control. The melt peak for the CrpeNPV-pif1 reactions is shown in Figure 6.4E, with a single peak observed for most samples. Two samples, namely G3 from passage 5 (grey lines) and GV from passage 4 (yellow lines), deviated from the typical melt curve. These two samples may have produced non-specific products or primer dimers due to low levels of CrpeNPV template gDNA. The last standard curve shown in Figure 6.4F was generated for the CrpeNPV qPCR analysis. The standards are each marked with a ○ while the unknown samples are each shown as ×. The amplification efficiency was 94 % indicating an ideal rate of product generation. The R^2 for the regression line generated from the CrpeNPV standards was 0.999 showing an ideal fit to the experimental data.

6.3.3.2. **Analysis of CrpeNPV to CrleGV OB ratio in the *T. leucotreta* passage assay**

Using the data generated by qPCR analysis of CrpeNPV and CrleGV in OBs recovered from each treatment across the passage assays, the ratio of NPV to GV could be determined. The initial composition of each virus treatment, referred to as P0, was determined by calculating the quantity of OBs from CrpeNPV and CrleGV transferred from the stock suspension, which was initially determined with a counting chamber and dark field microscopy. Thereafter, the concentration and ratio of NPV and GV in P1 to P5 were calculated using the data generated by qPCR.

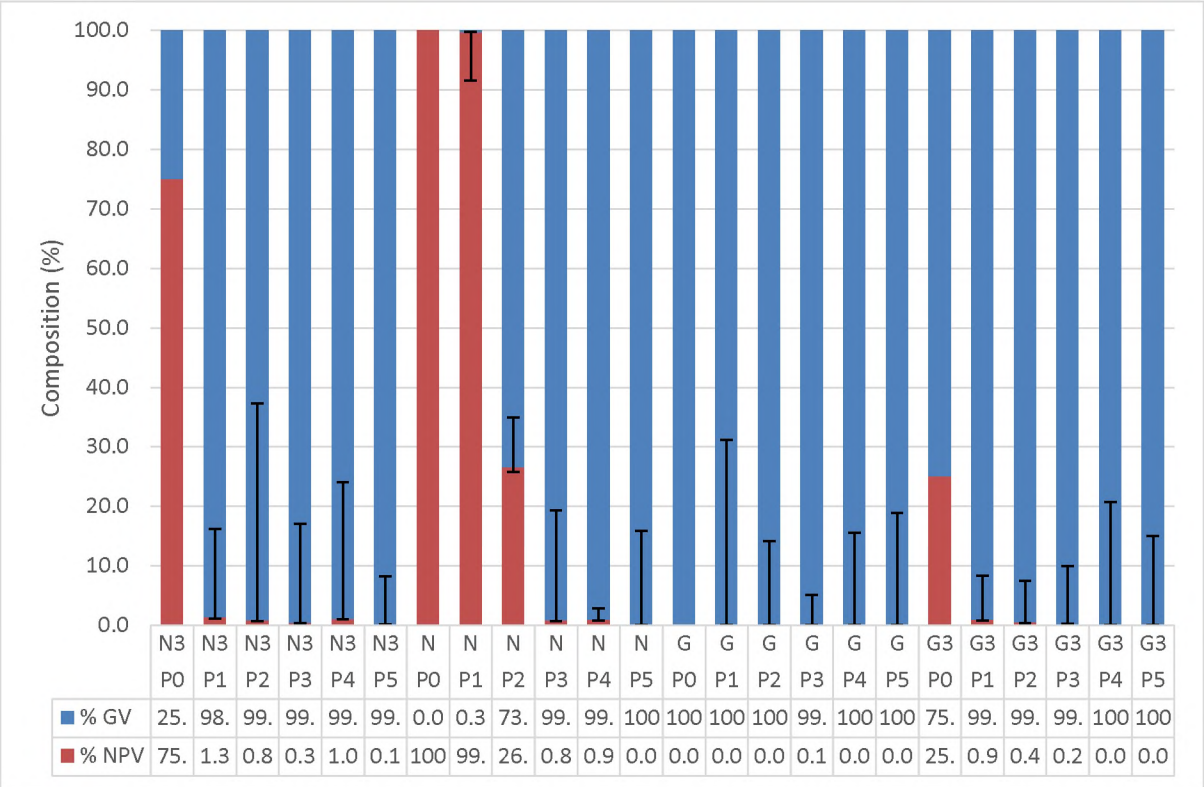

	N3 P0	N3 P1	N3 P2	N3 P3	N3 P4	N3 P5	N P0	N P1	N P2	N P3	N P4	N P5	G P0	G P1	G P2	G P3	G P4	G P5	G3 P0	G3 P1	G3 P2	G3 P3	G3 P4	G3 P5
% GV	25.	98.	99.	99.	99.	99.	0.0	0.3	73.	99.	99.	100	100	100	100	99.	100	100	75.	99.	99.	99.	100	100
% NPV	75.	1.3	0.8	0.3	1.0	0.1	100	99.	26.	0.8	0.9	0.0	0.0	0.0	0.0	0.1	0.0	0.0	25.	0.9	0.4	0.2	0.0	0.0

Figure 6.5. Ratio of CrleGV OBs in Blue to CrpeNPV OBs in red per mg recovered tissue from pooled larvae collected in P1 to P5. CrpeNPV dominant (N3), CrpeNPV (N), CrleGV (G), CrleGV (G3) treatments and the standard deviations. The initial ratio of virus calculated for each treatment is shown as P0.

Figure 6.5 shows the ratio of CrleGV and CrpeNPV in each of the four treatments across the five passages. The first treatment shown is the CrpeNPV dominant mixture referred to as N3 in the graph. The ratio of CrpeNPV OBs in recovered tissue was observed to immediately decrease from 75 % in the initial treatment PO to 1.3 % in the first passage (P1). Thereafter the ratio of CrpeNPV OBs remained at or below 1 % with CrleGV becoming the dominant virus in the mixture. The next treatment shown is the CrpeNPV only treatment referred to as N. After inoculation of *T. leucotreta* with this virus, a small amount of CrleGV, approximately 0.3 %, was detected in the recovered OBs from P1. The ratio of CrleGV to CrpeNPV rapidly increased in the following passages, rising to 73 % in passage 2 (P2). This increase of CrleGV OBs continued in passages 3 and 4 to around 99 % with no CrpeNPV OBs detected in the final passage (P5).

The CrleGV only treatment is the next set of results shown in Figure 6.5 labelled as G. The GV infection was maintained throughout all five passages, with a minor CrpeNPV signal detected in passage 3 (P3), representing approximately 0.1 % of the recovered OBs. Passages 2 and 5 were observed to produce an extremely weak CrpeNPV signal possibly indicating the presence

of this virus at a ratio of less than 0.01 %. The last treatment shown is the CrleGV dominant treatments (G3), where the initial dose (P0) was calculated to contain a 3:1 ratio of CrleGV to CrpeNPV. However, after the first passage the amount of CrpeNPV decreased to less than 1 % of the recovered OBs. Thereafter the percentage of CrpeNPV OBs continued to decrease, reaching 0 % of the mixture by passage 4 (P4).

6.3.4. Multiplex PCR and recombination analysis of CrpeNPV purified through *C. pomonella* larvae

Following the fifth and final passage of each treatment through *T. leucotreta* larvae, recovered OBs were applied to *C. pomonella* larvae to separate CrpeNPV OBs from the infections. A total of 5 infected cadavers were collected, referred to as CM1 to 5, all originating from the CrpeNPV dominant treatment.

6.3.4.1. Multiplex PCR analysis

OBs were recovered from five *C. pomonella* larvae and are referred to as CrpeNPV-CM1 to 5. Genomic DNA was extracted from these OBs and analysed using the mPCR technique developed in Chapter 4. The results from this analysis are shown in Figure 6.6.

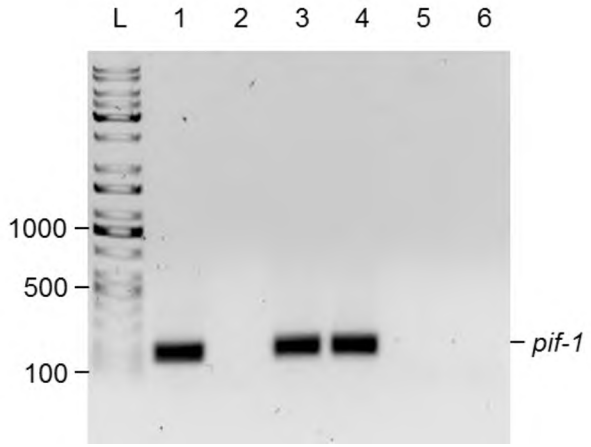

Figure 6.6. Inverted AGE image of the multiplex PCR analysis of CrpeNPV-CM OBs recovered from the NPV dominant treatment of passage 5 and purified through *C. pomonella* larvae. Lane 1 – CM1, Lane 2 – CM2, Lane 3 – CM3, Lane 4 – CM4, Lane 5, CM5 and Lane 6 – NTC. L – KAPA Universal DNA Ladder.

Multiplex PCR analysis of OBs recovered from the fifth passage of the CrpeNPV dominant treatment and purified through *C. pomonella* larvae is shown in Figure 6.6. A single band of approximately 200 bp was observed in lanes 1, 3 and 4. This band matches the expected size for the CrpeNPV-pif1 amplicon indicating the presence of CrpeNPV in the CM1, CM3, and CM4 samples. No bands were observed in lanes 2, 5 and 6.

6.3.4.2. **Restriction endonuclease profile analysis**

To examine possible recombination events which may have occurred between CrleGV and CrpeNPV, restriction endonuclease (REN) analysis was performed on gDNA extracted from the CM1, CM3, and CM4 OBs. *In silico* profiles were also generated using the complete CrpeNPV genome reported in Chapter 3. The enzymes *Nde*I and *Pst*I were used with the results shown in Table 6.4.

Table 6.4. Restriction endonuclease analysis of gDNA extracted from CM1, CM2 and CM3 CrpeNPV-CM OBs using A) *Nde*I and B) *Pst*I alongside a reference profile generated *in silico* from the complete CrpeNPV genome sequence. Band sizes shown in bp with *in vitro* fragment sizes approximated.

	***Nde*I**							***Pst*I**						
Band No.	**Ref**		**CM1**		**CM3**		**CM4**	**Ref**		**CM1**		**CM3**		**CM4**
1	28086	±	31363	±	30255	±	30404	22493	±	23046	±	23966	±	23966
2	15290	±	15852	±	15219	±	15044	14791	±	15071	±	15428	±	15428
3	13539	±	13782	±	13280	±	13155	13959	±	13979	±	14381	±	14381
4	12742	±	12233	±	12377	±	12262	13109	±	12972	±	13280	±	13280
5	9816	±	10100	±	9981	±	9918	12497	±	12233	±	12671	±	12671
6	8902	±	9264	±	8963	±	8981	10804	±	10747	±	11051	±	11051
7	7002	±	7156	±	7058	±	7024	8208	±	8183	±	8389	±	8389
8	6111	±	6153	±	6070	±	6083	7810	±	7823	±	7985	±	7985
9	4642	±	4640	±	4610	±	4652	5495	±	5450	±	5515	±	5547
10	3988	±	3925	±	3882	±	3912	2942	±	2759	±	2823	±	2807
11	2898	±	2807	±	2840	±	2864	2252	±	2052	±	2088	±	2100
12	2042	±	1994	±	1970	±	2012	1416	±	1267	±	1284		
13	696			±	672	±	683							
Total	115754		119271		117177		116992	115776		115582		118861		117606

The REN profiles generated with the *Nde*I and *Pst*I enzyme are shown in Table 6.4. Each profile showed a highly similar banding pattern to the reference profile, with the CM3 and CM4 samples having an identical number of fragments. The smallest fragment in the reference profile, of approximately 700 bp was not observed in the CM1 profile. The *Pst*I profiles for the three samples were each shown to have an identical number of fragments to the reference. All fragments were approximately the same size forming highly similar profiles to that of the respective reference. As the region encompassed by the largest *Pst*I and *Nde*I fragments do not overlap within the CrpeNPV reference genome sequence, the deviation observed in the sizes for these bands is likely a consequence of the technique used rather than a true recombination event between CrpeNPV and CrleGV.

6.3.4.3. **Analysis of the CrpeNPV-CM genome sequences**

The use of REN analyses did not show any substantial differences in the profiles generated for the three CrpeNPV-CM samples obtained from the NPV dominant treatment following passage 5. While some variation was observed, particularly in the larger fragments, this was likely a limitation of the REN technique. Therefore, additional analysis was required to confirm whether any recombination events had occurred. To do this, gDNA from each of the three CrpeNPV-CM isolates was extracted and fully sequenced using the MiSeq platform (Illumina, USA). For each CrpeNPV-CM isolate the complete genome sequence was determined using two different assembly methods, either *de novo* assembly or map to reference (MTR). The resulting CrpeNPV-CM genome sequences were aligned against the reference CrpeNPV (ThleNPV) sequence described in Chapter 3, with the percentage identities and assembly results shown in Table 6.5.

Table 6.5. Comparison between the CrpeNPV genome sequence and the sequences assembled from three CrpeNPV-CM isolates recovered from the final *T. leucotreta* passage and purified through *C. pomonella*. For each isolate the percentage identity, the number of differences and identities, the mean coverage and quality scores for each assembly are given.

CrpeNPV Isolate	Percentage Identity	Number of Differences	Number of Identities	Coverage		Q20 (%)	Q30 (%)
				Mean	Std Dev		
CM1 *de novo*	99.95	66	115646	699.3	214.9	95.0	92.8
CM1 MTR	99.96	66	115646	699.8	215.1	95.0	92.8
CM3 *de novo*	99.99	16	115696	388.1	138.8	94.3	91.8
CM3 MTR	99.99	16	115696	388.2	138.9	94.3	91.8
CM4 *de novo*	99.99	21	115963	362.5	113.2	95.0	92.8
CM4 MTR	99.99	24	115688	362.5	113.2	95.0	92.7

Table 6.5 shows the pairwise identity between the reference CrpeNPV genome sequence and three CrpeNPV-CM genome sequences (CM1, CM3, and CM4) obtained from the final serial passage. All assemblies were shown to have a greater than 99.9 % identity with both the CrpeNPV-CM3 and CM4 sequences having greater than 99.99 % pairwise identity and fewer than 25 nucleotide differences. The CM1 sequence was shown to have a slightly lower percentage identity due to a 51 bp region which was observed to have poor read coverage (Figure 6.7). Excluding this region, the CM1 genome sequence would also show a pairwise identity greater than 99.99 % against the reference CrpeNPV sequence with a total of 15

nucleotide differences. In all three CM isolates, all nucleotide differences (excluding the 51 bp gap) were observed to be spaced across the genome as single nucleotide polymorphisms or ambiguous nucleotides.

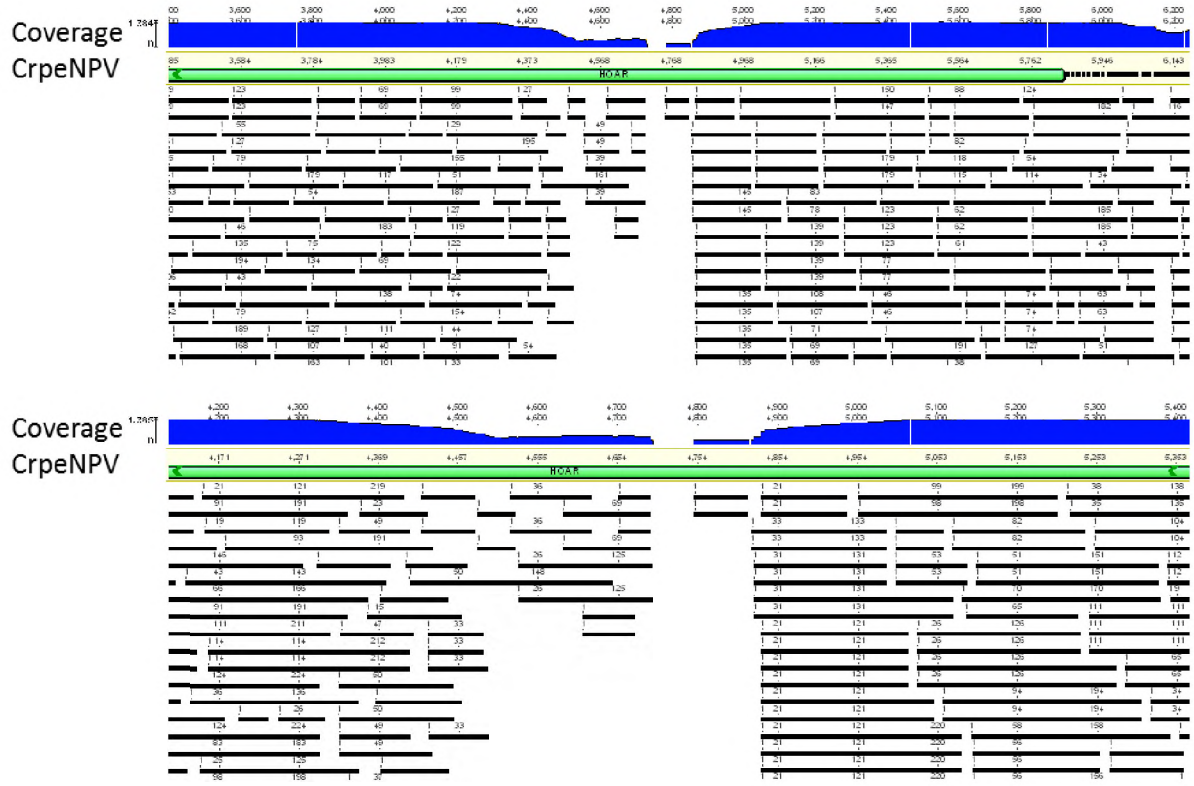

Figure 6.7. Comparison of the A) *de novo* and B) MTR assemblies for CrpeNPV-CM1 for the region containing a 51 bp gap. The blue chart shows the coverage for each nucleotide with this region falling within the HOAR gene shown with the green annotation. Black bars indicate individual reads mapped to the reference CrpeNPV genome.

Figure 6.7 above shows the region in the CrpeNPV-CM1 genome sequence where a 51 bp gap was observed in relation to the CrpeNPV complete genome sequence. This gap was observed in the HOAR gene between nucleotides 4699 and 4751with the region upstream of the gap shown to also have a lower coverage of around 8× compared to the downstream surrounding region which had a coverage of more than 300×. Following PCR amplification, sequencing, and alignment of this region in CrpeNPV-CM1 against the CrpeNPV genome sequence, it was revealed that this gap was the result of low read coverage during NGS. Alignment of the sequence obtained from the PCR analysis matched the region in the CrpeNPV genome sequence, indicating that this region in CrpeNPV-CM1 was identical to the respective region in the reference genome.

6.4. Discussion

In this chapter the interaction between CrpeNPV and CrleGV was investigated by serial passage of four treatments through *T. leucotreta* larvae five times. The four treatments applied matched those evaluated in the previous chapter: namely CrpeNPV alone, CrleGV alone, and 1:3 and 3:1 mixtures of CrpeNPV and CrleGV. OBs recovered from the final passage were further purified through *C. pomonella* larvae to isolate CrpeNPV, enabling examination of potential recombination events.

Following each passage (P1 to P5), larval cadavers were collected with the mass of the tissue recorded prior to extraction of OBs. All recovered samples across the various treatments were enumerated to determine the number of OBs produced per milligram of infected tissue. Interestingly, all larvae inoculated with CrleGV produced approximately 5×10^8 OBs.mg^{-1}, with the CrleGV and GV dominant treatments roughly reaching this concentration by passage 1 and the NPV dominant mixture by passage 3. Conversely, the NPV treatment showed lower OB concentrations for passage 1 and 2 gradually increasing to reach 5×10^8 OBs.mg^{-1} by passage 3. This increase is possibly due to the occurrence of CrleGV in this treatment by passage 2 as shown in both the mPCR and qPCR analysis. The concentration of OBs per milligram of larval tissue has been previously reported for AdhoNPV and AdorNPV in infected *Adoxophyes honmai* larvae (Ishii et al., 2002; Takahashi et al., 2008). These studies calculated approximately 3×10^8 OBs.mg^{-1} and 7.75×10^7 OBs.mg^{-1} for AdhoNPV and AdorNPV respectively. Given the close relation of CrpeNPV to AdhoNPV, as shown in Chapter 3, it is not surprising to see similar concentrations of OBs in the NPV treatment for the first two passages. However, once CrleGV was observed in CrpeNPV infected larvae, an increase in GV OB concentration was recorded. This may be due to CrleGV outcompeting CrpeNPV for resources in coinfected larvae, enabling increased amounts of OB production (Burden et al., 2003; Wennmann et al., 2015).

Multiplex PCR analysis was performed on gDNA extracted from OBs recovered for each treatment across all five passages. The appearance of CrleGV in the CrpeNPV treatment could be an indication of a covert GV infection shifting to an overt state due to stress factors related to the environmental conditions, the handling of insects or the NPV infection. As previously discussed, CrleGV isolates have been successfully isolated from healthy *T. leucotreta* colonies following induced stress on the larvae by overcrowding (Opoku-Debrah et al., 2013). One of these colonies, the MixC colony, is the same *T. leucotreta* colony used for these experiments and therefore it is possible that a covert CrleGV infection persists in this colony, becoming

overt once the survival of the treated larvae was compromised by the CrpeNPV infection. This process was reported in a review by Williams et al. (2017) whereby stress factors which threaten larval survival trigger baculoviruses to switch towards a horizontal mode of transmission resulting in increased virus replication and larval mortality. Of all various stress factors discussed in the introduction to this chapter, the superinfection of a second baculovirus into a covertly infected larva has been previously shown to be the strongest in eliciting an overt response (Cooper et al., 2003; Fuxa et al., 2002; Kouassi et al., 2009; Williams et al., 2017).

A surprising result was the detection of CrpeNPV in the control for P2 along with CrleGV in the P1 and P4 controls. Analysis of unpublished NGS data collected by UGMUG from the sequencing of CrleGV infected *T. leucotreta* homogenate samples spanning 15 years (see Section 4.3.4) showed the presence of CrpeNPV sequence reads in samples as early as 2001, possibly indicating a persistent NPV infection in this host. While this may appear to contradict the findings in this past section, it is important to consider what the lower template threshold for the mPCR analysis is for a positive reaction to occur, as discussed in Chapter 4, and the corresponding sensitivity of NGS. The presence of CrleGV may have been a covert infection in passage 1 and 4. It is, however, important to note that all larvae collected from control treatments were observed to have a healthy, pinkish appearance and were still actively feeding. Conversely, CrleGV and CrpeNPV treatments contained almost no living larvae, with those still alive having a milky-white appearance and exhibiting lethargic and non-responsive behaviour. The observation of virus in the controls could therefore be an indication of a covert CrleGV or CrpeNPV infection in one or two larvae which, once pooled with all the other control larvae, provided enough viral genomic template for detection by the mPCR technique. Alternatively, these results may be a caused by unintentional contamination and therefore necessitate the replication of this experiment in the future.

While the mPCR technique enabled screening of samples recovered from the passage assay for the presence of CrpeNPV and CrleGV, further analysis by qPCR was required to accurately determine the ratio of GV to NPV. Analysis of all samples recovered from the passage assay showed that CrleGV overwhelmingly became the dominant virus, with CrpeNPV comprising approximately 0.1 % of the NPV and NPV dominant treatments. These results suggest an antagonistic interaction between these viruses, which is defined as an improvement in replication of one virus at the expense of the other (Cheng and Lynn, 2009). While the type of interaction is often not reported in the literature for mixed baculovirus infections, similar results have been observed whereby the ratios present in the virus recovered from the final passage

converge upon a common ratio regardless of the make-up of the initial inoculum. The first example of this phenomenon was observed in three artificial treatments of two SfMNPV genotypes C and B, at ratios of 1:9, 5:5 and 9:1. These treatments were applied to *S. frugiperda* larvae with the composition of all treatments observed to change when passaged through the larvae five times (Simón et al., 2006). Examination of the all three treatments showed the resulting OBs to comprise a consistent 1:4 ratio of genotypes C and B respectively which interestingly mirrored the composition observed in the wild type virus. This may represent a stable equilibrium at which these genotypes can efficiently replicate and any deviation from this ratio is rapidly corrected to a more stable composition. An alternative example of shifts in genotype frequency was shown with an initial artificial mixture of two HearSNPV genotypes, SP1B and LB6, at a ratio at 1:1 which resulted in an approximate 6:1 ratio after serial passage of the virus five times in *H. armigera* larvae (Arrizubieta et al., 2015b). This final ratio was shown to cause increased virulence when applied to *H. armigera* larvae as compared to the original 1:1 mixture, potentially favouring improved transmission.

It is unclear which of these examples describe the interaction observed between CrpeNPV and CrleGV most accurately, if either. It is also unknown whether a persistent CrpeNPV and CrleGV infection in *T. leucotreta* larvae occurs and, if so, what ratio these viruses would tend towards in a wild type covert scenario. Analysis of unpublished NGS data from the *T. leucotreta* homogenate samples indicates that CrpeNPV was observed at ratios between 1:125 in 2001 to 1:26917 in 2007 with the ratio increasing to 1:2 when it was first identified in 2013. If these earlier ratios represent a stable convert infection that one might expect to see in wild-type CrpeNPV infected larvae, then the proportion of OBs obtained in the final passage may indeed mirror this extremely low ratio, mimicking a situation as reported for the SfMNPV genotypes by Simón et al. (2006). Speculatively, this may indicate that CrpeNPV favours a covert infection in *T. leucotreta* which may provide a mechanism for long term persistence as was suggested for Mamestra brassicae NPV by Burden et al., (2003). Alternatively, the change from a 3:1 or 1:3 ratio of GV and NPV, which was shown to have higher virulence, to essentially a pure CrleGV composition by passage 5, which was determined to have a comparatively lower virulence, may indicate a potential shift towards decreased host mortality.

The last section of this chapter investigated potential recombination events between CrleGV and CrpeNPV. Recombination in baculoviruses has been demonstrated between BmNPV and AcMNPV both *in vivo* and *in vitro* (Kamita et al., 2003; Kondo and Maeda, 1991). Analysis of purified CrpeNPV-CM gDNA recovered from passage 5 by REN and NGS analysis did not

show any homologous recombination between the CrleGV and CrpeNPV. A possible explanation for this may be the low level of homology between CrleGV and CrpeNPV. Kamita et al., (2003) reported a nucleotide sequence identity of more than 90 % for over 78 % of the BmNPV and AcMNPV and observed less than 1 % recombination in an *in vivo* system. In contrast, the genomes of CrleGV-CV3 and CrpeNPV showed a much lower percentage identity at 31.2 % across the core genes and 41.3 % across the entire genome sequences. This low level of identity may limit homologous recombination occurring between these species, however, future experiments involving mixed infections of AdhoNPV or AdorNPV with CrpeNPV may offer more noteworthy results and may be worth investigating.

In conclusion, this chapter aimed to investigate the interactions between CrpeNPV and CrleGV through consecutive infection of *T. leucotreta.* The qPCR results show that CrleGV rapidly became the dominant virus by the final passage in all treatments, with CrpeNPV often comprising less than 1 % of the OBs recovered. These results were also discussed in relation to potential covert infections for each virus, however additional analysis is required to show whether persistent infections in *T. leucotreta* are occurring. The final objective was to examine potential recombination between CrleGV and CrpeNPV, but this was not observed, possibly due to the low levels of nucleotide homology between these viruses.

Chapter 7

Field evaluation of CrpeNPV and CrleGV alone and in combination against *Thaumatotibia leucotreta*

7.1. Introduction

A previous chapter evaluated the biological activity of CrpeNPV and CrleGV both alone and in combinations against *T. leucotreta* in a laboratory setting. The results showed potential synergistic interactions in the mixed infections with improved virulence against neonate larvae. While this is an important result, it is necessary to translate it into an applied scenario by evaluating the efficacy of both CrleGV and CrpeNPV both alone and in combination in the field.

Field trials have been conducted for many baculoviruses worldwide, including Mamestra brassicae NPV (MabrNPV), PhopGV, LdMNPV, CpGV, HearNPV, and CrleGV with the latter three also evaluated in South Africa (Gómez-Bonilla et al., 2013; Goto et al., 2015; Gupta et al., 2016; Knox et al., 2015; S. D. Moore et al., 2004; Provast et al., 2008). The efficacy of CrpeNPV remains to be determined in the field against *T. leucotreta*. CrleGV, in contrast, has undergone several trials spanning over more than a decade (Moore et al., 2015). Early field trials, conducted between 2001 and 2003, involved application of unformulated CrleGV. Subsequently the virus was formulated into the commercial product, Cryptogran™, which has been utilised since 2003. Many of these trials included chemical pesticide treatment, with the results showing that CrleGV can achieve similar levels of reduction in infested fruit when compared against the controls (Moore et al., 2015). Applications of CrleGV in these trials also included the addition of a surfactant either Agral 90 (alkylated phenol-ethylene oxide; Plasskem, South Africa) or Break-Thru S240 (polyether trisiloxane; Evonik Africa, South Africa). Additionally, molasses was added to Cryptogran™ as an adjuvant in many of the trials, with this combination showing a significant improvement in reducing the number of infested fruit as compared to Cryptogran™ on its own (Moore et al., 2015). The continued addition of these surfactants and adjuvant is an important consideration that must be made to assist in improving the efficacy of CrleGV in the field. It is also important to consider when to apply the virus treatments, due to the known susceptibility of baculoviruses towards UV radiation

and the effect it could have during their evaluation (Arthurs et al., 2008; Shapiro, 1995). To mitigate the inactivation of baculovirus biopesticides, treatments should therefore be applied at or after sunset. This enables the greatest duration for viable virus OBs to encounter the target pest before UV inactivation begins (Moore et al., 2015). In the case of *T. leucotreta*, the application of treatments after sunset also coincides with the nocturnal habits of the adult moth (Moore, 2017; Stibick, 2007).

Few studies have investigated the efficacy of mixed baculovirus formulations for the control of insect pests in the field. Field trials conducted by Goto et al. (2015) evaluated the efficacy of MabrNPV, alone and in combination, with proteins derived from the capsules of XecnGV against *Mamestra brassicae* (Linnaeus) (Lepidoptera: Noctuidae). The results from these field trials indicated that the combinations resulted in a significant increase in infectivity and improved speed of kill as compared to the NPV when applied in isolation. A second example of combined baculoviruses for use in the field is that of AcMNPV and Spodoptera albula NPV (SpalNPV), which were formulated into the product VPN-ULTRA (Agrcola El Sol, Guatemala) (Beas-Catena et al., 2014; Haase et al., 2015; Jackson et al., 2008). This product has been used to control multiple insects in Guatemala, however, there is no published literature on the efficacy of this product. The application of CrpeNPV and CrleGV in different combinations in the field would therefore be important in understanding how these viruses interact in a natural environment. This would further inform the development of novel biopesticides for improved control of *T. leucotreta.*

Using the application procedures developed during the evaluation of CrleGV in the field by Moore et al. (2015), this chapter aimed to evaluate the efficacy of CrpeNPV and CrleGV alone and in combination against *T. leucotreta.* The 3:1 and 1:3 combinations of CrpeNPV and CrleGV described previously during the biological assay of these viruses in Chapter 5 were applied in the field on two occasions, once in December 2016 and again in March 2017, each at a different location. The results obtained could assist in determining whether the synergistic effects observed in the laboratory assays between these viruses can also occur in the field.

7.2. Materials and methods

Field trials for both CrpeNPV and CrleGV, alone and in combinations, were conducted on citrus trees on two separate occasions: once in December 2016 and again in March 2017. These dates were chosen to coincide with the period when fruit drop is at a peak as of result of FCM activity (Moore, 2017). FCM egg hatching also occurs during this period enabling exposure of

neonate larvae to the different treatments (S. Moore pers. comm). For both trials, a single-tree, randomised block format was used, with each treatment replicated 10 times. Unsprayed buffer trees were incorporated between each treated tree and on the borders of both trial sites. The first trial was conducted in an orchard at Far Away Farm (33°29'07.9"S 25°40'35.6"E) and the second at Sackville Farm (33°31'53.5"S 25°39'11.9"E) (Figure 7.1A and B respectively) both in the Sundays River Valley of the Eastern Cape Province (Figure 7.1C).

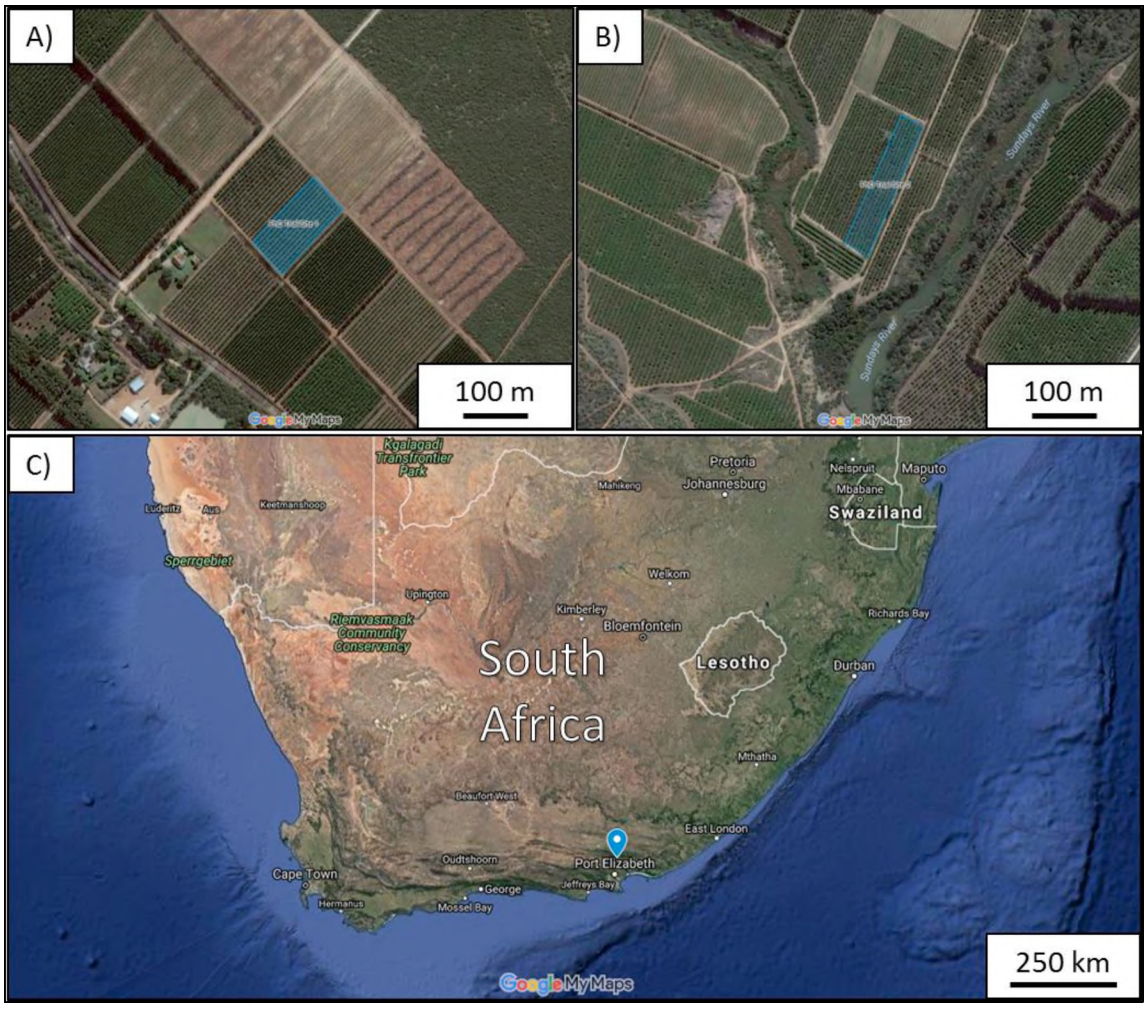

Figure 7.1. Aerial photographs of the A) Far Away and B) Sackville trial sites with the treatment blocks highlighted in blue. The location of Sundays River Valley is shown in panel C by the blue marker (Google Maps, USA).

7.2.1. **Virus formulation and application**

Trials were conducted using CrleGV as the commercial product Cryptogran™ and CrpeNPV, each produced by River Bioscience, both at a concentration of 5×10^{10} OBs.ml^{-1}. For the Far Away trial site, four high (H) (5×10^{6} OBs.ml^{-1}) and four low (L) (5×10^{5} OBs.ml^{-1}) concentration treatments of the viruses were prepared and sprayed alongside a control (no treatment) (Table 7.1). Four concentrations of a proprietary chemical product were also sprayed

alongside the virus treatments. However, the details for these treatments are excluded from this report. The four virus treatments were CrpeNPV (NPV), CrleGV (GV), a 3:1 (N3), and a 1:3 (G3) mixture of the two viruses.

Table 7.1. Treatments applied at the Far Away trial site at high (5×10^9 OBs.l^{-1}) and low (5×10^8 OBs.l^{-1}) concentrations.

	Treatment	Volume (ml) per 100 L		Volume applied (Mean L/tree)
		Cryptogran™	CrpeNPV	
	Control	-	-	-
High Concentration	CrleGV (GV H)	10	0	25
	CrpeNPV (NPV H)	0	10	24
	GV:NPV 3:1 (G3 H)	7.5	2.5	22.5
	GV:NPV 1:3 (N3 H)	2.5	7.5	28
Low Concentration	CrleGV (GV L)	1	0	25
	CrpeNPV (NPV L)	0	1	26
	GV:NPV 3:1 (GV L)	0.75	0.25	25
	GV:NPV 1:3 (NPV L)	0.25	0.75	25

Three virus treatments were applied at the Sackville site (Table 7.2) with CrleGV (GV) and CrpeNPV (NPV) each applied at a concentration of 5×10^6 OBs.ml^{-1}. A single 3:1 mixture of CrpeNPV and CrleGV (N3) respectively was also applied at a total concentration of 5×10^6 OBs.ml^{-1}. These treatments were applied alongside a control (no treatment) and eight chemical treatments, for which the details of seven were excluded from this study due to proprietary constraints. The remaining chemical treatment was the commercial product Runner 240 SC (methoxyfenozide; Dow AgroSciences, USA) referred to as Chem5.

Table 7.2. Treatments applied at the Sackville trial site, each at a concentration of 5×10^9 OBs.l^{-1}.

Treatment	Volume (ml) per 100 L		Volume applied (Mean L/tree)
	Cryptogran™	CrpeNPV	
Control	-	-	-
CrleGV (GV)	10	0	19
CrpeNPV (NPV)	0	10	20
GV:NPV 1:3 (N3)	2.5	7.5	18
Treatment	**Volume (ml) per 100 L**		**Volume applied (Mean L/tree)**
Runner (Chem5)	60		17.5

All virus treatments were applied after sunset to avoid any immediate inactivation of virus OBs due to exposure to UV radiation. All treatments were prepared in a Janisch spray machine and applied to trees using handguns with 2 mm nozzles at a pressure of 20 Bar (Figure 7.2). Virus treatments were combined with Break-Thru S240 at 5 ml per 100 L of water and Molasses at 250 ml per 100 L of water and mixed automatically by the spray machine, which had a centrally located powerful agitator in each tank. Trees were thoroughly sprayed, ensuring all fruit and leaves received the respective treatment while also ensuring the spray mist did not transfer onto adjacent or nearby trees (even though treated trees were buffered). After each treatment, the spray machine tanks were rinsed with water before preparing the next treatment.

Figure 7.2. The application of treatments using pressurised handguns onto citrus trees in Sundays River Valley.

The average daily temperature, duration of sunshine, humidity, rainfall, and wind speed were recorded from a nearby weather station in Port Elizabeth, Eastern Cape (Table 7.3). This weather station is approximately 30 km from where the trial sites were located.

Table 7.3. Average daily weather data, obtained from The Weather Company (IBM, USA) for a nearby weather station in Port Elizabeth (± 30 km from trial sites) for the days that treatments were applied.

Site	Date	Mean Temp (°C)	Sunshine duration (h:min)	Humidity (%)	Rainfall (mm)	Wind speed (km/h)
Far Away	06/12/16	24	14:19	63	0	23
	07/12/16	22	14:20	68	0	21
Sackville	29/03/17	18	11:48	80	0	10

7.2.2. Evaluation and Statistical analysis

Trails were evaluated by collecting and counting fruit drop from all data trees on a weekly basis starting three weeks after the treatments were applied as described by Moore et al. (2015). The Far Away trial was evaluated for 7 weeks, starting in January 2017, with the second week of intended evaluation (i.e. 4 weeks after treatment application) excluded due to orchard sanitation (clearing of fallen fruit) activities conducted by the farm owner under the trial trees, contrary to instruction. The Sackville trial was evaluated for 5 weeks, starting in April 2017. Dropped fruit were examined individually by dissection, with the number of *T. leucotreta* infested fruit counted per treatment for each week of evaluation. The number of infested fruit per week for each treatment was analysed using a Generalised Linear Model ANOVA and the LSD multiple range test using SPSS (IBM, USA). The mean difference between treatments was determined to at a significance level of 0.05.

7.3. Results

7.3.1. Far Away trial site

The Far Away trial site involved a total of 12 treatments alongside an untreated control. Four different virus treatments namely, CrpeNPV treatments (NPV), dominant NPV treatments (N3), dominant GV treatments (G3), and CrleGV treatments (GV), were applied each at high (H) and low (L) concentrations (Table 7.1). Alongside these treatments, a proprietary chemical pesticide was applied at four increasing concentrations referred to as Chem1 to Chem4 (Figure 7.3). Due to orchard sanitation activities conducted by the farm owner during the second week,

the three weeks of data analysed were week one, three, and four and this is referred to as the three-week evaluation.

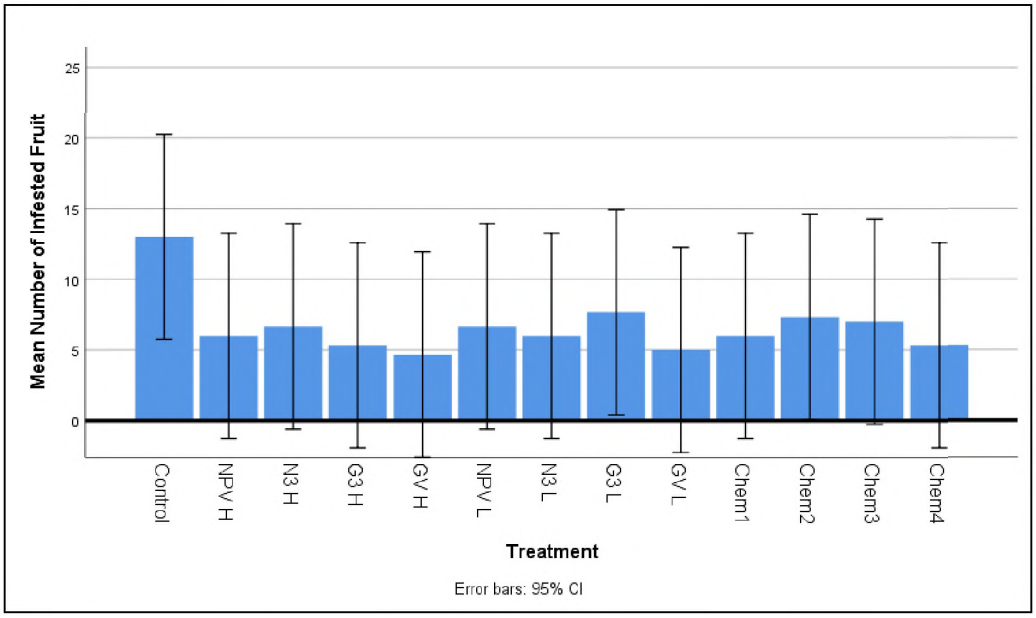

Figure 7.3. The mean number (std. error) of infested fruit per week for the Far Away Farm treatments after three weeks of evaluation. The virus treatments, each applied to ten trees, were CrpeNPV (NPV), NPV dominant (N3), GV dominant (G3) and CrleGV (GV) at high (H) and low (L) concentrations. A chemical treatment was also applied at four concentrations Chem1 (lowest) to Chem4 (highest).

The mean number of infested fruit was higher in the control than all other treatments, but these differences were not statistically significant (> 0.05) (Figure 7.3 and Supplementary Table 10.5). The lowest mean number of infested fruit was measured in the CrleGV treatments, particularly for the high concentration treatment (GV H). Although not significant, a reduction of between 48.7 % and 64.1 % was measured in the high concentration treatments compared to the control. This reduction dropped slightly to between 41.0 % and 61.5 % for the low concentration treatments compared to the control. The next lowest mean number of infested fruit was recorded in the Chem4 treatment, which was applied at the highest concentration of the four chemical applications. Similar to the virus treatments, a reduction of between 43.6 % and 59 % was measured in the chemical treatments when compared to the control.

Analysis of the Far Away trial site across the seven weeks showed most treatments to have only a slightly lower level of infested fruit than was observed in the control. Like the results measured for the first three weeks of evaluation, no significant difference was determined between the treatments and the control after seven weeks (Supplementary Table 10.6). The high concentration treatment of CrpeNPV was recorded to have the lowest mean number of

infested fruit after seven weeks. While not significant, a reduction in the percentage of infested fruit was still measured in almost all treatments when compared to the control. The exception to this was the CrleGV treatment applied at a low concentration (GV L) where a slight increase of 2.9 % was measured. For all treatments, the level of reduction was, however, lower than what was observed after the three weeks of evaluation. Results indicated that there was already a decline in efficacy of all treatments at the fourth week of data collection. Efficacy of chemical treatments seemed to have virtually disappeared at this time and efficacy of virus treatments seemed to disappear between the fifth and sixth week of data collecting. This indicated that there was a period of residual efficacy under these conditions in the field.

7.3.2. **Sackville trial site**

The Sackville trial site involved a total of 11 treatments applied alongside a control. Only three of these treatments were virus based, consisting of a CrleGV treatment (GV), a CrpeNPV treatment (NPV), and an NPV dominant treatment (N3). The remaining treatments were all chemical pesticides and are referred to as Chem1 to Chem8. The Chem1 and Chem2 treatments each comprise different chemical pesticides which were also evaluated in two combinations referred to as Chem3 and Chem4. The chemical treatments, Chem6 to Chem8, were different pesticides while Chem5 was the commercial pesticide Runner (Figure 7.4).

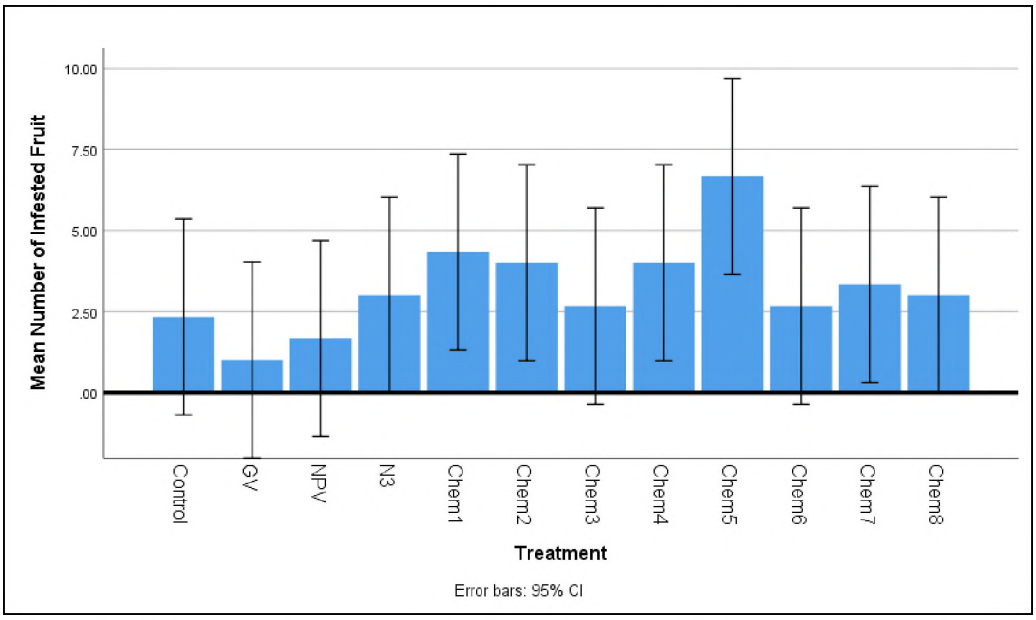

Figure 7.4. The mean number (std. error) of infested fruit per week for the Sackville Farm treatments after three weeks of evaluation. Three virus treatments, each applied to ten trees, were applied namely a CrleGV (GV), a CrpeNPV (NPV) and an NPV dominant (N3) mixture. Eight chemical treatments were also applied, Chem1 to Chem8.

The mean level of infestation between the treatments after three weeks in the Sackville trial site showed a large amount of variation (Figure 7.4). All chemical and the NPV dominant treatments had higher mean number of infected fruit compared to the control. Only the CrleGV and CrpeNPV dominant treatments showed a lower mean number of infested fruit when compared to the control. No treatment was significantly different from the control indicating large amounts of variation between the results recorded each week (Supplementary Table 10.7). A reduction in fruit infestation of 57.1 % and 28.6 % was observed in the CrleGV and CrpeNPV treatments when compared to the control after the first three weeks of evaluation. No other treatment showed a reduction in fruit infestation after three weeks. The mean number of infested fruit on the Chem5 (Runner) treatment was significantly higher than the control (0.047), CrleGV (0.012), and CrpeNPV (0.024) treatments.

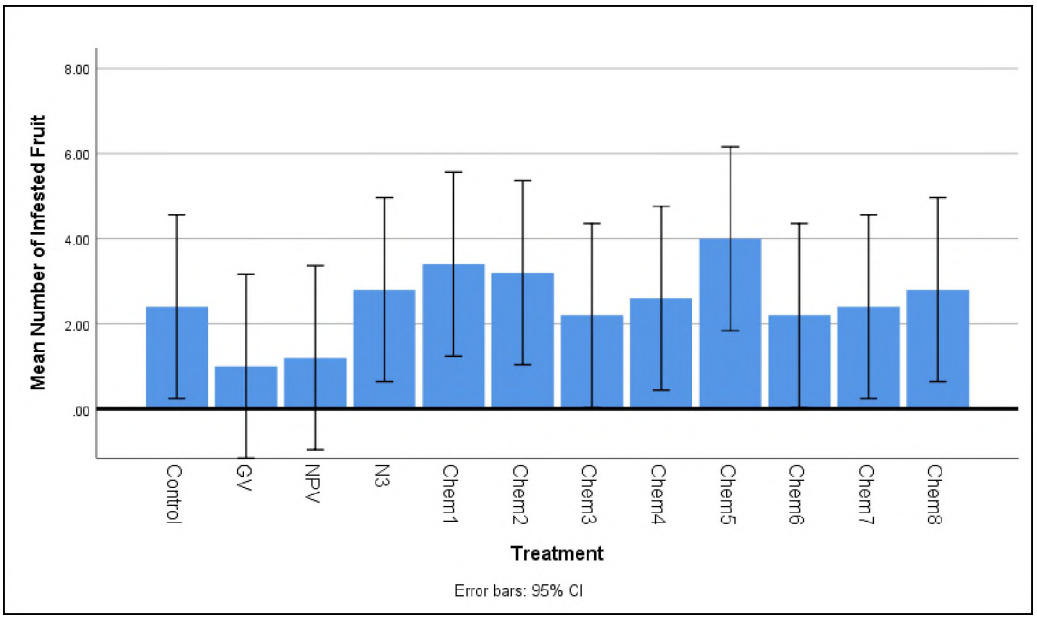

Figure 7.5. The mean number (std. error) of infested fruit per week for the Sackville Farm treatments after five weeks of evaluation. Three virus treatments, each applied to ten trees, were applied namely a CrleGV (GV), a CrpeNPV (NPV) and an NPV dominant (N3) mixture. Eight chemical treatments were also applied, Chem1 to Chem8.

The results for the Sackville trial site after five weeks (Figure 7.5) of evaluation did not differ much from what was recorded after three weeks. The same general trend was observed with no significant difference measured between the treatments and the control (Supplementary Table 10.8). The CrleGV and CrpeNPV treatments had the lowest mean number of infested fruit, although this was not significantly lower than any other treatment. The greatest reduction in fruit infestation was observed in the CrleGV and CrpeNPV treatments at 54.5 % and 45.5 %. A slight reduction in fruit infestation of 9.1 % was observed in the Chem6 treatment, while the

Chem3 and the Chem7 treatments showed no difference in percentage reduction when compared to the control after five weeks of evaluation.

7.4. Discussion

In this chapter, the efficacy of CrpeNPV and CrleGV either alone or in combinations were evaluated in the field. Two separate trials were conducted: the first on an orchard at Far Away Farm and a second at Sackville Farm. The first trial evaluated four virus-based treatments each at a high and low concentration. A chemical pesticide at four concentrations was applied alongside the virus treatments. The details for these were excluded due the proprietary nature of this product, with these products unregistered and under experimentation. The second trial evaluated three virus based treatments alongside eight chemical pesticides. The details for seven of the eight chemical treatments at the Sackville Farm trial were also excluded, again due to the proprietary nature of these products. The remaining chemical treatment, Runner, is a registered insecticide which is used to control *T. leucotreta* in citrus in South Africa. It has been tested in field trials against this pest and has been shown to be consistently the most effective of the registered chemical insecticides in reducing fruit infestation (S. Moore pers. comm, Moore et al., 2015).

The results obtained for the Far Away Farm field trial were found to be highly variable, whereby the mean number of infested fruit across all treatments for weeks 3 and 4 was recorded at 4.0 ± 3.1 and 3.9 ± 2.8 respectively. However, a dramatic increase in *T. leucotreta* larval infestation of fruit across all treatments was recorded for weeks 5, 6, and 7 with mean values of 22.9 ± 6.3, 49.9 ± 10.5, and 32.4 ± 7.2 respectively. While all treatments showed lower levels of mean infested fruit when compared to the control, this high degree of variation between weeks resulted in no significant differences.

Similarly, the Sackville trial did not show any significant decreases in the mean number of infested fruit for the treatments compared to the control. Interestingly, a reduction in the percentage of infested fruit was only measured in the CrleGV and CrpeNPV treatments with all other treatments recorded to have higher levels of infested fruit when compared to the control. The Runner (Chem5) application was the only treatment to show a significant difference to the control at the 3-week evaluation point, however, it was recorded to have significantly higher levels of infested fruit. This could be an incidental result, due to the lack of efficacy among all treatments. Alternatively, this increase in infested fruit might be due to a non-target effect by Runner, which potentially suppressed a natural enemy of *T. leucotreta*,

such as the egg parasitoid, *Trichogrammatoidea cryptophlebia* (Nagaraja) (Hymenoptera: Trichogrammatoidea) which is known to effectively suppress the pest (Moore and Hattingh, 2012; Newton and Odendaal, 1990). While non-target effects have not been demonstrated for the insecticide Runner (EPPO, 2013), there have been multiple reports demonstrating detrimental effects of other chemical insecticides, including insect growth regulators (IGR), on natural enemies (Cloyd and Dickinson, 2006; Prabhaker et al., 2007; Rothwangl et al., 2004; Wakgari and Giliomee, 2001, 2003). For example, a study by Liu and Stansly, (1997) evaluated the effect of the IGR insecticide pyriproxyfen against three *Bemisia tabaci* (Gennadius) (Hemiptera: Aleyrodidae) endoparasitoids. One of these endoparasitoids, *Encarsia formosa* (Gahan) (Hymenoptera: Aphelinidae), was affected by pyriproxyfen which resulted in reduced parasitism of *B. tabaci.* A similar study by Cloyd and Dickinson, (2006) investigated the effects of chemical insecticides on natural enemies of *Planococcus citri* (Risso) (Hemiptera: Pseudococcidae). Pyriproxyfen was recorded to increase mortality in the natural enemy, *Cryptolaemus montrouzieri* (Mulsant) (Coleoptera: Coccinellidae), by 20 %, while other chemical insecticides such as the neonicotinoids Clothianidin and Acetamiprid, resulted in a significant mortality of 70 % just 24 hours after application and 100 % after 48 hours. Another study examined the effects of chemical insecticides on the natural enemy, *Coccidoxenoides perminutus* (Timberlake) (Hymenoptera: Encyrtidae). This insect parasitises *P. citri,* a citrus pest in South Africa (Wakgari and Giliomee, 2003). Several IGRs were tested including the chemicals fenoxycarb, pyriproxyfen, and triflumuron. However, these did not cause a significant increase in *C. peregrinus* when compared to the control. Conversely, organophosphate chemistries such as parathion and methidathion were found to cause 100 % mortality in *C. perminutus*. While there is some evidence that IGR insecticides can influence natural enemies, the impact of Runner against *T. leucotreta* parasitoids was not examined. There was therefore no clarification for the reason of the increased fruit infestation in this treatment during the Sackville trial.

It is unclear why all the treatments, both virus and chemical, showed poor efficacy at these trial sites. It is important to consider that both CrleGV and Runner have been shown to be effective in reducing the mean number of infested fruit in a number of completed field trials (Moore et al., 2015). The decreased efficacy of CrleGV along with all other treatments might indicate that an external factor mitigated their effect against *T. leucotreta.* The average weather data over the time during which the Far Away field trials were conducted in this study, and those by Moore et al. (2015), are shown in Table 7.4.

Table 7.4. Average weather data obtained from The Weather Company (IBM, USA) for a nearby weather station in Port Elizabeth (± 30 km from trial sites) for the trial conducted at Far Away Farm in this study and by Moore et al. (2015) on the Far Away Farm in 2010/11 and 2013, all for the period from application to the last evaluation.

	Far Away Field Site		
	Dec-Feb 2010/11	**Apr-June 2013**	**Dec-Feb 2016/17**
Avg. max temp	24 °C	22 °C	26 °C
Avg. mean temp	20 °C	15 °C	21 °C
Avg. min temp	17 °C	9 °C	17 °C
Avg. rainfall	0.0 mm	0.7 mm	0.3 mm
Total rainfall	0.0 mm	37.34 mm	22.33 mm
Avg. wind speed	19 $km.h^{-1}$	15 $km.h^{-1}$	19 $km.h^{-1}$

In both field trials conducted at the Far Away Farm by Moore et al. (2015) in 2010/11 and 2013, a significant difference in infested fruit was recorded between the Cryptogran™ plus molasses treatment as compared to the control. All three trials had similar average temperatures (max, mean and min) and wind speeds during the period starting from initial application to the last week of evaluation (Table 7.4). Additionally, during the 2010/11 trial no rainfall was recorded, whereas 37.34 mm of rainfall was observed in the 2013 trial. The total rainfall for the Far Away trial in this study was 22.33 mm which was comparable to the 2013 trial, and therefore likely had no detrimental effect on the trial. Additionally, Kirkman, (2007) demonstrated that Cryptogran™ is rain fast. The overall similarity in the average weather data between these trials indicates that the immediate environmental conditions may not have been a major influencing factor in this study.

Another possible reason for the low efficacy in the trials may be related to higher than normal levels of recorded fruit drop in the Sundays River Valley in the 2016/17 season as reported by Stander, (2017). Abnormally elevated temperatures, low relative humidity, and high wind speed during the citrus flowering period in August 2016 was associated with increased fruit splitting and dropping. Insect pests were not identified as a major contributing factor towards the increase in recorded fruit drop, fruit splitting, and changes in fruit development in the lead up to this study. However, the increase in fruit dropping may have triggered changes in insect behaviour resulting in unusual levels of infestation which may have affected the results obtained. It has been reported that injury or premature ripening of citrus fruit increases the

number of *T. leucotreta* eggs laid on them, resulting in increased infestation (Newton, 1989). Furthermore, fruit splitting could enable neonate larvae to penetrate directly into the fruit, reducing contact with the treatments and consequently reducing their efficacy in the trials. However, the addition of molasses to virus treatments has been shown to attract neonate larvae, which then feed on the molasses and consequently remain on the surface of the fruit (Mwanza et al., 2016). This increases the possibility of coming into contact with virus OBs, resulting in improved efficacy (Mwanza et al., 2016). An increase in neonate feeding on the surface of virus-inoculated trees, due to the addition of molasses in the Far Away Farm and Sackville Farm trials in this study, may explain why these treatments showed the greatest reduction in fruit infestation.

In conclusion, this chapter aimed to evaluate the efficacy of CrpeNPV and CrleGV alone and in combination in the field against *T. leucotreta*. However, due to factors which remain unclear, no significant decrease in fruit infestation was observed between the virus or chemical treatments and the controls. Interestingly, the mean number of infested fruit was generally observed to be lower in the virus treatments than was recorded in the chemical treatments at both trial sites. It is possible that adverse field conditions contributed to the poor efficacy of the treatments, resulting in inconclusive findings. As such, it would prove worthwhile to repeat this field trial during the next available season to determine whether the results obtained were a result of the treatments or another mitigating factor.

Chapter 8

General discussion

8.1. Thesis overview

The identification of a novel NPV in CrleGV infected *T. leucotreta* larval homogenate samples was an important discovery which created opportunities that were investigated in this study. The first major objective of this study was to develop a method to purify the NPV OBs from mixed NPV-CrleGV samples as described in Chapter 2. The successful isolation and morphological examination of the NPV OBs was followed by analysis of the complete genome sequence in Chapter 3. This analysis revealed that the genome sequence of the novel NPV was identical to a baculovirus isolated from *C. peltastica* and was thereafter named CrpeNPV. Using the complete genome sequences of CrpeNPV and CrleGV, mPCR and qPCR assays, developed in Chapter 4, were used to screen samples for the presence of either virus and to quantify the amount of each virus in test samples. The biological activity of CrleGV and CrpeNPV, both alone and in combinations, was determined against *T. leucotreta* neonate larvae (Chapter 5). Following this, the interaction between CrpeNPV and CrleGV was studied, as discussed in Chapter 6, by successively passaging these viruses alone and in combinations through *T. leucotreta* larvae. The recovered OBs from each passage were studied using the mPCR and qPCR techniques. The OBs recovered from the final passage were further examined using NGS and REN analysis for potential recombination events. Lastly, CrpeNPV and CrleGV were evaluated in the field, both alone and in various combinations, to determine how effective they could be in reducing *T. leucotreta* infestation in citrus fruit.

8.2. The development of techniques to detect and characterise CrpeNPV

The detection, characterisation and development of novel baculoviruses as biopesticides is an important process to ensure continued control of agricultural pests. In South Africa, *T. leucotreta* is an important pest in the citrus industry. It poses a threat to the export market due to its classification as a phytosanitary risk. Although many baculoviruses have been developed into biopesticides (Moscardi, 1999; Moscardi et al., 2011), only one was known to infect *T. leucotreta*. This virus, CrleGV, has been formulated into the commercial biopesticides Cryptogran™ and Cryptex® and incorporated into an IPM programme for control of *T. leucotreta* in the field (Knox et al., 2015; S. Moore et al., 2004). The recent identification of a

novel NPV, initially referred to as ThleNPV in coinfected *T. leucotreta*, created the opportunity for developing novel biopesticides against this pest. However, to further characterise and evaluate this virus, a method was required to separate and purify ThleNPV OBs from coinfected *T. leucotreta* samples. Few studies have described baculovirus coinfections, with many of these preparing artificial mixtures from purified samples of the viruses and therefore avoiding the need to develop separation techniques (Lara-Reyna et al., 2003; Wennmann and Jehle, 2014). In this study, the isolation of ThleNPV OBs was achieved using an *in vivo* separation method whereby the heterologous host, *C. pomonella,* was exposed to a mixture of the NPV and CrleGV OBs. As reported by Jehle et al. (1995), CrleGV is unable to establish an infection in *C. pomonella*. On the contrary, ThleNPV can establish an infection in this host (Marsberg, 2016), providing a useful technique for isolating NPV OBs from mixed samples. ThleNPV OBs were examined by TEM and found to have single nucleocapsids per ODV as observed in other SNPVs (Rohrmann, 2013). Another interesting observation was the presence of multiple nucleocapsids in some CrleGV OBs which, although rare, has been observed before in this virus and in CpGV (Dhladhla, 2012; Falcon and Hess, 1985).

Following the isolation of ThleNPV, analysis of the complete genome sequence was carried out. The genome contained 126 ORFs, with all 37 core genes present across the 115,728 bp sequence. Alignment of the genome sequence of ThleNPV against CrpeNPV, which had been recently isolated from *C. peltastica* by Marsberg, (2016), showed these viruses to be identical. Consequently, ThleNPV was renamed as CrpeNPV. Importantly, the observation that ThleNPV and CrpeNPV are the same virus provided a source of purified NPV OBs isolated from *C. peltastica* which could be used in downstream experiments. The independent isolation of the same baculovirus from two or more separate hosts has occurred several times due to baculoviruses, particularly in NPVs. This is because NPVs often have multiple hosts. Examples of this include Rachiplusia ou MNPV (RoMNPV) and Plutella xylostella MNPV (PlxyMNPV), which were both shown to have high genetic similarity to AcMNPV (Harrison and Bonning, 2003; Harrison and Lynn, 2007). This has led to a change in the RoMNPV and PlxyMNPV reference genome sequences on GenBank redirecting to the AcMNPV record for all three viruses (Supplementary Table 10.1). To ensure CrpeNPV was a distinct baculovirus species, a phylogenetic analysis was performed using the core gene sequences from 58 baculoviruses. The results showed CrpeNPV forming a separate branch alongside AdhoNPV and AdorNPV. This distinction of CrpeNPV from other baculoviruses was further supported by the generation of gene parity plots and mauve alignments. For example, several large colinear regions, some

of which were inverted, were identified between CrpeNPV and AdhoNPV which indicated unique genome organisation and structure.

The genome sequences of both CrleGV and CrpeNPV were further used to develop molecular techniques to detect and quantify each of these viruses. An mPCR analysis was developed which could selectively detect either of these viruses in a single reaction, enabling rapid screening of samples. An mPCR technique has been used in another study for the detection of Epinotia aporema GV as a means of quality control in its production (Manzán et al., 2008). Similarly, the mPCR technique developed in this study could be useful as a quality control protocol, should CrpeNPV and/or combinations of CrpeNPV/CrleGV be commercially produced. A qPCR technique was also developed to quantify the amount of each virus in a sample. This technique has important applications in investigating CrleGV and CrpeNPV coinfections and could serve as an accurate indication of quality control should combinations of these viruses be formulated for commercial production.

8.3. The synergistic effect between CrleGV and CrpeNPV in coinfected *T. leucotreta* larvae

The identification of a second baculovirus capable of infecting *T. leucotreta* provided a unique opportunity to examine the effect on the host as well as interactions between the viruses during coinfection. Several studies have investigated the effects of mixed baculovirus genotypes during coinfections, but few have examined mixtures of different species (Arrizubieta et al., 2015a, 2015b; Biedma et al., 2015; Lara-Reyna et al., 2003; Wennmann and Jehle, 2014). Importantly, mixtures of baculoviruses have been shown to be able to improve insecticidal activity as compared to the viruses applied in isolation in laboratory bioassays (Biedma et al., 2015; Lara-Reyna et al., 2003)a. The potential for synergistic interactions was examined between CrpeNPV and CrleGV using biological assays, with each virus applied alone and in combinations of 1:3 and 3:1 respectively, against neonate *T. leucotreta*. The results from these assays gave an indication that a synergistic effect between these viruses was occurring, with decreased LC_{50} and LC_{90} values recorded in the combination treatments as compared to the same concentrations of each virus in isolation. Furthermore, this improvement was greater in the NPV dominant mixture particularly at LC_{90}. These results could have important implications for the development of novel baculovirus-based biopesticides against *T. leucotreta*. The biological activity of CrleGV and CrpeNPV in isolation were evaluated by Marsberg, (2016) against neonate *T. leucotreta* larvae. While the LC_{50} and LC_{90} values were higher in this study, it was observed that CrpeNPV was at least as effective as CrleGV when

used alone. Therefore, any improvement due to synergistic interactions could be beneficial in developing improved biopesticides for the control of *T. leucotreta*. Furthermore, combinations of these viruses, either formulated as mixtures or through the mixing of individual CrpeNPV and CrleGV products, could provide additional options for incorporation into IPM programmes in the field. CrleGV has been successfully utilised in the field for more than 10 years and has been shown to remain genetically and biologically stable across this duration (Moore et al., 2015; van der Merwe et al., 2017). Interestingly, resistance to CrleGV has not been recorded in *T. leucotreta* during this period, however, the discovery of *C. pomonella* populations resistant to CpGV-M emphasises the need for mitigation strategies to be prepared (Asser-Kaiser et al., 2007). The incorporation of CrpeNPV as a biopesticide could assist in mitigating the potential for resistance development in *T. leucotreta* by increasing the number of control options, preventing overuse of any one option. Additionally, combinations of CpGV-M with the CpGV-R5 genotype, which is capable of infecting resistant *C. pomonella,* resulted in both viruses establishing an infection (Graillot et al., 2016). Similarly, should resistance to either CrleGV or CrpeNPV occur in *T. leucotreta*, combinations of these viruses may enable both to establish infections and so facilitate continued control of this pest.

Another aspect worthy of investigation was the potential for interactions between CrleGV and CrpeNPV in coinfected *T. leucotreta* larvae. Serial passage of each virus individually and in the 3:1 and 1:3 combinations was performed on third and fourth instar *T. leucotreta* larvae. This technique has been used in other studies to better understand the interactions occurring between viruses in coinfections, such as changes in population dynamics, synergistic or antagonistic effects on replication, and potential effects on covert infections (Arrizubieta et al., 2015b; Cheng and Lynn, 2009; Simón et al., 2006). OBs recovered from each passage in this study were then analysed using the mPCR and qPCR assays described in Chapter 4. A dramatic shift in OB composition was recorded in all treatments throughout the passage assay. Larvae infected with CrleGV alone were observed to produce more OBs per milligram of tissue than those infected with CrpeNPV. The CrpeNPV dominant treatment yielded increased amounts of total OBs per milligram through each successive passage. However, the mPCR analysis indicated that this observation was likely due to CrleGV becoming increasingly dominant. To better understand the interactions occurring between these viruses during serial passage, gDNA was extracted from the recovered OB samples and analysed using qPCR. Interestingly, CrleGV became the dominant virus in all treatments including the CrpeNPV only treatment. This observation indicated two possible processes occurring during the coinfections. First, as

suggested by the results, CrleGV replication appears to outcompete CrpeNPV during infection in *T. leucotreta*. Secondly, both viruses appear to form covert infections in *T. leucotreta* with CrleGV detected in the CrpeNPV treatment and CrpeNPV detected in control larvae. The ability of baculoviruses to form covert infections has been documented in the literature, with superinfection observed to be a strong elicitor of an overt infection (Burden et al., 2003; Williams et al., 2017). These two processes, when combined, enabled CrleGV to become the dominant virus in all treatments by the final passage. These observations may have implications for both the production of CrpeNPV and CrleGV biopesticides as well as for their use in the field. The production of these viruses would likely need to occur in separate hosts, as CrpeNPV production would risk potential failure if a covertly infected *T. leucotreta* colony is used. The presence of CrleGV infection could rapidly outcompete CrpeNPV, leading to low levels of production. The identification of a potential covert CrpeNPV infection in *T. leucotreta* larvae also possess a potential risk to CrleGV production. A shift to an overt state could result in CrleGV formulated biopesticides becoming contaminated with CrpeNPV. Conversely, the use of CrpeNPV in the field could be advantageous in eliciting covert CrleGV infections in wild *T. leucotreta* populations to become overt, potentially increasing expected level of control.

While the evaluation of CrpeNPV and CrleGV in the laboratory showed potential for synergistic interactions due to improvements in biological activity, it is necessary to test both viruses alone and in combinations in the field. CrleGV has been evaluated in multiple field trials and has been shown to significantly reduce *T. leucotreta* infestation in citrus (Moore et al., 2015). Two separate trials were conducted using CrpeNPV and CrleGV, however, due to unfavourable field conditions, no significant differences were found between the chemical or biological treatments and the control. Virus treatments were recorded to reduce infestation levels more so than other treatments when compared against the control. It is therefore important to repeat these trials and further test the efficacy of CrpeNPV and CrleGV, both alone and in various combinations, in the field.

8.4. Future perspectives

As discussed in Chapter 6, a disparity between unpublished NGS data and the mPCR analysis of *T. leucotreta* homogenate samples was noted (Section 4.3.4). The NGS data indicated that CrpeNPV was present in *T. leucotreta* samples dating back as early as 2001. However, examination of the same samples with the mPCR analysis did not detect CrpeNPV. This disparity might be due to the lower template threshold limits for the mPCR technique, whereas NGS technologies may be more sensitive. It is therefore important to establish the minimum

and maximum amounts of gDNA template required for a positive result to be obtained when using the mPCR analysis. The sensitivity of mPCR was evaluated by Nealis et al. (2015), with oligonucleotide sets determined to affect sensitivity. The mPCR assay used was capable of detecting the viruses from 1 pg to 10 pg gDNA per reaction. Furthermore, it is also important to determine whether mixtures of CrpeNPV and CrleGV gDNA affect the minimum threshold for successful detection of either virus by the mPCR analysis. Determining the limits for the mPCR assay used in this study are necessary to ensure this technique can produce accurate results in both research and commercial settings.

A repeat of the passage assay experiments would also be of great interest to determine whether the results obtained in this study can be replicated. If possible, larvae should be collected before completely succumbing to the virus, enabling the quantification of virus in individual cadavers. Additionally, the non-synchronous infection and potential exclusion during superinfection of *T. leucotreta* larvae could also be carried out and evaluated in a similar manner to the passage assay. A study by Beperet et al. (2014) examined superinfection exclusion between AcMNPV and SfMNPV *in vitro*. This study reported superinfection exclusion 16 to 20 hours postinfection. A similar experiment could be conducted with CrpeNPV and CrleGV in *T. leucotreta* larvae. This experiment could involve the inoculation of larvae with CrpeNPV, followed by separate inoculations with CrleGV (or *vice versa*) at 2-hour intervals up to 24 or 48 hours to determine whether coinfection is inhibited *in vivo* after a certain time span. The qPCR and mPCR techniques developed in this study could be utilised and further improved for such an experiment. The inhibition of either CrleGV or CrpeNPV during a non-synchronous treatment could impact the way in which these viruses are applied in the field, whereby the application of the first virus may inhibit the second virus, decreasing the overall efficacy.

Another important line of research would involve the generation of *T. leucotreta* colonies that are resistant to either CrpeNPV or CrleGV in a laboratory setting. For example, resistance was generated by Nakai et al. (2017) in a laboratory colony of *A. honmai* against the baculovirus AdhoNPV. A significant reduction in LC_{50} was recorded after only three generations, with the resistance pathway determined to remain stable after exposure to the virus had been stopped. The replication of this experiment in a laboratory colony of *T. leucotreta* against CrpeNPV or CrleGV would assist in determining whether combinations of these viruses could overcome such resistance. Furthermore, colonies with resistance generated against CrpeNPV could be exposed to CrleGV or *vice versa* to determine if the resistance pathway is selective towards one or both viruses. These studies would enable mitigation strategies to be developed should

any such resistance develop, in field populations of *T. leucotreta.* In addition to experiments examining resistance, repeated exposure of CrleGV or CrpeNPV to *T. leucotreta* by serial passage could enable the selection of genotypes with improved virulence and speed of kill. The results obtained in this study indicate that CrleGV outcompetes CrpeNPV in *T. leucotreta.* However, of these two viruses, only CrpeNPV can replicate *C. pomonella.* These results may be due to differences in heterologous and homologous host ranges, with *T. leucotreta* being the former for CrpeNPV. It may therefore be possible to adapt CrpeNPV to *T. leucotreta*, as was done for CpGV to *Grapholita molesta* by Graillot et al. (2017), potentially generating improved isolates.

Lastly, research conducted by Opoku-Debrah et al. (2016) identified five distinct CrleGV genotypes from geographically isolated populations of *T. leucotreta.* It is important to determine whether combinations of CrpeNPV with each of these CrleGV genotypes could also exhibit a synergistic effect in *T. leucotreta.* Furthermore, the evaluation of CrpeNPV and combinations with the CrleGV genotypes could be performed on each geographic population of *T. leucotreta.* Similar to the results obtained by Opoku-Debrah et al. (2016), the identification of populations which are more susceptible to CrpeNPV or the combinations could assist in making informed decisions regarding the application of these viruses in the field, should they be formulated as biopesticides. It is also important to continue bioprospecting for novel baculoviruses and genotypes as they could also be further developed for use in the agricultural industry.

8.5. Conclusion

In conclusion, the primary aim of this study was to evaluate the potential for synergistic interactions between a novel baculovirus, CrpeNPV and CrleGV in *T. leucotreta* larvae for improved pest control. Biological assays with CrpeNPV and CrleGV alone and in combinations were conducted to evaluate whether synergistic effects could be recorded. The bioassays showed that mixtures of these viruses had improved virulence as compared to either virus in isolation. These results may enable the development of improved biopesticides for the control of *T. leucotreta* in the South African citrus industry. Interactions between these viruses were also studied, with CrleGV shown to outcompete CrpeNPV during serial passage. These results provide an initial view into how these viruses interact during coinfection, creating a foundation for continued research into baculovirus superinfections. Future research into the efficacy of CrpeNPV alone and in combination with CrleGV in the field is also required to develop novel biopesticide formulations.

References

Abdulkadir, F., Knox, C., Marsberg, T., Hill, M.P., Moore, S.D., 2015. Genetic and biological characterisation of a novel Plutella xylostella granulovirus, PlxyGV-SA. Biocontrol 60, 507–515.

Abdulkadir, F., Marsberg, T., Knox, C.M., Hill, M.P., Moore, S.D., 2013. Morphological and genetic characterization of a South African Plutella xylostella granulovirus (PlxyGV) isolate: short communication. African Entomol. 21, 168–171.

Ansell, C., 2008. Pesticide Regulation in the EU and California, Institure of Governmental Stuides.

Aragão-Silva, C.W., Andrade, M.S., Ardisson-Araújo, D.M.P., Fernandes, J.E.A., Morgado, F.S., Báo, S.N., Moraes, R.H.P., Wolff, J.L.C., Melo, F.L., Ribeiro, B.M., 2016. The complete genome of a baculovirus isolated from an insect of medical interest: Lonomia obliqua (Lepidoptera: Saturniidae). Sci. Rep. 6, 23127. doi:10.1038/srep23127

Ardisson-Araújo, D.M.P., de Melo, F.L., de Andrade, M., Sihler, W., Báo, S.N., Ribeiro, B.M., de Souza, M.L., Andrade, M.D.S., Sihler, W., Báo, S.N., Ribeiro, B.M., de Souza, M.L., 2014. Genome sequence of Erinnyis ello granulovirus (ErelGV), a natural cassava hornworm pesticide and the first sequenced sphingid-infecting betabaculovirus. BMC Genomics 15, 856. doi:10.1186/1471-2164-15-856

Ardisson-araújo, D.M.P., Lima, R.N., Melo, F.L., Clem, R.J., Huang, N., Báo, S.N., Sosa-gómez, D.R., Ribeiro, B.M., 2016. Genome sequence of Perigonia lusca single nucleopolyhedrovirus : insights into the evolution of a nucleotide metabolism enzyme in the family Baculoviridae. Nat. Publ. Gr. 1–14. doi:10.1038/srep24612

Arrizubieta, M., Simón, O., Torres-vila, L.M., Figueiredo, E., Mendiola, J., Mexia, A., Caballero, P., Williams, T., 2015a. Insecticidal efficacy and persistence of a co-occluded binary mixture of Helicoverpa armigera nucleopolyhedrovirus (HearNPV) variants in protected and field-grown tomato crops on the Iberian Peninsula. Pest Manag. Sci. 72, 660–670. doi:10.1002/ps.4035

Arrizubieta, M., Simón, O., Williams, T., Caballero, P., 2015b. A novel binary mixture of Helicoverpa armigera single nucleopolyhedrovirus genotypic variants has improved

insecticidal characteristics for control of cotton bollworms. Appl. Environ. Microbiol. 81, 3984–3993. doi:10.1128/AEM.00339-15

Arthurs, S.P., Lacey, L.A., Behle, R.W., 2008. Evaluation of lignins and particle films as solar protectants for the granulovirus of the codling moth, *Cydia pomonella*. Biocontrol Sci. Technol. 18, 829–839. doi:10.1080/09583150802376227

Arthurs, S.P., Lacey, L.A., Miliczky, E.R., 2007. Evaluation of the codling moth granulovirus and spinosad for codling moth control and impact on non-target species in pear orchards. Biol. Control 41, 99–109. doi:10.1016/j.biocontrol.2007.01.001

Asser-Kaiser, S., Fritsch, E., Undorf-Spahn, K., Kienzle, J., Eberle, K.E., Gund, N. a, Reineke, a, Zebitz, C.P.W., Heckel, D.G., Huber, J., Jehle, J. a, 2007. Rapid emergence of baculovirus resistance in codling moth due to dominant, sex-linked inheritance. Science 317, 1916–1918. doi:10.1126/science.1146542

Asser-Kaiser, S., Heckel, D.G., Jehle, J.A., 2010. Sex linkage of CpGV resistance in a heterogeneous field strain of the codling moth *Cydia pomonella* (L.). J. Invertebr. Pathol. 103, 59–64. doi:10.1016/j.jip.2009.10.005

Asser-Kaiser, S., Radtke, P., El-Salamouny, S., Winstanley, D., Jehle, J.A., 2011. Baculovirus resistance in codling moth (*Cydia pomonella* L.) caused by early block of virus replication. Virology 410, 360–367. doi:10.1016/j.virol.2010.11.021

Bajwa, W.I., Kogan, M., 2002. Compendium of IPM Definitions (CID)–What is IPM and how is it defined in the Worldwide Literature. IPPC Publ. 998.

Beas-Catena, A., Sanchez-Miron, A., Garcia-Camacho, F., Contreras-Gómez, A., Molina-Grima, E., 2014. Baculovirus biopesticides: An overview. J. Anim. Plant Sci. 24, 362–373.

Bedford, E.C.G., den Berg, M.A., De Villiers, E.A., 1998. Citrus pests in the Republic of South Africa. 2.

Beperet, I., Irons, S.L., Simon, O., King, L.A., Williams, T., Possee, R.D., Lopez-Ferber, M., Caballero, P., 2014. Superinfection Exclusion in Alphabaculovirus Infections Is Concomitant with Actin Reorganization. J. Virol. 88, 3548–3556. doi:10.1128/JVI.02974-13

Bianchi, F.J., Snoeijing, I., van der Werf, W., Mans, R.M., Smits, P.H., Vlak, J.M., 2000.

Biological activity of SeMNPV, AcMNPV, and three AcMNPV deletion mutants against *Spodoptera exigua* larvae (Lepidoptera: noctuidae). J. Invertebr. Pathol. 75, 28–35. doi:10.1006/jipa.1999.4907

Biedma, M.E., Salvador, R., Ferrelli, M.L., Sciocco-Cap, A., Romanowski, V., 2015. Effect of the interaction between Anticarsia gemmatalis multiple nucleopolyhedrovirus and Epinotia aporema granulovirus, on *A. gemmatalis* (Lepidoptera: Noctuidae) larvae. Biol. Control 91, 17–21. doi:10.1016/j.biocontrol.2015.07.006

Bielza, P., Denholm, I., Sterk, G., Leadbeater, A., Leonard, P., Jørgensen, L.N., 2008. Declaration of Ljubljana – The Impact of a Declining European Pesticide Portfolio on Resistance Management. Outlooks Pest Manag. 19, 246–248. doi:10.1564/19dec03

Briese, D.T., Mende, H. a., 1983. Selection for increased resistance to a granulosis virus in the potato moth, *Phthorimaea operculella* (Zeller) (Lepidoptera: Gelechiidae). Bull. Entomol. Res. 73, 1. doi:10.1017/S0007485300013730

Bristol Regional Environmental Records Centre, 2017. BRERC species records recorded over 15 years ago. [WWW Document]. doi:10.15468/h1ln5p

Burden, J.P.P., Nixon, C.P.P., Hodgkinson, A.E.E., Possee, R.D.D., Sait, S.M.M., King, L.A.A., Hails, R.S.S., 2003. Covert infections as a mechanism for long-term persistence of baculoviruses. Ecol. Lett. 6, 524–531. doi:10.1046/j.1461-0248.2003.00459.x

Butterfly Conservation, 2017. Macro-moth distribution records for the UK for the period pre 2000 from Butterfly Conservation. [WWW Document]. GBIF.org. doi:10.15468/xnm1lw

Carpenter, J., Bloem, S., Hofmeyr, H., 2007. Area-Wide Control Tactics for the False Codling Moth *Thaumatotibia leucotreta* in South Africa: a Potential Invasive Species, in: Area-Wide Control of Insect Pests. Springer Netherlands, Dordrecht, pp. 351–359. doi:10.1007/978-1-4020-6059-5_33

CGA, 2017. Citrus Growers' Association of Southern Africa Annual Report.

Chen, X., Sun, X., Hu, Z., Li, M., O'Reilly, D.R., Zuidema, D., Vlak, J.M., 2000. Genetic Engineering of Helicoverpa armigera Single-Nucleocapsid Nucleopolyhedrovirus as an Improved Pesticide. J. Invertebr. Pathol. 76, 140–146. doi:10.1006/jipa.2000.4963

Chen, Y.R., Wu, C.Y., Lee, S.T., Wu, Y.J., Lo, C.F., Tsai, M.F., Wang, C.H., 2008. Genomic and host range studies of Maruca vitrata nucleopolyhedrovirus. J. Gen. Virol. 89, 2315–

2330. doi:10.1099/vir.0.2008/001412-0

Cheng, X.W., Lynn, D.E., 2009. Chapter 5 Baculovirus Interactions. In Vitro and In Vivo. Adv. Appl. Microbiol. doi:10.1016/S0065-2164(09)01205-2

Clarke, J.F.G., 1955. Catalogue of the types specimens of Microlepidoptera in the British Museum (Natural History) described by Edward Meyrick / v.3.

Clavijo, G., Williams, T., Simón, O., Muñoz, D., Cerutti, M., López-Ferber, M., Caballero, P., 2009. Mixtures of complete and pif1- and pif2-deficient genotypes are required for increased potency of an insect nucleopolyhedrovirus. J. Virol. 83, 5127–36. doi:10.1128/JVI.02020-08

Cloyd, R.A., Dickinson, A., 2006. Effect of Insecticides on Mealybug Destroyer (Coleoptera: Coccinellidae) and Parasitoid, Leptomastix dactylopii (Hymenoptera: Encyrtidae), Natural Enemies of Citrus Mealybug (Homoptera: Pseudococcidae). J. Econ. Entomol. 99, 1596–1604. doi:10.1603/0022-0493-99.5.1596

Coombes, C.A., Hill, M.P., Moore, S.D., Dames, J.F., 2017. Short communications Potential of entomopathogenic fungal isolates for control of the soil-dwelling life stages of *Thaumatotibia leucotreta* Meyrick (Lepidoptera : Tortricidae) in citrus 25, 235–238. doi:10.4001/003.025.0235

Coombes, C.A., Hill, M.P., Moore, S.D., Dames, J.F., 2016. Entomopathogenic fungi as control agents of *Thaumatotibia leucotreta* in citrus orchards: field efficacy and persistence. BioControl 61, 729–739. doi:10.1007/s10526-016-9756-x

Coombes, C.A., Hill, M.P., Moore, S.D., Dames, J.F., Fullard, T., 2013. Persistence and virulence of promising entomopathogenic fungal isolates for use in citrus orchards in South Africa. Biocontrol Sci. Technol. 23, 1053–1066. doi:10.1080/09583157.2013.819489

Cooper, D., Cory, J.S., Theilmann, D.A., Myers, J.H., 2003. Nucleopolyhedroviruses of forest and western tent caterpillars: Cross-infectivity and evidence for activation of latent virus in high-density field populations. Ecol. Entomol. 28, 41–50. doi:10.1046/j.1365-2311.2003.00474.x

Cory, J.S., Clarke, E.E., Brown, M.L., Hails, R.S., O'Reilly, D.R., 2004. Microparasite manipulation of an insect: The influence of the egt gene on the interaction between a

baculovirus and its lepidopteran host. Funct. Ecol. 18, 443–450. doi:10.1111/j.0269-8463.2004.00853.x

Crook, N.E., James, J.D., Smith, I.R.L., Winstanley, D., 1997. Comprehensive physical map of the Cydia pomonella granulovirus genome and sequence analysis of the granulin gene region. J. Gen. Virol. 78, 965–974. doi:10.1099/0022-1317-78-4-965

Cross, R., Botha, T., Pinchuck, S., 2001. The preparation of biological material for electron microscopy. Rhodes Univ. Grahamst.

Cuartas, P.E., Barrera, G.P., Belaich, M.N., Barreto, E., Ghiringhelli, P.D., Villamizar, L.F., 2015. The Complete Sequence of the First Spodoptera frugiperda Betabaculovirus Genome: A Natural Multiple Recombinant Virus 394–421. doi:10.3390/v7010394

Cunningham, J.C., 1995. Baculoviruses as microbial insecticides. Nov. approaches to Integr. pest Manag. 261–292.

DAFF, 2017. Trends in the Agricultural Sector 2016.

DAFF, 2016. A profile of the South African Citrus Market Value Chain.

Daiber, C.C., 1980. A study of the biology of the false codling moth *Cryptophlebia leucotreta* (Meyr.): The adult and generations during the year. Phytophylactica 12, 182–193.

Daiber, C.C., 1979a. A study of the biology of the false codling moth (*Cryptophlebia leucortreta* (Meyr.)): The cocoon. Phytophylactica 11, 151–157.

Daiber, C.C., 1979b. A study of the biology of the false codling moth [(*Cryophlebia leucotreta* (Meyer.)]: The egg. Phytophylactica 11, 129–132.

Daiber, C.C., 1979c. A study of the biology of the false codling moth [*Cryptophlebia leucotreta* (Meyr.)]: The larva. Phytophylactica 11, 141–144.

David, W.A.L., Gardiner, B.O.C., 1966. Breeding *Pieris brassicae* apparently free from granulosis virus. J. Invertebr. Pathol. 8, 325–333. doi:http://dx.doi.org/10.1016/0022-2011(66)90045-0

David, W.A.L., Gardiner, B.O.C., 1965. The incidence of granulosis deaths in susceptible and resistant *Pieris brassicae* (Linnaeus) larvae following changes of population density, food, and temperature. J. Invertebr. Pathol. 7, 347–355.

Dhladhla, B.I.R., 2012. Enumeration of Insect Viruses using Microscopic and Molecular

Analyses ; South African isolate of Cryptophlebia leucotreta Granulovirus as a Case Study. Nelson Mandela Metropolitan University.

Eberle, K.E., 2010. Novel isolates of Cydia pomonella granulovirus (CpGV): deciphering the molecular mechanism for overcoming CpGV resistance in codling moth (*Cydia pomonella*).

Eberle, K.E., Asser-Kaiser, S., Sayed, S.M., Nguyen, H.T., Jehle, J.A., 2008. Overcoming the resistance of codling moth against conventional Cydia pomonella granulovirus (CpGV-M) by a new isolate CpGV-I12. J. Invertebr. Pathol. 98, 293–298. doi:10.1016/j.jip.2008.03.003

Eberle, K.E., Jehle, J.A., 2006. Field resistance of codling moth against Cydia pomonella granulovirus (CpGV) is autosomal and incompletely dominant inherited. J. Invertebr. Pathol. 93, 201–206. doi:10.1016/j.jip.2006.07.001

EPPO, 2013. Pest risk analysis for Thaumatotibia leucotreta.

Erlandson, M., 2008. Insect Pest Control by Viruses, in: Encyclopedia of Virology. Elsevier, pp. 125–133. doi:10.1016/B978-012374410-4.00432-5

European Commision, 2017. Legislation L 184. Off. J. Eur. Union 60, 1–76.

Falcon, L.A., Hess, R.T., 1985. Electron microscope observations of multiple occluded virions in the granulosis virus of the codling moth, *Cydia pomonella*. J. Invertebr. Pathol. 45, 356–359. doi:10.1016/0022-2011(85)90115-6

Friesen, P.D., 2007. Insect Viruses, in: Fields, B.N., Knipe, D.M., Howley, P.M. (Eds.), Fields Virology. Wolters Kluwer Health/Lippincott Williams & Wilkins, Philadelphia, pp. 709–721.

Fuxa, J.., Sun, J.-Z., Weidner, E.., LaMotte, L.., 1999. Stressors and Rearing Diseases of *Trichoplusia ni*: Evidence of Vertical Transmission of NPV and CPV. J. Invertebr. Pathol. 74, 149–155. doi:10.1006/jipa.1999.4869

Fuxa, J.R., Richter, A.R., Ameen, A.O., Hammock, B.D., 2002. Vertical transmission of TnSNPV, TnCPV, AcMNPV, and possibly recombinant NPV in *Trichoplusia ni*. J. Invertebr. Pathol. 79, 44–50. doi:10.1016/S0022-2011(02)00003-4

Garavaglia, M.J., Miele, S.A.B., Iserte, J.A., Belaich, M.N., Ghiringhelli, P.D., 2012. The ac53,

ac78, ac101, and ac103 Genes Are Newly Discovered Core Genes in the Family Baculoviridae. J. Virol. 86, 12069–12079. doi:10.1128/JVI.01873-12

Gebhardt, M.M., Eberle, K.E., Radtke, P., Jehle, J.A., 2014. Baculovirus resistance in codling moth is virus isolate-dependent and the consequence of a mutation in viral gene pe38. Proc. Natl. Acad. Sci. U. S. A. 111, 15711–15716. doi:10.1073/pnas.1411089111 [doi]

Gilligan, T.M., Epstein, M.E., Hoffman, K.M., 2011. Discovery of False Codling Moth, *Thaumatotibia Leucotreta* (Meyrick), in California (Lepidoptera: Tortricidae). Proc. Entomol. Soc. Washingt. 113, 426–435. doi:10.4289/0013-8797.113.4.426

Gómez-Bonilla, Y., López-Ferber, M., Caballero, P., Léry, X., Muñoz, D., 2011. Characterization of a Costa Rican granulovirus strain highly pathogenic against its indigenous hosts, *Phthorimaea operculella* and *Tecia solanivora*. Entomol. Exp. Appl. 140, 238–246. doi:10.1111/j.1570-7458.2011.01156.x

Gómez-Bonilla, Y., López-Ferber, M., Caballero, P., Murillo, R., Muñoz, D., 2013. Granulovirus formulations efficiently protect stored and field potatoes from *Phthorimaea operculella* and *Tecia solanivora* in Costa Rica. BioControl 58, 215–224. doi:10.1007/s10526-012-9473-z

Goto, C., Mukawa, S., Mitsunaga, T., 2015. Two Year Field Study to Evaluate the Efficacy of Mamestra brassicae Nucleopolyhedrovirus Combined with Proteins Derived from Xestia c-nigrum Granulovirus. Viruses 7, 1062–1078. doi:10.3390/v7031062

Graham, R.I., Tummala, Y., Rhodes, G., Cory, J.S., Shirras, A., Grzywacz, D., Wilson, K., 2015. Development of a real-time qPCR assay for quantification of covert baculovirus infections in a major african crop pest. Insects 6, 746–759. doi:10.3390/insects6030746

Graillot, B., Bayle, S., Blachere-Lopez, C., Besse, S., Siegwart, M., Lopez-Ferber, M., 2016. Biological Characteristics of Experimental Genotype Mixtures of Cydia Pomonella Granulovirus (CpGV): Ability to Control Susceptible and Resistant Pest Populations. Viruses 8, 147. doi:10.3390/v8050147

Graillot, B., Berling, M., Blachere-López, C., Siegwart, M., Besse, S., López-Ferber, M., 2014. Progressive Adaptation of a CpGV Isolate to Codling Moth Populations Resistant to CpGV-M. Viruses 6, 5135–5144. doi:10.3390/v6125135

Graillot, B., Blachère-López, C., Besse, S., Siegwart, M., López-Ferber, M., 2017. Host range

extension of Cydia pomonella granulovirus: adaptation to Oriental Fruit Moth, *Grapholita molesta*. BioControl 62, 19–27. doi:10.1007/s10526-016-9772-x

Grzywacz, D., Rabindra, R.J., Brown, M., Jones, K.A., Parnell, M., 2004. The Helicoverpa armigera NPV production manual.

Gupta, R.K., Gani, M., Kaul, V., Bhagat, R.M., Bali, K., Samnotra, R.K., 2016. Field evaluation of Lymantria obfuscata multiple nucleopolyhedrovirus for the management of Indian gypsy moth in Jammu & Kashmir, India. Crop Prot. 80, 149–158. doi:10.1016/j.cropro.2015.11.008

Haase, S., Sciocco-Cap, A., Romanowski, V., 2015. Baculovirus Insecticides in Latin America: Historical Overview, Current Status and Future Perspectives. Viruses 7, 2230–2267. doi:10.3390/v7052230

Han, G., Xu, J., Liu, Q., Li, C., Xu, H., Lu, Z., 2016. Genome of Cnaphalocrocis medinalis Granulovirus, the First Crambidae-Infecting Betabaculovirus Isolated from Rice Leaffolder to Sequenced. PLoS One 11, e0147882. doi:10.1371/journal.pone.0147882

Harrison, R., Hoover, K., 2012. Baculoviruses and Other Occluded Insect Viruses, in: Vega, F.E., Kaya, H.K. (Eds.), Insect Pathology. Elsevier, pp. 73–131. doi:10.1016/B978-0-12-384984-7.00004-X

Harrison, R.L., 2009. Structural divergence among genomes of closely related baculoviruses and its implications for baculovirus evolution. J. Invertebr. Pathol. 101, 181–186. doi:10.1016/j.jip.2009.03.012

Harrison, R.L., Bonning, B.C., 2003. Comparative analysis of the genomes of Rachiplusia ou and Autographa californica multiple nucleopolyhedroviruses. J. Gen. Virol. 84, 1827–1842. doi:10.1099/vir.0.19146-0

Harrison, R.L., Lynn, D.E., 2007. Genomic sequence analysis of a nucleopolyhedrovirus isolated from the diamondback moth, *Plutella xylostella*. Virus Genes 35, 857–873. doi:10.1007/s11262-007-0136-6

Hayakawa, T., Ko, R., Okano, K., Seong, S.-I., Goto, C., Maeda, S., 1999. Sequence Analysis of the Xestia c-nigrum Granulovirus Genome. Virology 262, 277–297.

Herniou, E.A., Luque, T., Chen, X., Vlak, J.M., Winstanley, D., Cory, J.S., O'Reilly, D.R., 2001. Use of whole genome sequence data to infer baculovirus phylogeny. J. Virol. 75,

8117–26. doi:10.1128/JVI.75.17.8117

Herniou, E.A., Olszewski, J.A., Cory, J.S., O'Reilly, D.R., 2003. The genome sequence and evolution of baculoviruses. Annu. Rev. Entomol. 48, 211–234.

Hofmeyr, J.H., Hofmeyr, M., Hattingh, V., Slabbert, J.P., 2016. Postharvest Phytosanitary Disinfestation of Thaumatotibia leucotreta (Lepidoptera: Tortricidae) in Citrus Fruit: Determination of Ionising Radiation and Cold Treatment Conditions for Inclusion in a Combination Treatment. African Entomol. 24, 208–216. doi:10.4001/003.024.0208

Hoover, K., Grove, M., Gardner, M., Hughes, D.P., McNeil, J., Slavicek, J., 2011. A gene for an extended phenotype. Science (80-.). 333, 1401.

Hostetter, D.L., Puttler, B., 1991. A New Broad Host Spectrum Nuclear Polyhedrosis Virus Isolated from a Celery Looper, *Anagrapha falcifera* (Kirby), (Lepidoptera: Noctuidae). Environ. Entomol. 20, 1480–1488. doi:10.1093/ee/20.5.1480

Hunter-Fujita, F.R., Entwistle, P.F., Evans, H.F., Crook, N.E., 1998. Insect viruses and pest management. John Wiley & Sons Ltd.

Ishii, T., Takatsuka, J., Nakai, M., Kunimi, Y., 2002. Growth Characteristics and Competitive Abilities of a Nucleopolyhedrovirus and an Entomopoxvirus in Larvae of the Smaller Tea Tortrix, *Adoxophyes honmai* (Lepidoptera: Tortricidae). Biol. Control 23, 96–105. doi:10.1006/bcon.2001.0988

Jackson, D.M., Lynn, D.E., Fuxa, J.R., Shepard, B.M., Shapiro, M., 2008. Efficacy of Entomopathogenic Viruses on Pickleworm Larvae and Cell Lines. J. Agric. Urban Entomol. 25, 81–97. doi:10.3954/1523-5475-25.2.81

Jackson, J.., Sutter, G.R., 1985. Pathology of a Granulosis Virus in the Army Cutworm , Euxoa auxiliaris (Lepidoptera : Noctuidae). J. Kansas Entomol. Soc. 58, 353–355.

Jehle, J.A., Fritsch, E., Nickel, A., Huber, J., Backhaus, H., 1995. TCl4.7: A Novel Lepidopteran Transposon Found in Cydia pomonella Granulosis Virus. Virology 207, 369–379. doi:10.1006/viro.1995.1096

Jehle, J.A., Lange, M., Wang, H., Hu, Z., Wang, Y., Hauschild, R., 2006. Molecular identification and phylogenetic analysis of baculoviruses from Lepidoptera. Virology 346, 180–193. doi:10.1016/j.virol.2005.10.032

Jehle, J.A., Sauer, A., Fritsch, E., Udorf-Spahn, K., 2014. Resistance to cydia pomonella granulovirus: Novel findings on its distribution and diversity. 16 th Int. Conf. Org. Fruit-Growin 244–246.

Jehle, Blissard, G.W., Bonning, B.C., Cory, J.S., Herniou, E.A., Rohrmann, G.F., Theilmann, D.A., Thiem, S.M., Vlak, J.M., 2006. On the classification and nomenclature of baculoviruses: A proposal for revision. Arch. Virol. 151, 1257–1266. doi:10.1007/s00705-006-0763-6

Jiang, Y., Deng, F., Rayner, S., Wang, H., Hu, Z., 2009. Evidence of a major role of GP64 in group I alphabaculovirus evolution. Virus Res. 142, 85–91. doi:10.1016/j.virusres.2009.01.015

Jones, D.T., Taylor, W.R., Thornton, J.M., 1992. The rapid generation of mutation data matrices from protein sequences. Comput. Appl. Biosci. CABIOS 8, 275–282.

Jukes, M.D., 2015. The isolation, genetic characterisation and biological activity of a South African Phthorimaea operculella granulovirus (PhopGV-SA) for the control of the Potato Tuber Moth, *Phthorimaea operculella* (Zeller).

Jukes, M.D., Knox, C.M., Hill, M.P., Moore, S.D., 2014. The isolation and genetic characterisation of a South African strain of Phthorimaea operculella granulovirus, PhopGV-SA. Virus Res. 183, 85–88. doi:10.1016/j.virusres.2014.01.013

Jung, S., Kim, Y., 2006. An Entomopathogenic Bacterium, Xenorhabdus nematophila K1, Enhances Baculovirus Pathogenicity against *Spodoptera exigua* and *Plutella xylostella*. J. Asia. Pac. Entomol. 9, 179–182. doi:10.1016/S1226-8615(08)60290-3

Kamita, S.G., Maeda, S., Hammock, B.D., 2003. High-frequency homologous recombination between baculoviruses involves DNA replication. J Virol 77, 13053–13061. doi:10.1128/JVI.77.24.13053

Katsuma, S., Shimada, T., 2015. The killing speed of egt-inactivated Bombyx mori nucleopolyhedrovirus depends on the developmental stage of *B. mori* larvae. J. Invertebr. Pathol. 126, 64–70.

Kearse, M., Moir, R., Wilson, A., Stones-Havas, S., Cheung, M., Sturrock, S., Buxton, S., Cooper, A., Markowitz, S., Duran, C., Thierer, T., Ashton, B., Meintjes, P., Drummond, A., 2012. Geneious Basic: an integrated and extendable desktop software platform for the

organization and analysis of sequence data. Bioinformatics 28, 1647–1649. doi:10.1093/bioinformatics/bts199 [doi]

Kemp, E.M., Woodward, D.T., Cory, J.S., 2011. Detection of single and mixed covert baculovirus infections in eastern spruce budworm, *Choristoneura fumiferana* populations. J. Invertebr. Pathol. 107, 202–205. doi:10.1016/j.jip.2011.05.015

Kimura, M., 1980. A simple method for estimating evolutionary rates of base substitutions through comparative studies of nucleotide sequences. J. Mol. Evol. 16, 111–120. doi:10.1007/BF01731581

Kirkman, W., 2007. Understanding and improving the residual efficacy of the Cryptophlebia leucotreta granulovirus (CRYPTOGRAN).

Knox, C., Moore, S.D., Luke, G.A., Hill, M.P., 2015. Baculovirus-based strategies for the management of insect pests : a focus on development and application in South Africa. Biocontrol Sci. Technol. 25, 1–20. doi:10.1080/09583157.2014.949222

Komai, F., 1999. A taxonomic review of the genus *Grapholita* and allied genera (Lepidoptera: Tortricidae) in the Palaearctic region. Entomol. Scand. 5--+.

Kondo, a, Maeda, S., 1991. Host range expansion by recombination of the baculoviruses Bombyx mori nuclear polyhedrosis virus and Autographa californica nuclear polyhedrosis virus. J. Virol. 65, 3625–32.

Kouassi, L.N., Tsuda, K., Goto, C., Mukawa, S., Sakamaki, Y., Kusigemati, K., Nakamura, M., 2009. Prevalence of latent virus in Spodoptera litura (Fabricius) (Lepidoptera: Noctuidae) and its activation by a heterologous virus. Appl. Entomol. Zool. 44, 95–102. doi:10.1303/aez.2009.95

Krejmer, M., Skrzecz, I., Wasag, B., Szewczyk, B., Rabalski, L., 2015. The genome of Dasychira pudibunda nucleopolyhedrovirus (DapuNPV) reveals novel genetic connection between baculoviruses infecting moths of the Lymantriidae family. BMC Genomics 16, 1–13. doi:10.1186/s12864-015-1963-9

Kumar, S., Nei, M., Dudley, J., Tamura, K., 2008. MEGA: a biologist-centric software for evolutionary analysis of DNA and protein sequences. Brief. Bioinform. 9, 299–306. doi:10.1093/bib/bbn017 [doi]

Kumar, S., Stecher, G., Tamura, K., 2016. MEGA7: Molecular Evolutionary Genetics Analysis

Version 7.0 for Bigger Datasets. Mol. Biol. Evol. 33, 1870–1874. doi:10.1093/molbev/msw054

Laarif, A., Ammar, A. Ben, Trabelsi, M., Hamouda, M.H. Ben, Ben Ammar, A., Trabelsi, M., Ben Hamouda, M., 2006. Histopathology and morphogenesis of the Granulovirus of the potato tuber moth *Phthorimaea operculella*. Tunis. J. Plant Prot. 1, 115–124.

Lacey, L.., Vail, P.., Hoffmann, D.., 2002. Comparative activity of baculoviruses against the codling moth *Cydia pomonella* and three other tortricid pests of tree fruit. J. Invertebr. Pathol. 80, 64–68. doi:10.1016/S0022-2011(02)00036-8

Lacey, L.A., Thomson, D., Vincent, C., Arthurs, S.P., 2008. Codling moth granulovirus: a comprehensive review. Biocontrol Sci. Technol. 18, 639–663. doi:10.1080/09583150802267046

Lange, M., Wang, H., Zhihong, H., Jehle, J.A., 2004. Towards a molecular identification and classification system of lepidopteran-specific baculoviruses. Virology 325, 36–47.

Lara-Reyna, J., Del Rincón-Castro, M.C., Ibarra, J.E., 2003. Synergism between the nucleopolyhedroviruses of *Autographa californica* and *Trichoplusia ni*. Acta Virol. 47, 189–94.

Lauzon, H.A.M., Lucarotti, C.J., Krell, P.J., Feng, Q., Retnakaran, A., Arif, B.M., 2004. Sequence and Organization of the Neodiprion lecontei Nucleopolyhedrovirus Genome 78, 7023–7035. doi:10.1128/JVI.78.13.7023

Li, J., Zhou, Y., Lei, C., Fang, W., Sun, X., 2015. Improvement in the UV resistance of baculoviruses by displaying nano-zinc oxide-binding peptides on the surfaces of their occlusion bodies. Appl. Microbiol. Biotechnol. 99, 6841–6853. doi:10.1007/s00253-015-6581-6

Li, Z., Gong, Y., Yin, C., Wang, L., Li, C., Pang, Y., 2003. Characterization of a novel ubiquitin-fusion gene Uba256 from Spodoptera litura nucleopolyhedrovirus. Gene 303, 111–119. doi:10.1016/S0378-1119(02)01140-X

Liu, T.-X., Stansly, P.A., 1997. Effects of Pyriproxyfen on Three Species of *Encarsia* (Hymenoptera: Aphelinidae), Endoparasitoids of *Bemisia argentifolii* (Homoptera: Aleyrodidae). J. Econ. Entomol. 90, 404–411. doi:10.1093/jee/90.2.404

López-Ferber, M., Simón, O., Williams, T., Caballero, P., 2003. Defective or effective?

Mutualistic interactions between virus genotypes. Proc. Biol. Sci. 270, 2249–55. doi:10.1098/rspb.2003.2498

Malan, A.P., Knoetze, R., Moore, S.D., 2011. Isolation and identification of entomopathogenic nematodes from citrus orchards in South Africa and their biocontrol potential against false codling moth. J. Invertebr. Pathol. 108, 115–125. doi:10.1016/j.jip.2011.07.006

Manzán, M.A., Aljinovic, E.M., Biedma, M.E., Sciocco-Cap, A., Ghiringhelli, P.D., Romanowski, V., 2008. Multiplex PCR and quality control of Epinotia aporema granulovirus production. Virus Genes 37, 203–211. doi:10.1007/s11262-008-0256-7

Marsberg, T., 2016. The isolation and genetic characterisation of a novel alphabaculovirus for the microbial control of *Cryptophlebia peltastica* and closely related tortricid pests. Rhodes University.

Mascarin, G.M., Delalibera, I., 2012. Insecticidal Activity of the Granulosis Virus in Combination with Neem Products and Talc Powder Against the Potato Tuberworm *Phthorimaea operculella* (Zeller) (Lepidoptera: Gelechiidae). Neotrop. Entomol. 41, 223–231. doi:10.1007/s13744-012-0044-x

Matindoost, L., Nielsen, L., Reid, S., 2015. Intracellular Trafficking of Baculovirus Particles: A Quantitative Study of the HearNPV/HzAM1 Cell and AcMNPV/Sf9 Cell Systems. Viruses 7, 2288–2307. doi:10.3390/v7052288

Moore, S., Hattingh, V., 2017. A review of control measures and risk mitigation options for false codling moth (FCM), *Thaumatotibia leucotreta*, and their efficacy 1–8.

Moore, S., Hattingh, V., 2012. A Review of Current Pre-harvest Control Options for False Codling Moth in Citrus in Southern Africa. South African Fruit J. 11, 82–85.

Moore, S., Kirkman, W., 2010. HELICOVIR TM : A virus for the biological control of bollworm. SA Fruit J. 9, 63–67.

Moore, S., Kirkman, W., Richards, G., Stephen, P., 2015. The Cryptophlebia Leucotreta Granulovirus—10 Years of Commercial Field Use. Viruses 7, 1284–1312. doi:10.3390/v7031284

Moore, S., Kirkman, W., Stephen, P., 2004. Cryptogran. A virus for the biological control of false codling moth. SA Fruit J. (South Africa).

Moore, S.D., 2017. Moths and Butterflies: False Codling Moth, in: Integrated Production Guidelines. pp. 1–9.

Moore, S.D., 2002. The development and evaluation of Cryptophlebia leucotreta Granulovirus (CrleGV) as a biological control agent for the management of False Codling Moth , *Cryptophlebia leucotreta*, on citrus. Rhodes University.

Moore, S.D., Hendry, D.A., Richards, G.I., 2011. Virulence of a South African isolate of the Cryptophlebia leucotreta granulovirus to *Thaumatotibia leucotreta* neonate larvae. BioControl 56, 341–352. doi:10.1007/s10526-010-9339-1

Moore, S.D., Pittaway, T., Bouwer, G., Fourie, J.G., 2004. Evaluation of Helicoverpa armigera Nucleopolyhedrovirus (HearNPV) for Control of *Helicoverpa armigera* (Lepidoptera: Noctuidae) on Citrus in South Africa. Biocontrol Sci. Technol. 14, 239–250. doi:10.1080/09583150310001655666

Moore, S.D., Richards, G.I., Chambers, C., Hendry, D., 2014. An improved larval diet for commercial mass rearing of the false codling moth, *Thaumatotibia leucotreta* (Meyrick)(Lepidoptera: Tortricidae): short communication. African Entomol. 22, 216–219.

Moscardi, F., 2007. A Nucleopolyhedrovirus for control of the velvetbean caterpillar in Brazilian Soybeans. Biol. Control A Glob. Perspect. eds.C.Vincent, MS Goethel, G.Lazarovits 344–352.

Moscardi, F., 1999. Assessment of the application of baculoviruses for control of Lepidoptera. Annu. Rev. Entomol. 44, 257–289. doi:10.1146/annurev.ento.44.1.257

Moscardi, F., de Souza, M.L., de Castro, M.E.B., Moscardi, M.L., Szewczyk, B., 2011. Baculovirus pesticides: present state and future perspectives, in: Microbes and Microbial Technology. Springer, pp. 415–445.

Motsoeneng, B.M., 2014. Genetic and biological characterisation of a novel South African Cydia pomonella granulovirus (CpGV-SA) isolate. Rhodes University.

Mwanza, P., Hilliar, S., Dealtry, G., Lee, M., Hill, M., Moore, S., 2016. Determination of reapplication frequency required for the Cryptophlebia leucotreta granulovirus : a factor of rate of virus breakdown and larval behaviour. IOBC-WPRS Bull. 113, 151–154.

Nakai, M., Takahashi, K., Iwata, K., Tanaka, K., Koyanagi, J., Ookuma, A., Takatsuka, J.,

Okuno, S., Kunimi, Y., 2017. Acquired resistance to a nucleopolyhedrovirus in the smaller tea tortrix *Adoxophyes honmai* (Lepidoptera: Tortricidae) after selection by serial viral administration. J. Invertebr. Pathol. 145, 23–30. doi:10.1016/j.jip.2017.03.003

Nealis, V.G., Turnquist, R., Morin, B., Graham, R.I., Lucarotti, C.J., 2015. Baculoviruses in populations of western spruce budworm. J. Invertebr. Pathol. 127, 76–80. doi:10.1016/j.jip.2015.03.005

Newton, P.J., 1989. The influence of citrus fruit condition on egg laying by the false codling moth, *Cryptophlebia leucotreta*. Entomol. Exp. Appl. 52, 113–117. doi:10.1111/j.1570-7458.1989.tb01257.x

Newton, P.J., Odendaal, W.J., 1990. Commercial inundative releases of *Trichogrammatoidea cryptophlebiae* [Hym.: Trichogrammatidae] against *Cryptophlebia leucotreta* [Lep.: Tortricidae] in citrus. Entomophaga 35, 545–556. doi:10.1007/BF02375089

Nysten, P.-H., 1808. Recherches sur les maladies des vers à soie et les moyens de les prévenir: suivies d'une instruction sur l'éducation de ces insectes. Impr. impériale.

Opoku-Debrah, J.K., 2008. Geographic variation in the susceptibility of false codling moth, *Thaumatotibia leucotreta*, populations to a granulovirus (CrleGV-SA).

Opoku-Debrah, J.K., Hill, M.P., Knox, C., Moore, S.D., 2016. Heterogeneity in virulence relationships between Cryptophlebia leucotreta granulovirus isolates and geographically distinct host populations: lessons from codling moth resistance to CpGV-M. BioControl 61, 449–459. doi:10.1007/s10526-016-9728-1

Opoku-Debrah, J.K., Hill, M.P., Knox, C., Moore, S.D., 2014. Comparison of the biology of geographically distinct populations of the citrus pest, *Thaumatotibia leucotreta* (Meyrick) (Lepidoptera: Tortricidae), in South Africa. African Entomol. 22, 530–537.

Opoku-Debrah, J.K., Hill, M.P., Knox, C., Moore, S.D., 2013. Overcrowding of false codling moth, *Thaumatotibia leucotreta* (Meyrick) leads to the isolation of five new Cryptophlebia leucotreta granulovirus (CrleGV-SA) isolates. J. Invertebr. Pathol. 112, 219–228. doi:10.1016/j.jip.2012.12.008

Pinedo, F.J.R., Moscardi, F., Luque, T., Olszewski, J.A., Ribeiro, B.M., 2003. Inactivation of the ecdysteroid UDP-glucosyltransferase (egt) gene of Anticarsia gemmatalis nucleopolyhedrovirus (AgMNPV) improves its virulence towards its insect host. Biol.

Control 27, 336–344. doi:10.1016/S1049-9644(03)00026-4

Possee, R.D., Griffiths, C.M., Hitchman, R.B., Chambers, A., Murguia-Meca, F., Danquah, J., Jeshtadi, A., King, L.A., 2010. Baculoviruses: biology, replication and exploitation, in: Asgari, S., Johnson, K.N. (Eds.), Insect Virology. Caister Academic Press, Norfolk, UK, pp. 35–57.

PPECB, 2017. PPECB Annual Report 2016/17. Cape Town.

Prabhaker, N., Morse, J.G., Castle, S.J., Naranjo, S.E., Henneberry, T.J., Toscano, N.C., 2007. Toxicity of seven foliar insecticides to four insect parasitoids attacking citrus and cotton pests. J. Econ. Entomol. 100, 1053–1061. doi:10.1603/0022-0493(2007)100[1053:TOSFIT]2.0.CO;2

Provast, C., Rasamimanana, H., Vincent, C., Valero, J., 2008. Virosoft CP4 field trials in an organic apple orchard, in: International Conference of Entomology. p. 1.

Reynolds, E.S.S., 1963. The use of lead citrate at high pH as an electron-opaque stain in electrion microscopy. J. Cell Biol. 17, 208–212. doi:10.1083/jcb.17.1.208

Roelvink, P.W., Corsaro, B.G., Granados, R.R., 1995. Characterization of the Helicoverpa armigera and Pseudaletia unipuncta granulovirus enhancin genes. J. Gen. Virol. 76, 2693–2705. doi:10.1099/0022-1317-76-11-2693

Rohrmann, G.F., 2014. Baculovirus nucleocapsid aggregation (MNPV vs SNPV): an evolutionary strategy, or a product of replication conditions? Virus Genes 49, 351–357. doi:10.1007/s11262-014-1113-5

Rohrmann, G.F., 2013. Baculovirus Molecular Biology, 3rd ed, Baculovirus Molecular Biology.

Rohrmann, G.F., Erlandson, M.A., Theilmann, A., 2015. Genome Sequence of an Alphabaculovirus Isolated from the Oak Looper , *Lambdina fiscellaria* , Contains a Putative 2-Kilobase-Pair Transposable Element Encoding a Transposase and a FLYWCH 3, 5–6. doi:10.1128/genomeA.00186-15.Copyright

Rothwangl, K.B., Cloyd, R. a, Wiedenmann, R.N., 2004. Effects of Insect Growth Regulators on Citrus Mealybug Parasitoid *Leptomastix dactylopii* (Hymenoptera: Encyrtidae). J. Econ. Entomol. 97, 1239–1244. doi:10.1603/0022-0493-97.4.1239

Sahayaraj, K., 2014. Basic and Applied Aspects of Biopesticides, Basic and Applied Aspects of Biopesticides. Springer India, New Delhi. doi:10.1007/978-81-322-1877-7

Sciocco-Cap, A., Parola, A.D., Goldberg, A. V., Ghiringhelli, P.D., Romanowski, V., 2001. Characterization of a Granulovirus Isolated from Epinotia aporema Wals. (Lepidoptera: Tortricidae) Larvae. Appl. Environ. Microbiol. 67, 3702–3706. doi:10.1128/AEM.67.8.3702-3706.2001

Senthil Kumar, C.M., Jacob, T.K., Devasahayam, S., D'Silva, S., Jinsha, J., Rajna, S., 2015. Occurrence and characterization of a tetrahedral nucleopolyhedrovirus from *Spilarctia obliqua* (Walker). J. Invertebr. Pathol. 132, 135–141. doi:10.1016/j.jip.2015.10.001

Serrano, A., Pijlman, G.P., Vlak, J.M., Muñoz, D., Williams, T., Caballero, P., 2015. Identification of Spodoptera exigua nucleopolyhedrovirus genes involved in pathogenicity and virulence. J. Invertebr. Pathol. 126, 43–50. doi:10.1016/j.jip.2015.01.008

Shapiro, M., 1995. Radiation Protection and Activity Enhancement of Viruses, in: Biorational Pest Control Agents. pp. 153–164. doi:10.1021/bk-1995-0595.ch010

Shokralla, S., Spall, J.L., Gibson, J.F., Hajibabaei, M., 2012. Next-generation sequencing technologies for environmental DNA research. Mol. Ecol. 21, 1794–1805.

Simón, O., Williams, T., Caballero, P., López-Ferber, M., 2006. Dynamics of deletion genotypes in an experimental insect virus population. Proc. R. Soc. B Biol. Sci. 273, 783–790. doi:10.1098/rspb.2005.3394

Sireesha, K., Rao, G.V.R., Rao, P.A., Kumar, P.L., 2010. Effect of different storage conditions on the virulence of Helicoverpa armigera nucleopolyhedrovirus. J. Entomol. Res. 34, 65–69.

Sosa Gómez, D.R., Moscardi, F., Santos, B., Alves, L.F.A., Alves, S.B., 2008. Produção e uso de vírus para o controle de pragas na América Latina. Control. Microbiano Pragas na Am. Lat. Brazil.

Stander, J., 2017. An investigation of excessive fruit drop in the Sundays River valley during the.

Steyn, W.P., Malan, A.P., Daneel, M.S., Slabbert, R.M., 2017. Entomopathogenic nematodes from north-eastern South Africa and their virulence against false codling moth,

Thaumatotibia leucotreta (Lepidoptera: Tortricidae). Biocontrol Sci. Technol. 27, 1265–1278. doi:10.1080/09583157.2017.1391174

Stibick, J., 2007. New pest response guidelines: False codling moth *Thaumatotibia leucotreta*. USDA–APHIS–PPQ–Emergency Domest. Programs, Riverdale, Maryl.

Stofberg, F.J., 1954. False codling moth of citrus. Farming in South Africa 29, 273–276.

Takahashi, M., Nakai, M., Nakanishi, K., Sato, T., Hilton, S., Winstanley, D., Kunimi, Y., 2008. Genetic and biological comparisons of four nucleopolyhedrovirus isolates that are infectious to *Adoxophyes honmai* (Lepidoptera: Tortricidae). Biol. Control 46, 542–546. doi:10.1016/j.biocontrol.2008.06.003

Tanada, Y., Hess, R.T., Omi, E.M., 1975. Invasion of a nuclear polyhedrosis virus in midgut of the armyworm, *Pseudaletia unipuncta*, and the enhancement of a synergistic enzyme. J. Invertebr. Pathol. 26, 99–104. doi:10.1016/0022-2011(75)90174-3

Tanada, Y., Hukuhara, T., 1971. Enhanced infection of a nuclear-polyhedrosis virus in larvae of the armyworm, *Pseudaletia unipuncta*, by a factor in the capsule of a granulosis virus. J. Invertebr. Pathol. 17, 116–126. doi:10.1016/0022-2011(71)90133-9

Tang, Q., Hu, Z., Yang, Y., Wu, H., Qiu, L., Chen, K., Li, G., 2015. Overexpression of Bm65 correlates with reduced susceptibility to inactivation by UV light. J. Invertebr. Pathol. 127, 87–92. doi:10.1016/j.jip.2015.03.003

Thomas, S.R., Elkinton, J.S., 2004. Pathogenicity and virulence. J. Invertebr. Pathol. 85, 146–151. doi:10.1016/j.jip.2004.01.006

Untergasser, A., Cutcutache, I., Koressaar, T., Ye, J., Faircloth, B.C., Remm, M., Rozen, S.G., 2012. Primer3—new capabilities and interfaces. Nucleic Acids Res. 40, e115–e115. doi:10.1093/nar/gks596

van der Merwe, M., Jukes, M., Rabalski, L., Knox, C., Opoku-Debrah, J., Moore, S., Krejmer-Rabalska, M., Szewczyk, B., Hill, M., 2017. Genome Analysis and Genetic Stability of the Cryptophlebia leucotreta Granulovirus (CrleGV-SA) after 15 Years of Commercial Use as a Biopesticide. Int. J. Mol. Sci. 18, 2327. doi:10.3390/ijms18112327

Van Strien, E.A., Jansen, B.J.H., Mans, R.M.W., Zuidema, D., Vlak, J.M., 1996. Sequence and transcriptional analysis of the ubiquitin gene cluster in the genome of Spodoptera exigua nucleopolyhedrovirus. J. Gen. Virol. 77, 2311–2319. doi:10.1099/0022-1317-77-9-2311

Vanreuse, W., Swinnen, K., Gielen, K., Vercayie, D., Driessens, G., Veraghtert, W., Desmet, P., 2017. Waarnemingen.be - Non-native animal occurrences in Flanders and the Brussels Capital Region, Belgium. Version 1.1. [WWW Document]. Natuurpunt. doi:10.15468/k2aiak

Venette, R.C., Davis, E.E., DaCosta, M., Heisler, H., Larson, M., 2003. Mini Risk Assessment False codling moth, *Thaumatotibia* (=*Cryptophlebia*) *leucotreta* (Meyrick) [Lepidoptera: Tortricidae] 1–30.

Vincent, C., Andermatt, M., Valero, J., 2007. Madex® and Virosoft®, viral biopesticides for codling moth control, in: Vincent, C., Goettel, M.S., Lazarovits, G. (Eds.), Biological Control: A Global Perspective: Case Studies from Around the World. Cabi, pp. 336–343.

Virto, C., Williams, T., Navarro, D., Tellez, M.M., Murillo, R., Caballero, P., 2017. Can mixtures of horizontally and vertically transmitted nucleopolyhedrovirus genotypes be effective for biological control of *Spodoptera exigua*? J. Pest Sci. (2004). 90, 331–343. doi:10.1007/s10340-016-0743-x

Wakgari, W., Giliomee, J., 2001. Effects of some conventional insecticides and insect growth regulators on different phenological stages of the white wax scale, *Ceroplastes destructor* Newstead (Hemiptera: Coccidae), and its primary parasitoid, *Aprostocetus ceroplastae* (Gira. Int. J. Pest Manag. 47, 179–184. doi:10.1080/09670870010011118

Wakgari, W.M., Giliomee, J.H., 2003. Natural enemies of three mealybug species (Hemiptera: Pseudococcidae) found on citrus and effects of some insecticides on the mealybug parasitoid *Coccidoxenoides peregrinus* (Hymenoptera: Encyrtidae) in South Africa. Bull. Entomol. Res. 93, 243–54. doi:10.1079/BER2003235

Wang, Q., Bosch, B.J., Vlak, J.M., van Oers, M.M., Rottier, P.J., van Lent, J.W.M., 2016. Budded baculovirus particle structure revisited. J. Invertebr. Pathol. 134, 15–22. doi:10.1016/j.jip.2015.12.001

Wang, Zhu, Z., Zhang, L., Hou, D., Wang, M., Arif, B., Kou, Z., Wang, H., Deng, F., Hu, Z., 2016. Genome Sequencing and Analysis of Catopsilia pomona nucleopolyhedrovirus: A Distinct Species in Group I Alphabaculovirus. PLoS One 11, e0155134. doi:10.1371/journal.pone.0155134

Wennmann, J.T., 2014. Diversity of Baculoviruses Isolated from Cutworms (*Agrotis* spp.).

Johannes Gutenberg-Universität.

Wennmann, J.T., Jehle, J.A., 2014. Detection and quantitation of Agrotis baculoviruses in mixed infections. J. Virol. Methods 197, 39–46. doi:10.1016/j.jviromet.2013.11.010

Wennmann, J.T., Kohler, T., Gueli Alletti, G., Jehle, J.A., 2015. Mortality of cutworm larvae is not enhanced by Agrotis segetum granulovirus and Agrotis segetum nucleopolyhedrovirus B coinfection relative to single infection by either virus. Appl. Environ. Microbiol. 81, 2893–2899. doi:10.1128/AEM.03726-14

Williams, T., Virto, C., Murillo, R., Caballero, P., 2017. Covert Infection of Insects by Baculoviruses. Front. Microbiol. 8, 1–13. doi:10.3389/fmicb.2017.01337

Zimba, K., Moore, S.D., Heshula, U., Hill, M.P., 2016. Agathis bishopi , a Larval Parasitoid of False Codling Moth *Thaumatotibia leucotreta* : Laboratory Rearing and Effect of Adult food on Parasitism and Longevity. African Entomol. 24, 153–161. doi:10.4001/003.024.0153

Zwart, M.P., van Oers, M.M., Cory, J.S., van Lent, J.W.M., van der Werf, W., Vlak, J.M., 2008. Development of a quantitative real-time PCR for determination of genotype frequencies for studies in baculovirus population biology. J. Virol. Methods 148, 146–54. doi:10.1016/j.jviromet.2007.10.022

Supplementary data

Table 10.1. Baculoviruses used to generate the phylogenetic tree for CrpeNPV.

Name	Abbreviation	Accession Number	Genome length (bp)	PubMed Ref. #
Autographa californica MNPV	AcMNPV	NC_001623.1	133894	8030224
Adoxophyes honmai NPV	AdhoNPV	NC_004690	113220	14599801
Adoxophyes orana NPV	AdorNPV	NC_011423	111724	18931089
Agrotis ipsilon MNPV	AgipMNPV	NC_011345	155122	Unpublished
Anticarsia gemmatalis NPV	AgNPV	NC_008520	132239	17030857

Agrotis segetum NPV	AgseNPV	NC_007921	147544	16476975	
Agrotis segetum NPV B	AgseNPV-B	NC_025960.	148981	25471493	
Antheraea pernyi NPV	AnpeNPV	NC_008035	126629	17650316	
Apocheima cinerarium NPV	ApciNPV	NC_018504	123876	Unpublished	
Bombyx mori NPV	BmNPV	NC_001962	128413	10355780	
Bombyx mandarina NPV	BomaNPV	NC_012672	126770	20221737	1
Buzura suppressaria NPV	BusuNPV	NC_023442	120420	24475121	
Choristoneura fumiferana DEF MNPV	CfDEFMNPV	NC_005137	131160	15784888	
Choristoneura fumiferana MNPV	CfMNPV	NC_004778	129593	15784887	
Chrysodeixis chalcites NPV	ChchNPV	NC_007151	149622	15958686	
Choristoneura murinana NPV	ChmuNPV	NC_023177	124688	24482509	2
Choristoneura occidentalis NPV	ChocNPV	NC_021925	128446	23861954	
Choristoneura rosaceana NPV	ChroNPV	NC_021924	129052	23861954	
Clanis bilineata NPV	ClbiNPV	NC_008293	135454	19243590	
Condylorrhiza vestigialis MNPV	CoveMNPV	NC_026430	125767	Unpublished	
Cydia pomonella GV	CpGV	NC_002816	123500	11562546	
Cryptophlebia peltastica NPV	CrpeSNPV	NA		NA	
Culex nigripalpus NPV	CuniNPV	NC_003084	108252	11602755	
Dasychira pudibunda NPV	DapuNPV	KP747440	136761	26449402	
Ecotropis obliqua NPV	EcobNPV	NC_008586	131204	17097707	

Epiphyas postvittana NPV	EppoNPV	NC_003083	118584	11907346	
Euproctis pseudoconspersa NPV	EupsNPV	NC_012639	141291	19347664	
Helicoverpa armigera MNPV	HearMNPV	NC_011615	154196	Unpublished	3
Helicoverpa armigera NPV	HearNPV	NC_003094	130759	15708604	
Helicoverpa SNPV AC53	HearSNPV-AC53	NC_024688	130442	26404605	4
Hemileuca sp. NPV	HespNPV	NC_021923	140633	23852342	
Hyphantria cunea NPV	HycuNPV	NC_007767	132959	16894193	
Helicoverpa zea SNPV	HzSNPV	NC_003349	130869	Unpublished	5
Lambdina fiscellaria NPV	LafiNPV	NC_026922	157977	26021909	
Lymantria dispar MNPV	LdMNPV	NC_001973	161046	9887315	
Leucania separata NPV	LeseNPV	NC_008348	168041	17763934	
Lymantria xylina MNPV	LyxyMNPV	NC_013953	156344	20167051	
Mamestra brassicae MNPV	MabrNPV-K1	NC_023681	152710	23712441	
Mamestra configurata NPV-A	MacoNPV-A	NC_003529	155060	11886270	
Mamestra configurata NPV-B	MacoNPV-B	NC_004117	158482	12083822	
Maruca vitrata MNPV	MaviMNPV	NC_008725	111953	18753242	
Neodiprion sertifer NPV	NeseNPV	NC_005905	86462	15194780	
Orgyia pseudotsugata MNPV	OpMNPV	NC_001875	131995	9126251	
Orgyia leucostigma NPV	OrleNPV	NC_010276	156179	Unpublished	
Peridroma NPV	PealNPV	NC_024625	151109	25838477	

Perigonia lusca SNPV	PeluSNPV	NC_027923	132831	27273152	
Philosamia cynthia ricini NPV	PhcyNPV	JX404026	125376	23425301	
Plutella xylostella MNPV	PlxyMNPV	NC_008349	134417	17671835	6
Pseudoplusia includens SNPV	PsinSNPV	NC_026268	139132	25765042	
Rachiplusia ou MNPV	RoMNPV	NC_004323	131526	12810877	7
Spodoptera exigua NPV	SeMNPV	NC_002169	135611	10567663	
Spodoptera frugiperda MNPV	SfMNPV	NC_009011	131331	18272770	
Spodoptera litura NPV	SpliNPV	NC_003102	139342	11531416	
Spodoptera litura NPV II	SpliNPV-II	NC_011616	148634	Unpublished	
Spodoptera littoralis NPV	SpltNPV	JX454574	137998	23219924	
Sucra jujuba NPV	SujuNPV	NC_028636	135952	25329074	
Thysanoplusia orichalcea NPV	ThorNPV-p2	NC_019945	132978	23043178	
Trichoplusia ni SNPV	TnSNPV	NC_007383	134394	15951000	

#: 1 – Renamed BmNPV (NC_001962), 2 – Renamed CfMNPV (NC_004778), 3 – Renamed MacoNPV (NC004117), 4 – Removed as RefSeq, 5 – Removed as RefSeq, 6 – Renamed AcMNPV (NC_001623), 7 – Renamed AcMNPV (NC_001623).

Table 10.2. gDNA concentrations used for mPCR analysis in Chapter 4

Experiment	Sample name	Concentration ng/µl	A260/280	A260/230
OB purification	50% Sucrose	-	-	-
	PhopGV	77.4	1.8	1.7
***C. pomonella* infection assay**	C_1	489.8	2.0	1.8
	C_6	75.9	1.8	1.0
	T. leucotreta homogenate	58.2	1.5	0.5
	CrleGV	12.2	1.9	1.2

mPCR validation	CrleGV	0.7	0	0
	CrpeNPV	17.6	2.6	0.4
***T. leucotreta* homogenates over 15-years**	2000	3.2	2.1	0.3
	2003	20.4	1.6	0.6
	2006	100.2	1.7	1.3
	2009	37.6	1.6	0.9
	2012	63.7	1.8	1.0
	2015	10.0	1.6	0.4
	2013	831.6	1.6	1.0
	2014	808.2	1.5	0.8
	2015	442.5	1.7	1.1
	2016	471.0	1.7	1.1
	CrpeNPV*	207.9	1.6	0.7
	CrleGV*	684.4	0.9	0.6

Table 10.3. gDNA concentrations used for mPCR analysis in Chapter 6

Passage	Sample	Concentration ng/µl	A260/280	A260/230
Passage 1 (P1)	N3	2.1	2.0	0.0
	NPV	1.0	0.6	0.2
	GV	1.1	0.7	0.0
	G3	2.0	1.4	0.0
	C	4.6	1.2	0.6
Passage 2 (P2)	N3	53.6	1.9	0.1
	NPV	29.6	1.8	0.1
	GV	37.3	1.8	0.2
	G3	26.1	1.8	1.1
	C	36.5	1.8	1.9
Passage 3 (P3)	N3	3.5	1.2	0.0
	NPV	3.6	1.2	0.1
	GV	12.7	1.7	0.1

	G3	10.3	1.6	0.2
	C	1.4	0.7	0.0
Passage 4 (P4)	N3	19.0	1.7	0.6
	NPV	36.0	1.7	0.5
	GV	35.5	1.7	0.1
	G3	72.2	1.9	1.6
	C	133.2	1.9	1.8
Passage 5 (P5)	N3	4.5	1.3	0.2
	NPV	5.2	1.3	0.1
	GV	0.9	0.7	0.0
	G3	4.3	2.0	0.0
	C	68.4	2.0	0.3

Table 10.4. gDNA concentrations used for qPCR analysis in Chapter 6

Passage	Sample	Concentration ng/µl	A260/280	A260/230
Passage 1 (P1)	N3	14.3	0.2	2.4
	NPV	26.0	0.5	1.9
	GV	13.8	0.5	2.0
	G3	13.5	0.7	1.5
Passage 2 (P2)	N3	23.3	0.6	2.0
	NPV	47.2	0.6	1.9
	GV	20.1	0.1	2.1
	G3	18.9	0.3	1.9
Passage 3 (P3)	N3	15.7	0.1	2.4
	NPV	11.4	0.1	2.2
	GV	17.1	0.1	2.1
	G3	11.4	0.2	2.6

	N3	13.0	0.1	2.2
Passage 4	NPV	14.8	0.1	2.3
(P4)	GV	13.7	0.1	2.7
	G3	25.2	0.4	2.0
	N3	16.2	0.3	2.4
Passage 5	NPV	9.8	0.1	2.4
(P5)	GV	11.9	0.3	2.3
	G3	11.9	0.0	2.8

Table 10.5. Multiple comparisons of the Far Away field trial using generalised linear model and the least significant differences after 3 weeks of evaluation.

(I) Treatment	(J) Treatment	Mean Difference (I-J)	Std. Error	Sig.	95% Confidence Interval	
					Lower Bound	Upper Bound
Control	**NPV H**	7.00	4.999	.173	-3.28	17.28
	N3 H	6.33	4.999	.216	-3.94	16.61
	G3 H	7.67	4.999	.137	-2.61	17.94
	GV H	8.33	4.999	.108	-1.94	18.61
	NPV L	6.33	4.999	.216	-3.94	16.61
	N3 L	7.00	4.999	.173	-3.28	17.28
	G3 L	5.33	4.999	.296	-4.94	15.61
	GV L	8.00	4.999	.122	-2.28	18.28
	Chem2	5.67	4.999	.267	-4.61	15.94
	Chem1	7.00	4.999	.173	-3.28	17.28
	Chem3	6.00	4.999	.241	-4.28	16.28
	Chem4	7.67	4.999	.137	-2.61	17.94
NPV H	**Control**	-7.00	4.999	.173	-17.28	3.28
	N3 H	-.67	4.999	.895	-10.94	9.61
	G3 H	.67	4.999	.895	-9.61	10.94

	GV H	1.33	4.999	.792	-8.94	11.61
	NPV L	-.67	4.999	.895	-10.94	9.61
	N3 L	.00	4.999	1.000	-10.28	10.28
	G3 L	-1.67	4.999	.742	-11.94	8.61
	GV L	1.00	4.999	.843	-9.28	11.28
	Chem2	-1.33	4.999	.792	-11.61	8.94
	Chem1	.00	4.999	1.000	-10.28	10.28
	Chem3	-1.00	4.999	.843	-11.28	9.28
	Chem4	.67	4.999	.895	-9.61	10.94
N3 H	**Control**	-6.33	4.999	.216	-16.61	3.94
	NPV H	.67	4.999	.895	-9.61	10.94
	G3 H	1.33	4.999	.792	-8.94	11.61
	GV H	2.00	4.999	.692	-8.28	12.28
	NPV L	.00	4.999	1.000	-10.28	10.28
	N3 L	.67	4.999	.895	-9.61	10.94
	G3 L	-1.00	4.999	.843	-11.28	9.28
	GV L	1.67	4.999	.742	-8.61	11.94
	Chem2	-.67	4.999	.895	-10.94	9.61
	Chem1	.67	4.999	.895	-9.61	10.94
	Chem3	-.33	4.999	.947	-10.61	9.94
	Chem4	1.33	4.999	.792	-8.94	11.61
G3 H	**Control**	-7.67	4.999	.137	-17.94	2.61
	NPV H	-.67	4.999	.895	-10.94	9.61
	N3 H	-1.33	4.999	.792	-11.61	8.94
	GV H	.67	4.999	.895	-9.61	10.94
	NPV L	-1.33	4.999	.792	-11.61	8.94
	N3 L	-.67	4.999	.895	-10.94	9.61
	G3 L	-2.33	4.999	.645	-12.61	7.94
	GV L	.33	4.999	.947	-9.94	10.61
	Chem2	-2.00	4.999	.692	-12.28	8.28
	Chem1	-.67	4.999	.895	-10.94	9.61
	Chem3	-1.67	4.999	.742	-11.94	8.61
	Chem4	.00	4.999	1.000	-10.28	10.28
GV H	**Control**	-8.33	4.999	.108	-18.61	1.94
	NPV H	-1.33	4.999	.792	-11.61	8.94
	N3 H	-2.00	4.999	.692	-12.28	8.28
	G3 H	-.67	4.999	.895	-10.94	9.61
	NPV L	-2.00	4.999	.692	-12.28	8.28
	N3 L	-1.33	4.999	.792	-11.61	8.94

	G3 L	-3.00	4.999	.554	-13.28	7.28
	GV L	-.33	4.999	.947	-10.61	9.94
	Chem2	-2.67	4.999	.598	-12.94	7.61
	Chem1	-1.33	4.999	.792	-11.61	8.94
	Chem3	-2.33	4.999	.645	-12.61	7.94
	Chem4	-.67	4.999	.895	-10.94	9.61
NPV L	**Control**	-6.33	4.999	.216	-16.61	3.94
	NPV H	.67	4.999	.895	-9.61	10.94
	N3 H	.00	4.999	1.000	-10.28	10.28
	G3 H	1.33	4.999	.792	-8.94	11.61
	GV H	2.00	4.999	.692	-8.28	12.28
	N3 L	.67	4.999	.895	-9.61	10.94
	G3 L	-1.00	4.999	.843	-11.28	9.28
	GV L	1.67	4.999	.742	-8.61	11.94
	Chem2	-.67	4.999	.895	-10.94	9.61
	Chem1	.67	4.999	.895	-9.61	10.94
	Chem3	-.33	4.999	.947	-10.61	9.94
	Chem4	1.33	4.999	.792	-8.94	11.61
N3 L	**Control**	-7.00	4.999	.173	-17.28	3.28
	NPV H	.00	4.999	1.000	-10.28	10.28
	N3 H	-.67	4.999	.895	-10.94	9.61
	G3 H	.67	4.999	.895	-9.61	10.94
	GV H	1.33	4.999	.792	-8.94	11.61
	NPV L	-.67	4.999	.895	-10.94	9.61
	G3 L	-1.67	4.999	.742	-11.94	8.61
	GV L	1.00	4.999	.843	-9.28	11.28
	Chem2	-1.33	4.999	.792	-11.61	8.94
	Chem1	.00	4.999	1.000	-10.28	10.28
	Chem3	-1.00	4.999	.843	-11.28	9.28
	Chem4	.67	4.999	.895	-9.61	10.94
G3 L	**Control**	-5.33	4.999	.296	-15.61	4.94
	NPV H	1.67	4.999	.742	-8.61	11.94
	N3 H	1.00	4.999	.843	-9.28	11.28
	G3 H	2.33	4.999	.645	-7.94	12.61
	GV H	3.00	4.999	.554	-7.28	13.28
	NPV L	1.00	4.999	.843	-9.28	11.28
	N3 L	1.67	4.999	.742	-8.61	11.94
	GV L	2.67	4.999	.598	-7.61	12.94
	Chem2	.33	4.999	.947	-9.94	10.61

	Chem1	1.67	4.999	.742	-8.61	11.94
	Chem3	.67	4.999	.895	-9.61	10.94
	Chem4	2.33	4.999	.645	-7.94	12.61
GV L	**Control**	-8.00	4.999	.122	-18.28	2.28
	NPV H	-1.00	4.999	.843	-11.28	9.28
	N3 H	-1.67	4.999	.742	-11.94	8.61
	G3 H	-.33	4.999	.947	-10.61	9.94
	GV H	.33	4.999	.947	-9.94	10.61
	NPV L	-1.67	4.999	.742	-11.94	8.61
	N3 L	-1.00	4.999	.843	-11.28	9.28
	G3 L	-2.67	4.999	.598	-12.94	7.61
	Chem2	-2.33	4.999	.645	-12.61	7.94
	Chem1	-1.00	4.999	.843	-11.28	9.28
	Chem3	-2.00	4.999	.692	-12.28	8.28
	Chem4	-.33	4.999	.947	-10.61	9.94
Chem1	**Control**	-7.00	4.999	.173	-17.28	3.28
	NPV H	.00	4.999	1.000	-10.28	10.28
	N3 H	-.67	4.999	.895	-10.94	9.61
	G3 H	.67	4.999	.895	-9.61	10.94
	GV H	1.33	4.999	.792	-8.94	11.61
	NPV L	-.67	4.999	.895	-10.94	9.61
	N3 L	.00	4.999	1.000	-10.28	10.28
	G3 L	-1.67	4.999	.742	-11.94	8.61
	GV L	1.00	4.999	.843	-9.28	11.28
	Chem2	-1.33	4.999	.792	-11.61	8.94
	Chem3	-1.00	4.999	.843	-11.28	9.28
	Chem4	.67	4.999	.895	-9.61	10.94
Chem2	**Control**	-5.67	4.999	.267	-15.94	4.61
	NPV H	1.33	4.999	.792	-8.94	11.61
	N3 H	.67	4.999	.895	-9.61	10.94
	G3 H	2.00	4.999	.692	-8.28	12.28
	GV H	2.67	4.999	.598	-7.61	12.94
	NPV L	.67	4.999	.895	-9.61	10.94
	N3 L	1.33	4.999	.792	-8.94	11.61
	G3 L	-.33	4.999	.947	-10.61	9.94
	GV L	2.33	4.999	.645	-7.94	12.61
	Chem1	1.33	4.999	.792	-8.94	11.61
	Chem3	.33	4.999	.947	-9.94	10.61
	Chem4	2.00	4.999	.692	-8.28	12.28
Chem3	**Control**	-6.00	4.999	.241	-16.28	4.28

	NPV H	1.00	4.999	.843	-9.28	11.28
	N3 H	.33	4.999	.947	-9.94	10.61
	G3 H	1.67	4.999	.742	-8.61	11.94
	GV H	2.33	4.999	.645	-7.94	12.61
	NPV L	.33	4.999	.947	-9.94	10.61
	N3 L	1.00	4.999	.843	-9.28	11.28
	G3 L	-.67	4.999	.895	-10.94	9.61
	GV L	2.00	4.999	.692	-8.28	12.28
	Chem2	-.33	4.999	.947	-10.61	9.94
	Chem1	1.00	4.999	.843	-9.28	11.28
	Chem4	1.67	4.999	.742	-8.61	11.94
Chem4	**Control**	-7.67	4.999	.137	-17.94	2.61
	NPV H	-.67	4.999	.895	-10.94	9.61
	N3 H	-1.33	4.999	.792	-11.61	8.94
	G3 H	.00	4.999	1.000	-10.28	10.28
	GV H	.67	4.999	.895	-9.61	10.94
	NPV L	-1.33	4.999	.792	-11.61	8.94
	N3 L	-.67	4.999	.895	-10.94	9.61
	G3 L	-2.33	4.999	.645	-12.61	7.94
	GV L	.33	4.999	.947	-9.94	10.61
	Chem2	-2.00	4.999	.692	-12.28	8.28
	Chem1	-.67	4.999	.895	-10.94	9.61
	Chem3	-1.67	4.999	.742	-11.94	8.61

Based on observed means.

The error term is Mean Square(Error) = 37.487.

Table 10.6. Multiple comparisons of the Far Away field trial using generalised linear model and the least significant differences after 7 weeks of evaluation.

(I) Treatment	(J) Treatment	Mean Difference (I-J)	Std. Error	Sig.	95% Confidence Interval	
					Lower Bound	Upper Bound
Control	**NPV H**	8.0000	11.01654	.470	-14.0015	30.0015
	N3 H	6.1667	11.01654	.578	-15.8349	28.1682
	G3 H	6.3333	11.01654	.567	-15.6682	28.3349
	GV H	2.5000	11.01654	.821	-19.5015	24.5015
	NPV L	4.3333	11.01654	.695	-17.6682	26.3349
	N3 L	.0000	11.01654	1.000	-22.0015	22.0015
	G3 L	1.0000	11.01654	.928	-21.0015	23.0015
	GV L	5.3333	11.01654	.630	-16.6682	27.3349

	Chem1	1.5000	11.01654	.892	-20.5015	23.5015
	Chem2	2.5000	11.01654	.821	-19.5015	24.5015
	Chem3	5.3333	11.01654	.630	-16.6682	27.3349
	Chem4	4.8333	11.01654	.662	-17.1682	26.8349
NPV H	**Control**	-8.0000	11.01654	.470	-30.0015	14.0015
	N3 H	-1.8333	11.01654	.868	-23.8349	20.1682
	G3 H	-1.6667	11.01654	.880	-23.6682	20.3349
	GV H	-5.5000	11.01654	.619	-27.5015	16.5015
	NPV L	-3.6667	11.01654	.740	-25.6682	18.3349
	N3 L	-8.0000	11.01654	.470	-30.0015	14.0015
	G3 L	-7.0000	11.01654	.527	-29.0015	15.0015
	GV L	-2.6667	11.01654	.809	-24.6682	19.3349
	Chem1	-6.5000	11.01654	.557	-28.5015	15.5015
	Chem2	-5.5000	11.01654	.619	-27.5015	16.5015
	Chem3	-2.6667	11.01654	.809	-24.6682	19.3349
	Chem4	-3.1667	11.01654	.775	-25.1682	18.8349
N3 H	**NPV H**	1.8333	11.01654	.868	-20.1682	23.8349
	Control	-6.1667	11.01654	.578	-28.1682	15.8349
	G3 H	.1667	11.01654	.988	-21.8349	22.1682
	GV H	-3.6667	11.01654	.740	-25.6682	18.3349
	NPV L	-1.8333	11.01654	.868	-23.8349	20.1682
	N3 L	-6.1667	11.01654	.578	-28.1682	15.8349
	G3 L	-5.1667	11.01654	.641	-27.1682	16.8349
	GV L	-.8333	11.01654	.940	-22.8349	21.1682
	Chem1	-4.6667	11.01654	.673	-26.6682	17.3349
	Chem2	-3.6667	11.01654	.740	-25.6682	18.3349
	Chem3	-.8333	11.01654	.940	-22.8349	21.1682
	Chem4	-1.3333	11.01654	.904	-23.3349	20.6682
G3 H	**NPV H**	1.6667	11.01654	.880	-20.3349	23.6682
	Control	-6.3333	11.01654	.567	-28.3349	15.6682
	N3 H	-.1667	11.01654	.988	-22.1682	21.8349
	GV H	-3.8333	11.01654	.729	-25.8349	18.1682
	NPV L	-2.0000	11.01654	.857	-24.0015	20.0015
	N3 L	-6.3333	11.01654	.567	-28.3349	15.6682
	G3 L	-5.3333	11.01654	.630	-27.3349	16.6682
	GV L	-1.0000	11.01654	.928	-23.0015	21.0015
	Chem1	-4.8333	11.01654	.662	-26.8349	17.1682
	Chem2	-3.8333	11.01654	.729	-25.8349	18.1682
	Chem3	-1.0000	11.01654	.928	-23.0015	21.0015
	Chem4	-1.5000	11.01654	.892	-23.5015	20.5015

GV H	**NPV H**	5.5000	11.01654	.619	-16.5015	27.5015
	Control	-2.5000	11.01654	.821	-24.5015	19.5015
	N3 H	3.6667	11.01654	.740	-18.3349	25.6682
	G3 H	3.8333	11.01654	.729	-18.1682	25.8349
	NPV L	1.8333	11.01654	.868	-20.1682	23.8349
	N3 L	-2.5000	11.01654	.821	-24.5015	19.5015
	G3 L	-1.5000	11.01654	.892	-23.5015	20.5015
	GV L	2.8333	11.01654	.798	-19.1682	24.8349
	Chem1	-1.0000	11.01654	.928	-23.0015	21.0015
	Chem2	.0000	11.01654	1.000	-22.0015	22.0015
	Chem3	2.8333	11.01654	.798	-19.1682	24.8349
	Chem4	2.3333	11.01654	.833	-19.6682	24.3349
NPV L	**NPV H**	3.6667	11.01654	.740	-18.3349	25.6682
	Control	-4.3333	11.01654	.695	-26.3349	17.6682
	N3 H	1.8333	11.01654	.868	-20.1682	23.8349
	G3 H	2.0000	11.01654	.857	-20.0015	24.0015
	GV H	-1.8333	11.01654	.868	-23.8349	20.1682
	N3 L	-4.3333	11.01654	.695	-26.3349	17.6682
	G3 L	-3.3333	11.01654	.763	-25.3349	18.6682
	GV L	1.0000	11.01654	.928	-21.0015	23.0015
	Chem1	-2.8333	11.01654	.798	-24.8349	19.1682
	Chem2	-1.8333	11.01654	.868	-23.8349	20.1682
	Chem3	1.0000	11.01654	.928	-21.0015	23.0015
	Chem4	.5000	11.01654	.964	-21.5015	22.5015
N3 L	**NPV H**	8.0000	11.01654	.470	-14.0015	30.0015
	Control	.0000	11.01654	1.000	-22.0015	22.0015
	N3 H	6.1667	11.01654	.578	-15.8349	28.1682
	G3 H	6.3333	11.01654	.567	-15.6682	28.3349
	GV H	2.5000	11.01654	.821	-19.5015	24.5015
	NPV L	4.3333	11.01654	.695	-17.6682	26.3349
	G3 L	1.0000	11.01654	.928	-21.0015	23.0015
	GV L	5.3333	11.01654	.630	-16.6682	27.3349
	Chem1	1.5000	11.01654	.892	-20.5015	23.5015
	Chem2	2.5000	11.01654	.821	-19.5015	24.5015
	Chem3	5.3333	11.01654	.630	-16.6682	27.3349
	Chem4	4.8333	11.01654	.662	-17.1682	26.8349
G3 L	**NPV H**	7.0000	11.01654	.527	-15.0015	29.0015
	Control	-1.0000	11.01654	.928	-23.0015	21.0015
	N3 H	5.1667	11.01654	.641	-16.8349	27.1682

	G3 H	5.3333	11.01654	.630	-16.6682	27.3349
	GV H	1.5000	11.01654	.892	-20.5015	23.5015
	NPV L	3.3333	11.01654	.763	-18.6682	25.3349
	N3 L	-1.0000	11.01654	.928	-23.0015	21.0015
	GV L	4.3333	11.01654	.695	-17.6682	26.3349
	Chem1	.5000	11.01654	.964	-21.5015	22.5015
	Chem2	1.5000	11.01654	.892	-20.5015	23.5015
	Chem3	4.3333	11.01654	.695	-17.6682	26.3349
	Chem4	3.8333	11.01654	.729	-18.1682	25.8349
GV L	**NPV H**	2.6667	11.01654	.809	-19.3349	24.6682
	Control	-5.3333	11.01654	.630	-27.3349	16.6682
	N3 H	.8333	11.01654	.940	-21.1682	22.8349
	G3 H	1.0000	11.01654	.928	-21.0015	23.0015
	GV H	-2.8333	11.01654	.798	-24.8349	19.1682
	NPV L	-1.0000	11.01654	.928	-23.0015	21.0015
	N3 L	-5.3333	11.01654	.630	-27.3349	16.6682
	G3 L	-4.3333	11.01654	.695	-26.3349	17.6682
	Chem1	-3.8333	11.01654	.729	-25.8349	18.1682
	Chem2	-2.8333	11.01654	.798	-24.8349	19.1682
	Chem3	.0000	11.01654	1.000	-22.0015	22.0015
	Chem4	-.5000	11.01654	.964	-22.5015	21.5015
Chem1	**NPV H**	6.5000	11.01654	.557	-15.5015	28.5015
	Control	-1.5000	11.01654	.892	-23.5015	20.5015
	N3 H	4.6667	11.01654	.673	-17.3349	26.6682
	G3 H	4.8333	11.01654	.662	-17.1682	26.8349
	GV H	1.0000	11.01654	.928	-21.0015	23.0015
	NPV L	2.8333	11.01654	.798	-19.1682	24.8349
	N3 L	-1.5000	11.01654	.892	-23.5015	20.5015
	G3 L	-.5000	11.01654	.964	-22.5015	21.5015
	GV L	3.8333	11.01654	.729	-18.1682	25.8349
	Chem2	1.0000	11.01654	.928	-21.0015	23.0015
	Chem3	3.8333	11.01654	.729	-18.1682	25.8349
	Chem4	3.3333	11.01654	.763	-18.6682	25.3349
Chem2	**NPV H**	5.5000	11.01654	.619	-16.5015	27.5015
	Control	-2.5000	11.01654	.821	-24.5015	19.5015
	N3 H	3.6667	11.01654	.740	-18.3349	25.6682
	G3 H	3.8333	11.01654	.729	-18.1682	25.8349
	GV H	.0000	11.01654	1.000	-22.0015	22.0015
	NPV L	1.8333	11.01654	.868	-20.1682	23.8349

	N3 L	-2.5000	11.01654	.821	-24.5015	19.5015
	G3 L	-1.5000	11.01654	.892	-23.5015	20.5015
	GV L	2.8333	11.01654	.798	-19.1682	24.8349
	Chem1	-1.0000	11.01654	.928	-23.0015	21.0015
	Chem3	2.8333	11.01654	.798	-19.1682	24.8349
	Chem4	2.3333	11.01654	.833	-19.6682	24.3349
Chem3	**NPV H**	2.6667	11.01654	.809	-19.3349	24.6682
	Control	-5.3333	11.01654	.630	-27.3349	16.6682
	N3 H	.8333	11.01654	.940	-21.1682	22.8349
	G3 H	1.0000	11.01654	.928	-21.0015	23.0015
	GV H	-2.8333	11.01654	.798	-24.8349	19.1682
	NPV L	-1.0000	11.01654	.928	-23.0015	21.0015
	N3 L	-5.3333	11.01654	.630	-27.3349	16.6682
	G3 L	-4.3333	11.01654	.695	-26.3349	17.6682
	GV L	.0000	11.01654	1.000	-22.0015	22.0015
	Chem1	-3.8333	11.01654	.729	-25.8349	18.1682
	Chem2	-2.8333	11.01654	.798	-24.8349	19.1682
	Chem4	-.5000	11.01654	.964	-22.5015	21.5015
Chem4	**NPV H**	3.1667	11.01654	.775	-18.8349	25.1682
	Control	-4.8333	11.01654	.662	-26.8349	17.1682
	N3 H	1.3333	11.01654	.904	-20.6682	23.3349
	G3 H	1.5000	11.01654	.892	-20.5015	23.5015
	GV H	-2.3333	11.01654	.833	-24.3349	19.6682
	NPV L	-.5000	11.01654	.964	-22.5015	21.5015
	N3 L	-4.8333	11.01654	.662	-26.8349	17.1682
	G3 L	-3.8333	11.01654	.729	-25.8349	18.1682
	GV L	.5000	11.01654	.964	-21.5015	22.5015
	Chem1	-3.3333	11.01654	.763	-25.3349	18.6682
	Chem2	-2.3333	11.01654	.833	-24.3349	19.6682
	Chem3	.5000	11.01654	.964	-21.5015	22.5015

Based on observed means.

The error term is Mean Square(Error) = 364.092.

Table 10.7. Multiple comparisons of the Sackville field trial using generalised linear model and the least significant differences after 3 weeks of evaluation.

(I) Treatment	(J) Treatment	Mean Difference (I-J)	Std. Error	Sig.	95% Confidence Interval	
					Lower Bound	Upper Bound
Control	**GV**	1.3333	2.07275	.526	-2.9446	5.6113
	NPV	.6667	2.07275	.751	-3.6113	4.9446

	N3	-.6667	2.07275	.751	-4.9446	3.6113
	Chem1	-2.0000	2.07275	.344	-6.2779	2.2779
	Chem2	-1.6667	2.07275	.429	-5.9446	2.6113
	Chem3	-.3333	2.07275	.874	-4.6113	3.9446
	Chem4	-1.6667	2.07275	.429	-5.9446	2.6113
	Chem5	-4.3333*	2.07275	.047	-8.6113	-.0554
	Chem6	-.3333	2.07275	.874	-4.6113	3.9446
	Chem7	-1.0000	2.07275	.634	-5.2779	3.2779
	Chem8	-.6667	2.07275	.751	-4.9446	3.6113
	Control	2.0000	2.07275	.344	-2.2779	6.2779
	GV	3.3333	2.07275	.121	-.9446	7.6113
	NPV	2.6667	2.07275	.211	-1.6113	6.9446
	N3	1.3333	2.07275	.526	-2.9446	5.6113
	Chem2	.3333	2.07275	.874	-3.9446	4.6113
Chem1	**Chem3**	1.6667	2.07275	.429	-2.6113	5.9446
	Chem4	.3333	2.07275	.874	-3.9446	4.6113
	Chem5	-2.3333	2.07275	.271	-6.6113	1.9446
	Chem6	1.6667	2.07275	.429	-2.6113	5.9446
	Chem7	1.0000	2.07275	.634	-3.2779	5.2779
	Chem8	1.3333	2.07275	.526	-2.9446	5.6113
	Control	1.6667	2.07275	.429	-2.6113	5.9446
	GV	3.0000	2.07275	.161	-1.2779	7.2779
	NPV	2.3333	2.07275	.271	-1.9446	6.6113
	N3	1.0000	2.07275	.634	-3.2779	5.2779
	Chem1	-.3333	2.07275	.874	-4.6113	3.9446
Chem2	**Chem3**	1.3333	2.07275	.526	-2.9446	5.6113
	Chem4	.0000	2.07275	1.000	-4.2779	4.2779
	Chem5	-2.6667	2.07275	.211	-6.9446	1.6113
	Chem6	1.3333	2.07275	.526	-2.9446	5.6113
	Chem7	.6667	2.07275	.751	-3.6113	4.9446
	Chem8	1.0000	2.07275	.634	-3.2779	5.2779
	Control	.3333	2.07275	.874	-3.9446	4.6113
	GV	1.6667	2.07275	.429	-2.6113	5.9446
	NPV	1.0000	2.07275	.634	-3.2779	5.2779
	N3	-.3333	2.07275	.874	-4.6113	3.9446
Chem3	**Chem1**	-1.6667	2.07275	.429	-5.9446	2.6113
	Chem2	-1.3333	2.07275	.526	-5.6113	2.9446
	Chem4	-1.3333	2.07275	.526	-5.6113	2.9446
	Chem5	-4.0000	2.07275	.066	-8.2779	.2779
	Chem6	.0000	2.07275	1.000	-4.2779	4.2779

	Chem7	-.6667	2.07275	.751	-4.9446	3.6113
	Chem8	-.3333	2.07275	.874	-4.6113	3.9446
Chem4	**Control**	1.6667	2.07275	.429	-2.6113	5.9446
	GV	3.0000	2.07275	.161	-1.2779	7.2779
	NPV	2.3333	2.07275	.271	-1.9446	6.6113
	N3	1.0000	2.07275	.634	-3.2779	5.2779
	Chem1	-.3333	2.07275	.874	-4.6113	3.9446
	Chem2	.0000	2.07275	1.000	-4.2779	4.2779
	Chem3	1.3333	2.07275	.526	-2.9446	5.6113
	Chem5	-2.6667	2.07275	.211	-6.9446	1.6113
	Chem6	1.3333	2.07275	.526	-2.9446	5.6113
	Chem7	.6667	2.07275	.751	-3.6113	4.9446
	Chem8	1.0000	2.07275	.634	-3.2779	5.2779
Chem5	**Control**	4.3333*	2.07275	.047	.0554	8.6113
	GV	5.6667*	2.07275	.012	1.3887	9.9446
	NPV	5.0000*	2.07275	.024	.7221	9.2779
	N3	3.6667	2.07275	.090	-.6113	7.9446
	Chem1	2.3333	2.07275	.271	-1.9446	6.6113
	Chem2	2.6667	2.07275	.211	-1.6113	6.9446
	Chem3	4.0000	2.07275	.066	-.2779	8.2779
	Chem4	2.6667	2.07275	.211	-1.6113	6.9446
	Chem6	4.0000	2.07275	.066	-.2779	8.2779
	Chem7	3.3333	2.07275	.121	-.9446	7.6113
	Chem8	3.6667	2.07275	.090	-.6113	7.9446
Chem6	**Control**	.3333	2.07275	.874	-3.9446	4.6113
	GV	1.6667	2.07275	.429	-2.6113	5.9446
	NPV	1.0000	2.07275	.634	-3.2779	5.2779
	N3	-.3333	2.07275	.874	-4.6113	3.9446
	Chem1	-1.6667	2.07275	.429	-5.9446	2.6113
	Chem2	-1.3333	2.07275	.526	-5.6113	2.9446
	Chem3	.0000	2.07275	1.000	-4.2779	4.2779
	Chem4	-1.3333	2.07275	.526	-5.6113	2.9446
	Chem5	-4.0000	2.07275	.066	-8.2779	.2779
	Chem7	-.6667	2.07275	.751	-4.9446	3.6113
	Chem8	-.3333	2.07275	.874	-4.6113	3.9446
Chem7	**Control**	1.0000	2.07275	.634	-3.2779	5.2779
	GV	2.3333	2.07275	.271	-1.9446	6.6113
	NPV	1.6667	2.07275	.429	-2.6113	5.9446
	N3	.3333	2.07275	.874	-3.9446	4.6113
	Chem1	-1.0000	2.07275	.634	-5.2779	3.2779

	Chem2	-.6667	2.07275	.751	-4.9446	3.6113
	Chem3	.6667	2.07275	.751	-3.6113	4.9446
	Chem4	-.6667	2.07275	.751	-4.9446	3.6113
	Chem5	-3.3333	2.07275	.121	-7.6113	.9446
	Chem6	.6667	2.07275	.751	-3.6113	4.9446
	Chem8	.3333	2.07275	.874	-3.9446	4.6113
Chem8	**Control**	.6667	2.07275	.751	-3.6113	4.9446
	GV	2.0000	2.07275	.344	-2.2779	6.2779
	NPV	1.3333	2.07275	.526	-2.9446	5.6113
	N3	.0000	2.07275	1.000	-4.2779	4.2779
	Chem1	-1.3333	2.07275	.526	-5.6113	2.9446
	Chem2	-1.0000	2.07275	.634	-5.2779	3.2779
	Chem3	.3333	2.07275	.874	-3.9446	4.6113
	Chem4	-1.0000	2.07275	.634	-5.2779	3.2779
	Chem5	-3.6667	2.07275	.090	-7.9446	.6113
	Chem6	.3333	2.07275	.874	-3.9446	4.6113
	Chem7	-.3333	2.07275	.874	-4.6113	3.9446
GV	**Control**	-1.3333	2.07275	.526	-5.6113	2.9446
	NPV	-.6667	2.07275	.751	-4.9446	3.6113
	N3	-2.0000	2.07275	.344	-6.2779	2.2779
	Chem1	-3.3333	2.07275	.121	-7.6113	.9446
	Chem2	-3.0000	2.07275	.161	-7.2779	1.2779
	Chem3	-1.6667	2.07275	.429	-5.9446	2.6113
	Chem4	-3.0000	2.07275	.161	-7.2779	1.2779
	Chem5	-5.6667*	2.07275	.012	-9.9446	-1.3887
	Chem6	-1.6667	2.07275	.429	-5.9446	2.6113
	Chem7	-2.3333	2.07275	.271	-6.6113	1.9446
	Chem8	-2.0000	2.07275	.344	-6.2779	2.2779
N3	**Control**	.6667	2.07275	.751	-3.6113	4.9446
	GV	2.0000	2.07275	.344	-2.2779	6.2779
	NPV	1.3333	2.07275	.526	-2.9446	5.6113
	Chem1	-1.3333	2.07275	.526	-5.6113	2.9446
	Chem2	-1.0000	2.07275	.634	-5.2779	3.2779
	Chem3	.3333	2.07275	.874	-3.9446	4.6113
	Chem4	-1.0000	2.07275	.634	-5.2779	3.2779
	Chem5	-3.6667	2.07275	.090	-7.9446	.6113
	Chem6	.3333	2.07275	.874	-3.9446	4.6113
	Chem7	-.3333	2.07275	.874	-4.6113	3.9446
	Chem8	.0000	2.07275	1.000	-4.2779	4.2779

	Control	-.6667	2.07275	.751	-4.9446	3.6113
	GV	.6667	2.07275	.751	-3.6113	4.9446
	N3	-1.3333	2.07275	.526	-5.6113	2.9446
	Chem1	-2.6667	2.07275	.211	-6.9446	1.6113
	Chem2	-2.3333	2.07275	.271	-6.6113	1.9446
NPV	**Chem3**	-1.0000	2.07275	.634	-5.2779	3.2779
	Chem4	-2.3333	2.07275	.271	-6.6113	1.9446
	Chem5	-5.0000*	2.07275	.024	-9.2779	-.7221
	Chem6	-1.0000	2.07275	.634	-5.2779	3.2779
	Chem7	-1.6667	2.07275	.429	-5.9446	2.6113
	Chem8	-1.3333	2.07275	.526	-5.6113	2.9446

Based on observed means.

The error term is Mean Square(Error) = 6.444.

***. The mean difference is significant at the 0.05 level.**

Table 10.8. Multiple comparisons of the Sackville field trial using generalised linear model and the least significant differences after 5 weeks of evaluation.

(I) Treatment	(J) Treatment	Mean Difference (I-J)	Std. Error	Sig.	95% Confidence Interval	
					Lower Bound	Upper Bound
	GV	1.4000	1.52096	.362	-1.6581	4.4581
	NPV	1.2000	1.52096	.434	-1.8581	4.2581
	N3	-.4000	1.52096	.794	-3.4581	2.6581
	Chem1	-1.0000	1.52096	.514	-4.0581	2.0581
	Chem2	-.8000	1.52096	.601	-3.8581	2.2581
Control	**Chem3**	.2000	1.52096	.896	-2.8581	3.2581
	Chem4	-.2000	1.52096	.896	-3.2581	2.8581
	Chem5	-1.6000	1.52096	.298	-4.6581	1.4581
	Chem6	.2000	1.52096	.896	-2.8581	3.2581
	Chem7	.0000	1.52096	1.000	-3.0581	3.0581
	Chem8	-.4000	1.52096	.794	-3.4581	2.6581
	Control	-1.4000	1.52096	.362	-4.4581	1.6581
	NPV	-.2000	1.52096	.896	-3.2581	2.8581
	N3	-1.8000	1.52096	.242	-4.8581	1.2581
	Chem1	-2.4000	1.52096	.121	-5.4581	.6581
GV	**Chem2**	-2.2000	1.52096	.155	-5.2581	.8581
	Chem3	-1.2000	1.52096	.434	-4.2581	1.8581
	Chem4	-1.6000	1.52096	.298	-4.6581	1.4581
	Chem5	-3.0000	1.52096	.054	-6.0581	.0581
	Chem6	-1.2000	1.52096	.434	-4.2581	1.8581

	Chem7	-1.4000	1.52096	.362	-4.4581	1.6581
	Chem8	-1.8000	1.52096	.242	-4.8581	1.2581
NPV	**GV**	.2000	1.52096	.896	-2.8581	3.2581
	Control	-1.2000	1.52096	.434	-4.2581	1.8581
	N3	-1.6000	1.52096	.298	-4.6581	1.4581
	Chem1	-2.2000	1.52096	.155	-5.2581	.8581
	Chem2	-2.0000	1.52096	.195	-5.0581	1.0581
	Chem3	-1.0000	1.52096	.514	-4.0581	2.0581
	Chem4	-1.4000	1.52096	.362	-4.4581	1.6581
	Chem5	-2.8000	1.52096	.072	-5.8581	.2581
	Chem6	-1.0000	1.52096	.514	-4.0581	2.0581
	Chem7	-1.2000	1.52096	.434	-4.2581	1.8581
	Chem8	-1.6000	1.52096	.298	-4.6581	1.4581
N3	**GV**	1.8000	1.52096	.242	-1.2581	4.8581
	Control	.4000	1.52096	.794	-2.6581	3.4581
	NPV	1.6000	1.52096	.298	-1.4581	4.6581
	Chem1	-.6000	1.52096	.695	-3.6581	2.4581
	Chem2	-.4000	1.52096	.794	-3.4581	2.6581
	Chem3	.6000	1.52096	.695	-2.4581	3.6581
	Chem4	.2000	1.52096	.896	-2.8581	3.2581
	Chem5	-1.2000	1.52096	.434	-4.2581	1.8581
	Chem6	.6000	1.52096	.695	-2.4581	3.6581
	Chem7	.4000	1.52096	.794	-2.6581	3.4581
	Chem8	.0000	1.52096	1.000	-3.0581	3.0581
Chem1	**GV**	2.4000	1.52096	.121	-.6581	5.4581
	Control	1.0000	1.52096	.514	-2.0581	4.0581
	NPV	2.2000	1.52096	.155	-.8581	5.2581
	N3	.6000	1.52096	.695	-2.4581	3.6581
	Chem2	.2000	1.52096	.896	-2.8581	3.2581
	Chem3	1.2000	1.52096	.434	-1.8581	4.2581
	Chem4	.8000	1.52096	.601	-2.2581	3.8581
	Chem5	-.6000	1.52096	.695	-3.6581	2.4581
	Chem6	1.2000	1.52096	.434	-1.8581	4.2581
	Chem7	1.0000	1.52096	.514	-2.0581	4.0581
	Chem8	.6000	1.52096	.695	-2.4581	3.6581
Chem2	**GV**	2.2000	1.52096	.155	-.8581	5.2581
	Control	.8000	1.52096	.601	-2.2581	3.8581
	NPV	2.0000	1.52096	.195	-1.0581	5.0581
	N3	.4000	1.52096	.794	-2.6581	3.4581
	Chem1	-.2000	1.52096	.896	-3.2581	2.8581

	Chem3	1.0000	1.52096	.514	-2.0581	4.0581
	Chem4	.6000	1.52096	.695	-2.4581	3.6581
	Chem5	-.8000	1.52096	.601	-3.8581	2.2581
	Chem6	1.0000	1.52096	.514	-2.0581	4.0581
	Chem7	.8000	1.52096	.601	-2.2581	3.8581
	Chem8	.4000	1.52096	.794	-2.6581	3.4581
	GV	1.2000	1.52096	.434	-1.8581	4.2581
	Control	-.2000	1.52096	.896	-3.2581	2.8581
	NPV	1.0000	1.52096	.514	-2.0581	4.0581
	N3	-.6000	1.52096	.695	-3.6581	2.4581
	Chem1	-1.2000	1.52096	.434	-4.2581	1.8581
Chem3	**Chem2**	-1.0000	1.52096	.514	-4.0581	2.0581
	Chem4	-.4000	1.52096	.794	-3.4581	2.6581
	Chem5	-1.8000	1.52096	.242	-4.8581	1.2581
	Chem6	.0000	1.52096	1.000	-3.0581	3.0581
	Chem7	-.2000	1.52096	.896	-3.2581	2.8581
	Chem8	-.6000	1.52096	.695	-3.6581	2.4581
	GV	1.6000	1.52096	.298	-1.4581	4.6581
	Control	.2000	1.52096	.896	-2.8581	3.2581
	NPV	1.4000	1.52096	.362	-1.6581	4.4581
	N3	-.2000	1.52096	.896	-3.2581	2.8581
	Chem1	-.8000	1.52096	.601	-3.8581	2.2581
Chem4	**Chem2**	-.6000	1.52096	.695	-3.6581	2.4581
	Chem3	.4000	1.52096	.794	-2.6581	3.4581
	Chem5	-1.4000	1.52096	.362	-4.4581	1.6581
	Chem6	.4000	1.52096	.794	-2.6581	3.4581
	Chem7	.2000	1.52096	.896	-2.8581	3.2581
	Chem8	-.2000	1.52096	.896	-3.2581	2.8581
	GV	3.0000	1.52096	.054	-.0581	6.0581
	Control	1.6000	1.52096	.298	-1.4581	4.6581
	NPV	2.8000	1.52096	.072	-.2581	5.8581
	N3	1.2000	1.52096	.434	-1.8581	4.2581
	Chem1	.6000	1.52096	.695	-2.4581	3.6581
Chem5	**Chem2**	.8000	1.52096	.601	-2.2581	3.8581
	Chem3	1.8000	1.52096	.242	-1.2581	4.8581
	Chem4	1.4000	1.52096	.362	-1.6581	4.4581
	Chem6	1.8000	1.52096	.242	-1.2581	4.8581
	Chem7	1.6000	1.52096	.298	-1.4581	4.6581
	Chem8	1.2000	1.52096	.434	-1.8581	4.2581

Chem6	GV	1.2000	1.52096	.434	-1.8581	4.2581
	Control	-.2000	1.52096	.896	-3.2581	2.8581
	NPV	1.0000	1.52096	.514	-2.0581	4.0581
	N3	-.6000	1.52096	.695	-3.6581	2.4581
	Chem1	-1.2000	1.52096	.434	-4.2581	1.8581
	Chem2	-1.0000	1.52096	.514	-4.0581	2.0581
	Chem3	.0000	1.52096	1.000	-3.0581	3.0581
	Chem4	-.4000	1.52096	.794	-3.4581	2.6581
	Chem5	-1.8000	1.52096	.242	-4.8581	1.2581
	Chem7	-.2000	1.52096	.896	-3.2581	2.8581
	Chem8	-.6000	1.52096	.695	-3.6581	2.4581
Chem7	GV	1.4000	1.52096	.362	-1.6581	4.4581
	Control	.0000	1.52096	1.000	-3.0581	3.0581
	NPV	1.2000	1.52096	.434	-1.8581	4.2581
	N3	-.4000	1.52096	.794	-3.4581	2.6581
	Chem1	-1.0000	1.52096	.514	-4.0581	2.0581
	Chem2	-.8000	1.52096	.601	-3.8581	2.2581
	Chem3	.2000	1.52096	.896	-2.8581	3.2581
	Chem4	-.2000	1.52096	.896	-3.2581	2.8581
	Chem5	-1.6000	1.52096	.298	-4.6581	1.4581
	Chem6	.2000	1.52096	.896	-2.8581	3.2581
	Chem8	-.4000	1.52096	.794	-3.4581	2.6581
Chem8	GV	1.8000	1.52096	.242	-1.2581	4.8581
	Control	.4000	1.52096	.794	-2.6581	3.4581
	NPV	1.6000	1.52096	.298	-1.4581	4.6581
	N3	.0000	1.52096	1.000	-3.0581	3.0581
	Chem1	-.6000	1.52096	.695	-3.6581	2.4581
	Chem2	-.4000	1.52096	.794	-3.4581	2.6581
	Chem3	.6000	1.52096	.695	-2.4581	3.6581
	Chem4	.2000	1.52096	.896	-2.8581	3.2581
	Chem5	-1.2000	1.52096	.434	-4.2581	1.8581
	Chem6	.6000	1.52096	.695	-2.4581	3.6581
	Chem7	.4000	1.52096	.794	-2.6581	3.4581

Based on observed means.

The error term is Mean Square(Error) = 5.783.